

Syracuse University

SURFACE

Dissertations - ALL

SURFACE

August 2020

EXPANDING THE POTENTIAL PRENYLOME: PRENYLATION OF SHORTENED TARGET SUBSTRATES BY FTASE AND DEVELOPMENT OF FRET-BASED SYSTEM FOR DETECTING POTENTIALLY "SHUNTED" PROTEINS

Sudhat Ashok
Syracuse University

Follow this and additional works at: <https://surface.syr.edu/etd>



Part of the [Physical Sciences and Mathematics Commons](#)

Recommended Citation

Ashok, Sudhat, "EXPANDING THE POTENTIAL PRENYLOME: PRENYLATION OF SHORTENED TARGET SUBSTRATES BY FTASE AND DEVELOPMENT OF FRET-BASED SYSTEM FOR DETECTING POTENTIALLY "SHUNTED" PROTEINS" (2020). *Dissertations - ALL*. 1185.
<https://surface.syr.edu/etd/1185>

This Dissertation is brought to you for free and open access by the SURFACE at SURFACE. It has been accepted for inclusion in Dissertations - ALL by an authorized administrator of SURFACE. For more information, please contact surface@syr.edu.

ABSTRACT

Protein prenylation is a posttranslational modification involving the attachment of a C15 or C20 isoprenoid group to a cysteine residue near the C-terminus of the target substrate by protein farnesyltransferase (FTase) or protein geranylgeranyltransferase type I (GGTase-I), respectively. Both of these protein prenyltransferases recognize a C-terminal "CaaX" sequence in their protein substrates, but recent studies in yeast- and mammalian-based systems have demonstrated FTase can also accept sequences that diverge in length from the canonical four-amino acid motif, such as the recently reported five-amino acid $C(x)_3X$ motif. In this work, we further expand the substrate scope of FTase by demonstrating sequence-dependent farnesylation of shorter three-amino acid "Cxx" C-terminal sequences using both genetic and biochemical assays. Surprisingly, biochemical assays utilizing purified mammalian FTase and Cxx substrates reveal prenyl donor promiscuity leading to both farnesylation and geranylgeranylation of these sequences. The work herein expands the substrate pool of sequences that can be potentially prenylated, further refines our understanding of substrate recognition by FTase and GGTase-I and suggests the possibility of a new class of prenylated proteins within proteomes.

To identify potential new Cxx substrates in human proteomes, we explored a FRET-based system using phosphodiesterase delta subunit (PDE δ) as the acceptor protein for potentially prenylated Cxx sequences. While not conclusive, this work lays the foundation for an assay not dependent on membrane localization as a signal for prenylation inside cells and suggests future studies to improve upon the utility of this assay. Lastly, this work demonstrates FTase's flexibility in accepting a prenyl donor analogue with an azobenzene moiety that can be modulated with light. This establishes a potential new avenue for mediating membrane localization behavior of prenylated proteins.

EXPANDING THE POTENTIAL PRENYLOME: PRENYLATION OF SHORTENED
TARGET SUBSTRATES BY FTASE AND DEVELOPMENT OF FRET-BASED SYSTEM
FOR DETECTING POTENTIALLY “SHUNTED” PROTEINS

by

Sudhat Ashok

M.Phil., Chemistry, Syracuse University, 2017
B.A., Psychology, SUNY Geneseo, 2014

Dissertation

Submitted in partial fulfillment of the requirements for the degree of
Doctor of Philosophy in Chemistry

Syracuse University
August 2020

Copyright © by Sudhat Ashok 2020
All Rights Reserved

ACKNOWLEDGEMENTS

There are several people that have been instrumental in my motivation to pursue this work and my development as a scientist. First, I must thank my advisor Dr. James Houglund for allowing me to work in his lab given my undergraduate background in psychology. His patience, guidance, and encouragement throughout the course of my graduate studies were invaluable and greatly appreciated. I am thankful for our discussions and the insights I gained. His mentoring has shaped my scientific thinking and made me confident in my abilities to incorporate research in my next endeavor as a physician. I would also like to thank Dr. Yan-Yueng Luk and Dr. Mark Braiman for their careful review of my work and providing suggestions to improve its overall quality throughout my tenure. I am also grateful to Dr. Douglas Frank, Dr. Davoud Mozhdehi, and Dr. John Franck for agreeing to serve on my defense committee and imparting insightful suggestions.

I thank my lab mates old and new, Mel, Michelle, Soumya, Liz, Kayleigh, Maria, Tasha, Jacob, Mariah, and Sadie for making my time in lab always enjoyable, no matter the experimental result. I want to especially thank Mel and Michelle for teaching me basic lab skills and showing me the “prenylation ropes”. You guys made coming into lab fun and I will value our time together.

I must also thank my partner Beryl. For always pushing me to achieve my potential and encouraging me to be the best version of myself. I am grateful for the time we have spent and cannot wait to navigate the next stage of our life together, medical school. I also thank Lee and Lisa for being incredible role models and for their support and guidance. Thank you to Dr. Michael Ruggiero for encouraging me to apply to the chemistry program at SU and more importantly, being a friend.

Finally, I thank my parents for their unconditional love and support. My parents have always been supportive of my decisions and for that I am grateful. Their sacrifices in moving to America are a major source for my motivation to pursue a career as a physician scientist. I also thank my brother Samrat for being a source of inspiration and my personal consumer reports expert, I know you will make a great psychiatrist soon.

TABLE OF CONTENTS

Chapter 1: Introduction

1.1	Protein Post-Translational Modifications.....	2
1.2	Prenylation and its enzymes.....	7
1.3	Structural, biochemical, and computational studies defining substrate selectivity of FTase and GGTase-I.....	13
1.4	Biological significance of prenylation.....	28
1.5	Importance and objectives.....	32
1.6	References.....	33

Chapter 2: Investigation of shortened “Cxx” target sequence recognition by FTase and GGTase-I

2.1	Introduction.....	64
2.2	Genetic screening in yeast reveals prenylation of Cxx sequences can occur <i>in vivo</i>	68
2.3	Farnesylation of Cxx peptide substrates by mammalian prenyltransferases.....	74
2.4	Geranylgeranylation of Cxx peptide sequences by FTase.....	90
2.5	Competition assay to assess FTase preference for FPP versus GGPP.....	93
2.6	Steady state analysis of dns-GCxx peptide prenylation by FTase.....	95
2.7	Prenylation of Cxx motifs by FTase is inhibited by tipifarnib.....	100
2.8	Investigating prenylation of Cxx c-terminal sequences via in cell fluorescence by localization studies.....	103
2.9	Investigating prenylation of Cxx c-terminal sequences in a biological context via protein lipidation quantification (PLQ).....	106
2.10	Conclusions.....	111
2.11	Materials and Methods.....	114
2.11.1	Miscellaneous Methods.....	114
2.11.2	Yeast strains.....	114
2.11.3	Yeast plasmids and oligo designs.....	115
2.11.4	a-factor mating pheromone screen, halo assay, and mating test.....	116
2.11.5	Thermotolerance screen and assays.....	118

2.11.6	Estimate of Cxx complexity in a-factor and thermotolerance screens.....	118
2.11.7	Immunoblot analysis for protein prenylation in yeast.....	119
2.11.8	Image analysis for yeast plates and immunoblot films.....	119
2.11.9	Expression and purification of FTase and GGTase-I.....	119
2.11.10	RP-HPLC-based assay for screening the reactivity of dns-GCxx peptides and assessing prenylation preference by FTase.....	120
2.11.11	Fluorescence-based assay for screening reactivity of dns-GCxx peptides, determining prenyl donor saturating concentration, and determining steady-state kinetic parameters.....	120
2.11.12	RP-HPLC-based and fluorescence-based assays for screening the reactivity of dns-GCxx peptides by GGTase-I.....	124
2.11.13	LC-MS analysis of dns-GCxx peptides modified by FTase.....	124
2.11.14	Determination of tipifarnib inhibition of dns-GCxx peptide prenylation.....	125
2.11.15	Construction of eGFP-KRas-CLL/-CWI/-CQL reporter protein plasmids.....	125
2.11.16	Site-directed mutagenesis of eGFP-KRas-CLL reporter protein to generate 6 remaining -Cxx sequences.....	126
2.11.17	Transfection and visualization of eGFP-KRas-Cxx fusion proteins in HEK293 cells.....	127
2.11.18	Site-directed mutagenesis of pJExpress414-eGFP-CVLL reporter protein to -CVLS/-CLL/-CVL sequences.....	128
2.11.19	Expression and purification of pJExpress414-eGFP-CVLS/-CVL/-CLL.....	129
2.11.20	Farnesylation of purified His ₆ -eGFP-CVLS/-CVL/-CLL.....	129
2.11.21	Site-directed mutagenesis of pCAF1-eGFP-CVLS vector to obtain -CVL/-CLL/-SVLS/-SVL/-SLL vectors.....	130
2.11.22	Preparation of HEK293 cells expressing eGFP-CVLS/-CVL/-CLL/-SVLS/-SVL/-SLL.....	131
2.11.23	Preparation and analysis of proteins by PLQ.....	131
2.12	References.....	133

Chapter 3: Investigating photo-switchable FPP analogs as donors for FTase

3.1	Introduction.....	145
3.2	WT FTase-catalyzed prenylation of dns-GCVLS peptide using Azo-FPP1.....	151

3.3	Azo-FPP1 exhibits sufficient reactivity with FTase to be considered for cellular studies.....	155
3.4	Conclusions.....	161
3.5	Materials and Methods.....	163
3.5.1	Synthetic schemes of Azo-FPP analogs.....	163
3.5.2	Assessing activity of Azo-FPP analogs with FTase and dns-GCVLS via RP-HPLC.....	164
3.5.3	Assessing activity of Azo-FPP analogs with GGTase-I and dns-GCVLL via RP-HPLC.....	165
3.5.4	Detection of Azo-FPP1 photoisomers via RP-HPLC analysis.....	165
3.5.5	Time course study to determine reactivity of <i>trans</i> - and <i>cis</i> -Azo-FPP1.....	166
3.5.6	Time course study to gauge reactivity of non-illuminated Azo-FPP1 in comparison to AlkC15OPP.....	167
3.6	References.....	168

Chapter 4: Development of a FRET assay to monitor protein prenylation within cells

4.1	Introduction.....	174
4.2	Establishing an <i>in vitro</i> FRET assay to assess binding of mCherry-PDE δ and prenylated eGFP-fusion peptide.....	179
4.3	Expression and purification of PDE δ and development of FRET assay using PDE δ and a prenylated dansyl-peptide.....	186
4.4	Investigating prenylation of non-canonical Cxx sequences in HEK293 cells via FLIM-FRET using GRK1 protein construct.....	191
4.5	Investigating prenylation of non-canonical Cxx sequences in HEK293 cells via FRET using modified eGFP-KRas protein constructs with mCherry-PDE δ	197
4.6	Conclusions.....	200
4.7	Materials and Methods.....	202
4.7.1	Construction of pET28a-mCherry-PDE δ bacterial vector.....	202
4.7.2	Expression and purification of pET28a-mCherry-PDE δ protein.....	203
4.7.3	Construction of pET28a-PDE δ bacterial vector.....	203
4.7.4	Expression and purification of pET28a-PDE δ	204
4.7.5	Farnesylation of purified eGFP-CVIA.....	205
4.7.6	FRET assay to probe mCherry-PDE δ binding prenylated eGFP-CVIA.....	205

4.7.7	Farnesylation and purification of dns-GCVLS.....	206
4.7.8	FRET assay to probe PDE δ binding prenylated dns-GCVLS.....	206
4.7.9	Generation of pCDNA-eGFP-GRK1ct18 mammalian vectors.....	207
4.7.10	Transfection and FLIM-FRET analysis of various eGFP-GRK1ct18 and eGFP-KRas fusion proteins in HEK293 cells.....	207
4.8	References.....	209

Chapter 5: Conclusions and Future Work

5.1	Summary.....	213
5.2	Future directions.....	215
5.2.1	Investigation of FTase vs. GGTase-I in Cxx substrate selectivity.....	215
5.2.2	Utilizing metabolic labeling to investigate prenylation of Cxx sequences in cells.....	216
5.2.3	Identification of endogenous Cxx proteins and the potential of a human shunt pathway.....	216
5.3	References.....	219

Appendices

Appendix I	Reprint permission for reference 104 (Chapter 1)	224
Appendix II	Reprint permission for reference 44 (Chapter 2)	232
Appendix III	Reprint permission for reference 2 (Chapter 3)	233
Appendix IV	Reprint permission for reference 18 (Chapter 4)	239
Appendix V	Curriculum Vitae.....	241

LIST OF FIGURES

Chapter 1: Introduction

Figure 1.1	Types of post-translational lipidations targeting proteins to the extracellular environment of a cell.....	5
Figure 1.2	Types of post-translational lipidations targeting proteins to membrane-bound organelles and/or the inner leaflet of the plasma membrane.....	6
Figure 1.3	The protein prenylation pathway.....	11
Figure 1.4	Transition state for FTase-catalyzed prenylation.....	12
Figure 1.5	Structures of mammalian FTase and GGTase-I.....	15
Figure 1.6	Selected FPP and GGPP analogues utilized for prenylated protein labeling and identification.....	26

Chapter 2: Investigation of shortened “Cxx” target sequence recognition by FTase and GGTase-I

Figure 2.1	Phenotypes of a-factor Cxx variants.....	72
Figure 2.2	Phenotypes and isoprenylation status of Ydj1p Cxx variants.....	73
Figure 2.3	FTase-catalyzed farnesylation of Cxx peptides confirmed by RP-HPLC analysis.....	88
Figure 2.4	LC-MS confirmation of FTase-catalyzed dns-GCxx peptide farnesylation.....	89
Figure 2.5	FTase-catalyzed geranylgeranylation of dns-GCxx peptides.....	91
Figure 2.6	LC-MS confirmation of FTase-catalyzed dns-GCxx peptide geranylgeranylation.....	92
Figure 2.7	Prenyl donor competition reveals FTase preference for FPP over GGPP for modifying dns-GCxx peptides.....	94
Figure 2.8	Steady state characterization of FTase-catalyzed dns-GCxx peptide farnesylation with FPP.....	97
Figure 2.9	Steady state characterization of FTase-catalyzed dns-GCxx peptide geranylgeranylation with GGPP.....	98
Figure 2.10	Inhibition of FTase-catalyzed farnesylation of dns-GCxx peptides by tipifarnib.....	101
Figure 2.11	Inhibition of FTase-catalyzed geranylgeranylation of dns-GCYL by tipifarnib.....	102
Figure 2.12	Fluorescence imaging of HEK293 cells expressing eGFP-KRas-C(x)(x) at 24 hours post transfection.....	105

Figure 2.13	Prenylation assessment of purified eGFP samples appended with various c-terminal motifs via PLQ at 520 nm.....	108
Figure 2.14	Prenylation assessment via PLQ of HEK293 cell lysate expressing eGFP-C(S)xx.....	110
Figure 2.15	Determination of saturating FPP and GGPP concentrations for FTase-catalyzed prenylation of dns-GCFT.....	123

Chapter 3: Investigating photo-switchable FPP analogs as donors for FTase

Figure 3.1	Structure and absorption spectra of trans- and cis-azobenzene.....	148
Figure 3.2	Structures of Azo-FPP1 and Azo-FPP2.....	149
Figure 3.3	Photophysical properties of Azo-FPP1.....	150
Figure 3.4	Modification of dns-GCVLS by FTase using Azo-FPP analogs as monitored by RP-HPLC.....	152
Figure 3.5	Modification of dns-GCVLL by GGTase-I using Azo-FPP analogs as monitored by RP-HPLC.....	153
Figure 3.6	RP-HPLC detection of modified dns-GCVLS with photoisomers of Azo-FPP1 generated by post-enzymatic reaction illumination.....	154
Figure 3.7	RP-HPLC detection of dns-GCVLS modified with trans-Azo-FPP1 at various time points under no illumination.....	157
Figure 3.8	RP-HPLC detection of dns-GCVLS modified with cis-Azo-FPP 1 at various time points after illumination with 365 nm light.....	158
Figure 3.9	Time course for FTase-catalyzed modification of dns-GCVLS by both photoisomers of Azo-FPP1.....	159
Figure 3.10	Time course for FTase-catalyzed modification of dns-GCVLS by both <i>trans</i> Azo-FPP1 and AlkC15OPP.....	160

Chapter 4: Development of a FRET assay to monitor protein prenylation within cells

Figure 4.1	Fluorescence resonance energy transfer.....	178
Figure 4.2	Expression and purification of His6-mCherry-PDE δ shown in white.....	181
Figure 4.3	Spectral characterization of His6-mCherry-PDE δ and eGFP-CVIA.....	184
Figure 4.4	FRET analysis to assess binding interaction of His6-mCherry-PDE δ with farnesylated and non-farnesylated eGFP-CVIA at 15 and 60 minutes' post-incubation.....	185

Figure 4.5	Serial dilution of purified His6-PDE δ analyzed by SDS-PAGE Gel under non-denaturing conditions, MW = 17.4 kDa, as shown in white.....	188
Figure 4.6	FRET measurements to determine binding interaction of PDE δ with farnesylated and non-farnesylated dns-GCVLS via plate-reader.....	189
Figure 4.7	FLIM-FRET measurements in HEK293 cells expressing either eGFP-GRK1-CVLS or eGFP-GRK1-AVLS.....	193
Figure 4.8	FLIM-FRET measurements in HEK293 cells co-expressing eGFP-GRK1-CVLS or eGFP-GRK1-AVLS or eGFP-GRK1-CVL and mCherry-PDE δ	196
Figure 4.9	FLIM-FRET measurements in HEK293 cells co-expressing eGFP-KRas and mCherry-PDE δ	199

LIST OF SCHEMES

Chapter 2: Investigation of shortened “Cxx” target sequence recognition by FTase and GGTase-I

Scheme 2.1 The protein farnesylation and processing pathway..... 67

Chapter 3: Investigating photo-switchable FPP analogs as donors for FTase

Scheme 3.1 Chemical synthesis of Azo-FPP1..... 163

Scheme 3.2 Chemical synthesis of Azo-FPP2..... 164

LIST OF TABLES

Chapter 2: Investigation of shortened “Cxx” target sequence recognition by FTase and GGTase-I

Table 2.1	Potential FTase substrate sequences within the human proteome.....	76
Table 2.2	Peptide information table for C-terminal Cxx sequences tested in the human genome.....	77
Table 2.3	Reactivity of Cxx peptides with mammalian FTase and prenyl donors.....	86
Table 2.4	Steady state reactivity of dns-GCxx peptides catalyzed by FTase.....	99

LIST OF ABBREVIATIONS

AdoHcy	S-Adenosylhomocysteine	FTI	Farnesyltransferase inhibitor
AdoMet	S-Adenosyl methionine	GDI	Guanine nucleoside dissociation inhibitors
AGOH	Anilinogeraniol	GGPP	Geranylgeranyl pyrophosphate
AGPP	Anilinogeranyl diphosphate	GGTase-I	Geranylgeranyltransferase type I
BGPP	Biotin- geranyl diphosphate	GPI	Glycosylphosphatidylinositol
CE	Capillary electrophoresis	PAGE	Polyacrylamide gel electrophoresis
CIP	Calf intestinal alkaline phosphatase	PBS	Phosphate Buffered Saline
CuAAC	Copper (I)- catalyzed alkyneazide cycloaddition	PCR	Polymerase Chain Reaction
DEAE	Diethylaminoethyl	HEK	Human embryonic kidney
DMSO	Dimethyl sulfoxide	HEPPSO	N-(2-Hydroxyethyl)piperazineN'-(2-hydroxypropanesulfonic acid)
DMEM	Dulbecco's Modified Eagle's Medium	HGPS	Hutchinson-Gilford Progeria Syndrome
DNA	Deoxyribonucleic acid	HPLC	High performance liquid chromatography
Dns	Dansyl fluorophore	ICMT	Isoprenylcysteine methyl transferase
dNTP	Deoxyribonucleotide Triphosphate	LC-MS	Liquid Chromatography-Mass spectrometry
<i>E. coli</i>	<i>Escherichia coli</i>	PDE δ	Phosphodiesterase δ
eGFP	Enhanced green fluorescent protein	PTM	Post-translational modification
ER	Endoplasmic reticulum	Rce1	Ras converting enzyme 1
FPLC	Fast protein liquid chromatography	SDS	Sodium dodecyl sulfate
FPP	Farnesyl pyrophosphate	TAMRA	Carboxytetramethylrhodamine
FTase	Farnesyltransferase	ZMPSTE24	Zinc metallopeptidase STE 24

Chapter 1: Introduction

Portions of this chapter including figures have been previously published and are reprinted with permission from the publisher, reference 104, Blanden, M. J.; Ashok, S. A.; Hougland, J. L., Mechanisms of CaaX Protein Processing: Protein Prenylation by FTase and GGTase-I, Reference Module in Chemistry, Molecular Sciences and Chemical Engineering, Elsevier, 2020.

1.1 Protein Post-Translational Modifications

The central dogma of molecular biology dictates that each organism's genetic code determines its proteome. That is, DNA is transcribed to RNA, and RNA is translated to proteins that are essential for proper functioning and development of every organism. However, many organisms have proteomes that are far more diverse and complex than would be simply predicted from its genome. For example, the human genome is estimated to have 20,000-25,000 open reading frames while the total number of molecularly distinct protein forms in the human proteome is estimated to be more than a million.^{1,2} These numbers show that a single gene can code for distinct protein forms. This diversity can be attributed to two phenomena in a cell. First, at the transcriptional level, use of multiple promoter and termination sites, alternate mRNA splicing, and/or recombination yields protein variation. Second, protein modifications at the co-translational and post-translational levels result in distinct forms as well.³

Post-translational modifications (PTMs) refer to covalent chemical modifications of target proteins, with these modifications influencing protein structure, localization, stability, and protein-protein interactions.⁴⁻⁷ Protein lipidation is one class of PTMs in which proteins are altered by attachment of various lipid groups such as fatty acids, isoprenoids, sterols, phospholipids and glycosylphosphatidylinositol (GPI) anchors.^{8,9} While lipidation commonly serves to enhance protein affinity for cell membranes, this modification has been found to both facilitate protein-protein interactions and play a role in protein stability.^{8,9}

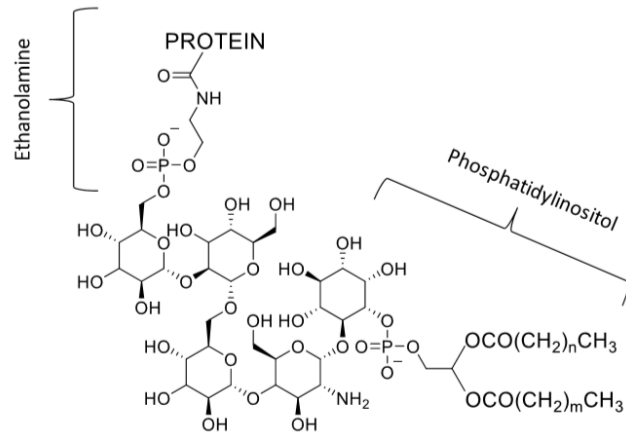
Protein lipidation modifications can be broadly classified into two categories: those that occur in the luminal compartments of the endoplasmic reticulum (ER) and Golgi bodies as part of secretory pathways, directing the modified proteins to targets outside the cell or the extracellular face of the plasma membrane; and those that occur on the cytoplasmic face of

membranes, targeting the modified proteins to the inner membrane leaflet or membranous compartments in cells. Glycosylphosphatidylinositol (GPI) anchors and cholesterol attachments represent the former of the two categories of lipid modifications that occur in the ER and Golgi lumen (Figure 1.1). The GPI moiety is composed of a phospholipid, sugars, and ethanolamine and is attached to the C-terminal carboxylate of a protein through its ethanolamine functional group. This attachment is involved in cell signaling, prion disease pathogenesis, and protein incorporation into lipid rafts.¹⁰⁻¹⁶ Similarly, cholesterol attachment occurs at the C-terminus of target proteins via an ester linkage.¹⁷⁻²¹ This modification is predominantly found in the Hedgehog protein family with the modified proteins playing roles in tissue repair and regeneration, organ development and stem cell maintenance.^{17, 22-25}

Protein myristoylation, palmitoylation, and prenylation belong to the second class of lipid modifications that occur on the cytoplasmic face of organelles or in the cytoplasm itself, targeting the modified proteins to the inner leaflet of the plasma membrane in addition to facilitating associations with other cellular compartments such as the Golgi, ER, and lipid vesicles (Figure 1.2).^{8, 9, 26} Protein myristoylation is the attachment of a 14-carbon myristic acid moiety to an N-terminal glycine residue on the target protein through an amide linkage. This modification plays a key role in cellular signaling pathways and is also known to act as a regulatory switch for proteins' spatial distribution inside cells.^{9, 10, 26-33} Palmitoylation usually involves the reversible addition of a 16-carbon palmitic acid moiety to a cysteine residue via a thioester bond, however, serine and threonine residues are also found to be palmitoylated on select proteins.^{8-10, 34, 35} The reversible nature of this modification via thioester hydrolysis allows modified proteins to shuttle between a membrane-bound or membrane-unbound state.³⁶⁻⁴² This modification is known to serve important roles in protein-protein interactions, protein trafficking

and stability.^{10, 43-50} Lastly, prenylation is the irreversible attachment of a 15-or 20-carbon isoprenoid chain to a cysteine residue near the C-terminus of a target protein. Prenylation plays an important role in cell signaling by aiding the localization of modified proteins to the plasma membrane and protein-protein interactions.⁵¹⁻⁵⁵

(A)



(B)

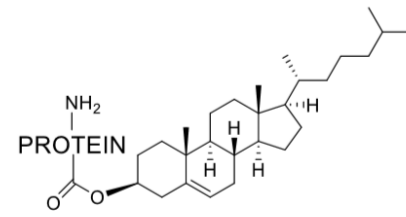


Figure 1.1: Types of post-translational lipidations targeting proteins to the extracellular environment of a cell. A) Glycophosphatidylinositol (GPI) anchors consist of an ethanolamine group, a sugar chain (D-mannose and D-glucosamine), and a phosphatidylinositol group. Mannose hydroxyl groups can also consist of various substitutions of long chain fatty acids.¹³ B) A protein-cholesterol ester bond.⁵⁶

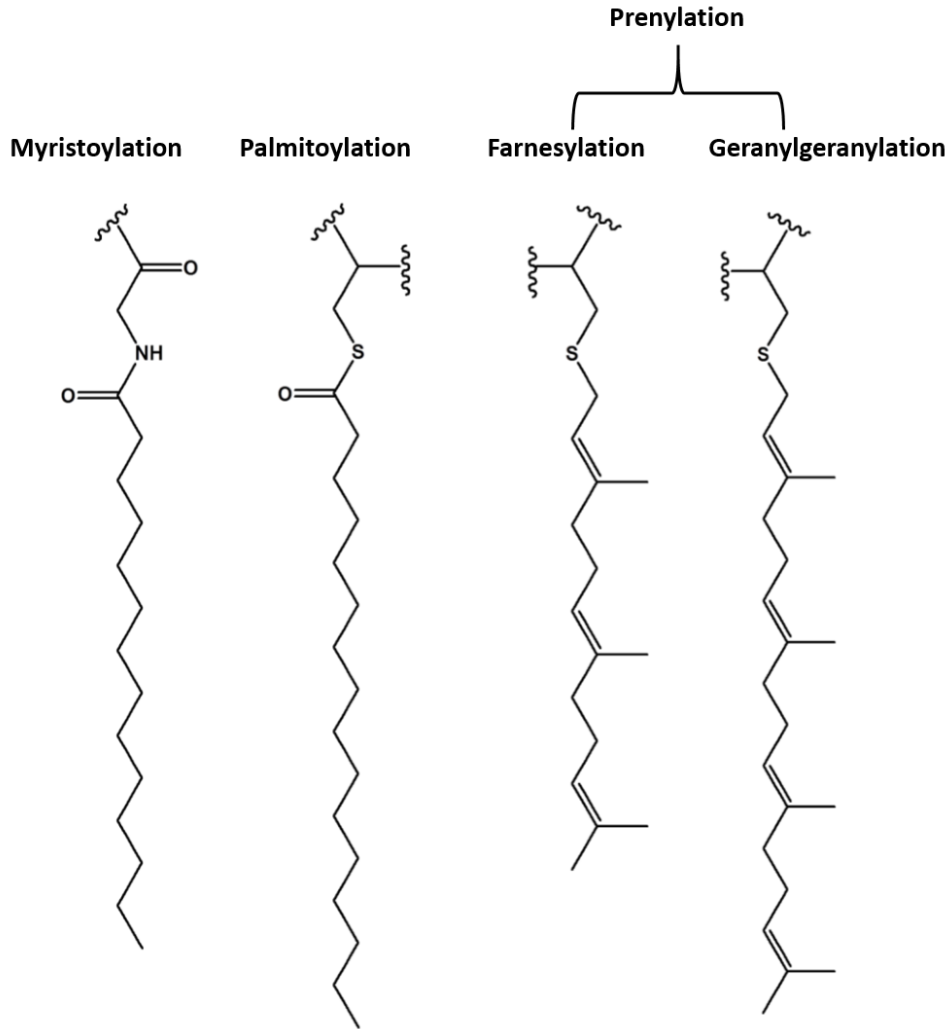


Figure 1.2: Types of post-translational lipidations targeting proteins to membrane-bound organelles and/or the inner leaflet of the plasma membrane. Myristoylation forms an amide bond to the N-terminal amino group of proteins; Palmitoylation occurs on a cysteine residue through a thioester linkage; Prenylation (farnesylation or geranylgeranylation) involves the formation of a thioether bond on a cysteine residue near the C-terminus.

1.2 Prenylation and its enzymes

Prenylation is a post-translational modification wherein a hydrophobic isoprenoid group, either a farnesyl or geranylgeranyl group, is transferred to a cysteine residue near the C-terminus of a target protein.^{7, 52, 53} This modification is necessary for membrane localization of many proteins which play important roles in signaling pathways and cellular processes. Prenylation can be catalyzed by protein farnesyltransferase (FTase) or protein geranylgeranyltransferase type I (GGTase-I), which differ in amino acid sequence recognition and the isoprenoid substrate to be attached.⁵² FTase catalyzes the addition of a 15-carbon isoprenoid group from farnesyl pyrophosphate (FPP), while GGTase-I catalyzes the addition of a 20-carbon isoprenoid group from geranylgeranyl pyrophosphate (GGPP, Figure 1.3).^{7, 52-55} GGTase-II is a third enzyme responsible for addition of a 20-carbon isoprenoid chain. It requires a Rab escort protein (REP) for substrate recognition, with REP binding to the substrate to be prenylated and presenting it to the catalytic site of GGTase-II for prenylation.⁵⁷ The target sequence for GGTase-II is also distinct from FTase and GGTase-I, with this enzyme modifying a variety of motifs from the Rab family of proteins including CC, CXC, CCXX, CCXXX, where C is a cysteine that undergoes modification.⁵⁸⁻⁶¹ Recently, a fourth protein prenyltransferase GGTase3 was identified as a novel human enzyme that modifies a ubiquitin ligase, FBXL2, with a 20-carbon geranylgeranyl isoprenoid group.⁶² This discovery expands our appreciation for the potential extent of prenylation within the proteome.

FTase and GGTase-I are both heterodimeric metalloenzymes comprising of an identical α subunit with differing β subunits.^{63, 64} The active site for both enzymes lies at the interface of the α and β subunits and is mainly composed of residues in the β subunit.⁶⁵ Both enzymes follow an ordered sequential mechanism wherein the isoprenoid binds first followed by binding of the

peptide or protein substrate. A subsequent conformational change in the first two units of the prenyl donor (FPP or GGPP) brings C1 of the prenyl donor near the cysteine side chain thiol to be modified.^{7, 66-70} In FTase, the negatively charged diphosphate group of the isoprenoid is stabilized during catalysis through interaction with a bound Mg^{2+} ion (Figure 1.4).^{70, 71} GGTase-I does not require a magnesium ion for reaction with GGPP, with lysine 311 β partially replacing the catalytic benefit provided by the magnesium ion in FTase.^{66, 72} A catalytic Zn^{2+} ion enhances peptide substrate binding and activates the cysteine thiol group for nucleophilic attack (Figure 1.4).⁷³ The pKa of the thiol is lowered due to coordination with the Zn^{2+} resulting in the formation of a Zn^{2+} -coordinated thiolate anion at physiological pH. This thiolate anion performs a nucleophilic attack on the alpha carbon of FPP or GGPP to form a thioether bond between the cysteine residue of the peptide/protein substrate and the lipid.^{71, 73-75} The modification step of this reaction is fast and the overall rate of the reaction depends on the slow product release step under saturating conditions.^{76, 77} The prenylated product is released upon binding of a new molecule of the respective prenyl donor followed by a conformation change in the peptide substrate.^{69, 78-80}

FTase and GGTase-I are proposed to recognize their substrates by the presence of a “CaaX” motif near the C-terminus of proteins. ‘C’ is the cysteine to be prenylated, ‘a’ is any aliphatic amino acid, and ‘X’ is an amino acid which determines enzyme specificity.^{63, 77, 81} FTase substrates typically have an X residue of serine, methionine, alanine, or glutamine, while GGTase-I usually recognizes leucine or phenylalanine at the X residue position. Some substrates may also be recognized by both enzymes as targets for prenylation.⁸²⁻⁸⁵ Recent evidence, however, from both yeast and mammalian systems supports the expansion of the FTase substrate pool with the discovery of farnesylated C(x)₃X sequences.⁸⁶ This again highlights the potential extent of prenylation in proteomes. Following prenylation of the CaaX sequence, a majority of

prenylated proteins undergo further post-processing steps which are essential for their final incorporation into the plasma membrane. The first step involves proteolysis of the last three amino acids by the CaaX protease Rce1p or Ste24p in the endoplasmic reticulum (ER), resulting in a negatively charged carboxyl group on the C-terminal cysteine which is then methylated by the S-adenosylmethionine (AdoMet) dependent isoprenylcysteine methyltransferase (ICMT) (Figure 1.3).⁸⁷⁻⁹³ Acting together, these two modifications increase protein hydrophobicity and lead to localization of prenylated proteins to the cell membrane. Structural and functional studies suggest that both enzymes process their substrates on the cytoplasmic surface of the ER.^{91, 94-97} A crystal structure of human metalloprotease Ste24p showed that the catalytic site lies at the apex of the enzyme's membrane-spanning chamber. On the cytoplasmic side of the membrane, a Zn²⁺ ion is coordinated by His residues from the HEXXH zinc metalloprotease motif (HELGH in Ste24p), where the Glu residue is predicted to be the catalytic residue that activates the attacking water molecule based on similarities with other metalloproteases and mutagenesis analysis.^{98, 99} Moreover, the substrate-binding site was predicted to be between the Zn²⁺ ion and a β sheet strand of the metalloprotease, containing hydrophobic pockets proposed to influence enzyme specificity.⁹⁹ More recently, a crystal structure of beetle ICMT revealed a breadth of information regarding the enzyme's ability to catalyze the reaction between two energetically unfavourable reactants, AdoMet and prenylcysteine substrates.¹⁰⁰ Specifically, ICMT exhibits two distinct entry routes for the cytosolic AdoMet and ER bound prenylated substrate. The active site was determined to be on the cytosolic leaflet of the membrane and exhibits a slender tunnel that brings the methyl group of AdoMet in proximity to prenylcysteine substrate, where the C-terminal carboxylate is stabilized and oriented for attack through hydrogen bonding with positively charged residues.¹⁰⁰ Overall, all three modification steps are deemed necessary for

function of most prenylated proteins. However, recent reports suggest that certain proteins in yeast undergo prenylation without subsequent proteolysis or methylation in what has been deemed the “shunt pathway”, with evidence of these processing steps being deleterious to the protein’s function.^{88, 101}

While these post-translational modifications increase the hydrophobicity of prenylated proteins, evidence also suggests that in order for these proteins to associate with the plasma membrane an additional secondary signal is often required.^{102, 103} For example, some proteins contain a polybasic region upstream of the CaaX site which promotes plasma membrane localization via electrostatic interactions with the negatively charged bilayer membrane. Other proteins require an additional lipid modification such as palmitoylation of residues upstream of the prenylated cysteine, which further enhances substrate hydrophobicity.

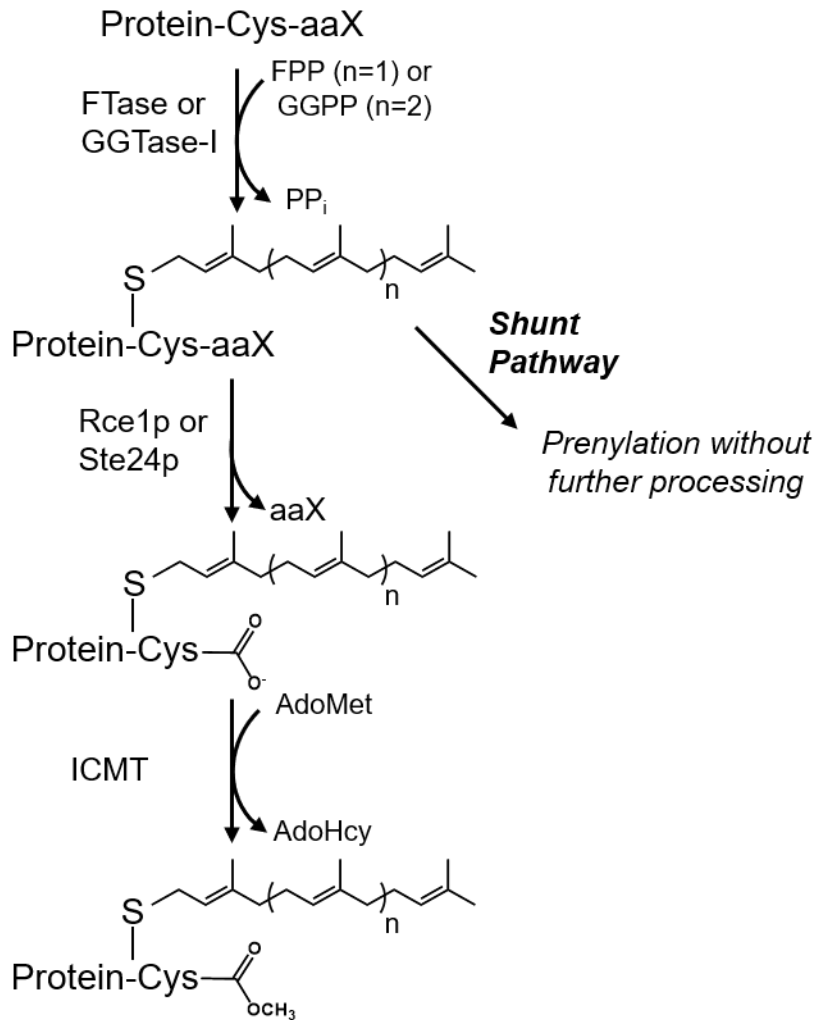


Figure 1.3: The protein prenylation pathway. The canonical protein prenylation pathway consists of three modification steps: isoprenoid addition, proteolysis, and carboxymethylation. A shunt pathway for proteins undergoing only prenylation absent subsequent processing has recently been reported.¹⁰⁴ This figure has been reused with permission from reference 104 (Appendix I).

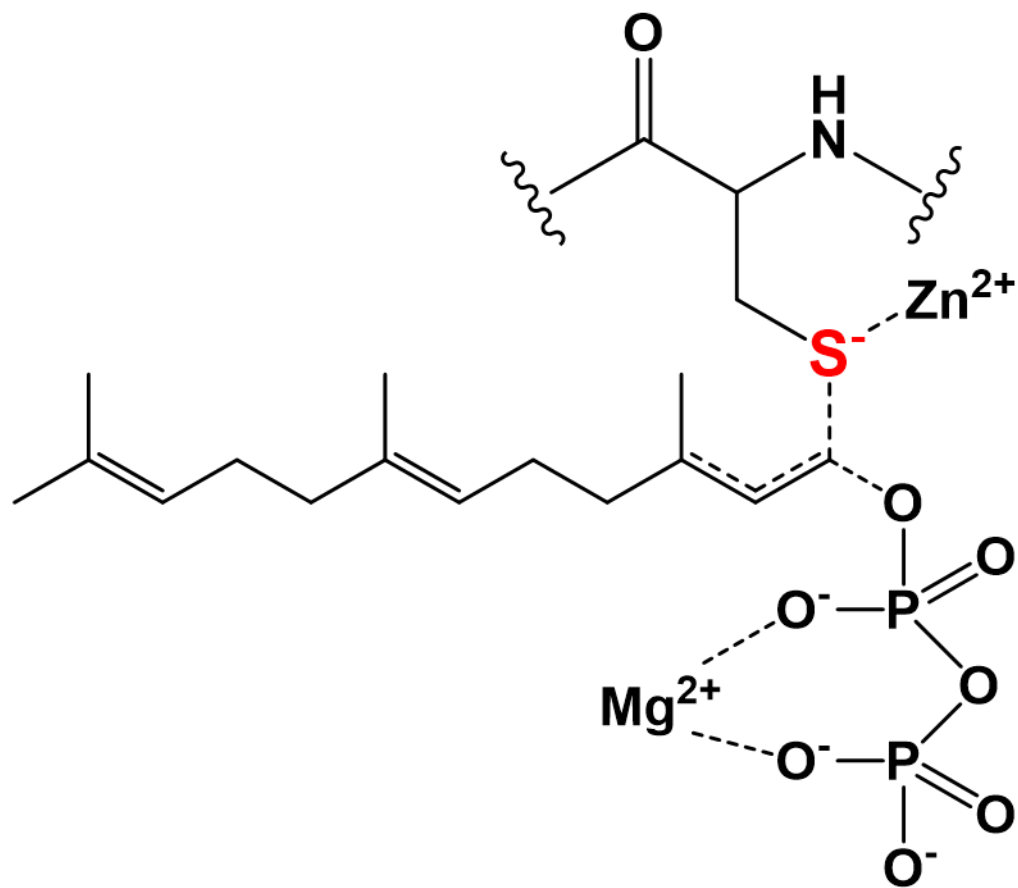


Figure 1.4: Transition state for FTase-catalyzed prenylation. The cysteine side chain thiol coordinates to the catalytic zinc ion, leading to an increase in nucleophilicity due to the lower pK_a of the zinc-coordinated thiolate. The pyrophosphate leaving group coordinates to a magnesium ion, with this interaction enhancing the prenylation rate ~ 700 -fold.¹⁰⁴ This figure has been reused with permission from reference 104 (Appendix I).

1.3 Structural, biochemical, and computational studies defining substrate selectivity of FTase and GGTase-I

To understand the biological impact of prenylation, it is important to define the extent and nature of the prenylated proteome. Numerous studies have aimed to gain insight into the substrate specificity for prenyl donor and CaaX substrates of prenyltransferases through various techniques such as structural studies, structure-function studies, peptide library studies and computational approaches.^{63, 105-110} Studies have also utilized radiolabeling, affinity tagging and similar techniques to identify prenylated proteins in cells as described below.^{105, 111-114}

Prenylation and the corresponding requirement of a CaaX motif were first described more than 30 years ago, when yeast mating pheromone a-factor, Ras GTPases, and nuclear lamins were found to be lipid-modified.¹¹⁵⁻¹¹⁹ Since their identification, studies of FTase and GGTase-I have focused on substrate selectivity and their preference for amino acids within the CaaX motif.¹²⁰ Several structural studies revealed that FTase and GGTase-I are both heterodimeric metalloenzymes consisting of an identical α subunit and distinct but homologous β subunits (Figure 1.5).^{63, 64, 66, 121} The active site for both enzymes lies at the interface of the α and β subunits and is predominantly composed of residues in the β subunit. The most obvious functional difference between FTase and GGTase-I, their respective preferences for FPP and GGPP as prenyl donor cosubstrates, was readily explained by comparison of their structures in complex with FPP and GGPP mimics.^{66, 85, 121} The binding sites for GGPP in GGTase-I and FPP in FTase are very comparable, constituting a cavity lined with conserved aromatic residues. However, selectivity of FTase for the shorter FPP substrate is determined by the presence of bulky tryptophan and tyrosine residues (W102 β and Y365 β) which block binding by the larger 20-carbon GGPP prenyl donor.⁶⁶ In comparison, GGTase-I has smaller threonine and

phenylalanine residues at the corresponding positions which allows this enzyme to accommodate the fourth isoprene unit of GGPP.⁶⁶ The amino acid contacts responsible for determining isoprenoid substrate selectivity were further confirmed via targeted mutagenesis of FTase to enable its use of GGPP as the prenyl donor.¹²² The FTase isoprenoid preference was converted by performing single and double mutations of the two bulky residues which contact FPP to their smaller counterparts in GGTase-I. Interestingly, mutating a single W102 β residue in FTase to threonine was sufficient for efficient catalysis with the longer GGPP prenyl donor. Of note, these mutations only changed FTase preference for its prenyl donor but did not change the peptide substrate preference to favor sequences recognized by GGTase-I.¹²²

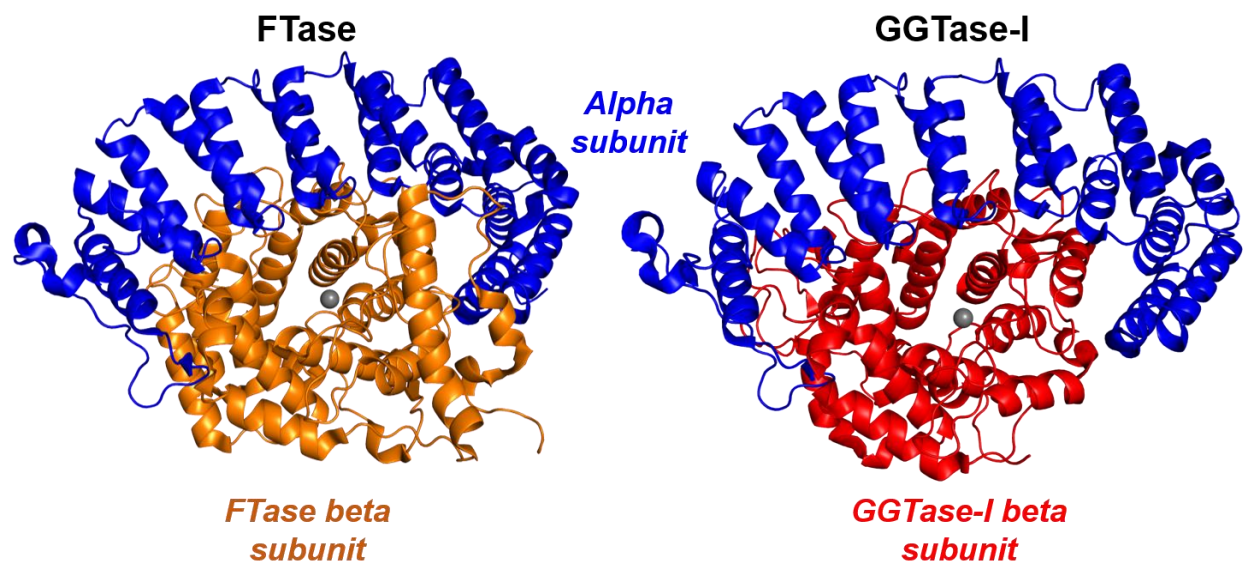


Figure 1.5: Structures of mammalian FTase and GGTase-I. Alpha subunits are shown in blue, with the FTase beta subunit in orange and the GGTase-I beta subunit in red. The catalytic zinc ions in both structures are depicted as grey spheres. Figure generated from PDB 1D8D (FTase) and 1TNO (GGTase-I) using Pymol.¹⁰⁴ This figure has been reused with permission from reference 104 (Appendix I).

In structural studies to identify the enzyme-substrate contacts responsible for FTase and GGTase-I CaaX peptide substrate selectivity, a series of peptide substrates were co-crystallized with FTase and GGTase-I. These substrates incorporated a series of different amino acids at the a₁, a₂, and X positions to explore the structural determinants governing peptide specificity for FTase and GGTase-I.⁸⁵ This study revealed that the various CaaX sequences adopt essentially the same conformation along one side of the funnel-shaped active site in both prenyltransferases except for the C-terminal X residue as discussed below. These structures showed the a₁ residue in a solvent-exposed conformation at the interface of the α and β subunits, consistent with the relaxed selectivity observed at the a₁ position in biochemical studies.¹²³⁻¹²⁵ Although FTase and GGTase-I generally exhibit broad amino acid tolerance at the a₁ position, the amino acids most commonly found at this position include V, A, K, and N, with the presence of a polar amino acid at this position proposed to enhance substrate binding via direct or water-mediated hydrogen bonding with the enzymes.⁸⁵

The a₂ and X residues, on the contrary, form interactions with enzyme residues within a solvent-excluded binding pocket. With this restricted location, steric and electrostatic interactions greatly influence amino acid specificity as compared to the a₁ position.^{82, 84, 85, 126} The a₂ binding pocket in FTase, for example, is composed of both the residues of the β subunit (W102 β , W106 β , and Y361 β) and the third isoprene unit of FPP. Specificity at this position was therefore proposed to be restricted to nonpolar residues such as I, L, and V. A similar binding site and specificity prediction is seen in GGTase-I with its analogous T49 β , F53 β , and L321 β residues.⁸⁵

Structural studies of FTase enzyme-substrate complexes with peptide substrates bearing varying amino acids at the C-terminal X position suggest that FTase utilizes two complementary

binding pockets for the X residue, which defines specificity at this position within the substrate sequence.⁸⁵ An X residue of S, Q and M interact with a binding pocket comprised of Y131 α , A98 β , S99 β , W102 β , H149 β , A151 β and P152 β . This differs from substrates terminating in F, L, H and N that interact with a separate binding pocket comprised of L96 β , S99 β , W102 β , W106 β , A151 β , the third isoprene unit of FPP and the a₂ residue. GGTase-I differs greatly in its X residue specificity in that it is composed of one binding pocket which contains the residues T49 β , H121 β , A123 β , F174 β , as well as the fourth isoprene unit of GGPP and the a₂ residue of the peptide substrate. GGTase-I prefers hydrophobic residues such as L, F, I, M and V given this hydrophobic binding pocket. In comparing the interactions of the a₁, a₂, and X residues with FTase and GGTase-I, it is the differences in X residue binding in these two enzymes that largely give them their varied preference for substrate targets and can allow for predictions of whether a substrate is more likely to be farnesylated or geranylgeranylated.⁸⁵

Functional studies utilizing peptide libraries have also proved useful for determining substrates recognized by FTase and GGTase-I, as well as defining what components of these substrates engender their recognition. Changes in peptide reactivity are correlated to changes in amino acid properties such as size or charge thereby, providing insights into the substrate recognition strategies employed by prenyltransferases. This method is based on monitoring reactivity of fluorescently tagged short peptides with prenyltransferases.^{73, 84, 123-130} For example, several peptide studies use a dansyl fluorophore attached to the N-terminus of the peptide allowing monitoring of prenylation via fluorescence assays.¹³¹ Utilizing the environmentally sensitive dansyl fluorophore facilitates real-time monitoring of prenylation through fluorescence enhancement upon cysteine alkylation with the hydrophobic farnesyl or geranylgeranyl groups.

The availability of high-throughput fluorescence assays has made peptide reactivity studies amenable for analyzing large peptide libraries.^{82, 123, 125-127, 132} CaaX peptide libraries have been employed in multiple studies to examine these effects by varying a₁, a₂, and X positions on fluorescent peptides.^{123, 126, 127} A study by Hartman and co-workers tested the specificity of prenyltransferases at the 'X' position of the substrate by investigating the TKCVIX peptide library derived from the K-Ras4B sequence TKCVIM.⁷⁷ This study showed that the specificity for FTase versus GGTase-I arises from peptide reactivity rather than relative binding affinity and that the reactivity strongly correlates with the hydrophobicity, volume and structure of the 'X' residue. FTase and GGTase-I were found to exhibit contrasting hydrophobicity preferences at the 'X' position, with GGTase-I preferring the more hydrophobic 'X' residues.⁷⁷ Krzysiak and co-workers also highlighted the ability for some substrates to undergo both farnesylation and geranylgeranylation depending on the amino acid at the X position, a phenomenon known as "leaky prenylation".⁸⁴

Study of the a₂ position has provided further insight into the structure-function relationship of prenyltransferases with their substrates.¹²⁶ In this study, the relative reactivity of a series of peptides which varied at the a₂ position (-GCV_{a2}S and -GCV_{a2}A) revealed that a₂ selectivity of FTase substrates depends on both size and hydrophobicity of the residue, with the enzyme discriminating against polar amino acids and both the largest and the smallest amino acids at this position. Moreover, this study found evidence for context dependent a₂ recognition, wherein the a₂ selectivity was influenced by the 'X' residue of the CaaX motif.¹²⁶ In a subsequent study, structure-targeted mutagenesis of GGTase-I was applied in combination with a series of dansyl-peptide substrates to better understand selectivity at the a₂ position.¹²⁷ Mutations of residues within GGTase-I, predicted to interact with the a₂ residue of the substrate, drastically

change substrate selectivity at the a_2 position. In addition, these variant GGTase-I enzymes not only accept non-natural peptide substrates in which the a_2 residue bears a charge, they are able to retain reactivity with a natural substrate (dns-GCVLL). In comparison to FTase variants with similarly reengineered substrate selectivities, it is evident that these two enzymes employ analogous mechanisms for substrate recognition with distinct sets of active site residues. These biochemical studies support the substrate recognition interactions predicted by structural studies of FTase and GGTase-I.^{63, 85}

In another study, Hougland and co-workers investigated the FTase substrate selectivity patterns by analyzing the reactivity of large scale peptide libraries whose sequences were derived from C-termini of human proteins.¹²³ The peptides from these libraries were screened under both multiple turnover conditions (MTO, $[E] \ll [S]$) and single turnover conditions (STO, $[E] \gg [S]$). MTO conditions most closely represent the scenario inside the cell where multiple substrates compete for prenylation by FTase or GGTase-I. From this study, it was found that of the roughly 300 C-terminal -Cxxx sequences tested, 67% were farnesylated under single-turnover conditions ($[E] \gg [S]$), suggesting that there are peptide sequence-dependent effects within the FTase catalytic cycle on steps such as the binding of FPP to the enzyme-farnesylated peptide complex and/or release of the farnesylated product. Moreover, the amino acid distribution at both the a_2 and X positions influences the preference for MTO vs STO reactivity, with non-canonical amino acids at both positions favoring STO reactivity. This provided insight into the role played by these positions on substrate binding, chemistry, and product release during farnesylation. For MTO peptides, specificity occurs before or at the step of farnesylation, while STO peptides exhibit a rate-limiting step at product release. The discovery that different substrate classes exist for FTase provides valuable insights into the regulation and reactivity of

FTase within the cell as well as the development of therapeutics for prenylation-dependent diseases.

Building upon the structural and biochemical data, several computational approaches have been developed to enable large scale prediction of prenylated proteins. Maurer-Stroh and Eisenhaber developed the algorithm PrePS to predict prenyltransferase substrates.¹⁰⁹ PrePS is based on data from experimentally derived recognition motifs to predict the likelihood of new motifs acting as a substrate for farnesylation or geranylgeranylation. This data resulted in learning sets which consist of 692 FTase and 486 GGTase-I substrates which were developed through a series of methods including a search of literature and BLASTP analysis with known prenylated substrates against an NCBI database. In addition, an 11 amino acid sequence upstream of the prenylcysteine was added to refine the algorithm. With this refinement of PrePS, the algorithm expands the rules which predict the prenylation of a substrate to a 15-amino acid sequence. However, due to the experimentally based nature of the algorithm development, PrePS has the potential for many false negatives for a given set of motifs with a reported false negative prediction near 40% when compared to substrates identified in peptide library screenings.^{108, 123}

FlexPepBind is another computational approach for predicting FTase substrates, developed by London and coworkers in 2011.¹⁰⁸ This algorithm predicts peptide binding through a structure-based modeling approach by aligning different peptide sequences onto a template peptide-receptor complex. Using the structure of the binding site of FTase, FlexPepBind is a more powerful tool than PrePS as it is not limited to information based on experimental data and was able to identify a range of novel potential targets in the human genome. In validation experiments, authors were able to verify 26 of the 29 tested peptides as being able to bind to FTase in *in vitro* assays. In comparison to PrePS, FlexPepBind is predicted to have a 44% true

positive rate and a 2% false positive rate but eliminates the large number of false negative predictions seen with PrePS.

A recent statistical analysis of the number of substrates capable of undergoing prenylation in yeast suggests that many prediction tools are biased against non-canonical motifs which may undergo prenylation but not the subsequent processing steps of proteolysis and methylation.¹³³ To remedy this bias, authors used yeast Hsp40 Ydj1p chaperone as a genetic reporter. Ydj1p is prenylated but is subject to the shunt pathway in which the prenylated protein does not undergo further processing steps and stays cytosolic. Prenylated Ydj1p produces a thermotolerant phenotype in yeast which serves as a proxy for the authors to monitor the prenylation state of Ydj1p given different mutations within the Cxxx motif. Using this genetic screen, the authors evaluated over 67,000 recombination events, correlating to 93.5% of the possible amino acid combinations in the Cxxx motif. The sequences found capable of undergoing prenylation using Ydj1p did not greatly overlap with those found in other screenings that utilized common targets such as Ras, suggesting a much larger set of motifs capable of prenylation than was previously thought. This includes a largely unbiased preference at each position in the motif to accept amino acids that vary in their hydrophobicity, size, and charge. In contrast to other predictive algorithms, very few sequences identified using the Ydj1p-based screening were identified as having a high probability of prenylation by FlexPepBind and PrePS with results of 27% and 7%, respectively. However, it is important to note that this discrepancy may reflect different substrate selectivities for the mammalian and yeast enzymes.

Many of the techniques used to study prenylation, while useful, examine the prenylation state of proteins *in vitro*. Use of fluorescent proteins within cells has been an indispensable technique in the study of prenylation at endogenous levels, providing better insight into both the

biological significance of prenylation and the effects of prenyltransferase inhibitors. The earliest examples of fluorescent localization studies include immunofluorescence microscopy. One study investigated the ability of prenyltransferase inhibitors to selectively target oncogenic Ras isoforms in cancer cells.¹³⁴ Upon treatment with two FTIs which block Ras protein farnesylation, cells studied with immunofluorescence of nuclear lamins did not show an impact on lamin ability to be farnesylated as reflected by proper localization to the nuclear membrane and metabolic labeling. This work provided some of the first insight into the effect of prenyltransferase inhibitors at a cellular level to better understand their potential as therapeutics.

Localization studies have evolved over the years to include conjugation of fluorescent proteins directly to the protein of interest.^{86, 127, 128, 135-142} In this method, an N-terminal fluorescent protein is appended to a protein of interest allowing direct visualization of protein localization. Fluorescence and protein localization at cellular membranes serves as a proxy for protein prenylation, whereas diffuse fluorescence throughout the cell indicates cytoplasmic localization. The latter implies a protein either not undergoing prenylation or becoming prenylated without further processing as noted in the shunt pathway. These fluorescent reporter proteins have been used to determine the sequence requirements and roles of CaaX modifications. Early studies into the role of post-prenylation processing include use of these fusion proteins to observe the effect of proteolysis and methylation on localization of prenylated proteins. In defining the mammalian Rce1 gene and its role in localization, Young and coworkers used Rce1^{+/+} and Rce1^{-/-} fibroblast cells transfected with a fusion protein containing green fluorescent protein and mouse Ki-Ras. Fluorescence was localized to the plasma membrane in Rce1^{+/+} cells but diffuse in Rce1^{-/-} cells, identifying proteolysis as necessary for Ras localization and introducing a new target for potential inhibitors.¹³⁸

A study in 2008 by Der et al. supported the requirement of proteolysis and methylation of Rho proteins following prenylation in determining cellular localization and protein function.¹³⁹ With green fluorescent protein cloned to several Rho proteins and grown in both wild-type cells and cells lacking either Rce1 ($Rce1^{-/-}$) or ICMT ($Icmt^{-/-}$), it was found that sensitivity to Rce1p and ICMT differed between Rho proteins. RhoB appeared to be more sensitive to loss of Rce1p, while RhoA was more dependent on ICMT as evidenced by the loss of fluorescent protein at the cell membrane.

Prenylated reporter protein cellular localization has also been employed to define the intrinsic reactivity required for a given FTase substrate sequence to be prenylated within a mammalian cell.¹²⁸ Development of a fluorescent reporter fusion protein terminating in C-terminal CaaX sequences with known levels of reactivity with FTase allowed for a calibrated sensor for protein farnesylation, with membrane localization indicating modification of the reporter protein. This study showed that in addition to the intrinsic reactivity of the reporter protein with FTase, the expression level of the reporter played a role in the extent of farnesylation of the reporter protein pool within the cell. This finding strongly suggested that results from overexpression studies of FTase substrates must be interpreted critically. Further, analysis of these panels of reactivity-defined reporter proteins provided the first cell-based quantitative measurements of FTase activity and provided potential reactivity thresholds for biologically relevant FTase substrates.

Another method for facilitating the detection of prenylated proteins is direct *in vivo* determination. The first approaches towards defining protein prenyltransferase selectivity included studies using radiolabeled ^3H FPP and GGPP for protein labeling, as well as radiolabeled precursors of these prenyl donors.^{112, 143, 144} In these studies, cells were grown in the

presence of these radiolabeled donors with subsequent ^3H incorporation into proteins endogenously prenylated in cells. This method was limited in its ability to provide a high yield of labeled protein against competing endogenous FPP or GGPP and in the limitation of pulling down the target protein from cells. While antibodies have been developed to aid in the selection of prenylated proteins from cells, they are unable to discriminate prenylation from other lipid posttranslational modifications.¹⁴⁵

Improvements upon this approach have centered around development of FPP and GGPP analogs that are functionalized with immunogenic tags, affinity tags or tags for chemoselective biorthogonal labeling (Figure 1.6). For example, Spielmann and co-workers showed the application of an immunogenic tag by using anilinogeraniol (AGOH) to detect FTase substrates.¹⁴⁶ Anilinogeraniol is an analog of an upstream precursor of FPP. It is converted to 8-anilinogeranyl diphosphate (AGPP) *in vivo* and replaces the third isoprene unit of FPP with an aniline moiety that then serves as an epitope for detection by Western blot.^{146, 147} Further, Alexandrov and co-workers developed biotin-geranyl diphosphate (BGPP) for use as an affinity tag.¹⁴⁸ BGPP only allowed for the efficient identification of GGTase-II substrates as the bulky nature of the biotin group was found to interfere with the protein substrate binding for FTase and GGTase-I. Reengineered FTase and GGTase-I variants that were capable of utilizing BGPP as a donor for protein modification were developed. Cell lysates were incubated with BGPP and wild-type or mutant prenyltransferases, with biotin-tagged proteins being subsequently pulled down using streptavidin beads and identified via mass spectrometry. This resulted in the identification of many Rab proteins as GGTase-II substrates, as well as various substrates which were identified from the lysates containing engineered FTase and GGTase-I.¹⁴⁸

Recently, new alkyne-tagged isoprenoid analogues which closely mimic FPP and GGPP have been used for direct detection of prenylated proteins via mass spectrometry.¹⁴⁹ These analogues not only allow for identification and quantification of prenyltransferase targets, they are able to maintain their transferase specificity and allow for a proteome-scale investigation of prenylated proteins at endogenous levels. Upon addition of the alkyne tagged analogue, proteins are captured via click CuAAC ligation to azide-containing reagents which have been functionalized with fluorophores or affinity tags such as biotin. These functionalizations allow for enrichment of the prenylated proteins and subsequent analysis via LC-MS/MS. In this study, proteins were identified at various stages of post-prenylation processing including ones in which cleavage of -aaX residues occurred but the protein (or the C-terminus) did not undergo subsequent methylation. The analogues also proved useful in determining the effects of prenyltransferase inhibitors (PTIs) across the prenylated proteome thus, providing a new avenue into the design of therapeutics that target prenylation specific diseases.

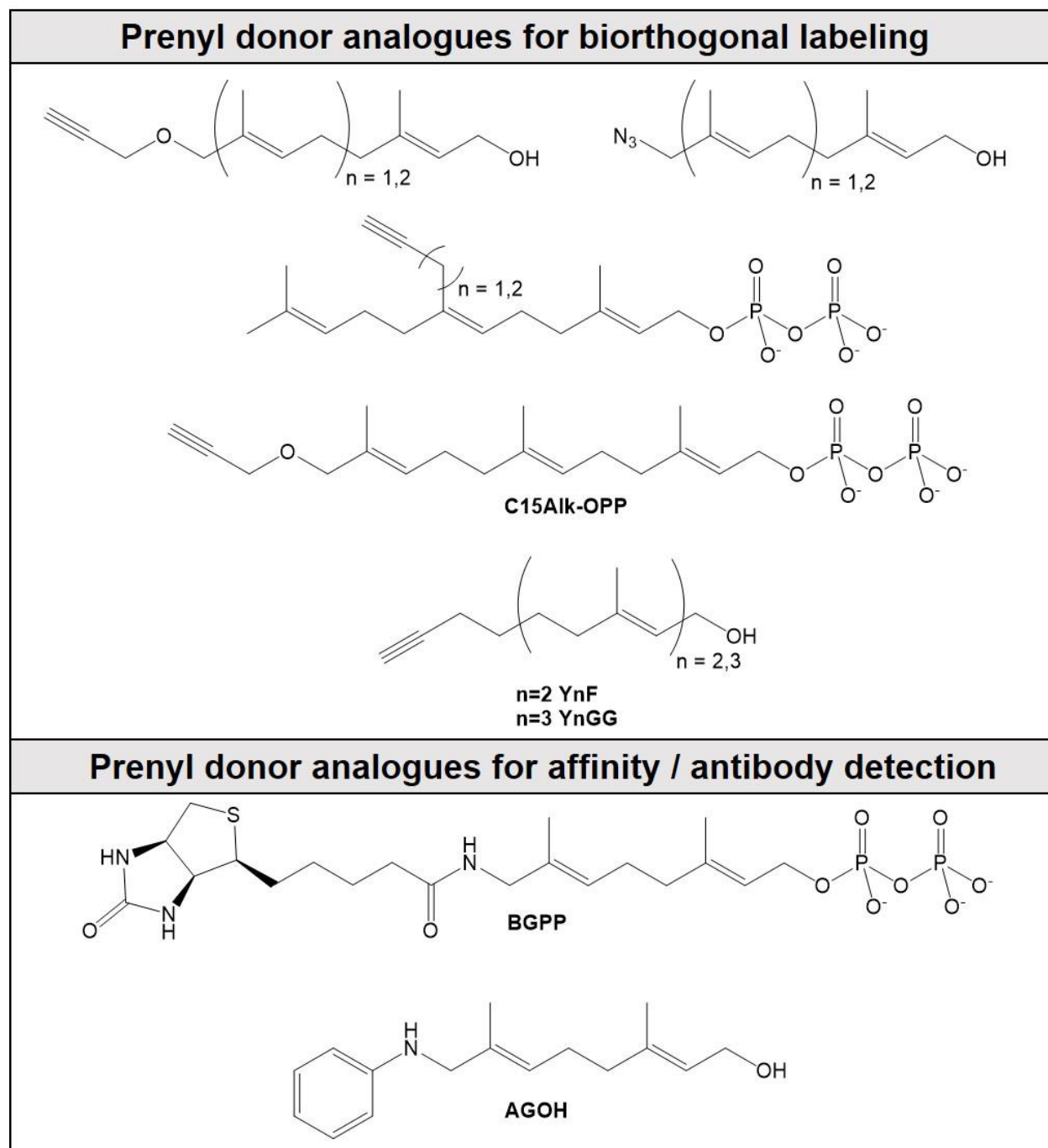


Figure 1.6: Selected FPP and GGPP analogues utilized for prenylated protein labeling and identification.¹⁰⁴ This figure has been reused with permission from reference 104 (Appendix I).

Overall, these analogues have enabled high-throughput identification of several FTase and GGTase-I substrates including members of the Ras, Rho, Rac, Rheb, Rab protein family members that were known to be prenylated.¹⁵⁰⁻¹⁵³ However, this approach also has certain limitations. Specifically, the use of FPP and GGPP analogues may alter the protein substrate specificity since the isoprenoid forms a part of the protein substrate binding pocket.¹⁵⁴⁻¹⁵⁶ Further, the use of mutant enzymes with certain analogues may not reflect the behavior of the wild type enzyme.¹²² Lastly, analogues used in several studies failed to identify known prenylated proteins, reflecting inefficient incorporation of the analog into substrates because of competition with endogenous prenyl donors.¹⁴⁸ In light of the limitations associated with chemical analogues and recent observations in yeast suggesting the prenylation of non-canonical C(x)₃X and Cxx motifs in the context of a heat-shock protein, Ydj1p (see chapter 2), it is important that we expand our approaches for the identification of potential prenyltransferase substrates.

1.4 Biological significance of prenylation

Prenylation plays an important role in signal transduction, control of cell differentiation and proliferation, cell survival and death, and cell migration.¹⁵⁷⁻¹⁶¹ This post-translational modification has been implicated in numerous diseases, with cancer receiving the most attention. The well-known GTPases H-Ras, N-Ras, K-Ras4 and N-Ras are involved in signal transduction and cell growth and have known oncogenic forms that are in an “always active” form, causing over-proliferation of cells.¹⁶²⁻¹⁶⁸ Prenylation is also not only crucial for plasma membrane localization and normal biological function of Ras proteins, but also for the transformation of cells by oncogenic Ras.^{60, 169, 170} Therefore, targeting Ras prenylation for mitigating oncogenesis has been of great interest.

Proteins beyond Ras family members have also been of interest in studying the role of prenylation in cancer. Certain members of the Rap family of proteins are implicated in tumorigenesis. For example, mutational activation of Rap1A signaling is associated with myeloproliferative disorder, a type of cancer involving aberrant development of blood cells. Abnormal Rap1 activity has also been linked to prostate cancer and osteosarcoma,¹⁷¹⁻¹⁷⁴ while Rap2B protein has been reported to promote invasion, proliferation and migration in breast cancer.¹⁷¹ The Rho proteins which are predominantly geranylgeranylated are involved in regulation of actin cytoskeleton. Both RhoA and RhoB play a role in actin stress fibers and focal adhesions formation.¹⁷⁵⁻¹⁷⁸ CDC42 is associated with control of cell cycle, cell polarity, and filopodia formation. And Rac is involved in the regulation of lamellipodia and membrane ruffles, which are motile cell surface formations that are crucial for cell motility.^{179, 180} Several of these Rho proteins have been linked to angiogenesis and metastasis.¹⁸¹⁻¹⁸³

With prenylation heavily implicated in cancer and tumor growth as described, several farnesyltransferase inhibitors (FTI) and geranylgeranyltransferase inhibitors (GGTI) have been explored as potential therapeutics.¹⁸⁴⁻¹⁸⁷ Despite the wide range of developed FTIs and GGITs, all have shown limited success at the clinical level for treating cancer.^{184, 188-190} The low level of effectiveness for these inhibitors in cells and human patients stems from the observation that there is no correlation between inhibition of tumor growth and the mutations of Ras. While Ras is mutated and involved in cancer, the efficacy of these prenyltransferase inhibitors potentially lies in their ability to inhibit both prenyltransferases.^{191, 192} For example, K-Ras and N-Ras have been found to undergo geranylgeranylation when subjected to FTI treatment.¹⁹³ This realization highlights the importance of identifying other proteins that undergo prenylation in order to design new, better therapeutic inhibitors or improve upon previously developed ones.

Protein prenylation of prelamin A has also been implicated in Hutchinson-Gilford progeria syndrome (HGPS). HGPS is a rare genetic disorder that manifests with reduced weight gain, loss of body fat, alopecia, and a variety of bone and dental abnormalities resulting in premature aging and death caused by myocardial infarction or stroke during teenage years.¹⁹⁴ Following prenylation and subsequent CaaX proteolysis, the final step in lamin maturation involves cleavage of the C-terminal 15 amino acid peptide by the endoprotease ZMPSTE24.¹⁹⁵⁻¹⁹⁷ However, in HGPS, the ZMPSTE24 cleavage site is lost due to alternative splicing of the prelamin A transcript due to a point mutation in *LMNA*, resulting in an in-frame deletion of 50 amino acids.^{198, 199} Consequently, the farnesylated and carboxymethylated prelamin A accumulate on the nuclear envelope leading to misshapen cell nuclei and ultimately to the phenotypic manifestations of HGPS. Several clinical trials for the use of FTIs as therapeutic agents were initiated after promising results in cells and mice.²⁰⁰⁻²⁰³ The use of FTIs such as

lonafarnib, pravastatin, and zoledronic acid increased life expectancy for children with progeria and improved their quality of life through measurement of weight gain and arterial density.²⁰⁴⁻²⁰⁷ Moreover, FTI treatment was also shown to decrease neurological symptoms such as seizures and headaches in one study, which are common comorbidities in HGPS patients.²⁰⁸ It is important to note however, that while FTIs proved useful in managing progeria symptoms and helped prolong life, they do not represent a cure for the disease. Investigations are focusing on gene therapy through stem cells and CRISPR-Cas9 gene editing as a potential avenue for curing patients who suffer from HGPS.²⁰⁹

Prenylation is also involved in infectious diseases. More specifically, *Legionella pneumophila*, a gram-negative pathogenic bacterium that causes Legionnaires' disease, was found to encode proteins that undergo prenylation.²¹⁰⁻²¹² This bacterium employs a Dot/Icm secretion system where it introduces numerous effectors that modulate and allow for bacterial proliferation as well as induce host cell apoptosis.²¹³⁻²¹⁵ The F-box effector Ankyrin B (AnkB) protein is one such vital effector that enables bacterial proliferation. It was shown that prenylation of this effector protein by the host's prenylation machinery is essential for anchoring the protein to the LCV membrane. This supports prenyltransferase inhibitors as attractive therapeutic agents to pursue for the treatment of Legionnaires' disease.²¹²

Candida albicans is a yeast organism where the role of prenylation has been studied to gain a better understanding of the etiology of various types of yeast infections.^{216, 217} A genetic study by Song and coworkers reported that RAM2, a gene that encodes the common alpha-subunit of both FTase and GGTase-I, is essential for *C. albicans* survival, suggesting that protein prenylation is an essential modification in the development of this organism.²¹⁸ Indeed, genetic and pharmacological interventions that target the *C. albicans* GGTase-I resulted in a

morphologically abnormal phenotype. However, this treatment failed to inhibit yeast growth, most likely due to the cross-reactivity with FTase.²¹⁷

There has also been much interest in the prenylated proteome of the protozoan parasite, *Plasmodium falciparum*, which causes malaria. Studies show that *P.falciparum* exhibits protein prenyltransferase activity and can incorporate both farnesyl and geranylgeranyl moieties onto protein substrates.²¹⁹⁻²²¹ Howe and coworkers noted that inhibition of isoprenoid biosynthesis by chemical treatment blocks protein prenylation and is lethal to cultured *P.falciparum*, suggesting a critical role for prenylation in this parasite's growth.²²² Other studies report that parasite prenyltransferase activity inhibition blocks parasite replication.²²³⁻²²⁵ Taken together, these studies demonstrate the essential nature of prenylation for parasitic growth and provide an alternative potential avenue for the treatment of malaria as drug resistance to current antimalarials develops.^{226, 227}

1.5 Importance and objectives

As discussed, prenylation serves as an important post-translational modification step for the proper functioning of several proteins that are implicated in many diseases. With over 1166 proteins estimated to contain a CaaX motif in the human proteome, gaining a more comprehensive picture of the prenylome represents a key step in understanding the roles played by prenylation in protein maturation and disease. While current investigations into the prenylome have limited their scope of investigation into the four amino acid C-terminal CaaX motif, recent evidence for prenylation of non-canonical C(x)3X sequences in yeast and mammalian systems calls for the expansion of the classically recognized prenylation motif.⁸⁶

This work aims to further expand the substrate selectivity of FTase by presenting evidence for the prenylation of a new motif, Cxx, by both yeast and mammalian enzymes through yeast genetic screening and biochemical characterization at the peptide and protein level. In addition to sequences identified from yeast genetic screening, a library of potential Cxx prenylation motifs was generated and tested for activity with mammalian FTase. In addition, studies were performed to assess the viability of FPP analogues with azo-benzene moieties that can be modulated with light as potential FTase donor substrates. In the last data chapter, efforts to develop a FRET-based system using phosphodiesterase delta subunit (PDE δ) as the acceptor protein for potentially prenylated Cxx sequences are presented. The main objective of this work is to characterize, identify, and expand upon the list of proteins that can be potentially prenylated in both in vitro and cellular contexts using a Cxx C-terminal motif.

1.6 References

1. Consortium, I. H. G. S., Finishing the euchromatic sequence of the human genome. *Nature* **2004**, *431* (7011), 931.
2. Jensen, O. N., Modification-specific proteomics: characterization of post-translational modifications by mass spectrometry. *Current opinion in chemical biology* **2004**, *8* (1), 33-41.
3. Ayoubi, T.; Van De Ven, W., Regulation of gene expression by alternative promoters. *The FASEB Journal* **1996**, *10* (4), 453-460.
4. Mann, M.; Jensen, O. N., Proteomic analysis of post-translational modifications. *Nature biotechnology* **2003**, *21* (3), 255-261.
5. Walsh, C., *Posttranslational modification of proteins: expanding nature's inventory*. Roberts and Company Publishers: 2006.
6. Prabakaran, S.; Lippens, G.; Steen, H.; Gunawardena, J., Post-translational modification: nature's escape from genetic imprisonment and the basis for dynamic information encoding. *Wiley Interdisciplinary Reviews: Systems Biology and Medicine* **2012**, *4* (6), 565-583.
7. Benetka, W.; Koranda, M.; Eisenhaber, F., Protein prenylation: An (almost) comprehensive overview on discovery history, enzymology, and significance in physiology and disease. *Monatshefte für Chemie/Chemical Monthly* **2006**, *137* (10), 1241.
8. Resh, M. D., Covalent lipid modifications of proteins. *Current Biology* **2013**, *23* (10), R431-R435.
9. Ganesan, L.; Levental, I., Pharmacological inhibition of protein lipidation. *The Journal of membrane biology* **2015**, *248* (6), 929-941.
10. Nadolski, M. J.; Linder, M. E., Protein lipidation. *The FEBS journal* **2007**, *274* (20), 5202-5210.

11. Nosjean, O., Mammalian GPI proteins: sorting, membrane resistance and functions. *Biochim Biophys Acta* **1997**, *1331*, 153-186.
12. Paulick, M. G.; Bertozzi, C. R., The glycosylphosphatidylinositol anchor: a complex membrane-anchoring structure for proteins. *Biochemistry* **2008**, *47* (27), 6991-7000.
13. Ferguson, M., The structure, biosynthesis and functions of glycosylphosphatidylinositol anchors, and the contributions of trypanosome research. *Journal of cell science* **1999**, *112* (17), 2799-2809.
14. Eisenhaber, B.; Maurer-Stroh, S.; Novatchkova, M.; Schneider, G.; Eisenhaber, F., Enzymes and auxiliary factors for GPI lipid anchor biosynthesis and post-translational transfer to proteins. *Bioessays* **2003**, *25* (4), 367-385.
15. Tiede, A.; Bastisch, I.; Schubert, J.; Orlean, P.; Schmidt, R. E., Biosynthesis of glycosylphosphatidylinositols in mammals and unicellular microbes. *Biological chemistry* **1999**, *380* (5), 503-524.
16. Chesebro, B.; Trifilo, M.; Race, R.; Meade-White, K.; Teng, C.; LaCasse, R.; Raymond, L.; Favara, C.; Baron, G.; Priola, S., Anchorless prion protein results in infectious amyloid disease without clinical scrapie. *Science* **2005**, *308* (5727), 1435-1439.
17. Ciepla, P.; Magee, A. I.; Tate, E. W., Cholesterylation: a tail of hedgehog. Portland Press Ltd.: 2015.
18. Chen, X.; Tukachinsky, H.; Huang, C.-H.; Jao, C.; Chu, Y.-R.; Tang, H.-Y.; Mueller, B.; Schulman, S.; Rapoport, T. A.; Salic, A., Processing and turnover of the Hedgehog protein in the endoplasmic reticulum. *Journal of Cell Biology* **2011**, *192* (5), 825-838.
19. Lee, J. J.; Ekker, S. C.; von Kessler, D. P.; Porter, J. A.; Sun, B. I.; Beachy, P. A., Autoproteolysis in hedgehog protein biogenesis. *Science* **1994**, *266* (5190), 1528-1537.

20. Porter, J. A.; von Kessler, D. P.; Ekker, S. C.; Young, K. E.; Lee, J. J.; Moses, K.; Beachy, P. A., The product of hedgehog autoproteolytic cleavage active in local and long-range signalling. *Nature* **1995**, *374* (6520), 363-366.
21. Porter, J. A.; Ekker, S. C.; Park, W.-J.; Von Kessler, D. P.; Young, K. E.; Chen, C.-H.; Ma, Y.; Woods, A. S.; Cotter, R. J.; Koonin, E. V., Hedgehog patterning activity: role of a lipophilic modification mediated by the carboxy-terminal autoprocessing domain. *Cell* **1996**, *86* (1), 21-34.
22. Porter, J. A.; Young, K. E.; Beachy, P. A., Cholesterol modification of hedgehog signaling proteins in animal development. *Science* **1996**, *274* (5285), 255-259.
23. Heal, W. P.; Jovanovic, B.; Bessin, S.; Wright, M. H.; Magee, A. I.; Tate, E. W., Bioorthogonal chemical tagging of protein cholesterylation in living cells. *Chemical communications* **2011**, *47* (14), 4081-4083.
24. Bürglin, T. R., The Hedgehog protein family. *Genome biology* **2008**, *9* (11), 241.
25. Heretsch, P.; Tzagkaroulaki, L.; Giannis, A., Modulators of the hedgehog signaling pathway. *Bioorganic & medicinal chemistry* **2010**, *18* (18), 6613-6624.
26. Resh, M. D., Trafficking and signaling by fatty-acylated and prenylated proteins. *Nature chemical biology* **2006**, *2* (11), 584-590.
27. Martin, D. D.; Beauchamp, E.; Berthiaume, L. G., Post-translational myristoylation: Fat matters in cellular life and death. *Biochimie* **2011**, *93* (1), 18-31.
28. Resh, M. D., Fatty acylation of proteins: new insights into membrane targeting of myristoylated and palmitoylated proteins. *Biochimica et Biophysica Acta (BBA)-Molecular Cell Research* **1999**, *1451* (1), 1-16.

29. Towler, D.; Eubanks, S.; Towery, D.; Adams, S.; Glaser, L., Amino-terminal processing of proteins by N-myristoylation. Substrate specificity of N-myristoyl transferase. *Journal of Biological Chemistry* **1987**, *262* (3), 1030-1036.
30. Boutin, J. A., Myristoylation. *Cellular signalling* **1997**, *9* (1), 15-35.
31. Farazi, T. A.; Waksman, G.; Gordon, J. I., The biology and enzymology of protein N-myristoylation. *Journal of biological chemistry* **2001**, *276* (43), 39501-39504.
32. Zha, J.; Weiler, S.; Oh, K. J.; Wei, M. C.; Korsmeyer, S. J., Posttranslational N-myristoylation of BID as a molecular switch for targeting mitochondria and apoptosis. *Science* **2000**, *290* (5497), 1761-1765.
33. Tang, C.; Loeliger, E.; Luncsford, P.; Kinde, I.; Beckett, D.; Summers, M. F., Entropic switch regulates myristate exposure in the HIV-1 matrix protein. *Proceedings of the National Academy of Sciences* **2004**, *101* (2), 517-522.
34. Fukata, Y.; Fukata, M., Protein palmitoylation in neuronal development and synaptic plasticity. *Nature Reviews Neuroscience* **2010**, *11* (3), 161.
35. Webb, Y.; Hermida-Matsumoto, L.; Resh, M. D., Inhibition of protein palmitoylation, raft localization, and T cell signaling by 2-bromopalmitate and polyunsaturated fatty acids. *Journal of Biological Chemistry* **2000**, *275* (1), 261-270.
36. Smotrýs, J. E.; Linder, M. E., Palmitoylation of intracellular signaling proteins: regulation and function. *Annual review of biochemistry* **2004**, *73* (1), 559-587.
37. Resh, M. D., Palmitoylation of ligands, receptors, and intracellular signaling molecules. *Sci. Stke* **2006**, *2006* (359), re14-re14.

38. Roth, A. F.; Wan, J.; Bailey, A. O.; Sun, B.; Kuchar, J. A.; Green, W. N.; Phinney, B. S.; Yates III, J. R.; Davis, N. G., Global analysis of protein palmitoylation in yeast. *Cell* **2006**, *125* (5), 1003-1013.
39. Duncan, J. A.; Gilman, A. G., A cytoplasmic acyl-protein thioesterase that removes palmitate from G protein α subunits and p21RAS. *Journal of Biological Chemistry* **1998**, *273* (25), 15830-15837.
40. Rocks, O.; Gerauer, M.; Vartak, N.; Koch, S.; Huang, Z.-P.; Pechlivanis, M.; Kuhlmann, J.; Brunsveld, L.; Chandra, A.; Ellinger, B., The palmitoylation machinery is a spatially organizing system for peripheral membrane proteins. *Cell* **2010**, *141* (3), 458-471.
41. Levental, I.; Grzybek, M.; Simons, K., Greasing their way: lipid modifications determine protein association with membrane rafts. *Biochemistry* **2010**, *49* (30), 6305-6316.
42. Greaves, J.; Chamberlain, L. H., DHHC palmitoyl transferases: substrate interactions and (patho) physiology. *Trends in biochemical sciences* **2011**, *36* (5), 245-253.
43. Greaves, J.; Chamberlain, L. H., Palmitoylation-dependent protein sorting. *J Cell Biol* **2007**, *176* (3), 249-254.
44. Linder, M. E.; Deschenes, R. J., Palmitoylation: policing protein stability and traffic. *Nature reviews Molecular cell biology* **2007**, *8* (1), 74-84.
45. Blaskovic, S.; Blanc, M.; van der Goot, F. G., What does S-palmitoylation do to membrane proteins? *The FEBS journal* **2013**, *280* (12), 2766-2774.
46. Zevian, S.; Winterwood, N. E.; Stipp, C. S., Structure-function analysis of tetraspanin CD151 reveals distinct requirements for tumor cell behaviors mediated by $\alpha 3\beta 1$ versus $\alpha 6\beta 4$ integrin. *Journal of Biological Chemistry* **2011**, *286* (9), 7496-7506.

47. McCormick, P. J.; Dumaresq-Doiron, K.; Pluviose, A. S.; Pichette, V.; Tosato, G.; Lefrancois, S., Palmitoylation controls recycling in lysosomal sorting and trafficking. *Traffic* **2008**, *9* (11), 1984-1997.
48. Lam, K. K.; Davey, M.; Sun, B.; Roth, A. F.; Davis, N. G.; Conibear, E., Palmitoylation by the DHHC protein Pfa4 regulates the ER exit of Chs3. *The Journal of cell biology* **2006**, *174* (1), 19-25.
49. Valdez-Taubas, J.; Pelham, H., Swf1-dependent palmitoylation of the SNARE Tlg1 prevents its ubiquitination and degradation. *The EMBO journal* **2005**, *24* (14), 2524-2532.
50. Kihara, A.; Kurotsu, F.; Sano, T.; Iwaki, S.; Igarashi, Y., Long-chain base kinase Lcb4 Is anchored to the membrane through its palmitoylation by Akr1. *Molecular and cellular biology* **2005**, *25* (21), 9189-9197.
51. Kamiya, Y.; Sakurai, A.; Tamura, S.; Takahashi, N.; Abe, K.; Tsuchiya, E.; Fukui, S.; Kitada, C.; Fujino, M., Structure of rhodotorucine A, a novel lipopeptide, inducing mating tube formation in *Rhodospiridiumtoruloides*. *Biochemical and biophysical research communications* **1978**, *83* (3), 1077-1083.
52. Casey, P. J.; Seabra, M. C., Protein prenyltransferases. *Journal of Biological Chemistry* **1996**, *271* (10), 5289-5292.
53. Zhang, F. L.; Casey, P. J., Protein prenylation: molecular mechanisms and functional consequences. *Annual review of biochemistry* **1996**, *65* (1), 241-269.
54. Marshall, C. J., Protein prenylation: a mediator of protein-protein interactions. *Science* **1993**, *259* (5103), 1865-1866.
55. Casey, P. J., Lipid modifications of G proteins. *Current opinion in cell biology* **1994**, *6* (2), 219-225.

56. Mann, R. K.; Beachy, P. A., Cholesterol modification of proteins. *Biochimica et Biophysica Acta (BBA)-Molecular and Cell Biology of Lipids* **2000**, *1529* (1-3), 188-202.
57. Shen, F.; Seabra, M. C., Mechanism of digeranylgeranylation of Rab proteins. Formation of a complex between monogeranylgeranyl-Rab and Rab escort protein. *The Journal of biological chemistry* **1996**, *271* (7), 3692-8.
58. Leung, K. F.; Baron, R.; Seabra, M. C., Thematic review series: lipid posttranslational modifications. geranylgeranylation of Rab GTPases. *Journal of lipid research* **2006**, *47* (3), 467-75.
59. Guo, Z.; Wu, Y. W.; Das, D.; Delon, C.; Cramer, J.; Yu, S.; Thuns, S.; Lupilova, N.; Waldmann, H.; Brunsveld, L.; Goody, R. S.; Alexandrov, K.; Blankenfeldt, W., Structures of RabGGTase-substrate/product complexes provide insights into the evolution of protein prenylation. *Embo j* **2008**, *27* (18), 2444-56.
60. Khosravi-Far, R.; Clark, G. J.; Abe, K.; Cox, A. D.; McLain, T.; Lutz, R. J.; Sinensky, M.; Der, C. J., Ras (CXXX) and Rab (CC/CXC) prenylation signal sequences are unique and functionally distinct. *The Journal of biological chemistry* **1992**, *267* (34), 24363-8.
61. Stenmark, H.; Olkkonen, V. M., The Rab GTPase family. *Genome Biol* **2001**, *2* (5), Reviews3007.
62. Kuchay, S.; Wang, H.; Marzio, A.; Jain, K.; Homer, H.; Fehrenbacher, N.; Philips, M. R.; Zheng, N.; Pagano, M., GGTase3 is a newly identified geranylgeranyltransferase targeting a ubiquitin ligase. *Nature structural & molecular biology* **2019**, *26* (7), 628-636.
63. Lane, K. T.; Beese, L. S., Thematic review series: lipid posttranslational modifications. Structural biology of protein farnesyltransferase and geranylgeranyltransferase type I. *Journal of lipid research* **2006**, *47* (4), 681-99.

64. Seabra, M. C.; Reiss, Y.; Casey, P. J.; Brown, M. S.; Goldstein, J. L., Protein farnesyltransferase and geranylgeranyltransferase share a common alpha subunit. *Cell* **1991**, *65* (3), 429-34.
65. Hast, M. A.; Beese, L. S., Structural Biochemistry of CaaX Protein Prenyltransferases. In *The Enzymes*, Tamanoi, F.; Hrycyna, C. A.; Bergo, M. O., Eds. Academic Press: 2011; Vol. 29, pp 235-257.
66. Taylor, J. S.; Reid, T. S.; Terry, K. L.; Casey, P. J.; Beese, L. S., Structure of mammalian protein geranylgeranyltransferase type-I. *EMBO J* **2003**, *22* (22), 5963-74.
67. Bowers, K. E.; Fierke, C. A., Positively charged side chains in protein farnesyltransferase enhance catalysis by stabilizing the formation of the diphosphate leaving group. *Biochemistry* **2004**, *43* (18), 5256-65.
68. Long, S. B.; Hancock, P. J.; Kral, A. M.; Hellinga, H. W.; Beese, L. S., The crystal structure of human protein farnesyltransferase reveals the basis for inhibition by CaaX tetrapeptides and their mimetics. *Proceedings of the National Academy of Sciences of the United States of America* **2001**, *98* (23), 12948-53.
69. Long, S. B.; Casey, P. J.; Beese, L. S., Reaction path of protein farnesyltransferase at atomic resolution. *Nature* **2002**, *419* (6907), 645-50.
70. Pickett, J. S.; Bowers, K. E.; Hartman, H. L.; Fu, H. W.; Embry, A. C.; Casey, P. J.; Fierke, C. A., Kinetic studies of protein farnesyltransferase mutants establish active substrate conformation. *Biochemistry* **2003**, *42* (32), 9741-8.
71. Saderholm, M. J.; Hightower, K. E.; Fierke, C. A., Role of metals in the reaction catalyzed by protein farnesyltransferase. *Biochemistry* **2000**, *39* (40), 12398-405.

72. Hartman, H. L.; Bowers, K. E.; Fierke, C. A., Lysine beta311 of protein geranylgeranyltransferase type I partially replaces magnesium. *The Journal of biological chemistry* **2004**, *279* (29), 30546-53.
73. Hightower, K. E.; Huang, C. C.; Casey, P. J.; Fierke, C. A., H-Ras peptide and protein substrates bind protein farnesyltransferase as an ionized thiolate. *Biochemistry* **1998**, *37* (44), 15555-62.
74. Huang, C. C.; Casey, P. J.; Fierke, C. A., Evidence for a catalytic role of zinc in protein farnesyltransferase. Spectroscopy of Co²⁺-farnesyltransferase indicates metal coordination of the substrate thiolate. *The Journal of biological chemistry* **1997**, *272* (1), 20-3.
75. Hightower, K. E.; De, S.; Weinbaum, C.; Spence, R. A.; Casey, P. J., Lysine(164)alpha of protein farnesyltransferase is important for both CaaX substrate binding and catalysis. *Biochem J* **2001**, *360* (Pt 3), 625-631.
76. Furfine, E. S.; Leban, J. J.; Landavazo, A.; Moomaw, J. F.; Casey, P. J., Protein farnesyltransferase: kinetics of farnesyl pyrophosphate binding and product release. *Biochemistry* **1995**, *34* (20), 6857-62.
77. Benetka, W.; Koranda, M.; Eisenhaber, F., Protein Prenylation: An (Almost) Comprehensive Overview on Discovery History, Enzymology, and Significance in Physiology and Disease. *Monatsh Chem* **2006**, *137*, 1241-1281.
78. Tschantz, W. R.; Furfine, E. S.; Casey, P. J., Substrate binding is required for release of product from mammalian protein farnesyltransferase. *The Journal of biological chemistry* **1997**, *272* (15), 9989-93.
79. Stradley, S. J.; Rizo, J.; Gierasch, L. M., Conformation of a heptapeptide substrate bound to protein farnesyltransferase. *Biochemistry* **1993**, *32* (47), 12586-12590.

80. Roskoski, R.; Ritchie, P. A., Time-dependent inhibition of protein farnesyltransferase by a benzodiazepine peptide mimetic. *Biochemistry* **2001**, *40* (31), 9329-9335.
81. Caplin, B. E.; Ohya, Y.; Marshall, M. S., Amino acid residues that define both the isoprenoid and CAAX preferences of the *Saccharomyces cerevisiae* protein farnesyltransferase. Creating the perfect farnesyltransferase. *The Journal of biological chemistry* **1998**, *273* (16), 9472-9.
82. Hartman, H. L.; Hicks, K. A.; Fierke, C. A., Peptide specificity of protein prenyltransferases is determined mainly by reactivity rather than binding affinity. *Biochemistry* **2005**, *44* (46), 15314-24.
83. Hicks, K. A.; Hartman, H. L.; Fierke, C. A., Upstream polybasic region in peptides enhances dual specificity for prenylation by both farnesyltransferase and geranylgeranyltransferase type I. *Biochemistry* **2005**, *44* (46), 15325-33.
84. Krzysiak, A. J.; Aditya, A. V.; Hougland, J. L.; Fierke, C. A.; Gibbs, R. A., Synthesis and screening of a CaaL peptide library versus FTase reveals a surprising number of substrates. *Bioorganic & medicinal chemistry letters* **2010**, *20* (2), 767-70.
85. Reid, T. S.; Terry, K. L.; Casey, P. J.; Beese, L. S., Crystallographic analysis of CaaX prenyltransferases complexed with substrates defines rules of protein substrate selectivity. *Journal of molecular biology* **2004**, *343* (2), 417-33.
86. Blanden, M. J.; Suazo, K. F.; Hildebrandt, E. R.; Hardgrove, D. S.; Patel, M.; Saunders, W. P.; Distefano, M. D.; Schmidt, W. K.; Hougland, J. L., Efficient farnesylation of an extended C-terminal C(x)3X sequence motif expands the scope of the prenylated proteome. *The Journal of biological chemistry* **2018**, *293* (8), 2770-2785.

87. Boyartchuk, V. L.; Ashby, M. N.; Rine, J., Modulation of Ras and a-factor function by carboxyl-terminal proteolysis. *Science* **1997**, *275* (5307), 1796-800.
88. Winter-Vann, A. M.; Casey, P. J., Post-prenylation-processing enzymes as new targets in oncogenesis. *Nature reviews. Cancer* **2005**, *5* (5), 405-12.
89. Bergo, M. O.; Wahlstrom, A. M.; Fong, L. G.; Young, S. G., Genetic analyses of the role of RCE1 in RAS membrane association and transformation. *Methods in enzymology* **2008**, *438*, 367-89.
90. Hollander, I.; Frommer, E.; Mallon, R., Human ras-converting enzyme (hRCE1) endoproteolytic activity on K-ras-derived peptides. *Analytical biochemistry* **2000**, *286* (1), 129-37.
91. Yang, J.; Kulkarni, K.; Manolaridis, I.; Zhang, Z.; Dodd, R. B.; Mas-Droux, C.; Barford, D., Mechanism of isoprenylcysteine carboxyl methylation from the crystal structure of the integral membrane methyltransferase ICMT. *Molecular cell* **2011**, *44* (6), 997-1004.
92. Gutierrez, L.; Magee, A. I.; Marshall, C. J.; Hancock, J. F., Post-translational processing of p21ras is two-step and involves carboxyl-methylation and carboxy-terminal proteolysis. *Embo j* **1989**, *8* (4), 1093-8.
93. Dolence, J. M.; Steward, L. E.; Dolence, E. K.; Wong, D. H.; Poulter, C. D., Studies with recombinant *Saccharomyces cerevisiae* CaaX prenyl protease Rce1p. *Biochemistry* **2000**, *39* (14), 4096-104.
94. Manolaridis, I.; Kulkarni, K.; Dodd, R. B.; Ogasawara, S.; Zhang, Z.; Bineva, G.; Reilly, N. O.; Hanrahan, S. J.; Thompson, A. J.; Cronin, N.; Iwata, S.; Barford, D., Mechanism of farnesylated CAAX protein processing by the intramembrane protease Rce1. *Nature* **2013**, *504* (7479), 301-5.

95. Diver, M. M.; Long, S. B., Mutational analysis of the integral membrane methyltransferase isoprenylcysteine carboxyl methyltransferase (ICMT) reveals potential substrate binding sites. *The Journal of biological chemistry* **2014**, *289* (38), 26007-20.
96. Plummer, L. J.; Hildebrandt, E. R.; Porter, S. B.; Rogers, V. A.; McCracken, J.; Schmidt, W. K., Mutational analysis of the ras converting enzyme reveals a requirement for glutamate and histidine residues. *The Journal of biological chemistry* **2006**, *281* (8), 4596-605.
97. Hildebrandt, E. R.; Davis, D. M.; Deaton, J.; Krishnankutty, R. K.; Lilla, E.; Schmidt, W. K., Topology of the yeast Ras converting enzyme as inferred from cysteine accessibility studies. *Biochemistry* **2013**, *52* (38), 6601-14.
98. Pryor, E. E.; Horanyi, P. S.; Clark, K. M.; Fedoriw, N.; Connelly, S. M.; Koszelak-Rosenblum, M.; Zhu, G.; Malkowski, M. G.; Wiener, M. C.; Dumont, M. E., Structure of the Integral Membrane Protein CAAX Protease Ste24p. *Science (New York, N.Y.)* **2013**, *339* (6127), 1600-1604.
99. Quigley, A.; Dong, Y. Y.; Pike, A. C.; Dong, L.; Shrestha, L.; Berridge, G.; Stansfeld, P. J.; Sansom, M. S.; Edwards, A. M.; Bountra, C.; von Delft, F.; Bullock, A. N.; Burgess-Brown, N. A.; Carpenter, E. P., The structural basis of ZMPSTE24-dependent laminopathies. *Science* **2013**, *339* (6127), 1604-7.
100. Diver, M. M.; Pedi, L.; Koide, A.; Koide, S.; Long, S. B., Atomic structure of the eukaryotic intramembrane RAS methyltransferase ICMT. *Nature* **2018**, *553* (7689), 526-529.
101. Hildebrandt, E. R.; Cheng, M.; Zhao, P.; Kim, J. H.; Wells, L.; Schmidt, W. K., A shunt pathway limits the CaaX processing of Hsp40 Ydj1p and regulates Ydj1p-dependent phenotypes. *eLife* **2016**, *5*, e15899.

102. Hancock, J. F.; Paterson, H.; Marshall, C. J., A polybasic domain or palmitoylation is required in addition to the CAAX motif to localize p21ras to the plasma membrane. *Cell* **1990**, *63* (1), 133-9.
103. Choy, E.; Chiu, V. K.; Silletti, J.; Feoktistov, M.; Morimoto, T.; Michaelson, D.; Ivanov, I. E.; Philips, M. R., Endomembrane trafficking of ras: the CAAX motif targets proteins to the ER and Golgi. *Cell* **1999**, *98* (1), 69-80.
104. Blanden, M. J.; Ashok, S.; Hougland, J. L., Mechanisms of CaaX Protein Processing: Protein Prenylation by FTase and GGTase-I. **2020**.
105. Zverina, E. A.; Lamphear, C. L.; Wright, E. N.; Fierke, C. A., Recent advances in protein prenyltransferases: substrate identification, regulation, and disease interventions. *Curr Opin Chem Biol* **2012**, *16* (5), 544-552.
106. Cui, G.; Merz, K. M., Jr., Computational studies of the farnesyltransferase ternary complex part II: the conformational activation of farnesyldiphosphate. *Biochemistry* **2007**, *46* (43), 12375-81.
107. Cui, G.; Wang, B.; Merz, K. M., Jr., Computational studies of the farnesyltransferase ternary complex part I: substrate binding. *Biochemistry* **2005**, *44* (50), 16513-23.
108. London, N.; Lamphear, C. L.; Hougland, J. L.; Fierke, C. A.; Schueler-Furman, O., Identification of a novel class of farnesylation targets by structure-based modeling of binding specificity. *PLoS Comput Biol* **2011**, *7* (10), e1002170-e1002170.
109. Maurer-Stroh, S.; Eisenhaber, F., Refinement and prediction of protein prenylation motifs. *Genome Biol* **2005**, *6* (6), R55.

110. Maurer-Stroh, S.; Koranda, M.; Benetka, W.; Schneider, G.; Sirota, F. L.; Eisenhaber, F., Towards complete sets of farnesylated and geranylgeranylated proteins. *PLoS Comput Biol* **2007**, *3* (4), e66.
111. Wang, Y.-C.; Distefano, M. D., Synthetic isoprenoid analogues for the study of prenylated proteins: Fluorescent imaging and proteomic applications. *Bioorganic Chemistry* **2016**, *64*, 59-65.
112. Gibbs, B. S.; Zahn, T. J.; Mu, Y.; Sebolt-Leopold, J. S.; Gibbs, R. A., Novel farnesol and geranylgeraniol analogues: A potential new class of anticancer agents directed against protein prenylation. *Journal of medicinal chemistry* **1999**, *42* (19), 3800-8.
113. Corsini, A.; Farnsworth, C. C.; McGeady, P.; Gelb, M. H.; Glomset, J. A., Incorporation of radiolabeled prenyl alcohols and their analogs into mammalian cell proteins. A useful tool for studying protein prenylation. *Methods in molecular biology (Clifton, N.J.)* **1999**, *116*, 125-44.
114. Benetka, W.; Koranda, M.; Maurer-Stroh, S.; Pittner, F.; Eisenhaber, F., Farnesylation or geranylgeranylation? Efficient assays for testing protein prenylation in vitro and in vivo. *BMC biochemistry* **2006**, *7*, 6.
115. Clarke, S.; Vogel, J. P.; Deschenes, R. J.; Stock, J., Posttranslational modification of the Ha-ras oncogene protein: evidence for a third class of protein carboxyl methyltransferases. *Proceedings of the National Academy of Sciences of the United States of America* **1988**, *85* (13), 4643-7.
116. Kitten, G. T.; Nigg, E. A., The CaaX motif is required for isoprenylation, carboxyl methylation, and nuclear membrane association of lamin B2. *J Cell Biol* **1991**, *113* (1), 13-23.

117. Powers, S.; Michaelis, S.; Broek, D.; Santa Anna, S.; Field, J.; Herskowitz, I.; Wigler, M., RAM, a gene of yeast required for a functional modification of RAS proteins and for production of mating pheromone a-factor. *Cell* **1986**, *47* (3), 413-22.
118. Vorburger, K.; Kitten, G. T.; Nigg, E. A., Modification of nuclear lamin proteins by a mevalonic acid derivative occurs in reticulocyte lysates and requires the cysteine residue of the C-terminal CXXM motif. *Embo j* **1989**, *8* (13), 4007-13.
119. Farnsworth, C. C.; Wolda, S. L.; Gelb, M. H.; Glomset, J. A., Human lamin B contains a farnesylated cysteine residue. *The Journal of biological chemistry* **1989**, *264* (34), 20422-9.
120. Zhang, F. L.; Casey, P. J., Protein prenylation: molecular mechanisms and functional consequences. *Annual review of biochemistry* **1996**, *65*, 241-69.
121. Strickland, C. L.; Windsor, W. T.; Syto, R.; Wang, L.; Bond, R.; Wu, Z.; Schwartz, J.; Le, H. V.; Beese, L. S.; Weber, P. C., Crystal structure of farnesyl protein transferase complexed with a CaaX peptide and farnesyl diphosphate analogue. *Biochemistry* **1998**, *37* (47), 16601-11.
122. Terry, K. L.; Casey, P. J.; Beese, L. S., Conversion of protein farnesyltransferase to a geranylgeranyltransferase. *Biochemistry* **2006**, *45* (32), 9746-55.
123. Hougland, J. L.; Hicks, K. A.; Hartman, H. L.; Kelly, R. A.; Watt, T. J.; Fierke, C. A., Identification of novel peptide substrates for protein farnesyltransferase reveals two substrate classes with distinct sequence selectivities. *Journal of molecular biology* **2010**, *395* (1), 176-90.
124. Reiss, Y.; Stradley, S. J.; Gierasch, L. M.; Brown, M. S.; Goldstein, J. L., Sequence requirement for peptide recognition by rat brain p21ras protein farnesyltransferase. *Proceedings of the National Academy of Sciences of the United States of America* **1991**, *88* (3), 732-6.

125. Moores, S. L.; Schaber, M. D.; Mosser, S. D.; Rands, E.; O'Hara, M. B.; Garsky, V. M.; Marshall, M. S.; Pompliano, D. L.; Gibbs, J. B., Sequence dependence of protein isoprenylation. *The Journal of biological chemistry* **1991**, *266* (22), 14603-10.
126. Hougland, J. L.; Lamphear, C. L.; Scott, S. A.; Gibbs, R. A.; Fierke, C. A., Context-Dependent Substrate Recognition by Protein Farnesyltransferase. *Biochemistry* **2009**, *48* (8), 1691-1701.
127. Gangopadhyay, S. A.; Losito, E. L.; Hougland, J. L., Targeted Reengineering of Protein Geranylgeranyltransferase Type I Selectivity Functionally Implicates Active-Site Residues in Protein-Substrate Recognition. *Biochemistry* **2014**, *53* (2), 434-446.
128. Flynn, S. C.; Lindgren, D. E.; Hougland, J. L., Quantitative determination of cellular farnesyltransferase activity: towards defining the minimum substrate reactivity for biologically relevant protein farnesylation. *Chembiochem : a European journal of chemical biology* **2014**, *15* (15), 2205-10.
129. Krzysiak, A. J.; Scott, S. A.; Hicks, K. A.; Fierke, C. A.; Gibbs, R. A., Evaluation of protein farnesyltransferase substrate specificity using synthetic peptide libraries. *Bioorganic & medicinal chemistry letters* **2007**, *17* (20), 5548-5551.
130. Boutin, J. A.; Marande, W.; Petit, L.; Loynel, A.; Desmet, C.; Canet, E.; Fauchere, J. L., Investigation of S-farnesyl transferase substrate specificity with combinatorial tetrapeptide libraries. *Cell Signal* **1999**, *11* (1), 59-69.
131. Pompliano, D. L.; Gomez, R. P.; Anthony, N. J., Intramolecular fluorescence enhancement: a continuous assay of Ras farnesyl:protein transferase. *J Am Chem Soc* **1992**, *114* (20), 7945-7946.

132. Wang, Y.-C.; Dozier, J. K.; Beese, L. S.; Distefano, M. D., Rapid analysis of protein farnesyltransferase substrate specificity using peptide libraries and isoprenoid diphosphate analogues. *ACS chemical biology* **2014**, *9* (8), 1726-1735.
133. Berger, B. M.; Kim, J. H.; Hildebrandt, E. R.; Davis, I. C.; Morgan, M. C.; Houglan, J. L.; Schmidt, W. K., Protein Isoprenylation in Yeast Targets COOH-Terminal Sequences Not Adhering to the CaaX Consensus. *Genetics* **2018**, *210* (4), 1301-1316.
134. Nagase, T.; Kawata, S.; Tamura, S.; Matsuda, Y.; Inui, Y.; Yamasaki, E.; Ishiguro, H.; Ito, T.; Miyagawa, J.; Mitsui, H.; Yamamoto, K.; Kinoshita, M.; Matsuzawa, Y., Manumycin and gliotoxin derivative KT7595 block Ras farnesylation and cell growth but do not disturb lamin farnesylation and localization in human tumour cells. *British journal of cancer* **1997**, *76* (8), 1001-10.
135. Zhang, Y.; Blanden, M. J.; Sudheer, C.; Gangopadhyay, S. A.; Rashidian, M.; Houglan, J. L.; Distefano, M. D., Simultaneous Site-Specific Dual Protein Labeling Using Protein Prenyltransferases. *Bioconjugate chemistry* **2015**, *26* (12), 2542-53.
136. Suazo, K. F.; Hurben, A. K.; Liu, K.; Xu, F.; Thao, P.; Sudheer, C.; Li, L.; Distefano, M. D., Metabolic Labeling of Prenylated Proteins Using Alkyne-Modified Isoprenoid Analogues. *Current protocols in chemical biology* **2018**, *10* (3), e46.
137. Thissen, J. A.; Gross, J. M.; Subramanian, K.; Meyer, T.; Casey, P. J., Prenylation-dependent association of Ki-Ras with microtubules. Evidence for a role in subcellular trafficking. *The Journal of biological chemistry* **1997**, *272* (48), 30362-70.
138. Kim, E.; Ambroziak, P.; Otto, J. C.; Taylor, B.; Ashby, M.; Shannon, K.; Casey, P. J.; Young, S. G., Disruption of the mouse Rce1 gene results in defective Ras processing and mislocalization of Ras within cells. *The Journal of biological chemistry* **1999**, *274* (13), 8383-90.

139. Roberts, P. J.; Mitin, N.; Keller, P. J.; Chenette, E. J.; Madigan, J. P.; Currin, R. O.; Cox, A. D.; Wilson, O.; Kirschmeier, P.; Der, C. J., Rho Family GTPase modification and dependence on CAAX motif-signaled posttranslational modification. *The Journal of biological chemistry* **2008**, *283* (37), 25150-63.
140. Manandhar, S. P.; Hildebrandt, E. R.; Jacobsen, W. H.; Santangelo, G. M.; Schmidt, W. K., Chemical inhibition of CaaX protease activity disrupts yeast Ras localization. *Yeast (Chichester, England)* **2010**, *27* (6), 327-43.
141. Winter-Vann, A. M.; Baron, R. A.; Wong, W.; dela Cruz, J.; York, J. D.; Gooden, D. M.; Bergo, M. O.; Young, S. G.; Toone, E. J.; Casey, P. J., A small-molecule inhibitor of isoprenylcysteine carboxyl methyltransferase with antitumor activity in cancer cells. *Proceedings of the National Academy of Sciences of the United States of America* **2005**, *102* (12), 4336-41.
142. Berzat, A. C.; Brady, D. C.; Fiordalisi, J. J.; Cox, A. D., Using Inhibitors of Prenylation to Block Localization and Transforming Activity. *Methods in enzymology* **2006**, *407*, 575-597.
143. Andres, D. A.; Crick, D. C.; Finlin, B. S.; Waechter, C. J., Rapid identification of cysteine-linked isoprenyl groups by metabolic labeling with [³H]farnesol and [³H]geranylgeraniol. *Methods in molecular biology (Clifton, N.J.)* **1999**, *116*, 107-23.
144. Hancock, J. F., Reticulocyte lysate assay for in vitro translation and posttranslational modification of Ras proteins. *Methods in enzymology* **1995**, *255*, 60-5.
145. Mumby, S. M.; Buss, J. E., Metabolic radiolabeling techniques for identification of prenylated and fatty acylated proteins. *Methods* **1990**, *1* (3), 216-220.
146. Troutman, J. M.; Roberts, M. J.; Andres, D. A.; Spielmann, H. P., Tools to analyze protein farnesylation in cells. *Bioconjugate chemistry* **2005**, *16* (5), 1209-17.

147. Chehade, K. A.; Andres, D. A.; Morimoto, H.; Spielmann, H. P., Design and synthesis of a transferable farnesyl pyrophosphate analogue to Ras by protein farnesyltransferase. *The Journal of organic chemistry* **2000**, *65* (10), 3027-33.
148. Nguyen, U. T.; Guo, Z.; Delon, C.; Wu, Y.; Deraeve, C.; Franzel, B.; Bon, R. S.; Blankenfeldt, W.; Goody, R. S.; Waldmann, H.; Wolters, D.; Alexandrov, K., Analysis of the eukaryotic prenolome by isoprenoid affinity tagging. *Nat Chem Biol* **2009**, *5* (4), 227-35.
149. Storck, E. M.; Morales-Sanfrutos, J.; Serwa, R. A.; Panyain, N.; Lanyon-Hogg, T.; Tolmachova, T.; Ventimiglia, L. N.; Martin-Serrano, J.; Seabra, M. C.; Wojciak-Stothard, B.; Tate, E. W., Dual chemical probes enable quantitative system-wide analysis of protein prenylation and prenylation dynamics. *Nature chemistry* **2019**, *11* (6), 552-561.
150. Kho, Y.; Kim, S. C.; Jiang, C.; Barma, D.; Kwon, S. W.; Cheng, J.; Jaunbergs, J.; Weinbaum, C.; Tamanoi, F.; Falck, J.; Zhao, Y., A tagging-via-substrate technology for detection and proteomics of farnesylated proteins. *Proceedings of the National Academy of Sciences of the United States of America* **2004**, *101* (34), 12479-12484.
151. Chan, L. N.; Hart, C.; Guo, L.; Nyberg, T.; Davies, B. S.; Fong, L. G.; Young, S. G.; Agnew, B. J.; Tamanoi, F., A novel approach to tag and identify geranylgeranylated proteins. *Electrophoresis* **2009**, *30* (20), 3598-606.
152. Berry, A. F.; Heal, W. P.; Tarafder, A. K.; Tolmachova, T.; Baron, R. A.; Seabra, M. C.; Tate, E. W., Rapid multilabel detection of geranylgeranylated proteins by using bioorthogonal ligation chemistry. *Chembiochem : a European journal of chemical biology* **2010**, *11* (6), 771-3.

153. DeGraw, A. J.; Palsuledesai, C.; Ochocki, J. D.; Dozier, J. K.; Lenevich, S.; Rashidian, M.; Distefano, M. D., Evaluation of alkyne-modified isoprenoids as chemical reporters of protein prenylation. *Chemical biology & drug design* **2010**, *76* (6), 460-71.
154. Reigard, S. A.; Zahn, T. J.; Haworth, K. B.; Hicks, K. A.; Fierke, C. A.; Gibbs, R. A., Interplay of isoprenoid and peptide substrate specificity in protein farnesyltransferase. *Biochemistry* **2005**, *44* (33), 11214-11223.
155. Krzysiak, A. J.; Rawat, D. S.; Scott, S. A.; Pais, J. E.; Handley, M.; Harrison, M. L.; Fierke, C. A.; Gibbs, R. A., Combinatorial modulation of protein prenylation. *ACS chemical biology* **2007**, *2* (6), 385-389.
156. Troutman, J. M.; Subramanian, T.; Andres, D. A.; Spielmann, H. P., Selective modification of CaaX peptides with ortho-substituted anilinogeranyl lipids by protein farnesyl transferase: competitive substrates and potent inhibitors from a library of farnesyl diphosphate analogues. *Biochemistry* **2007**, *46* (40), 11310-11321.
157. Takai, Y.; Sasaki, T.; Matozaki, T., Small GTP-binding proteins. *Physiological reviews* **2001**, *81* (1), 153-208.
158. Bar-Sagi, D.; Hall, A., Ras and Rho GTPases: a family reunion. *Cell* **2000**, *103* (2), 227-38.
159. Downward, J., Ras signalling and apoptosis. *Current opinion in genetics & development* **1998**, *8* (1), 49-54.
160. Downward, J., Targeting RAS signalling pathways in cancer therapy. *Nature reviews. Cancer* **2003**, *3* (1), 11-22.
161. Shields, J. M.; Pruitt, K.; McFall, A.; Shaub, A.; Der, C. J., Understanding Ras: 'it ain't over 'til it's over'. *Trends Cell Biol* **2000**, *10* (4), 147-54.

162. Malumbres, M.; Barbacid, M., RAS oncogenes: the first 30 years. *Nature reviews. Cancer* **2003**, *3* (6), 459-65.
163. Bos, J. L., ras oncogenes in human cancer: a review. *Cancer Res* **1989**, *49* (17), 4682-9.
164. Bos, J. L., p21ras: an oncoprotein functioning in growth factor-induced signal transduction. *Eur J Cancer* **1995**, *31A* (7-8), 1051-4.
165. Campbell, P. M.; Der, C. J., Oncogenic Ras and its role in tumor cell invasion and metastasis. *Semin Cancer Biol* **2004**, *14* (2), 105-14.
166. Hahn, W. C.; Counter, C. M.; Lundberg, A. S.; Beijersbergen, R. L.; Brooks, M. W.; Weinberg, R. A., Creation of human tumour cells with defined genetic elements. *Nature* **1999**, *400* (6743), 464-8.
167. Scheffzek, K.; Ahmadian, M. R.; Kabsch, W.; Wiesmuller, L.; Lautwein, A.; Schmitz, F.; Wittinghofer, A., The Ras-RasGAP complex: structural basis for GTPase activation and its loss in oncogenic Ras mutants. *Science* **1997**, *277* (5324), 333-8.
168. McCormick, F., Ras-related proteins in signal transduction and growth control. *Molecular reproduction and development* **1995**, *42* (4), 500-6.
169. Hancock, J. F.; Magee, A. I.; Childs, J. E.; Marshall, C. J., All ras proteins are polyisoprenylated but only some are palmitoylated. *Cell* **1989**, *57* (7), 1167-77.
170. Cox, A. D.; Der, C. J., The ras/cholesterol connection: implications for ras oncogenicity. *Crit Rev Oncog* **1992**, *3* (4), 365-400.
171. Di, J.; Huang, H.; Qu, D.; Tang, J.; Cao, W.; Lu, Z.; Cheng, Q.; Yang, J.; Bai, J.; Zhang, Y.; Zheng, J., Rap2B promotes proliferation, migration, and invasion of human breast cancer through calcium-related ERK1/2 signaling pathway. *Scientific reports* **2015**, *5*, 12363.

172. Itoh, M.; Nelson, C. M.; Myers, C. A.; Bissell, M. J., Rap1 integrates tissue polarity, lumen formation, and tumorigenic potential in human breast epithelial cells. *Cancer Res* **2007**, *67* (10), 4759-66.
173. Bailey, C. L.; Kelly, P.; Casey, P. J., Activation of Rap1 promotes prostate cancer metastasis. *Cancer Res* **2009**, *69* (12), 4962-8.
174. Yajnik, V.; Paulding, C.; Sordella, R.; McClatchey, A. I.; Saito, M.; Wahrer, D. C.; Reynolds, P.; Bell, D. W.; Lake, R.; van den Heuvel, S.; Settleman, J.; Haber, D. A., DOCK4, a GTPase activator, is disrupted during tumorigenesis. *Cell* **2003**, *112* (5), 673-84.
175. Hori, Y.; Kikuchi, A.; Isomura, M.; Katayama, M.; Miura, Y.; Fujioka, H.; Kaibuchi, K.; Takai, Y., Post-translational modifications of the C-terminal region of the rho protein are important for its interaction with membranes and the stimulatory and inhibitory GDP/GTP exchange proteins. *Oncogene* **1991**, *6* (4), 515-22.
176. Adamson, P.; Marshall, C. J.; Hall, A.; Tilbrook, P. A., Post-translational modifications of p21rho proteins. *The Journal of biological chemistry* **1992**, *267* (28), 20033-8.
177. Allal, C.; Favre, G.; Couderc, B.; Salicio, S.; Sixou, S.; Hamilton, A. D.; Sebti, S. M.; Lajoie-Mazenc, I.; Pradines, A., RhoA prenylation is required for promotion of cell growth and transformation and cytoskeleton organization but not for induction of serum response element transcription. *The Journal of biological chemistry* **2000**, *275* (40), 31001-8.
178. Ridley, A. J.; Hall, A., The small GTP-binding protein rho regulates the assembly of focal adhesions and actin stress fibers in response to growth factors. *Cell* **1992**, *70* (3), 389-99.
179. Evers, E. E.; Zondag, G. C.; Malliri, A.; Price, L. S.; ten Klooster, J. P.; van der Kammen, R. A.; Collard, J. G., Rho family proteins in cell adhesion and cell migration. *Eur J Cancer* **2000**, *36* (10), 1269-74.

180. Ridley, A. J.; Paterson, H. F.; Johnston, C. L.; Diekmann, D.; Hall, A., The small GTP-binding protein rac regulates growth factor-induced membrane ruffling. *Cell* **1992**, *70* (3), 401-10.
181. Schmitz, A. A.; Govek, E. E.; Bottner, B.; Van Aelst, L., Rho GTPases: signaling, migration, and invasion. *Exp Cell Res* **2000**, *261* (1), 1-12.
182. Jaffe, A. B.; Hall, A., Rho GTPases in transformation and metastasis. *Adv Cancer Res* **2002**, *84*, 57-80.
183. Kusama, T.; Mukai, M.; Iwasaki, T.; Tatsuta, M.; Matsumoto, Y.; Akedo, H.; Nakamura, H., Inhibition of epidermal growth factor-induced RhoA translocation and invasion of human pancreatic cancer cells by 3-hydroxy-3-methylglutaryl-coenzyme a reductase inhibitors. *Cancer Res* **2001**, *61* (12), 4885-91.
184. Ochocki, J. D.; Distefano, M. D., Prenyltransferase inhibitors: treating human ailments from cancer to parasitic infections. *Medchemcomm* **2013**, *4* (3), 476-492.
185. Gelb, M. H.; Brunsveld, L.; Hrycyna, C. A.; Michaelis, S.; Tamanoi, F.; Van Voorhis, W. C.; Waldmann, H., Therapeutic intervention based on protein prenylation and associated modifications. *Nature chemical biology* **2006**, *2* (10), 518-528.
186. Sousa, S. F.; Fernandes, P. A.; Ramos, M. J., Farnesyltransferase inhibitors: a detailed chemical view on an elusive biological problem. *Current medicinal chemistry* **2008**, *15* (15), 1478-1492.
187. Berndt, N.; Hamilton, A. D.; Sebt, S. M., Targeting protein prenylation for cancer therapy. *Nature Reviews Cancer* **2011**, *11* (11), 775-791.
188. Zujewski, J.; Horak, I.; Bol, C.; Woestenborghs, R.; Bowden, C.; End, D.; Piotrovsky, V.; Chiao, J.; Belly, R.; Todd, A., Phase I and pharmacokinetic study of farnesyl

protein transferase inhibitor R115777 in advanced cancer. *Journal of Clinical Oncology* **2000**, *18* (4), 927-927.

189. Sun, J.; Qian, Y.; Hamilton, A. D.; Sebti, S. M., Both farnesyltransferase and geranylgeranyltransferase I inhibitors are required for inhibition of oncogenic K-Ras prenylation but each alone is sufficient to suppress human tumor growth in nude mouse xenografts. *Oncogene* **1998**, *16* (11), 1467-1473.

190. Morgan, M.; Ganser, A.; Reuter, C., Therapeutic efficacy of prenylation inhibitors in the treatment of myeloid leukemia. *Leukemia* **2003**, *17* (8), 1482-1498.

191. Sepp-Lorenzino, L.; Ma, Z.; Rands, E.; Kohl, N. E.; Gibbs, J. B.; Oliff, A.; Rosen, N., A peptidomimetic inhibitor of farnesyl: protein transferase blocks the anchorage-dependent and-independent growth of human tumor cell lines. *Cancer Research* **1995**, *55* (22), 5302-5309.

192. Kurzrock, R.; Kantarjian, H. M.; Cortes, J. E.; Singhania, N.; Thomas, D. A.; Wilson, E. F.; Wright, J. J.; Freireich, E. J.; Talpaz, M.; Sebti, S. d. M., Farnesyltransferase inhibitor R115777 in myelodysplastic syndrome: clinical and biologic activities in the phase 1 setting. *Blood* **2003**, *102* (13), 4527-4534.

193. Whyte, D. B.; Kirschmeier, P.; Hockenberry, T. N.; Nunez-Oliva, I.; James, L.; Catino, J. J.; Bishop, W. R.; Pai, J.-K., K-and N-Ras are geranylgeranylated in cells treated with farnesyl protein transferase inhibitors. *Journal of Biological Chemistry* **1997**, *272* (22), 14459-14464.

194. DeBusk, F. L., The Hutchinson-Gilford progeria syndrome. Report of 4 cases and review of the literature. *J Pediatr* **1972**, *80* (4), 697-724.

195. Sinensky, M.; Fantle, K.; Trujillo, M.; McLain, T.; Kupfer, A.; Dalton, M., The processing pathway of prelamin A. *J Cell Sci* **1994**, *107* (Pt 1), 61-7.

196. Pendas, A. M.; Zhou, Z.; Cadinanos, J.; Freije, J. M.; Wang, J.; Hultenby, K.; Astudillo, A.; Wernerson, A.; Rodriguez, F.; Tryggvason, K.; Lopez-Otin, C., Defective prelamin A processing and muscular and adipocyte alterations in Zmpste24 metalloproteinase-deficient mice. *Nat Genet* **2002**, *31* (1), 94-9.
197. Bergo, M. O.; Gavino, B.; Ross, J.; Schmidt, W. K.; Hong, C.; Kendall, L. V.; Mohr, A.; Meta, M.; Genant, H.; Jiang, Y.; Wisner, E. R.; Van Bruggen, N.; Carano, R. A.; Michaelis, S.; Griffey, S. M.; Young, S. G., Zmpste24 deficiency in mice causes spontaneous bone fractures, muscle weakness, and a prelamin A processing defect. *Proceedings of the National Academy of Sciences of the United States of America* **2002**, *99* (20), 13049-54.
198. Eriksson, M.; Brown, W. T.; Gordon, L. B.; Glynn, M. W.; Singer, J.; Scott, L.; Erdos, M. R.; Robbins, C. M.; Moses, T. Y.; Berglund, P.; Dutra, A.; Pak, E.; Durkin, S.; Csoka, A. B.; Boehnke, M.; Glover, T. W.; Collins, F. S., Recurrent de novo point mutations in lamin A cause Hutchinson-Gilford progeria syndrome. *Nature* **2003**, *423* (6937), 293-8.
199. Moulson, C. L.; Fong, L. G.; Gardner, J. M.; Farber, E. A.; Go, G.; Passariello, A.; Grange, D. K.; Young, S. G.; Miner, J. H., Increased progerin expression associated with unusual LMNA mutations causes severe progeroid syndromes. *Hum Mutat* **2007**, *28* (9), 882-9.
200. Mehta, I. S.; Eskiw, C. H.; Arican, H. D.; Kill, I. R.; Bridger, J. M., Farnesyltransferase inhibitor treatment restores chromosome territory positions and active chromosome dynamics in Hutchinson-Gilford progeria syndrome cells. *Genome biology* **2011**, *12* (8), 1-14.
201. Wang, Y.; Östlund, C.; Worman, H., Blocking protein farnesylation improves nuclear shape abnormalities in keratinocytes of mice expressing the prelamin A variant in Hutchinson-Gilford progeria syndrome. *Nucleus* **2010**, *1* (5), 432-439.

202. Yang, S. H.; Chang, S. Y.; Ren, S.; Wang, Y.; Andres, D. A.; Spielmann, H. P.; Fong, L. G.; Young, S. G., Absence of progeria-like disease phenotypes in knock-in mice expressing a non-farnesylated version of progerin. *Human molecular genetics* **2011**, *20* (3), 436-444.
203. Yang, S. H.; Chang, S. Y.; Andres, D. A.; Spielmann, H. P.; Young, S. G.; Fong, L. G., Assessing the efficacy of protein farnesyltransferase inhibitors in mouse models of progeria. *Journal of lipid research* **2010**, *51* (2), 400-405.
204. Capell, B. C.; Erdos, M. R.; Madigan, J. P.; Fiordalisi, J. J.; Varga, R.; Conneely, K. N.; Gordon, L. B.; Der, C. J.; Cox, A. D.; Collins, F. S., Inhibiting farnesylation of progerin prevents the characteristic nuclear blebbing of Hutchinson-Gilford progeria syndrome. *Proceedings of the National Academy of Sciences* **2005**, *102* (36), 12879-12884.
205. Young, S. G.; Yang, S. H.; Davies, B. S.; Jung, H.-J.; Fong, L. G., Targeting protein prenylation in progeria. *Science translational medicine* **2013**, *5* (171), 171ps3-171ps3.
206. Gordon, L. B.; Shappell, H.; Massaro, J.; D'Agostino, R. B.; Brazier, J.; Campbell, S. E.; Kleinman, M. E.; Kieran, M. W., Association of lonafarnib treatment vs no treatment with mortality rate in patients with Hutchinson-Gilford progeria syndrome. *Jama* **2018**, *319* (16), 1687-1695.
207. Gordon, L. B.; Kleinman, M. E.; Massaro, J.; D'Agostino Sr, R. B.; Shappell, H.; Gerhard-Herman, M.; Smoot, L. B.; Gordon, C. M.; Cleveland, R. H.; Nazarian, A., Clinical trial of the protein farnesylation inhibitors lonafarnib, pravastatin, and zoledronic acid in children with Hutchinson-Gilford progeria syndrome. *Circulation* **2016**, *134* (2), 114-125.
208. Ullrich, N. J.; Kieran, M. W.; Miller, D. T.; Gordon, L. B.; Cho, Y.-J.; Silvera, V. M.; Giobbie-Hurder, A.; Neuberg, D.; Kleinman, M. E., Neurologic features of Hutchinson-Gilford progeria syndrome after lonafarnib treatment. *Neurology* **2013**, *81* (5), 427-430.

209. Compagnucci, C.; Bertini, E., The potential of iPSCs for the treatment of premature aging disorders. *International journal of molecular sciences* **2017**, *18* (11), 2350.
210. Price, C. T.; Jones, S. C.; Amundson, K. E.; Kwaik, Y. A., Host-mediated post-translational prenylation of novel dot/icm-translocated effectors of legionella pneumophila. *Front Microbiol* **2010**, *1*, 131.
211. Al-Quadan, T.; Price, C. T.; London, N.; Schueler-Furman, O.; AbuKwaik, Y., Anchoring of bacterial effectors to host membranes through host-mediated lipidation by prenylation: a common paradigm. *Trends Microbiol* **2011**, *19* (12), 573-9.
212. Price, C. T.; Al-Quadan, T.; Santic, M.; Jones, S. C.; Abu Kwaik, Y., Exploitation of conserved eukaryotic host cell farnesylation machinery by an F-box effector of Legionella pneumophila. *J Exp Med* **2010**, *207* (8), 1713-26.
213. Al-Khodor, S.; Price, C. T.; Habyarimana, F.; Kalia, A.; Abu Kwaik, Y., A Dot/Icm-translocated ankyrin protein of Legionella pneumophila is required for intracellular proliferation within human macrophages and protozoa. *Mol Microbiol* **2008**, *70* (4), 908-23.
214. Price, C. T.; Al-Khodor, S.; Al-Quadan, T.; Santic, M.; Habyarimana, F.; Kalia, A.; Kwaik, Y. A., Molecular mimicry by an F-box effector of Legionella pneumophila hijacks a conserved polyubiquitination machinery within macrophages and protozoa. *PLoS Pathog* **2009**, *5* (12), e1000704.
215. Lomma, M.; Dervins-Ravault, D.; Rolando, M.; Nora, T.; Newton, H. J.; Sansom, F. M.; Sahr, T.; Gomez-Valero, L.; Jules, M.; Hartland, E. L.; Buchrieser, C., The Legionella pneumophila F-box protein Lpp2082 (AnkB) modulates ubiquitination of the host protein parvin B and promotes intracellular replication. *Cell Microbiol* **2010**, *12* (9), 1272-91.

216. Smalera, I.; Williamson, J. M.; Baginsky, W.; Leiting, B.; Mazur, P., Expression and characterization of protein geranylgeranyltransferase type I from the pathogenic yeast *Candida albicans* and identification of yeast selective enzyme inhibitors. *Biochim Biophys Acta* **2000**, *1480* (1-2), 132-44.
217. Kelly, R.; Card, D.; Register, E.; Mazur, P.; Kelly, T.; Tanaka, K. I.; Onishi, J.; Williamson, J. M.; Fan, H.; Satoh, T.; Kurtz, M., Geranylgeranyltransferase I of *Candida albicans*: null mutants or enzyme inhibitors produce unexpected phenotypes. *J Bacteriol* **2000**, *182* (3), 704-13.
218. Song, J. L.; White, T. C., RAM2: an essential gene in the prenylation pathway of *Candida albicans*. *Microbiology* **2003**, *149* (Pt 1), 249-59.
219. Suazo, K. F.; Schaber, C.; Palsuledesai, C. C.; Odom John, A. R.; Distefano, M. D., Global proteomic analysis of prenylated proteins in *Plasmodium falciparum* using an alkyne-modified isoprenoid analogue. *Scientific reports* **2016**, *6*, 38615.
220. Chakrabarti, D.; Azam, T.; DelVecchio, C.; Qiu, L.; Park, Y. I.; Allen, C. M., Protein prenyl transferase activities of *Plasmodium falciparum*. *Molecular and biochemical parasitology* **1998**, *94* (2), 175-84.
221. Chakrabarti, D.; Da Silva, T.; Barger, J.; Paquette, S.; Patel, H.; Patterson, S.; Allen, C. M., Protein farnesyltransferase and protein prenylation in *Plasmodium falciparum*. *The Journal of biological chemistry* **2002**, *277* (44), 42066-73.
222. Howe, R.; Kelly, M.; Jimah, J.; Hodge, D.; Odom, A. R., Isoprenoid biosynthesis inhibition disrupts Rab5 localization and food vacuolar integrity in *Plasmodium falciparum*. *Eukaryotic cell* **2013**, *12* (2), 215-23.

223. Wiesner, J.; Kettler, K.; Sakowski, J.; Ortmann, R.; Katzin, A. M.; Kimura, E. A.; Silber, K.; Klebe, G.; Jomaa, H.; Schlitzer, M., Farnesyltransferase inhibitors inhibit the growth of malaria parasites in vitro and in vivo. *Angew Chem Int Ed Engl* **2004**, *43* (2), 251-4.
224. Glenn, M. P.; Chang, S. Y.; Hucke, O.; Verlinde, C. L.; Rivas, K.; Horney, C.; Yokoyama, K.; Buckner, F. S.; Pendyala, P. R.; Chakrabarti, D.; Gelb, M.; Van Voorhis, W. C.; Sebti, S. M.; Hamilton, A. D., Structurally simple farnesyltransferase inhibitors arrest the growth of malaria parasites. *Angew Chem Int Ed Engl* **2005**, *44* (31), 4903-6.
225. Glenn, M. P.; Chang, S. Y.; Horney, C.; Rivas, K.; Yokoyama, K.; Pusateri, E. E.; Fletcher, S.; Cummings, C. G.; Buckner, F. S.; Pendyala, P. R.; Chakrabarti, D.; Sebti, S. M.; Gelb, M.; Van Voorhis, W. C.; Hamilton, A. D., Structurally simple, potent, Plasmodium selective farnesyltransferase inhibitors that arrest the growth of malaria parasites. *Journal of medicinal chemistry* **2006**, *49* (19), 5710-27.
226. Ashley, E. A.; Dhorda, M.; Fairhurst, R. M.; Amaratunga, C.; Lim, P.; Suon, S.; Sreng, S.; Anderson, J. M.; Mao, S.; Sam, B.; Sopha, C.; Chuor, C. M.; Nguon, C.; Sovannaroeth, S.; Pukrittayakamee, S.; Jittamala, P.; Chotivanich, K.; Chutasmit, K.; Suchatsoonthorn, C.; Runcharoen, R.; Hien, T. T.; Thuy-Nhien, N. T.; Thanh, N. V.; Phu, N. H.; Htut, Y.; Han, K. T.; Aye, K. H.; Mokuolu, O. A.; Olaosebikan, R. R.; Folaranmi, O. O.; Mayxay, M.; Khanthavong, M.; Hongvanthong, B.; Newton, P. N.; Onyamboko, M. A.; Fanello, C. I.; Tshefu, A. K.; Mishra, N.; Valecha, N.; Phyto, A. P.; Nosten, F.; Yi, P.; Tripura, R.; Borrmann, S.; Bashraheil, M.; Peshu, J.; Faiz, M. A.; Ghose, A.; Hossain, M. A.; Samad, R.; Rahman, M. R.; Hasan, M. M.; Islam, A.; Miotto, O.; Amato, R.; MacInnis, B.; Stalker, J.; Kwiatkowski, D. P.; Bozdech, Z.; Jeeyapant, A.; Cheah, P. Y.; Sakulthaew, T.; Chalk, J.; Intharabut, B.; Silamut, K.; Lee, S. J.; Vihokhern, B.; Kunasol, C.; Imwong, M.;

Tarning, J.; Taylor, W. J.; Yeung, S.; Woodrow, C. J.; Flegg, J. A.; Das, D.; Smith, J.; Venkatesan, M.; Plowe, C. V.; Stepniewska, K.; Guerin, P. J.; Dondorp, A. M.; Day, N. P.; White, N. J.; Tracking Resistance to Artemisinin, C., Spread of artemisinin resistance in *Plasmodium falciparum* malaria. *N Engl J Med* **2014**, *371* (5), 411-23.

227. von Seidlein, L.; Dondorp, A., Fighting fire with fire: mass antimalarial drug administrations in an era of antimalarial resistance. *Expert Rev Anti Infect Ther* **2015**, *13* (6), 715-30.

Chapter 2: Investigation of shortened “Cxx” target sequence recognition by FTase and GGTase-I

Portions of this chapter including figures and experimental results have been published and reprinted with permission from the publisher, reference 44, Ashok, S.; Hildebrandt, E. R.; Ruiz, C. S.; Hardgrove, D. S.; Coreno, D. W.; Schmidt, W. K.; Hougland, J. L., Protein farnesyltransferase catalyzes unanticipated farnesylation and geranylgeranylation of shortened target sequences. *Biochemistry* **2020**, *59* (11), 1149-1162. Copyright (2020) American Chemical Society.

Co-author contributions include: ERH, CSR, DSH, and WKS performed the yeast screens and yeast-based biological assays. DWC assisted with FTase expression and purification and steady-state analysis.

2.1 Introduction

Protein lipidation is a posttranslational modification (PTM) that plays an essential role in the proper biological function of many proteins including protein trafficking and protein-protein interactions.¹⁻⁹ Prenylation is one such modification wherein proteins are modified by the covalent attachment of an isoprenoid group to a cysteine residue near the C-terminus of the substrate protein. FTase catalyzes cysteine alkylation with a 15-carbon (C15) farnesyl group from farnesyl diphosphate (FPP) (Scheme 2.1), whereas GGTase-I performs this reaction with a 20-carbon (C20) geranylgeranyl group.^{2-6,9} Prenylation augments the hydrophobicity of modified proteins, which can influence membrane association and/or protein-protein interactions that are essential to the biological function of many prenylated proteins.^{7,8,10-12}

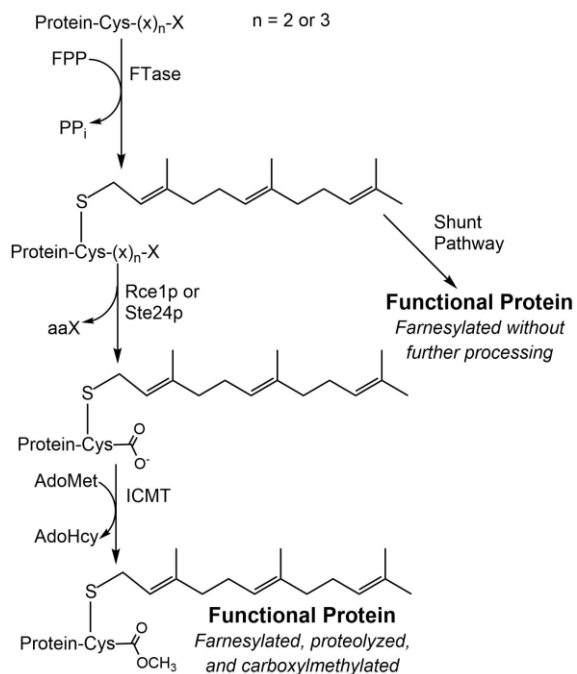
Following prenylation of the cysteine residue, many prenylated proteins undergo two additional processing steps.^{13,14} Proteolytic removal of the amino acids C-terminal to the prenylcysteine is performed by the Rce1p or Ste24p proteases, and the C-terminal prenylcysteine is subsequently methylated by isoprenylcysteine carboxyl methyltransferase (ICMT). These additional post-prenylation modifications are vital for the proper function of many prenylated proteins.¹⁴⁻¹⁷ These additional modifications are not, however, necessarily coupled to prenylation as has been commonly accepted. For example, farnesylation of yeast Ydj1p HSP40 occurs without proteolysis or methylation.^{18,19} While farnesylation is required for optimal Ydj1p function, proteolysis and carboxymethylation are detrimental to Ydj1p's role. Continuing studies indicate that the protein prenylation pathway is more complex than originally proposed.

The 'CaaX' motif has served as the defining paradigm for substrate selectivity for FTase and GGTase-I for three decades, beginning with the discoveries of prenylation in the context of yeast mating factors, Ras GTPases, and nuclear lamins.²⁰⁻³⁰ This sequence consists of an

invariant cysteine residue that is alkylated on its side-chain thiol, two amino acids commonly described to be aliphatic, and an X residue that can vary and influences peptide reactivity with FTase versus GGTase-I.^{25, 26, 31} The expanding number of known prenylated proteins stimulated biochemical, cell-based, and structural examinations of substrate determinants for selectivity by FTase and/or GGTase-I, which defined rules governing selectivity at each amino acid position within the CaaX motif.^{4, 26, 29, 32-37} Structural studies provided a needed framework for understanding FTase and GGTase-I substrate selectivity by revealing specific molecular interactions involved in recognizing both the CaaX substrate sequence and the FPP and GGPP prenyl donor cosubstrates.^{25, 26, 38, 39} Studies guided by FTase and GGTase-I structural models have allowed for efficient reengineering of both peptide and prenyl donor selectivity, reinforcing the importance of the interactions observed in these models for enzyme-substrate recognition.^{36, 40, 41} More recently, bioinformatics and computational/docking approaches have facilitated prediction of CaaX motifs as likely FTase and/or GGTase-I substrates.^{27, 28, 30, 42}

Expanding upon the well-established ability of protein prenyltransferases to recognize and modify CaaX sequences, recent work supports the ability of FTase to modify cysteine residues in other sequence contexts. Both yeast and mammalian FTase can accept longer five amino acid 'C(x)₃X' sequences as substrates.⁶ We now show that both yeast and mammalian FTase can prenylate shorter three-amino acid Cxx sequences. We demonstrate that yeast FTase can modify Cxx sequences *in vivo* in the context of Ydj1p Hsp40 while mammalian FTase can modify Cxx reporter peptides *in vitro*. Surprisingly, we found that mammalian FTase can accept both FPP and GGPP as the prenyl donor cosubstrate for modification of certain Cxx substrate sequences in the first reported example of wild type FTase catalyzing peptide geranylgeranylation with comparable efficiency to farnesylation.⁴³ This new class of FTase

substrates and the potential for their promiscuous modification with farnesyl and geranylgeranyl groups increases the complexity of protein prenylation, expanding the potential range of prenylation within proteomes and the roles played by these prenylated proteins in biological systems.



Scheme 2.1. The protein farnesylation and processing pathway. FTase catalyzes the covalent attachment of a 15-carbon farnesyl group to proteins terminating in CaaX (n=2) or C(x)₃X (n=3) sequences, with subsequent proteolytic and carboxymethylation steps required for many but not all farnesylated proteins. Modification of CaaX (n=2) sequences is well-documented in various organisms; modification of C(x)₃X sequences (n=3) has not yet been verified for a naturally occurring protein but has been demonstrated using an *in vivo* reporter. This figure has been reused with permission from reference 44 (Appendix II).

2.2 Genetic screening in yeast reveals prenylation of Cxx sequences can occur *in vivo*

Note: This data was collected and analyzed by our collaborator Walter K. Schmidt (University of Georgia).

Our research group recently reported that pentapeptide C_(x)₃X sequences can support prenylation of yeast genetic reporters based on the **a**-factor mating pheromone and Ydj1p Hsp40 chaperone.⁶ Using these same reporters and complementary selection screens, our studies show that certain tripeptide Cxx sequences are also recognized and modified by yeast FTase *in vivo*.

The biological activity of the yeast **a**-factor mating pheromone normally depends on farnesylation, proteolysis, and carboxymethylation of the CVIA CaaX motif associated with its precursor. To explore whether shorter sequences could be similarly modified, a genetic selection scheme using a plasmid library of **a**-factor-Cxx variants was examined. Using *MATa mfa1 mfa2* yeast that cannot make **a**-factor on their own, the plasmid-encoding **a**-factor mutants were introduced, and the **a**-factor halo assay was performed. In this assay, *MATa* cells are either spotted or replica printed onto a thin lawn of *MATα sst2-1* yeast that are super sensitive to **a**-factor mating pheromone. The release of **a**-factor by *MATa* cells results in a zone of *MATα* cell growth inhibition (i.e. halo) surrounding the *MATa* cells. We pursued a yeast mating approach (i.e. positive selection) over the halo assay approach (i.e. screening) for easier identification of **a**-factor producing colonies.

Out of ~8,100 colonies screened; 45 diploid colonies were identified. The corresponding haploid parents were recovered from the replica master and scored for their **a**-factor production phenotype using the halo assay. A subset of 19 colonies having the strongest halo production was identified and associated plasmids were recovered and sequenced.⁴⁴ A reduced set of 10 plasmids

represented the unique Cxx sequences after eliminating duplicate sequences (i.e. CII, CTI, and CVI). We estimate that ~99% of Cxx sequence space was evaluated during the selection strategy (see the Materials and Methods for description of coverage estimate). The plasmids were retransformed into *MATa mfa1 mfa2* yeast and retested for the ability to confer **a**-factor production using the halo assay (Figure 2.1a). The halos formed with Cxx sequences were similar in size to each other and all smaller than that associated with wild type **a**-factor (CVIA), implying overall less **a**-factor production was associated with this wide variety of Cxx sequences. Of note, the **a**-factor halo assay is an extremely sensitive and qualitative method for measuring **a**-factor production that quickly saturates at low levels of pheromone.¹⁸

A quantitative mating assay of **a**-factor production revealed that Cxx sequences were far less effective at promoting mating than wild type **a**-factor (Figure 2.1b); similar results were previously observed with longer C(x)₃X sequences.⁶ Nonetheless, mating for Cxx sequences was reproducible and higher than that observed for unprenylated **a**-factor variants (i.e. **a**-factor-C, -CV, -AVI, and -SVI) for which no mating was ever observed. Following mating analysis, we assessed whether increased expression of genes associated with **a**-factor production could improve mating of **a**-factor-CVI (Figure 2.1c). While over-expressed *RAMI* (FTase β subunit) and *STE24* (protease) had comparable levels of mating to the vector control, over-expressed *RCE1* (CaaX protease) improved mating, suggesting that proteolysis of CVI by Rce1p may be limiting for production of **a**-factor in this instance.

By comparison to the **a**-factor reporter, the Hsp40 Ydj1p only requires farnesylation of its CASQ CaaX motif to support its role in yeast thermotolerance. It does not undergo CaaX proteolysis and carboxymethylation, which are detrimental to its function.^{6, 18, 19, 45} Ydj1p thus served as a more direct reporter for farnesylation of Cxx sequences. A plasmid library of Ydj1p

Cxx mutants was transformed into *ydj1Δ* yeast in order to identify thermotolerant colonies .⁶ Out of ~1,200 colonies screened, 13 thermotolerant colonies were identified. The associated plasmids were recovered and sequenced. A reduced set of 10 plasmids represented the unique sequences after eliminating duplicate sequences (CAL, CEV, and CLL). We estimate that ~82% of Cxx sequences were evaluated during the screen (see the Materials and Methods for description of coverage estimate). The ability of these Cxx sequences to support prenylation was confirmed using a thermotolerance assay (Figure 2.2a). Moreover, several Cxx sequences identified in the **a**-factor halo assays were transferred onto Ydj1p and evaluated (i.e. CTI, CII, CFV and CVI). The growth observed for all mutants was qualitatively better than that observed for a non-prenylated Ydj1p mutants that fail to grow at 40 °C (i.e. AVI and SVI). Most test sequences exhibited a thermotolerance phenotype like that observed for wildtype Ydj1p (CASQ) that is prenylated but uncleaved, while a few displayed an intermediate phenotype similar to that observed for a prenylated and cleaved Ydj1p mutant (CTLM).

In addition to the thermotolerance phenotypic manifestations, prenylation of Ydj1p affects its mobility in SDS-PAGE counterintuitively such that the farnesylated protein has increased mobility (i.e. smaller apparent kDa) relative to unprenylated. The latter can be produced by expression in a FTase-deficient yeast strain (i.e. *ram1*). All the Ydj1p Cxx hits exhibited prenylation, albeit partially in most cases (Figure 2.2b). Importantly, Ydj1p-AVI and -SVI variants were neither thermotolerant nor displayed a gel-shift, implying lack of prenylation and consistent with results derived using **a**-factor-AVI and -SVI. To confirm that observed gel-shift phenotypes were not due to plasmid-based overexpression of the Ydj1p reporter, each Cxx hit was subsequently integrated into the genome as the sole copy of Ydj1p and gel-shift reassessed; thermotolerance was also assessed. More complete prenylation of Ydj1p-Cxx

variants was quantifiably observed, with several displaying complete modification (Figures 2.2b). The Cxx sequences recovered with the **a**-factor reporter (i.e. CTI, CII, CFV and CVI) were generally prenylated to a higher extent than those directly recovered with the Ydj1p reporter as assessed by gel-shift, while two displayed weaker thermotolerance (i.e. CFV and CVI). These results are consistent with the hypothesis that **a**-factor-derived sequences are likely more extensively modified after initial prenylation (i.e. cleaved and carboxylmethylated), which is known to diminish Ydj1p-based thermotolerance.^{18, 19} Overall, complete or near complete prenylation of Cxx sequences in the context of Ydj1p *supports* the possibility that such sequences may be modified when in a natural protein context.

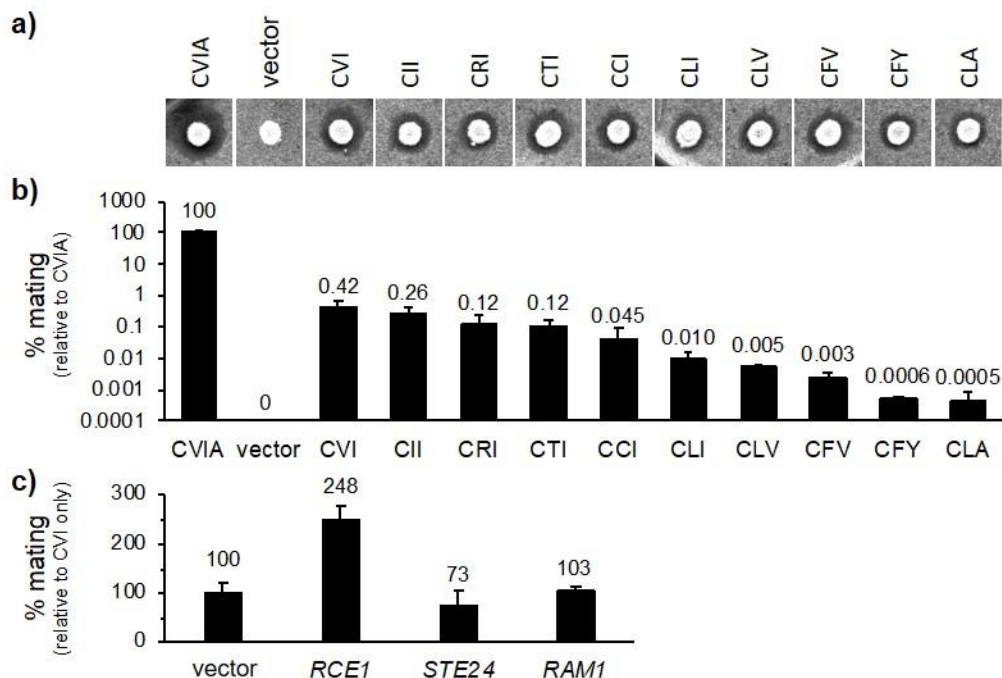


Figure 2.1. Phenotypes of *a*-factor Cxx variants. a) The spot halo assay is a highly sensitive and qualitative measure of *a*-factor production. SM2331 (*MATa mfa1 mfa2*) was transformed with plasmids encoding *a*-factor mutants or vector (*CEN LEU2*), resultant strains cultured as spots on YPD for 48 hours at 30 °C, and spots replica transferred onto a thin lawn of RC757 (*MATa sst2-1*). A zone of growth inhibition (i.e. halo) indicates pheromone production. b) The mating assay is used for relative measures of *a*-factor production. The *MATa* strains described in panel a) were tested in combination with IH1793 (*MAT α lys1*). All values are relative to diploid production (i.e. mating events) observed with *MATa* yeast expressing wildtype *a*-factor (CVIA; set to 100% mating efficiency). Mating values were determined from two experiments in which each sample was minimally evaluated in duplicate. c) The mating efficiencies for *a*-factor-CVI were determined as described in panel b) under conditions where the indicated CaaX modifying enzyme was overexpressed via a 2μ plasmid. All values are relative to diploid production (i.e. mating events) observed with an empty vector 2μ plasmid. Values represent the average of three biological replicates. *RCE1* encodes the Ras Converting Enzyme 1 (Rce1p) CaaX protease. *STE24* encodes Sterile Protein 24 (Ste24p). Both Rce1p and Ste24p can cleave the *a*-factor CaaX motif. *RAM1* encodes the FTase β subunit, whose overexpression improves FTase activity in some yeast strains.⁴⁶ This figure has been reused with permission from reference 44 (Appendix II). This data was collected and analyzed by our collaborator Walter K. Schmidt (University of Georgia).

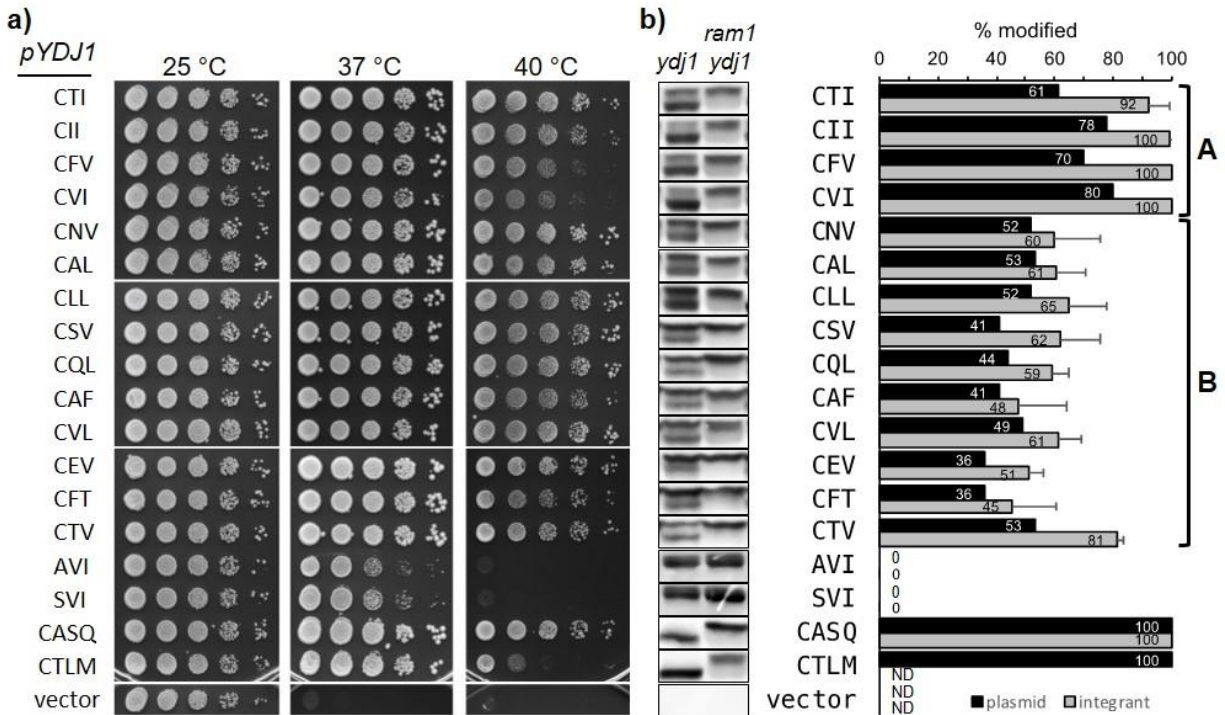


Figure 2.2. Phenotypes and isoprenylation status of Ydj1p Cxx variants. a) The indicated Ydj1p Cxx variants were transformed into the yWS2544 (*ydj1::NAT^R*) strain background and assessed for farnesyl-dependent biological activity using a thermotolerance assay. At 37 °C, yeast cannot grow in the absence of Ydj1p (i.e. vector). At 40 °C, yeast cannot grow in the absence of farnesylated Ydj1p (i.e. AVI and SVI), and shunted Ydj1p (i.e. CASQ) supports better growth than cleaved and carboxymethylated Ydj1p (i.e. CTLM); shunted refers to sequences that are farnesylated but not additionally modified (see Scheme 1). Each set of spots represents a 10-fold dilution series derived from a saturated culture initially grown in selective media. b) The mobility shift assay assesses the prenylation level of each Ydj1p Cxx variant. It relies on the observation that unmodified and farnesylated Ydj1p can be separated by SDS-PAGE, with the farnesylated species exhibiting a counterintuitive smaller apparent molecular mass relative to unmodified. Whole cell extracts were prepared as two sets then analyzed by SDS-PAGE and anti-Ydj1p immunoblot. One set was prepared from yWS2544 and yWS2542 (*ram1::KAN^R ydj1::NAT^R*) strain backgrounds that were transformed with the same plasmids used for thermotolerance testing; see panel a); *RAM1* encodes the FTase β subunit, and its absence eliminates endogenous FTase activity. Bands associated with the yWS2544 extracts shown in panel b) were quantified using ImageJ, and these values were used to plot the percent modification for each Cxx sequence (black bars, single biological replicate). ND – not determined; A – Cxx sequences initially identified using *a*-factor reporter and subsequently transferred onto Ydj1p; B – Cxx sequences directly identified using Ydj1p reporter. This figure has been reused with permission from reference 44 (Appendix II). This data was collected and analyzed by your collaborator Walter K. Schmidt (University of Georgia).

2.3 Farnesylation of Cxx peptide substrates by mammalian prenyltransferases

Yeast and mammalian FTase orthologs have been shown to exhibit non-identical but largely overlapping peptide selectivities.⁴⁷ Accordingly, the ability of purified mammalian FTase and GGTase-I to prenylate Cxx sequences was determined in the context of fluorescently labeled synthetic peptides (i.e. dns-GCxx). To supplement the 10 Cxx sequences selected from those identified as prenylation substrates by genetic screening (see Figures 2.1 and 2.2), a peptide panel of Cxx sequences derived from the human proteome was constructed. A Prosite database scan revealed 1074 human proteins with C-terminal Cxx sequences, with 847 of these not contained within longer CaaX or C(x)₃X sequences or associated with CC or CxC sequences that can serve as Rab GGTase-II substrates (Table 2.1).⁴⁸ From this pool, 75 candidate Cxx sequences were selected for detailed analysis based on the requirements of annotated membrane localization of the parent protein; conservation of the cysteine in at least two other species; evidence of protein expression; and lack of any predicted transmembrane helices (Table 2.2). This list of human-derived sequences included 12 sequences that were identified by genetic screening in yeast.

The panel of 85 dns-GCxx peptides were screened for prenylation activity with rat FTase and GGTase-I using RP-HPLC to directly detect the prenylated product.⁶ Farnesylation of 64 of the 85 peptide sequences was confirmed, with the extent of peptide farnesylation following overnight incubation (~16 hours) varying across these 64 sequences and 26 peptides reacting to completion (Table 2.3 and Figure 2.3). The varying reactivity of these Cxx peptides suggests that FTase exhibits sequence selectivity with these truncated prenylation motifs rather than recognizing the cysteine thiol sidechain alone. In contrast to FTase, peptide geranylgeranylation

with GGTase-I and GGPP under analogous conditions was not observed, indicating that these shorter peptide sequences do not serve as GGTase-I substrates.

To confirm dns-GCxx farnesylation, two representative dns-GCxx peptides were found to be modified by FTase via mass spectrometry (Figure 2.4). Two major ions were observed for dns-GCYL, corresponding to the farnesylated peptide ($M+H = 892$ Da) and a higher molecular weight peak consistent with oxidation of the farnesyl cysteine thioether to a sulfone, ($S=O$, $M+16+H = 908$ Da) as noted in mass spectrometry of related molecules.⁴⁹ For dns-GCWI, only one major species was identified, corresponding to an oxidized farnesylated product ($S=O$, $M+16+H = 931$ Da).

Table 2.1. Potential FTase substrate sequences within the human proteome

Potential FTase substrate sequences	Prosit search string ^b	Number of sequences
<i>unconstrained searches</i>		
Cxx	Cxx>	1074
CaaX	Cxxx>	1208
C(x) ₃ X	Cxxxx>	1015
<i>constrained searches^a</i>		
Cxx not within CaaX or C(x) ₃ X	{c}C-{c}C{c}{c}>	847
CaaX without downstream Cys	C{c}{c}{c}>	1062
C(x) ₃ X without downstream Cys	C{c}{c}{c}{c}>	824

^anoted constraints were applied to ignore Cxx sequences that were part of a longer sequence (e.g. CCxx and CxCxx) and potential GGTase-II consensus sequences (e.g. CxC, xCC).

^blower case c denotes positions where Cys was a negative constraint; > denotes the C-terminal constraint.

Table 2.2. Peptide information table for C-terminal Cxx sequences tested in the human genome.

Human-derived sequences	Uniprot ID	Protein	Notes
CAF*	P36551	Oxygen-dependent coproporphyrinogen-III oxidase, mitochondrial	Isoform 2 only
	Q8NI17	Interleukin-31 receptor subunit alpha	Isoform 11 only
CAG	Q9NP78	ATP-binding cassette sub-family B member 9	Isoform 5 only
	A8MXD5	Glutaredoxin domain-containing cysteine-rich protein 1	Isoform 1 only
CAL*	Q9NUI1	Peroxisomal 2,4-dienoyl-CoA reductase	Isoform 2 only
	Q1HG43	Dual oxidase maturation factor 1	Isoforms 1 & 3 only
	Q6IA86	Elongator complex protein 2	Isoforms 1, 2, 3, 5, 6, & 7 only
	O15504	Nucleoporin-like protein 2	Isoform 2 only
	Q9UKA8	Calcipressin-3	Isoforms 1, 2, 5, & 6 only
CAP	P19419	ETS domain-containing protein Elk-1	Isoform 2 only
	Q6NT32	Carboxylesterase 5A	Isoforms 1, 2, 3, & 4 only
	P10914	Interferon regulatory factor 1	Isoform 1 only
	P15941	Mucin-1	Isoform 13 only
CAV	Q8N4H5	Mitochondrial import receptor subunit TOM5 homolog	Isoform 2 only
CDI	Q8N1A6	UPF0462 protein C4orf33	Isoform 1 only
	O95475	Homeobox protein SIX6	Isoform 1 only
CDP	O14990	Protein phosphatase inhibitor 2 family member C	Isoform 1 only
CDV	O95343	Homeobox protein SIX3	Isoform 1 only
CEF	Q8IWL1	Pulmonary surfactant-associated protein A2	Isoform 1 only
	Q8IWL2	Pulmonary surfactant-associated protein A1	Isoforms 1 & 2 only
	P35247	Pulmonary surfactant-associated protein D	Isoform 1 only
	P04155	Trefoil factor 1	Isoform 1 only
CEG	P78346	Ribonuclease P protein subunit p30	Isoform 1 only
	P0CG00	Putative zinc finger and SCAN domain-containing protein 5D	Isoform 1 only
CEV*	P56559	ADP-ribosylation factor-like protein 4C	Isoform 2 only
	Q7L8W6	Diphthine--ammonia ligase	Isoform 2 only
	Q86UE6	Leucine-rich repeat transmembrane neuronal protein 1	Isoform 1 only
	O43300	Leucine-rich repeat transmembrane neuronal protein 2	Isoform 1 only

	Q86VH5	Leucine-rich repeat transmembrane neuronal protein 3	Isoform 2 only
CEY	A1A4Y4	Immunity-related GTPase family M protein	Isoform 1 only
CFS	P31358	CAMPATH-1 antigen	Isoform 1 only
	Q86YW9	Mediator of RNA polymerase II transcription subunit 12-like protein	Isoforms 2 & 3 only
CFT*	Q8N957	Ankyrin repeat and fibronectin type-III domain-containing protein 1	Isoform 1 only
	Q13111	Chromatin assembly factor 1 subunit A	Isoform 2 only
	O15440	Multidrug resistance-associated protein 5	Isoform 2 only
CFV*	P05997	Collagen alpha-2(V) chain	Isoform 1 only
	Q96L33	Rho-related GTP-binding protein RhoV	Isoform 1 only
CGF	P0DML2	Chorionic somatomammotropin hormone 1	Isoform 1 only
	P0DML3	Chorionic somatomammotropin hormone 2	Isoforms 1 & 3 only
	Q14406	Chorionic somatomammotropin hormone-like 1	Isoforms 1, 2, 3, & 4 only
	Q13772	Nuclear receptor coactivator 4	Isoform 4 only
	P01242	Growth hormone variant	Isoforms 1 & 3 only
	P01241	Somatotropin	Isoforms 1, 2, 3, 4, & 5 only
CGI	Q8WVE0	EEF1A lysine methyltransferase 1	Isoform 1 only
	O15533	Tapasin	Isoform 2 only
CGV	Q15059	Bromodomain-containing protein 3	Isoform 2 only
	P61626	Lysozyme C	Isoform 1 only
	Q9BRL7	Vesicle-trafficking protein SEC22c	Isoform 1 only
CHF	O60548	Forkhead box protein D2	Isoform 1 only
CHP	Q9H3Y6	Tyrosine-protein kinase Srms	Isoform 1 only
CIE	Q96DP5	Methionyl-tRNA formyltransferase, mitochondrial	Isoform 1 only
	Q9Y6K9	NF-kappa-B essential modulator	Isoforms 1, 2, & 3 only
CII*	Q5T1H1	Protein eyes shut homolog	Isoform 2 only
	Q96CV9	Optineurin	Isoforms 1, 2, & 3 only
	Q6WBX8	Cell cycle checkpoint control protein RAD9B	Isoforms 1 & 4 only
	P82675	28S ribosomal protein S5, mitochondrial	Isoform 2 only
CIL	P08174	Complement decay-accelerating factor	Isoform 3 only
	Q13278	Putative protein RIG	Isoform 1 only
CIQ	Q96NS5	Ankyrin repeat and SOCS box protein 16	Isoform 1 only
	Q6ZVN8	Hemojuvelin	Isoform 1, 2, & 3 only
CKH	O14905	Protein Wnt-9b	Isoform 1 only

CKI	P26371	Keratin-associated protein 5-9	Isoform 1 only
	P61244	Protein max	Isoform 5 only
	Q7RTM1	Proton channel OTOP1	Isoform 1 only
CKK	O76000	Putative olfactory receptor 2B3	Isoform 1 only
	P25398	40S ribosomal protein S12	Isoform 1 only
	O43147	Small G protein signaling modulator 2	Isoform 5 only
	P04179	Superoxide dismutase [Mn], mitochondrial	Isoforms 1, 2, 3, & 4 only
CKP	P28335	5-hydroxytryptamine receptor 2C	Isoform 2 only
	Q15131	Cyclin-dependent kinase 10	Isoforms 1, 2, 3, & 7 only
CKS	P16671	Platelet glycoprotein 4	Isoform 2 only
	Q9NYP9	Protein Mis18-alpha	Isoform 1 only
	P08949	Neuromedin-B	Isoform 2 only
	Q9Y3N9	Olfactory receptor 2W1	Isoform 1 only
CKV	P30443	HLA class I histocompatibility antigen, A-1 alpha chain	Isoform 1 only
	P01892	HLA class I histocompatibility antigen, A-2 alpha chain	Isoform 1 only
	P04439	HLA class I histocompatibility antigen, A-3 alpha chain	Isoform 1 only
	P13746	HLA class I histocompatibility antigen, A-11 alpha chain	Isoforms 1 & 2 only
	P30447	HLA class I histocompatibility antigen, A-23 alpha chain	Isoform 1 only
	P05534	HLA class I histocompatibility antigen, A-24 alpha chain	Isoform 1 only
	P18462	HLA class I histocompatibility antigen, A-25 alpha chain	Isoform 1 only
	P30450	HLA class I histocompatibility antigen, A-26 alpha chain	Isoform 1 only
	P30512	HLA class I histocompatibility antigen, A-29 alpha chain	Isoform 1 only
	P16188	HLA class I histocompatibility antigen, A-30 alpha chain	Isoform 1 only
	P16189	HLA class I histocompatibility antigen, A-31 alpha chain	Isoform 1 only
	P10314	HLA class I histocompatibility antigen, A-32 alpha chain	Isoform 1 only
	P16190	HLA class I histocompatibility antigen, A-33 alpha chain	Isoform 1 only
	P30453	HLA class I histocompatibility antigen, A-34 alpha chain	Isoform 1 only
	P30455	HLA class I histocompatibility antigen, A-36 alpha chain	Isoform 1 only

	P30456	HLA class I histocompatibility antigen, A-43 alpha chain	Isoform 1 only
	P30457	HLA class I histocompatibility antigen, A-66 alpha chain	Isoform 1 only
	P01891	HLA class I histocompatibility antigen, A-68 alpha chain	Isoform 1 only
	P10316	HLA class I histocompatibility antigen, A-69 alpha chain	Isoform 1 only
	P30459	HLA class I histocompatibility antigen, A-74 alpha chain	Isoform 1 only
	Q09160	HLA class I histocompatibility antigen, A-80 alpha chain	Isoform 1 only
	Q9Y271	Cysteinyl leukotriene receptor 1	Isoform 1 only
	Q14680	Maternal embryonic leucine zipper kinase	Isoforms 1, 2, 3, 4, 5, 6, 7, & 8 only
CLD	Q8NBU5	ATPase family AAA domain-containing protein 1	Isoform 1 only
	Q9BSJ5	Uncharacterized protein C17orf80	Isoforms 1 & 2 only
	O95402	Mediator of RNA polymerase II transcription subunit 26	Isoform 1 only
	Q9UJV8	Purine-rich element-binding protein gamma	Isoform 1 only
	Q8WVN8	Ubiquitin-conjugating enzyme E2 Q2	Isoform 2 only
CLG	Q9UNE2	Rab effector Noc2	Isoforms 1 & 2 only
	Q9BU02	Thiamine-triphosphatase	Isoform 1 only
CLK	Q8IX21	SMC5-SMC6 complex localization factor protein 2	Isoform 2 only
	Q8TDI7	Transmembrane channel-like protein 2	Isoform 4 only
	P61081	NEDD8-conjugating enzyme Ubc12	Isoform 1 only
	Q86YA3	Protein ZGRF1	Isoform 3 only
CLL*	Q6ZUX7	LHFPL tetraspan subfamily member 2 protein	Isoform 1 only
	Q9NVC6	Mediator of RNA polymerase II transcription subunit 17	Isoform 1 only
	Q75NE6	Putative microRNA 17 host gene protein	Isoform 1 only
	Q00765	Receptor expression-enhancing protein 5	Isoform 2 only
	Q7Z2W9	39S ribosomal protein L21, mitochondrial	Isoforms 1 & 2 only
	Q96I59	Probable asparagine--tRNA ligase, mitochondrial	Isoforms 1 & 2 only
CLP	P02545	Prelamin-A/C	Isoform 4 only
	Q9Y5Y2	Cytosolic Fe-S cluster assembly factor NUBP2	Isoform 1 only
	Q9Y6I8	Peroxisomal membrane protein 4	Isoform 2 only
	Q96HL8	SH3 domain-containing YSC84-like protein 1	Isoform 5 only
	Q9P2F9	Zinc finger protein 319	Isoform 1 only
CLV*	Q9H694	Protein bicaudal C homolog 1	Isoform 2 only
	O60308	Centrosomal protein of 104 kDa	Isoform 2 only

	Q14166	Tubulin--tyrosine ligase-like protein 12	Isoform 1 only
CMF	Q6NVY1	3-hydroxyisobutyryl-CoA hydrolase, mitochondrial	Isoform 2 only
	Q9GZX9	Twisted gastrulation protein homolog 1	Isoform 1 only
CNL	Q9C091	GREB1-like protein	Isoform 4 only
	P29728	2'-5'-oligoadenylate synthase 2	Isoform 3 only
	P22234	Multifunctional protein ADE2	Isoforms 1 & 2 only
	Q9UJT1	Tubulin delta chain	Isoforms 1, 2, 3, 4, 5, & 6 only
CNR	O15194	CTD small phosphatase-like protein	Isoform 1 & 2 only
CPG	Q6ZMM2	ADAMTS-like protein 5	Isoform 1 & 2 only
	Q8TDQ1	CMRF35-like molecule 1	Isoform 2, 4, & 5 only
	Q8N9R0	Putative uncharacterized protein encoded by LINC00304	Isoform 1 only
	Q6TCH4	Membrane progesterin receptor delta	Isoform 2 only
	Q9Y6S9	Ribosomal protein S6 kinase-like 1	Isoform 2 only
CPH	Q8NFI3	Cytosolic endo-beta-N-acetylglucosaminidase	Isoform 3 only
	Q9Y5X2	Sorting nexin-8	Isoform 1 only
CPI	Q9BSY4	Coiled-coil-helix-coiled-coil-helix domain-containing protein 5	Isoform 2 only
	Q9GZS3	WD repeat-containing protein 61	Isoform 1 only
CPK	Q9H9Q2	COP9 signalosome complex subunit 7b	Isoform 3 only
	Q3SYA9	Putative POM121-like protein 1	Isoform 1 only
	Q96LQ0	Protein phosphatase 1 regulatory subunit 36	Isoform 1 only
CPL	P30926	Neuronal acetylcholine receptor subunit beta-4	Isoform 2 only
	Q9UP79	A disintegrin and metalloproteinase with thrombospondin motifs 8	Isoform 1 only
	P38398	Breast cancer type 1 susceptibility protein	Isoform 2 only
	Q8TDM6	Disks large homolog 5	Isoforms 1, 2, 4, & 5 only
CPP	Q7Z695	Uncharacterized aarF domain-containing protein kinase 2	Isoform 1 only
	Q00975	Voltage-dependent N-type calcium channel subunit alpha-1B	Isoforms 2 only
	P56202	Cathepsin W	Isoform 1 only
	Q00535	Cyclin-dependent-like kinase 5	Isoform 1 & 2 only
	Q8NEG7	Protein DENND6B	Isoform 1 only
	O15527	N-glycosylase/DNA lyase	Isoform 2 only
	O75818	Ribonuclease P protein subunit p40	Isoforms 1 & 2 only
CPR	O95863	Zinc finger protein SNAI1	Isoform 1 only

	O43435	T-box transcription factor TBX1	Isoform 3 only
CPT	P25067	Collagen alpha-2(VIII) chain	Isoform 1 only
	Q99689	Fasciculation and elongation protein zeta-1	Isoform 1 only
	Q9UHY8	Fasciculation and elongation protein zeta-2	Isoforms 1 & 2 only
	Q93038	Tumor necrosis factor receptor superfamily member 25	Isoforms 5 & 6 only
CPV	P60981	Dextrin	Isoforms 1 & 2 only
	P55265	Double-stranded RNA-specific adenosine deaminase	Isoforms 1, 2, 3, 4, & 5 only
	Q7Z7L9	Zinc finger and SCAN domain-containing protein 2	Isoform 4 only
CPY	P51460	Insulin-like 3	Isoform 1 only
CQA	Q92784	Zinc finger protein DPF3	Isoform 1 only
	Q5VZR4	Hippocampus abundant transcript-like protein 2	Isoform 1 only
	P09086	POU domain, class 2, transcription factor 2	Isoform 4 only
CQL*	Q8WXX0	Dynein heavy chain 7, axonemal	Isoform 4 only
	P55082	Microfibril-associated glycoprotein 3	Isoforms 1 & 2 only
CQS	P04054	Phospholipase A2	Isoform 1 only
	A6NFN3	RNA binding protein fox-1 homolog 3	Isoform 2 only
CQV	Q96M34	Testis-specific expressed protein 55	Isoform 1 only
	P0C0L4	Complement C4-A	Isoforms 1 & 2 only
	P0C0L5	Complement C4-B	Isoform 1 only
	Q8IWL8	Saitohin	Isoform 1 only
CRD	Q86UQ0	Zinc finger protein 589	Isoforms 1 & 2 only
CRE	Q96CX2	BTB/POZ domain-containing protein KCTD12	Isoform 1 only
	Q15615	Olfactory receptor 4D1	Isoform 1 only
CRF	P09466	Glycodelin	Isoforms 1, 2, & 3 only
CRL	Q8TDW5	Synaptotagmin-like protein 5	Isoforms 1 & 2 only
CRQ	P08908	5-hydroxytryptamine receptor 1A	Isoform 1 only
	Q6P2C8	Mediator of RNA polymerase II transcription subunit 27	Isoforms 1 & 2 only
	Q4G0F5	Vacuolar protein sorting-associated protein 26B	Isoform 1 only
CRV	Q9Y2C4	Nuclease EXOG, mitochondrial	Isoform 2 only
CSA	Q1MX18	Protein inscuteable homolog	Isoform 6 only
	Q8N983	39S ribosomal protein L43, mitochondrial	Isoform 1 only
	P51811	Membrane transport protein XK	Isoform 1 only
CSF	Q9BTY2	Plasma alpha-L-fucosidase	Isoform 2 only

	Q6QHF9	Peroxisomal N(1)-acetyl-spermine/spermidine oxidase	Isoform 8 only
	Q9Y2Y8	Proteoglycan 3	Isoform 1 only
	P12757	Ski-like protein	Isoform 2 only
CSG	P41223	Protein BUD31 homolog	Isoform 1 only
	O43866	CD5 antigen-like	Isoform 1 only
	Q96KN8	Phospholipase A and acyltransferase 5	Isoform 2 only
	Q12794	Hyaluronidase-1	Isoform 4 only
	Q9BXT6	RNA helicase Mov10l1	Isoform 5 only
CSI	Q9Y2T5	G-protein coupled receptor 52	Isoform 1 only
	Q9Y5Q9	General transcription factor 3C polypeptide 3	Isoform 1 only
CSK	Q53EZ4	Centrosomal protein of 55 kDa	Isoform 1 only
	P04275	von Willebrand factor	Isoform 1 only
CSL	Q9P2M7	Cingulin	Isoform 2 only
	O95278	Laforin	Isoforms 1, 3, 6, 7, & 8 only
	O75593	Forkhead box protein H1	Isoform 1 only
	Q6KB66	Keratin, type II cytoskeletal 80	Isoform 2 only
	P14598	Neutrophil cytosol factor 1	Isoform 2 only
	Q9NQB0	Transcription factor 7-like 2	Isoform 12 only
	Q96N03	V-set and transmembrane domain-containing protein 2-like protein	Isoform 1 only
	Q9ULD5	Zinc finger protein 777	Isoform 1 only
CSQ	Q5HY92	Fidgetin	Isoform 1 only
	Q8IVF1	NUT family member 2A	Isoform 1 only
	A6NNL0	NUT family member 2B	Isoform 1 only
	Q5VT03	NUT family member 2D	Isoform 1 only
	B1AL46	NUT family member 2E	Isoform 1 only
	A1L443	NUT family member 2F	Isoform 1 only
	Q5VZR2	NUT family member 2G	Isoform 1 only
	P33764	Protein S100-A3	Isoform 1 only
CSS	Q5T1V6	Probable ATP-dependent RNA helicase DDX59	Isoform 2 only
	Q9H0R5	Guanylate-binding protein 3	Isoform 4 only
	P05112	Interleukin-4	Isoforms 1 & 2 only
	Q86X10	Ral GTPase-activating protein subunit beta	Isoforms 1, 2, 3, & 4 only
	Q9NY57	Serine/threonine-protein kinase 32B	Isoforms 1 & 2 only
CST	Q9BPY3	Protein FAM118B	Isoform 1 only
	Q8TC05	Nuclear protein MDM1	Isoform 3 only
	P16471	Prolactin receptor	Isoform 9 only
	Q7Z4G4	tRNA (guanine(10)-N2)-methyltransferase homolog	Isoform 3 only

CSV*	Q9UEW3	Macrophage receptor MARCO	Isoforms 1 & 2 only
	Q9H3H1	tRNA dimethylallyltransferase	Isoforms 1, 2, 3, 4, 5, & 6 only
	A8MW92	PHD finger protein 20-like protein 1	Isoform 1 only
	Q9UKA9	Polypyrimidine tract-binding protein 2	Isoforms 5 & 6 only
	O95969	Secretoglobin family 1D member 2	Isoform 1 only
CSY	P13727	Bone marrow proteoglycan	Isoforms 1 & 2 only
	A4D1P6	WD repeat-containing protein 91	Isoform 3 only
CTE	Q9H3K6	BolA-like protein 2	Isoform 2 only
	Q14204	Cytoplasmic dynein 1 heavy chain 1	Isoform 1 only
	Q14141	Septin-6	Isoform 1 only
	Q6PF04	Zinc finger protein 613	Isoforms 1 & 2 only
CTH	P02790	Hemopexin	Isoform 1 only
CTP	Q9UBL6	Copine-7	Isoforms 1 & 2 only
	Q5T1A1	DC-STAMP domain-containing protein 2	Isoform 2 only
	O43776	Asparagine--tRNA ligase, cytoplasmic	Isoform 1 only
CTS	P28222	5-hydroxytryptamine receptor 1B	Isoform 1 only
	Q6UX04	Spliceosome-associated protein CWC27 homolog	Isoform 2 only
	O15534	Period circadian protein homolog 1	Isoform 1 only
CTV*	A6H8Y1	Transcription factor TFIIB component B" homolog	Isoform 2 only
	O75044	SLIT-ROBO Rho GTPase-activating protein 2	Isoform 1 only
CVF	P59541	Taste receptor type 2 member 30	Isoform 1 only
	P29144	Tripeptidyl-peptidase 2	Isoform 1 only
CVG	Q96PK6	RNA-binding protein 14	Isoform 3 only
	Q9BWF3	RNA-binding protein 4	Isoform 3 only
	Q9Y336	Sialic acid-binding Ig-like lectin 9	Isoform 2 only
CVK	P01008	Antithrombin-III	Isoform 1 only
	Q9C0E2	Exportin-4	Isoform 1 only
CVL*	Q32MH5	Protein FAM214A	Isoform 2 only
	P23510	Tumor necrosis factor ligand superfamily member 4	Isoforms 1 & 2 only
CVM	Q12946	Forkhead box protein F1	Isoform 1 only
	Q12947	Forkhead box protein F2	Isoform 1 only
	Q9NS66	Probable G-protein coupled receptor 173	Isoform 1 only
CVY	Q14156	Protein EFR3 homolog A	Isoforms 1, 2, & 3 only
	Q9Y2G0	Protein EFR3 homolog B	Isoforms 1 & 2 only
	Q6ZUU3	FOXL2 neighbor protein	Isoform 1 only

	Q92750	Transcription initiation factor TFIID subunit 4B	Isoform 2 only
CWF	Q9UF11	Pleckstrin homology domain-containing family B member 1	Isoforms 1, 2, 3, & 4 only
CWI	Q68EM7	Rho GTPase-activating protein 17	Isoform 5 only
CYL	Q9BQ51	Programmed cell death 1 ligand 2	Isoform 3 only

*sequences that were also recovered from yeast genetic screening

Table 2.3. Reactivity of Cxx peptides with mammalian FTase and prenyl donors^{a,b}

<i>Complete prenylation by both prenyl donors (3 total)^b</i>			
CFT ^c	CFV ^d	CMF	
<i>Complete prenylation with FPP; partial prenylation with GGPP (22 total)^b</i>			
CAF ^c	CIL	CQA	CVL ^c
CAL ^c	CLL ^c	CQL ^c	CWF
CAV	CLV ^d	CQV	CWI
CEV ^c	CNV ^c	CSI	CYL
CFS	CPI	CSV ^c	
CII ^d	CPV	CTV ^c	
<i>Complete prenylation with FPP; no prenylation with GGPP (1 total)^b</i>			
CGI			
<i>Complete prenylation with GGPP; partial prenylation with FPP (2 total)^b</i>			
CGF	CVF		
<i>Partial prenylation with FPP and GGPP (11 total)^b</i>			
CEF	CLP	CSY	CVM
CHF	CPL	CTS	CVY
CLG	CSF	CVG	
<i>Partial prenylation with FPP; no prenylation with GGPP (25 total)^b</i>			
CAG	CIE	CPH	CST
CAP	CIQ	CPT	CTH
CDI	CKI	CRL	CTP
CDV	CKV	CRV	CVK
CEG	CLD	CSA	
CEY	CLK	CSL	
CHP	CNL	CSQ	
<i>Non-reactive with either prenyl donor (21 total)^b</i>			
CDP	CNR	CQS	CSK
CGV	CPG	CRD	CSS
CKH	CPK	CRE	CTE
CKK	CPP	CRF	
CKP	CPR	CRQ	
CKS	CPY	CSG	
<i>Peptide sequences from α-factor screen that were not tested (7 total)</i>			
CVI ^d	CTI ^d	CLI ^d	CLA ^d
CRI ^d	CCI ^d	CFY ^d	

^a Sequences were analyzed in the context of the indicated dns-GCxx peptide; each dns-GCxx peptide (3 μ M) was reacted with FTase (200 nM) and FPP or GGPP (10 μ M) and products analyzed by RP-HPLC as described in Materials and Methods.

^b Peptide reactivity was assigned into one of three levels: “Complete”, 85% or greater substrate to product conversion by peak integration; “Partial”, detectable substrate to product conversion (up to 84%); or no detectable product.

^c Peptide sequence identified from Ydj1p screen.

^d Peptide sequence identified from **a**-factor screen.

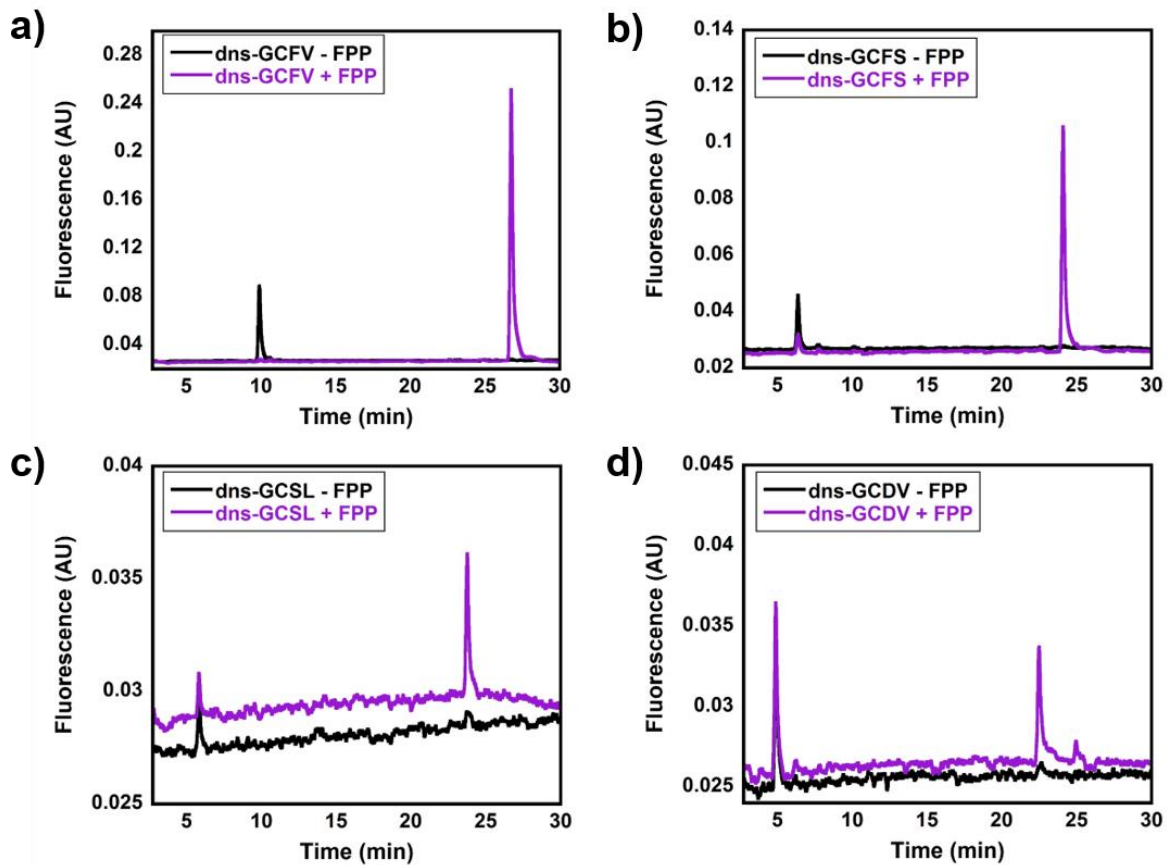


Figure 2.3. FTase-catalyzed farnesylation of Cxx peptides confirmed by RP-HPLC analysis. a) dns-GCFV; b) dns-GCFS; c) dns-GCSL; d) dns-GCDV. Purple and black lines denote reactions with or without 10 μ M FPP, respectively. Reactions and RP-HPLC analysis were carried out as described in Materials and Methods. This figure has been reused with permission from reference 44 (Appendix II).

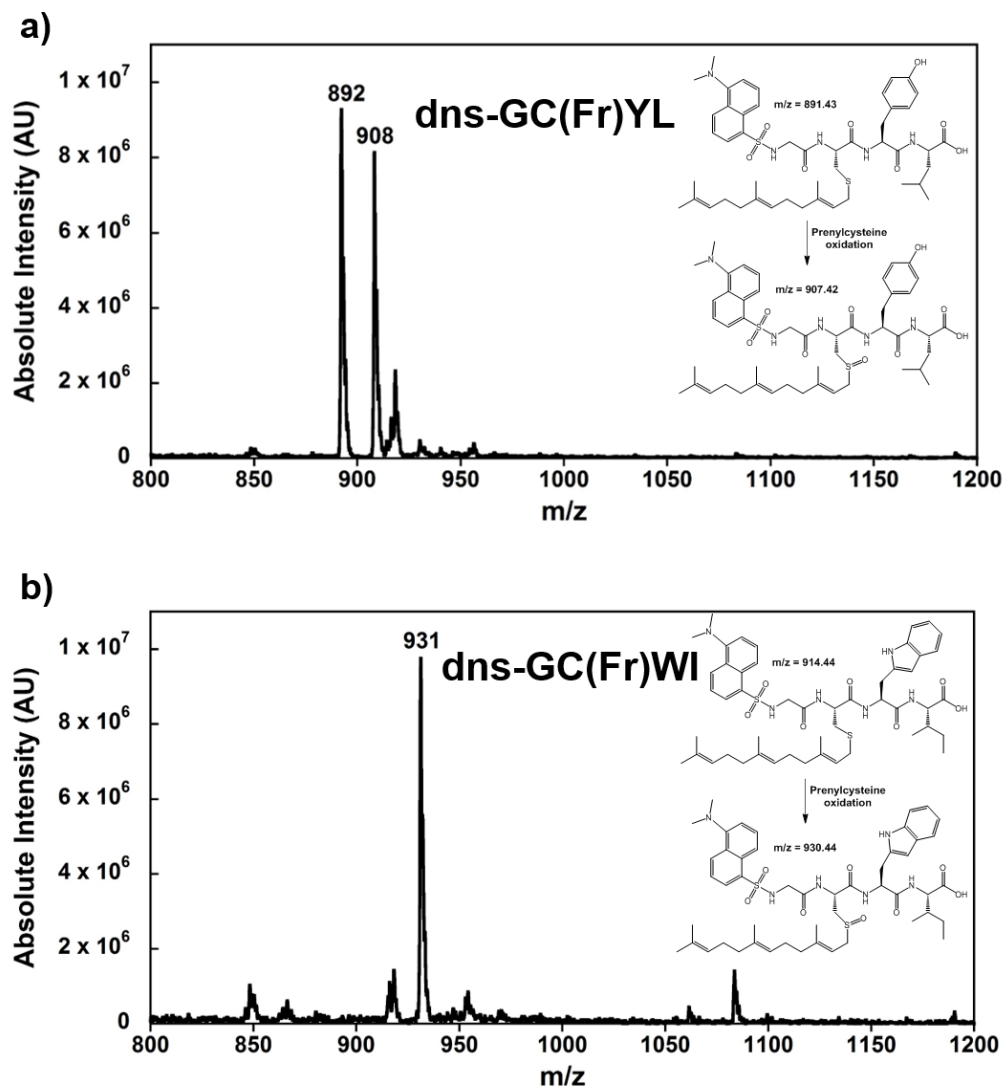


Figure 2.4. LC-MS confirmation of FTase-catalyzed dns-GCxx peptide farnesylation. a) LC-MS analysis of farnesylated dns-GCYL, with peaks at 892 m/z and 908 m/z corresponding to non-oxidized and oxidized farnesylated peptide, respectively; b) LC-MS analysis of farnesylated dns-GCWI, with peak at 931 m/z representing the oxidized farnesylated peptide. (Fr) denotes the farnesylation of cysteine sidechain. This figure has been reused with permission from reference 44 (Appendix II). LC-MS analysis of prenylated peptides was assisted by Tongyin Zheng from the Castañeda Lab (Syracuse University).

2.4 Geranylgeranylation of Cxx peptide sequences by FTase

The selectivity of FTase for FPP over GGPP as prenyl donor has been attributed to steric clashes between FTase active site residues and the larger GGPP isoprenoid chain when it occupies the active site. Certain engineered FTase active site mutations have been shown to relieve this clash.^{39,41,50} With the Cxx sequences being one amino acid shorter than the established CaaX prenylation motif, we hypothesized that FTase might be able to accommodate the larger isoprenoid donor GGPP for prenylation. Indeed, geranylgeranylation was observed for 38 of the 85 dns-Cxx peptides by RP-HPLC when reactions contained FTase and GGPP (Figure 2.5 and Table 2.3). FTase-catalyzed geranylgeranylation of Cxx peptides displayed sequence-dependent variation of peptide reactivity as well with only 5 peptides exhibiting complete or near-complete modification. Geranylgeranylation of two representative dns-GCxx peptides, dns-GCFT (S=O, M+16+H = 948 Da) and dns-GCYL (S=O, M+16+H = 976 Da), was verified by mass spectrometry (Figure 2.6).

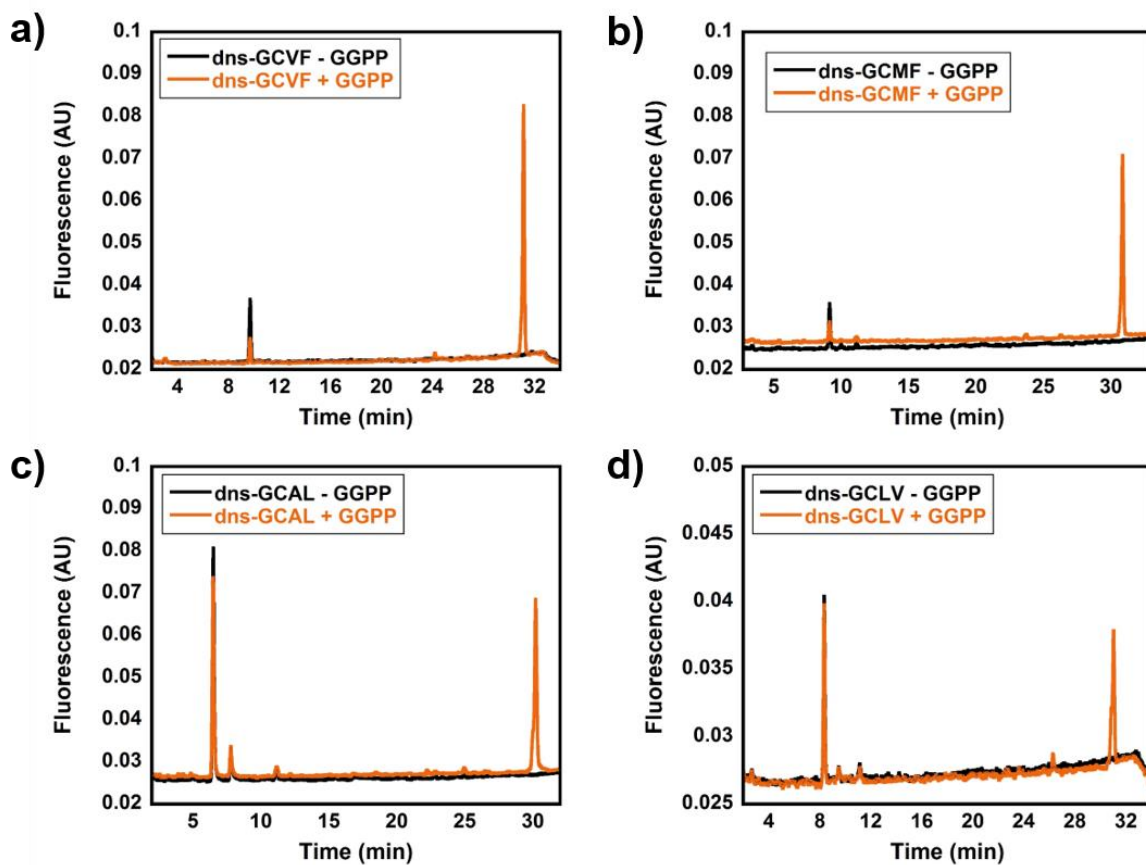


Figure 2.5. FTase-catalyzed geranylgeranylation of dns-GCxx peptides. a) dns-GCVF; b) dns-GCMF; c) dns-GCAL; d) dns-GCLV. Orange and black lines denote reactions with or without 10 μ M GGPP, respectively. Reactions and RP-HPLC analysis were carried out as described in Materials and Methods. This figure has been reused with permission from reference 44 (Appendix II).

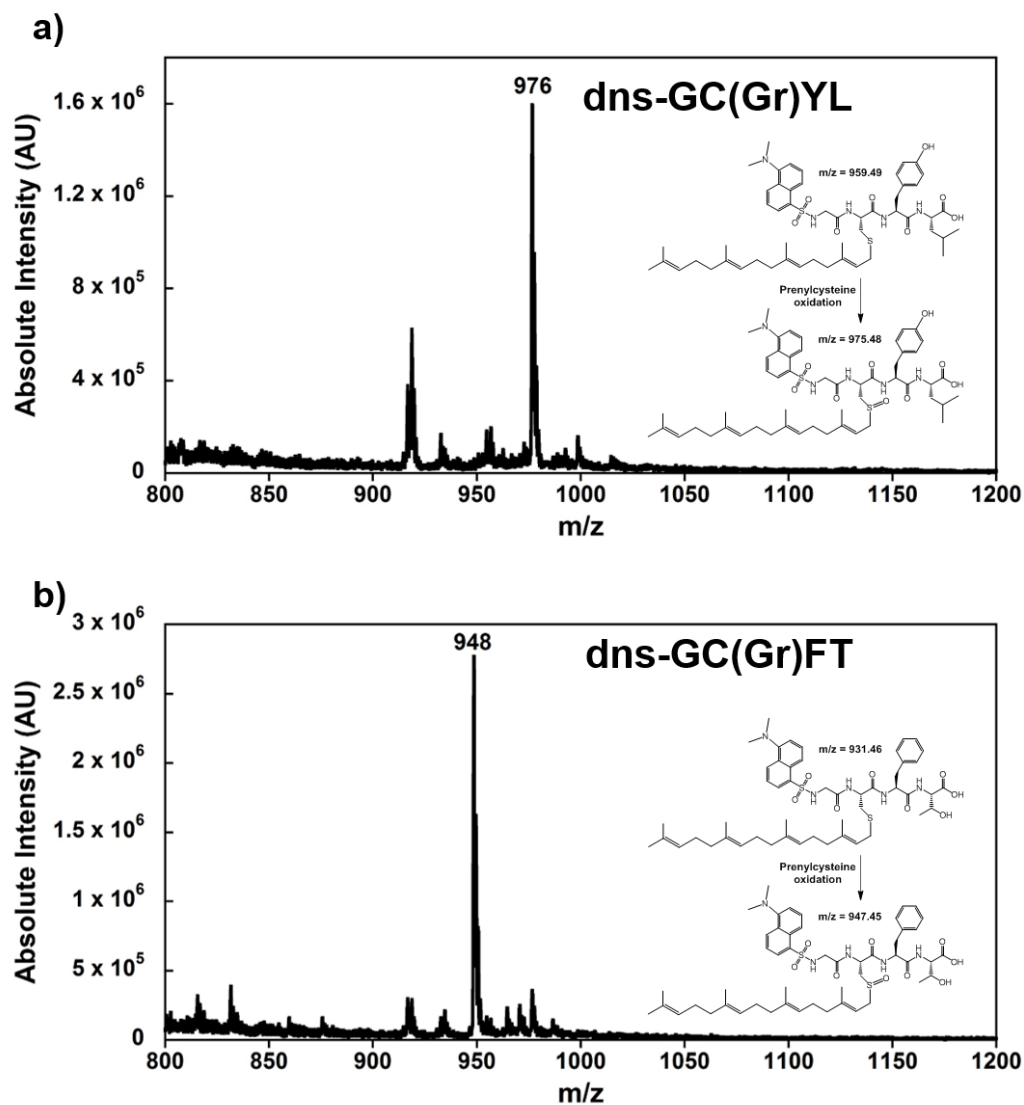


Figure 2.6. LC-MS confirmation of FTase-catalyzed dns-GCxx peptide geranylgeranylation. a) LC-MS analysis of geranylgeranylated dns-GCYL, with peak at 976 m/z corresponding to the oxidized geranylgeranylated peptide; b) LC-MS analysis of geranylgeranylated dns-GCFT, with peak at 948 m/z representing the oxidized geranylgeranylated peptide. (Gr) denotes the geranylgeranylation of cysteine sidechain. This figure has been reused with permission from reference 44 (Appendix II). LC-MS analysis of prenylated peptides was assisted by Tongyin Zheng from the Castañeda lab (Syracuse University).

2.5 Competition assay to assess FTase preference for FPP versus GGPP

We used a direct competition assay to delineate the relative lipid preference for FTase between FPP and GGPP given that it can use either to modify Cxx sequences. The five peptides (dns-GCFT, dns-GCFV, dns-GCGF, dns-GCMF and dns-GCVF) that displayed the highest activity with GGPP in the RP-HPLC assay were selected to assess lipid preference by FTase (Tables 2.3). Each peptide was incubated with FTase and 10 μ M total prenyl donor, where the molar ratio of lipid varied from 100% GGPP to 100% FPP. Following the overnight reaction (~16 hours), the modification associated with the product (farnesylation or geranylgeranylation) was determined by its RP-HPLC retention time (Figure 2.7a). For each peptide, the relative amount of geranylgeranylated product decreased in favor of farnesylation even when GGPP comprised the majority (i.e. 75%) of the prenyl pool available (Figure 2.7b-f). Unsurprisingly, this indicates a strong preference for FPP as an FTase co-substrate under most conditions but allows for unexpected use of GGPP in the absence of a farnesyl donor.

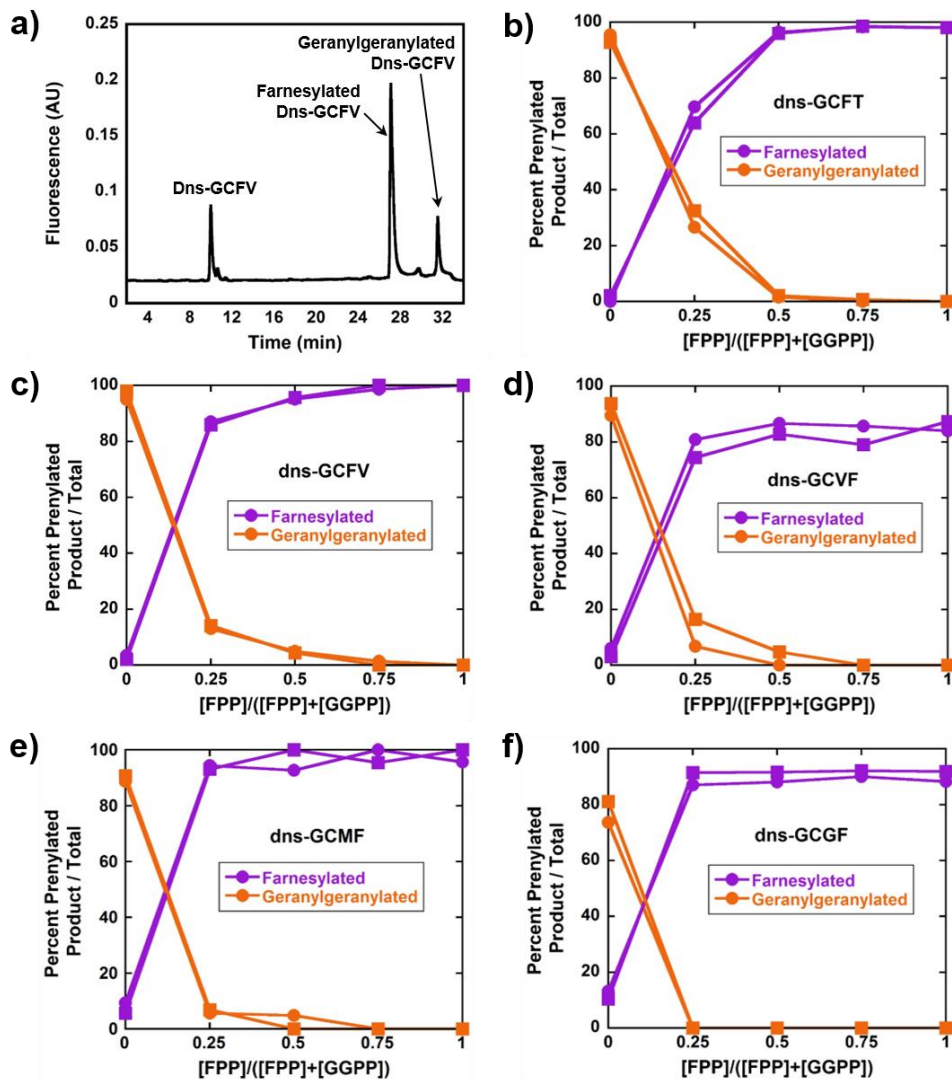


Figure 2.7. Prenyl donor competition reveals FTase preference for FPP over GGPP for modifying dns-GCxx peptides. a) Representative chromatogram for prenyl donor competition experiment with the dns-GCFV peptide and a 25:75 FPP:GGPP ratio; b) Product distribution for dns-GCFT; c) Product distribution for dns-GCFV; d) Product distribution for dns-GCVF; e) Product distribution for dns-GCMF; f) Product distribution for dns-GCGF. Purple and orange lines and symbols denote farnesylated and geranylgeranylated products, respectively. Each plot represents two independent trials per peptide reaction. Reactions were performed and analyzed as described in Materials and Methods. This figure has been reused with permission from reference 44 (Appendix II).

2.6 Steady state analysis of dns-GCxx peptide prenylation by FTase

For steady-state analysis of Cxx prenylation by FTase and GGTase-I, we used an established fluorescence-based assay that employs the environmentally sensitive dansyl fluorophore which allows continuous monitoring of peptide prenylation.^{51,52} As described in section 1.3, upon prenylation, dansylated peptides exhibit fluorescence enhancement which permits for more facile measurement of initial reaction rates compared to HPLC-based assays (Figures 2.8 and 2.9). Surprisingly, only 12 of the 85 peptides in our study set displayed fluorescence enhancement when reacted with FTase and FPP, consistent with peptide farnesylation. By comparison, 64 peptides were found to be farnesylated by RP-HPLC analysis under identical reaction conditions (Table 2.3). The high false negative rate for detecting peptide farnesylation through the fluorescence-based assay mirrors that observed for longer C(x)₃X peptides sequences,⁶ suggesting limitations on the utility of the fluorescence-based assay for determining peptide reactivity with FTase. Importantly, no false positives were observed with the fluorescence-based assay for peptides that were deemed unreactive by RP-HPLC analysis. In reactions with FTase and GGPP, 4 of the 85 peptides exhibited fluorescence enhancement (dns-GCFT, dns-GCII, dns-GCLL, and dns-GCYL). None of the 85 dns-GCxx peptides yielded fluorescence enhancement when reacted with mammalian GGTase-I and GGPP, consistent with the lack of Cxx peptide reactivity with GGTase-I as noted by RP-HPLC analysis.

Steady-state characterization of peptide reactivity was performed for dns-GCxx peptides exhibiting fluorescence enhancement upon prenylation with either FPP or GGPP in the presence of saturating (10 μ M) prenyl donor cosubstrate (Table 2.4 and Figures 2.8 and 2.9). Saturation of prenylation velocity was not observed within the experimentally accessible peptide concentration range for any of the peptides tested, allowing only measurement of k_{cat}/K_m for these FTase

substrates. In reaction with FPP, dns-GCxx peptides exhibited much less reactivity as compared to highly reactive CaaX sequences, such as the H-Ras derived CVLS sequence.⁵³ For example, one of the more active dns-GCLL peptide sequence was farnesylated ~40-fold less efficiently by FTase than dns-GCVLS under subsaturating (k_{cat}/K_m) conditions. For the Cxx peptides for which steady state reactivity with both FTase and GGPP could be determined, all peptides exhibited comparable reactivity (within 2-fold) in the presence of saturating FPP or GGPP.

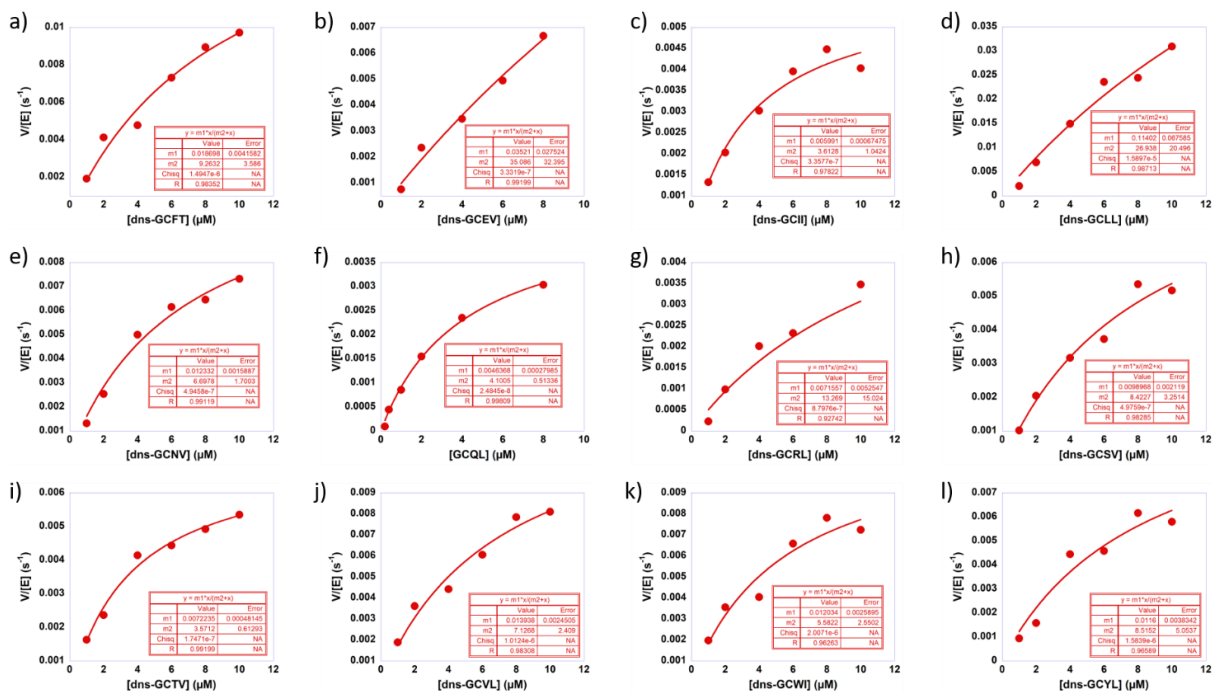


Figure 2.8. Steady state characterization of FTase-catalyzed dns-GCxx peptide farnesylation with FPP. a-l) Representative plots for dependence of farnesylation activity on peptide substrate concentration catalyzed by FTase in the presence of 10 μM FPP: a) dns-GCFT; b) dns-GCEV; c) dns-GCII; d) dns-GCLL; e) dns-GCNV; f) dns-GCQL; g) dns-GCRL; h) dns-GCSV; i) dns-GCTV; j) dns-GCVL; k) dns-GCWI; l) dns-GCYL. The curve represents the best fit to the Michaelis-Menten equation. Reactions were performed and analyzed as described in Materials and Methods. This figure has been reused with permission from reference 44 (Appendix II).

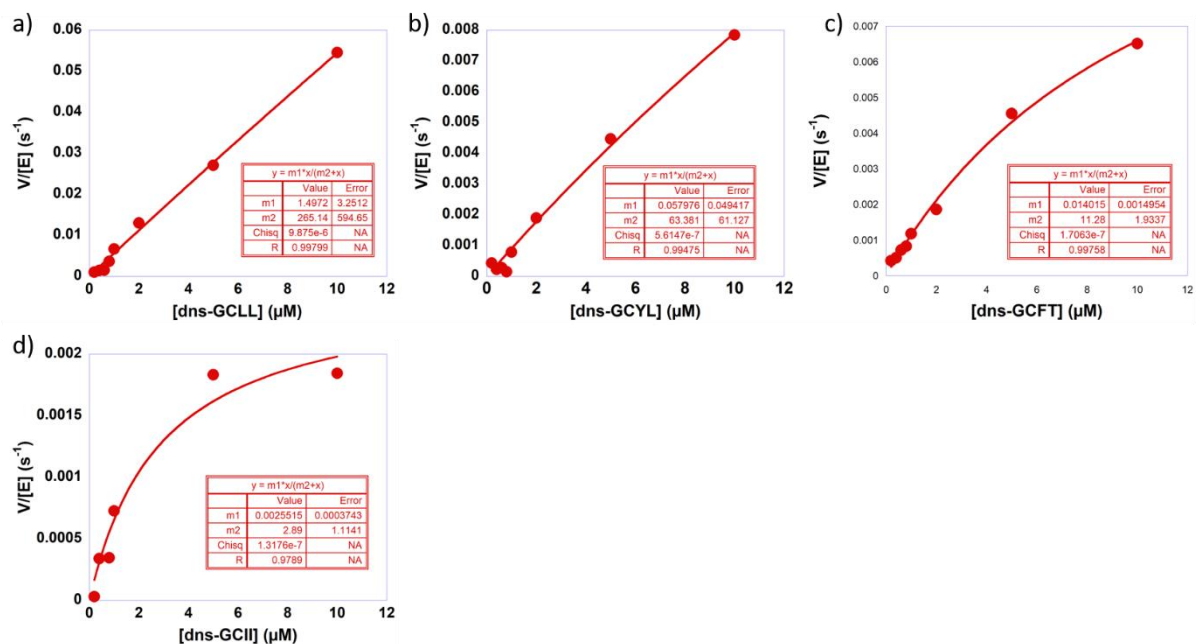


Figure 2.9. Steady state characterization of FTase-catalyzed dns-GCxx peptide geranylgeranylation with GGPP. a-d) Representative plots for dependence of farnesylation activity on peptide substrate concentration catalyzed by FTase in the presence of 10 μM GGPP: a) dns-GCLL; b) dns-GCYL; c) dns-GCFT; d) dns-GCII. The curve represents the best fit to the Michaelis-Menten equation. Reactions were performed and analyzed as described in Materials and Methods. This figure has been reused with permission from reference 44 (Appendix II).

Table 2.4. Steady state reactivity of dns-GCxx peptides catalyzed by FTase^a

dns-GCxx sequence	Prenyl donor	
	10 μ M FPP	10 μ M GGPP
	k_{cat}/K_m ($M^{-1} s^{-1}$)	k_{cat}/K_m ($M^{-1} s^{-1}$)
dns-GCEV	950 \pm 200	nd ^b
dns-GCFT	1900 \pm 70	1700 \pm 300
dns-GCII	1400 \pm 200	700 \pm 100
dns-GCLL	4000 \pm 100	6100 \pm 1000
dns-GCNV	1900 \pm 100	nd
dns-GCQL	2500 \pm 90	nd
dns-GCRL	340 \pm 100	nd
dns-GCSV	1000 \pm 90	nd
dns-GCTV	1900 \pm 40	nd
dns-GCVL	2200 \pm 200	nd
dns-GCWI	2600 \pm 200	nd
dns-GCYL	1300 \pm 100	920 \pm 30
dns-GCVLS	170000 \pm 40000 ^c	nd

^aSteady state analyses were carried out at saturating FPP or GGPP (10 μ M) and varying peptide concentrations (0.5 – 10 μ M) as described in Materials and Methods. Reported values are the average of at least three independent determinations, with the error indicating the standard deviation.

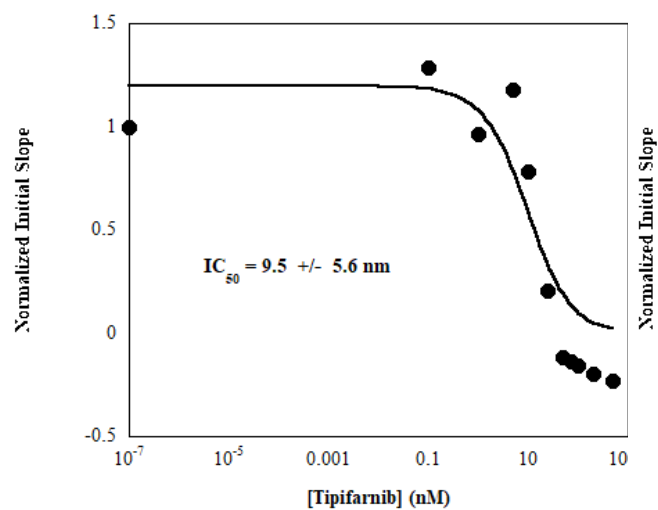
^bNo detectable activity. This assay has a lower limit for measuring k_{cat}/K_m of 0.4 $M^{-1} s^{-1}$ per reference 29.

^cPreviously reported per reference 29.

2.7 Prenylation of Cxx motifs by FTase is inhibited by tipifarnib

There are several FTase inhibitors that have been developed as targets for cancer treatment.^{54,55} One such inhibitor is tipifarnib, also known as Zarnestra, which is currently under investigation as a treatment for squamous cell carcinomas with HRas mutations.⁵⁶ This compound prevents the prenylation of C-terminal motifs by binding at the peptide substrate binding site of FTase. When treated with varying amounts of tipifarnib, farnesylation of dns-GCWI and dns-GCYL by FTase was efficiently blocked with an IC₅₀ value of 9.5 +/- 5.6 nM and 6.8 +/- 7.9 nM, respectively (Figure 2.10A and B). In addition, tipifarnib blocked geranylgeranylation by FTase of dns-GCYL with an IC₅₀ value of 7.4 +/- 12.2 nM (Figure 2.11). These results suggest prenylation of these shortened Cxx sequences occurs through the same binding interaction as of classical CaaX motifs.

A)



B)

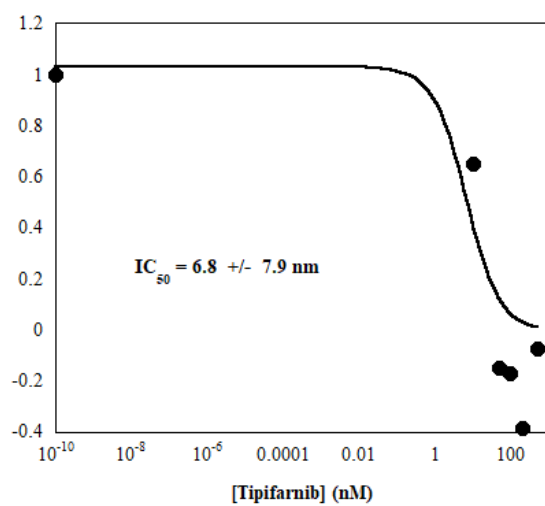


Figure 2.10. Inhibition of FTase-catalyzed farnesylation of dns-GCxx peptides by tipifarnib. A) dns-GCWI; B) dns-GCYL. Initial slopes were normalized to reactions without tipifarnib and IC_{50} values were calculated as described in Materials and Methods.

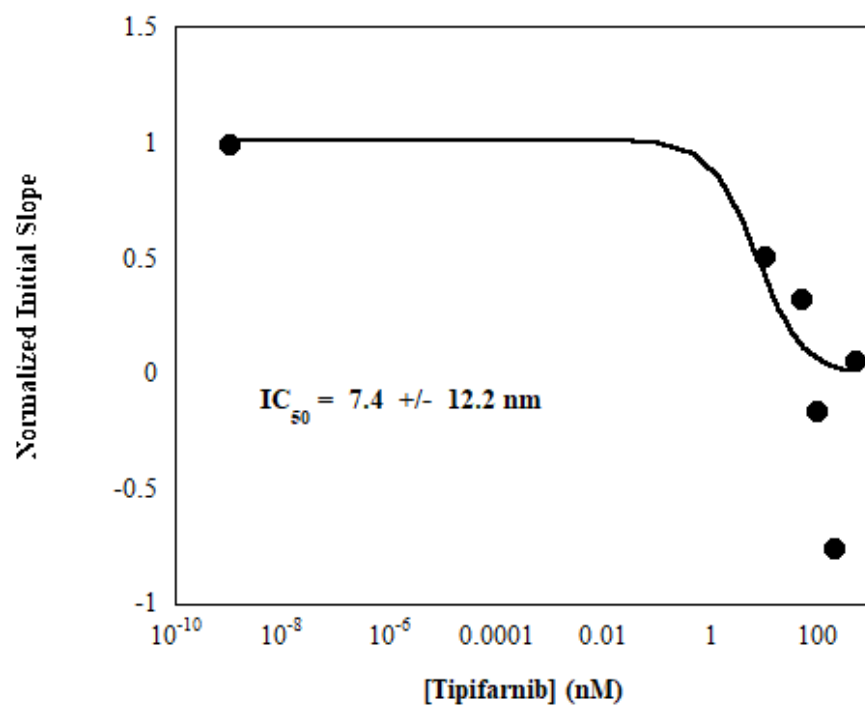


Figure 2.11. Inhibition of FTase-catalyzed geranylgeranylation of dns-GCYL by tipifarnib. Initial slopes were normalized to reactions without tipifarnib and IC_{50} values were calculated as described in Materials and Methods.

2.8 Investigating prenylation of Cxx c-terminal sequences via in cell fluorescence

localization studies

To be considered biologically relevant in mammalian systems, proteins terminating in Cxx sequences must exhibit sufficient reactivity to be modified by endogenous FTase within an intact human cell. The minimum reactivity is estimated to be in the range of $k_{cat}/K_m = 0.5-2 \times 10^4 \text{ M}^{-1}\text{s}^{-1}$ when peptide reactivity was determined in an *in vitro* assay using purified FTase.⁵⁷ The reactivity of several dns-GCxx peptides with purified FTase (see Table 2.4) falls closer to the lower limit of the range determined in the aforementioned study, suggesting that these shorter prenylation motifs might be reactive enough to support protein prenylation within mammalian cells. In addition, the apparent reactivity observed for several Cxx sequences within yeast cells suggests the ability of these motifs to be modified in a biological context.

We tested for the ability of 9 Cxx C-terminus sequences to undergo prenylation in HEK293 cells using a pEGFP-KRas vector (gift from Casey Lab, Duke University), which has the canonical motif -CVIM at its C-terminus. The vector was modified to contain the Cxx sequence of interest through PCR and subsequent ligation (see Materials and Methods). The use of an eGFP-KRas fusion protein serves as a proxy for directly detecting prenylation through visualization of eGFP fluorescence at the membrane (prenylated) or diffused throughout the cell (not prenylated, or prenylated but not processed).⁵⁸ The 9 sequences tested in this study included, -CLL, -CQI, -CQL, -CSI, -CQV, -CMF, -CQA, -CFV, and -CVF. These sequences represented the most active sequences from the 85 sequences investigated *in vitro* using purified FTase based on either steady-state analysis or RP-HPLC analysis (see Tables 2.3 and 2.4).

Transfection of 6×10^4 cells with 1 μg DNA and 2 μL Turbofect (Promega) in a 24-well plate was found to be the ideal transfection condition with 24-hour incubation post-transfection.

Of the 9 sequences tested, all were found to be diffuse throughout the cell, which does not provide evidence these proteins are modified inside cells (Figure 2.12). The positive control containing the canonical -CVIM sequence was confirmed to be membrane localized. While not promising, these results do not conclusively indicate that Cxx sequences are not modified inside mammalian cells. It is highly plausible that these sequences do not undergo the subsequent post-processing steps required for them to be shuttled to the cell membrane after prenylation. Analysis of these non-canonical sequences in a mammalian system requires a different approach that is not reliant on membrane localization to serve as the signal for detecting prenylation.

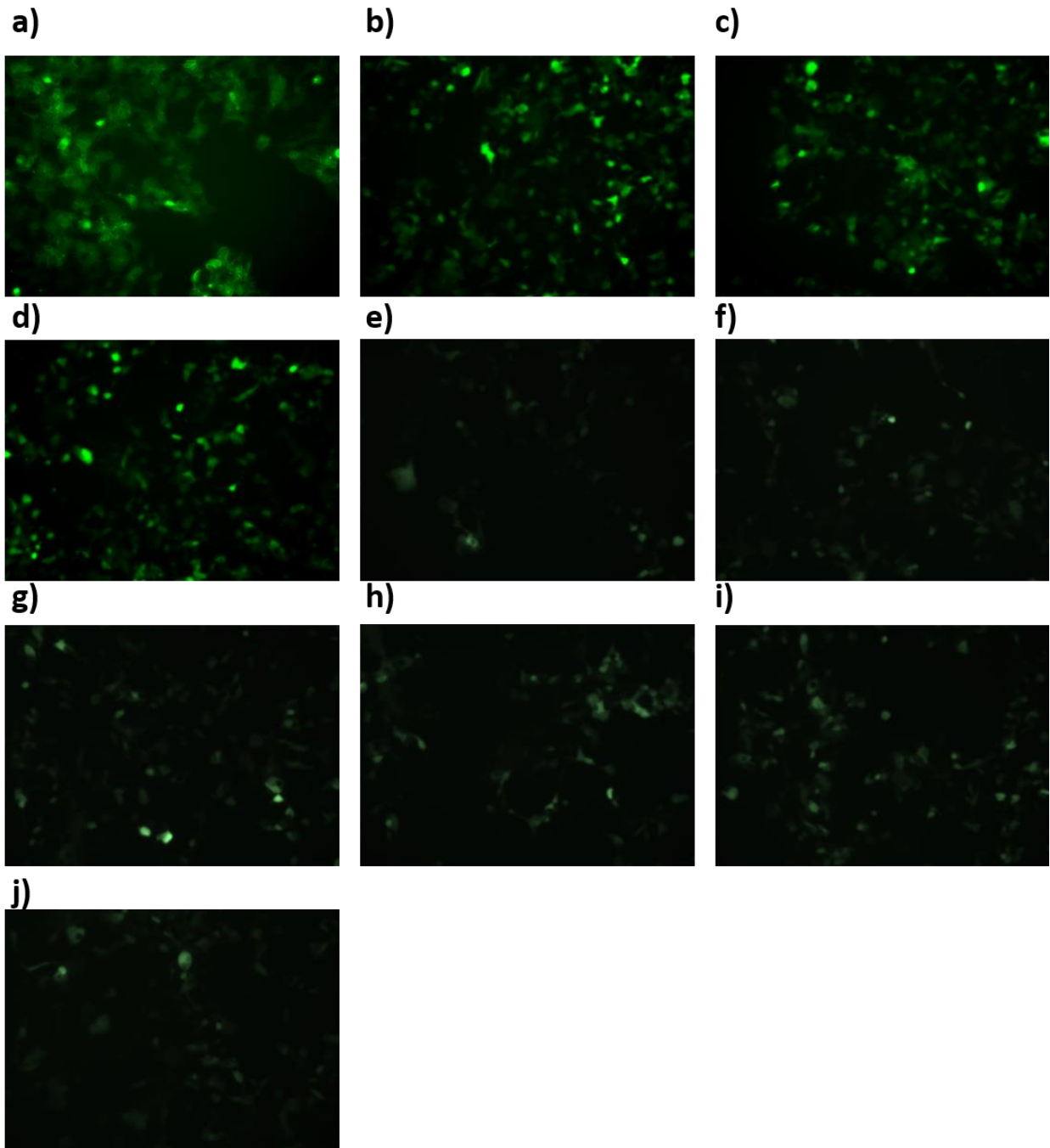


Figure 2.12. Fluorescence imaging of HEK293 cells expressing eGFP-KRas-C(x)(x) at 24 hours post transfection. a) -CVIM (positive control). b) -CLL. c) -CWI. d) -CQL. e) -CSI. f) -CQV. g) -CMF. h) -CQA. i) -CFV. j) -CVF. All images were collected at 20x magnification with 470/40 nm excitation filter, a 495 nm beam splitter and a 525/50 nm emission filter.

2.9 Investigating prenylation of Cxx c-terminal sequences in a biological context via protein lipidation quantification (PLQ)

Note: The PLQ data was collected and analyzed by Stanislav Beloborodov in the Krylov Lab (York University).

Despite not observing evidence for membrane localization of the modified eGFP-KRas protein that had Cxx sequences appended at its C-terminus, we could not conclusively interpret that these sequences were not modified inside HEK293 cells because these motifs may not undergo the subsequent post-processing steps required for them to be shuttled to the cell membrane following prenylation. To further evaluate the biological relevance of non-canonical Cxx sequences, we utilized another strategy for directly detecting protein lipidation inside a mammalian system that is not reliant on membrane localization as a proxy for prenylation.

One such approach is Protein Lipidation Quantification (PLQ), which is derived from an established method of Micellar Electro-Kinetic Chromatography (MEKC) that utilizes detergent micelles to provide molecular separation during capillary electrophoresis.⁵⁹⁻⁶¹ In this method, a detergent such as SDS is used to form micelles in the running buffer with which the analyte can interact. These micelles serve as pseudo-stationary phase and travel relatively slowly through the capillary tube compared to free analyte or buffer because of an electrophoretic drag associated with the viscosity and charge of the micelle as it moves through the electric field within the capillary. The electrophoretic mobility of the micelle is opposite to the direction of the electroosmotic flow (EOF) in the capillary resulting in micelle-associated analytes that exhibit a slower overall velocity towards the cathode. PLQ has been successfully used to separate prenylated full length fluorescent protein with a C-terminus CaaX motif in in-cell studies.⁶¹

Before we could probe prenylation of non-canonical Cxx motifs in a mammalian system via PLQ, we established standards using bacterially expressed and purified eGFP proteins appended with a canonical motif, -CVLS and two non-canonical motifs of the form, -CLL and -CVL. The plasmids for these proteins were obtained by performing site-directed mutagenesis on a pJExpress414-eGFP-CVDS plasmid (see Materials and Methods). This plasmid has a His-tag at the N-terminus allowing for Ni²⁺-resin based purification. Following expression and purification of eGFP-CVLS, eGFP-CVL, and eGFP-CLL, reactions were carried out to farnesylate the purified proteins with purified FTase enzyme and FPP donor (see Materials and Methods). Negative controls were performed in parallel without FPP. Reactions were incubated overnight under foil and then stored in -80°C the following day. PLQ analysis was performed by our collaborators in the Krylov Lab, York University. The results in Figure 2.13 show that we were able to detect the non-prenylated eGFP-CVLS/-CVL/-CLL and their prenylated counterparts at a longer retention time. However, it is important to note that the prenylated eGFP-Cxx protein products are modified to a smaller extent compared to the eGFP-CVLS positive control suggesting that these shorter sequences are not as reactive as CVLS, which is in agreement with our steady-state analysis (Section 2.6). Nonetheless, this study laid the groundwork for using PLQ to analyze prenylation of eGFP-CVLS/-CVL/-CLL proteins in a mammalian cellular context.

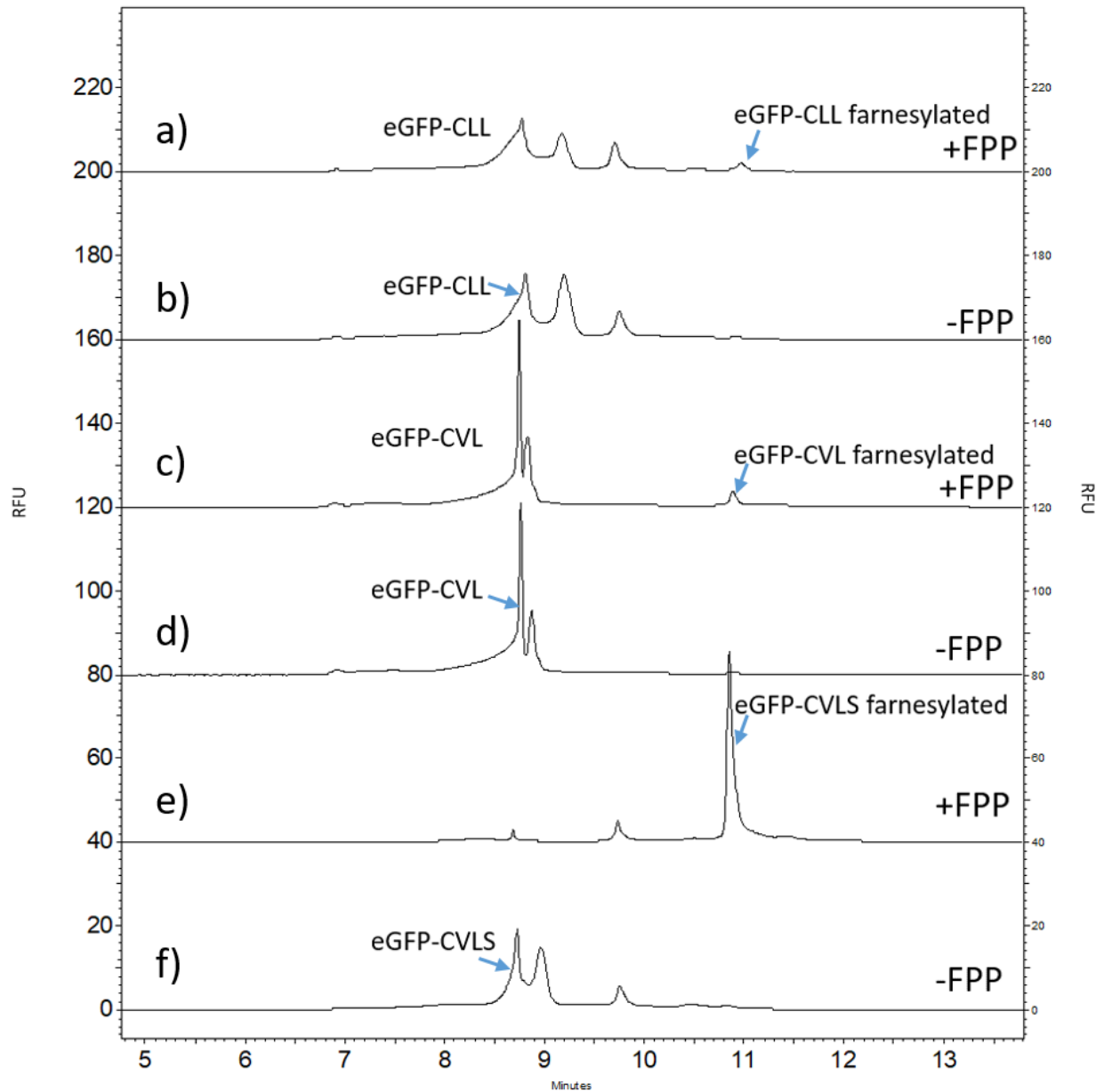


Figure 2.13. Prenylation assessment of purified eGFP samples appended with various c-terminal motifs via PLQ at 520 nm: a) eGFP-CLL in presence of FTase and FPP. b) eGFP-CLL in presence of FTase only. c) eGFP-CVL in presence of FTase and FPP. d) eGFP-CVL in presence of FTase only. e) eGFP-CVLS (positive control) in presence of FTase and FPP. f) eGFP-CVLS in presence of FTase only. PLQ analysis was performed by Stanislav Beloborodov from the Krylov Lab (York University).

After establishing bacterial standards as described, we transfected HEK293 cells with eGFP reporter proteins fused to canonical and non-canonical peptide sequences at the C-terminus to determine if prenylation of non-canonical Cxx sequences inside cells could be detected by PLQ. Six total plasmids were transfected, including pCAF1-eGFP-CVLS/-CVL/-CLL and their respective serine negative controls of the form, pCAF1-eGFP-SVLS/-SVL/-SLL. The serine mutants should block prenylation. Transfection of 2×10^5 with 4 μ g DNA and 6 μ L Turbofect (Promega) in a 6-well plate was found to be the ideal transfection condition with 24-hour incubation post-transfection (see Materials and Methods). Robust eGFP expression was confirmed via fluorescence imaging, following which cells were collected by scraping, re-suspended in 1X PBS, harvested by centrifugation, and stored immediately in -80°C .

The results obtained did not provide evidence for prenylation of non-canonical Cxx sequences in a mammalian context as both -Cxx sequences and their serine negative controls displayed the same pattern of detection (Figure 2.14). We were able to detect the prenylated eGFP-CVLS protein, confirming that the system is viable for this study, with the serine mutant not shown to be prenylated. Of note, we observed additional peaks that may represent different phosphorylation states of the serine residues in the proteins tested; this phenomenon will be the focus of further studies.

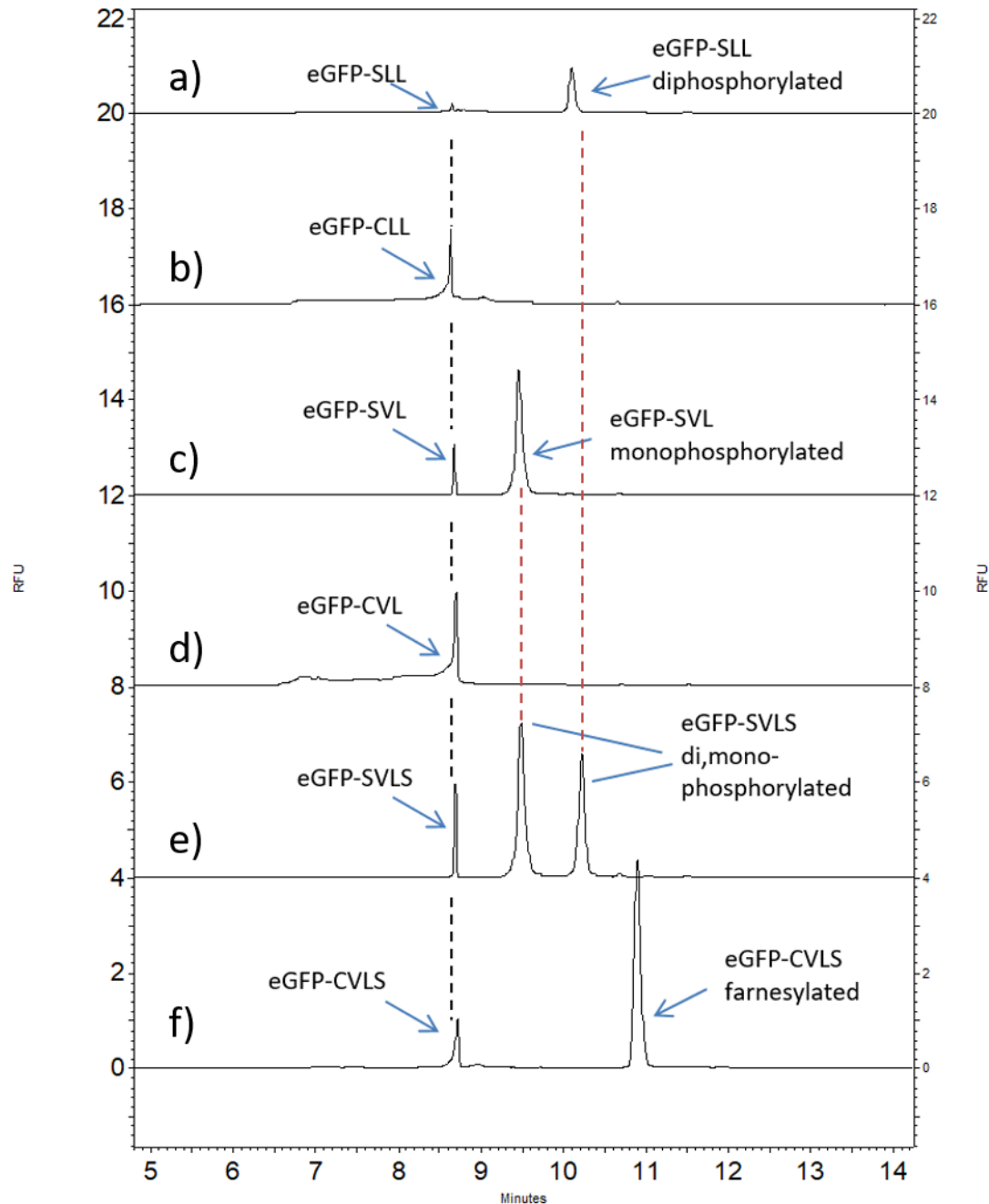


Figure 2.14. Prenylation assessment via PLQ of HEK293 cell lysate expressing eGFP-C(S)xx: a) -SLL. b) -CLL. c) -SVL. d) -CVL. e) -SVLS. f) -CVLS. Blue arrows indicate peaks representing both the unmodified eGFP sample and modified products. Black dotted lines serve as reference points for retention times of the unmodified substrates, while red dotted lines serve as reference points for potentially phosphorylated products. The mono- and di-phosphorylated labeled products are assigned purely hypothetically and require further investigation. PLQ analysis was performed by Stanislav Beloborodov in the Krylov Lab (York University).

2.10 Conclusions

Prenylation by FTase and GGTase-I is an important post-translational modification within eukaryotic proteomes. The canonical CaaX C-terminal motif is generally accepted as the most prevalent class of substrates for these enzymes. The recent finding that FTase can target longer C(x)₃X sequences has expanded the potential substrate scope for this enzyme,⁶ which we have further expanded by our current findings that FTase can accept shorter Cxx sequences. The Cxx sequences that we identified *in vivo* using yeast-based a-factor and Ydj1 reporter assays were also among the most reactive in *in vitro* studies using human FTase, suggesting these identified Cxx sequences have potential biological relevance. In this study, we additionally demonstrate that mammalian FTase can utilize GGPP as the prenyl donor for modification of a subset of Cxx sequences. While FTase can be mutated to allow GGPP to serve as the prenyl donor,⁴¹ this is the first reported example of wild type FTase catalyzing peptide geranylgeranylation with comparable efficiency to farnesylation of the same sequences. Our findings support the further investigation of proteins terminating in Cxx sequences in cellular systems to determine their prenylation status and impact of such modification on the biological activities of Cxx proteins.

This work expands both the peptide and prenyl donor substrate pools for FTase, which further highlights the truly remarkable degree of substrate flexibility exhibited by this enzyme. By contrast, the inability of GGTase-I to accept dns-GCxx sequences as substrates demonstrates that it displays stricter peptide length and sequence determinants than FTase. While the outcome of our FPP/GGPP competition assay clearly shows FTase prefers FPP over GGPP as a prenyl donor, the promiscuous utilization of GGPP as a prenyl donor could lead to alternative prenylation when FPP levels are depleted. It is also possible that certain Cxx sequences can be

preferentially geranylgeranylated by FTase, as it is well established for CaaX sequences that there is interplay between peptide sequence and prenyl donor selectivity.^{53, 62-64} Indeed, in this study using **a**-factor and Ydj1p reporters, while we assume the Cxx sequences are modified with farnesyl, we cannot formally discount that geranylgeranylation has also occurred. We expect to gain a better understanding of how FTase utilizes FPP and GGPP for prenylation of Cxx sequences through future structural and computational modeling studies of peptides from this new substrate class in complex with FTase and prenyl donors.

In interpreting the biochemical significance of FTase-catalyzed Cxx sequence prenylation, it is important to consider whether these sequences are being recognized as peptide/protein sequences or merely as thiols with appended functional groups. Previous work has shown FTase can farnesylate nonpeptidic thiols such as dithiothreitol and methyl thioglycolate (MTG).⁶⁵ That study demonstrated that thiol coordination to the catalytic zinc ion of FTase can lead to substrate binding, but peptide interactions enhance binding and catalysis. Our data suggests that the latter occurs with Cxx sequences. First, the steady state parameters (k_{cat}/K_m) determined for Cxx sequences range from 200- to 2300-fold higher than the highest k_{cat}/K_m reported for a nonpeptidic thiol (MTG, $1.7 \text{ M}^{-1}\text{s}^{-1}$).⁶⁵ Second, the substrate selectivity between Cxx peptides exhibited in FTase reactions with both FPP and GGPP prenyl donors indicates the peptide sequence strongly influences the ability of FTase to accept these peptides as substrates. Together, our findings support that the Cxx substrates are recognized by FTase as peptide sequences, although with lower reactivity than CaaX sequences.

Looking to the future, assessing the impact of Cxx sequence prenylation in biological systems represents the most important research avenue motivated by our current findings. Within yeast, we have demonstrated the ability of these sequences to support effective prenylation of

Ydj1p and a Ydj1p-based thermotolerance phenotype, indicating that Cxx sequences can exhibit biologically relevant reactivity. While no prenylated Cxx proteins have been identified by mass spectrometry-based proteomics studies utilizing chemically modified prenyl donors,⁶⁶⁻⁷¹ this may reflect multiple factors including reduced reactivity with prenyl donor analogues used for proteomics analysis, low Cxx sequence reactivity or protein abundance, or mass spectrometry complications such as neutral loss or peptide oxidation. The lack of evidence for the prenylation of Cxx sequences inside cells suggests that the sequences tested in this study are not reactive enough to be modified by FTase in our cell-based assay. The subset of Cxx sequences derived from the human proteome that were examined in this work are less reactive than canonical CaaX sequences (e.g. dns-GCLL peptide is ~40 fold less reactive than dns-GCVLS),⁵³ but the reactivity of dns-GCLL lies near the range established as viable for prenylation within a mammalian cell.⁵⁷ Thus, prenylated yeast and human Cxx proteins remain an intriguing possibility with a significant number of proteins bearing Cxx-terminal sequences predicted in the human proteome (Table 2.1). In addition to the selectivity rules defining Cxx sequence reactivity with FTase with both FPP and GGPP prenyl donors, cell-based studies of novel prenylated Cxx sequences will be essential for defining the biological roles potentially played by these proteins and the expanding importance of prenylation within proteomes.

2.11 Materials and Methods

2.11.1 Miscellaneous Methods: All *in vitro* FTase and GGTase-I assays were performed at 33 °C. All curve fitting was performed with KaleidaGraph (Synergy Software, Reading, PA). Geranylgeranyl diphosphate (GGPP) and farnesyl diphosphate (FPP) were purchased from Isoprenoids.com (Tampa, FL). Peptides were commercially synthesized (Sigma-Genosys, The Woodlands, TX) and exhibited >90% purity, as determined by RP-HPLC or after semi-prep purification via RP-HPLC. Peptides were solubilized in ethanol containing 10% (v/v) DMSO and stored at -80 °C. Peptide concentrations were determined spectrophotometrically using Ellman's reagent. The isoprenoid analog C15Alk-OPP was prepared as previously described.⁷²

2.11.2 Yeast strains (These experiments were performed in the Schmidt laboratory,

University of Georgia): Several of the yeast strains used in this study have been previously described: IH1793 (*MAT α lys1*), RC757 (*MAT α sst2-1 rme his6 met1 can1 cyh2*), SM2331 (*MAT α trp1 leu2 ura3 his4 can1 mfa1 mfa2*), BY4741 (*MAT α his3 Δ 1 leu2 Δ 0 met15 Δ 0 ura3 Δ 0*), yWS304 (*MAT α his3 Δ 1 leu2 Δ 0 met15 Δ 0 ura3 Δ 0 ydj1::KAN^R*).⁷³⁻⁷⁶ Multiple other strains were created for this study.⁴⁴ yWS2542 (*MAT α his3 Δ 1 leu2 Δ 0 met15 Δ 0 ura3 Δ 0 ram1::KAN^R ydj1::NAT^R*) was created by replacing the *YDJ1* open reading frame with the nourseothricin resistance cassette (NAT^R) in yWS1632 (*MAT α his3 Δ 1 leu2 Δ 0 met15 Δ 0 ura3 Δ 0 ram1::KAN^R*). This was accomplished by transformation of the strain with a restriction enzyme digestion of pWS1623 (*BamHI*, *HindIII*, *PvuII*) and selection on yeast rich media agar plates (YPD) containing 100 μ g/ml nourseothricin. yWS2544 (*MAT α his3 Δ 1 leu2 Δ 0 met15 Δ 0 ura3 Δ 0 ydj1::NAT^R*) was made in similar fashion using BY4741 as the parent strain. yWS2938-2951 and yWS2958-2959 were created by integrating Ydj1p-Cxx mutants into the *ydj1::NAT^R* locus of

yWS2544. Integrating DNA fragments were derived by restriction digestion from appropriate *CEN URA3 YDJI-Cxx* plasmids (*BamHI*, *XhoI*, *PvuI*, *BglI*). Candidate colonies were scored for improved thermotolerance and concomitant loss of nourseothricin resistance. The gene replacements and integrations were confirmed by PCR using primers external and internal to the integrated fragment and sequencing of PCR products derived from the Cxx encoding genomic DNA. Yeast strains were propagated at 30 °C (IH1793, RC757, SM2331, yWS2938-2952, yWS2958-2959) or room temperature (yWS2542, yWS2544) on either YPD or appropriate selective media when plasmid transformed.

2.11.3 Yeast plasmids and oligo designs (These experiments were performed in the Schmidt

laboratory, University of Georgia): The plasmids used in this study were either pre-existing or newly constructed for this study as noted.⁴⁴ Unless noted otherwise, new constructs were created *in vivo* by recombination of a linearized parent plasmid and appropriate PCR amplified DNA fragments. Plasmids encoding **a**-factor mutants (i.e. CVI, CV, C, AVI, SVI) were created using parent plasmids pWS610 (*MluI*) or pWS817 (*PstI*, *MluI*). Plasmids encoding Ydj1p mutants (i.e. CTI, CII, CFV, CVI, AVI, SVI) were created using parent plasmid pWS1132 (*NheI*, or *NheI* and *AflIII*).^{6, 77} pWS1623 (*CEN URA3 ydj1::NAT^R*) was created using a NAT^R PCR product and pWS1132 (*NheI* and *BsaBI*). The NAT^R PCR product was derived from p4339 and was designed to have flanking sequence identical to the 5' and 3' UTRs of the *YDJI* ORF. pWS114 (*2μ URA3 RCE1*) was constructed by subcloning the *BglI* fragment from pSM1275 (*CEN URA3 RCE1*) into the *BglI* site of pSM217.^{75, 78} pWS1808 (*2μ URA3 RAM1*) was constructed in two steps. First, pWS1767 (*CEN URA3 RAM1*) was created through *in vivo* recombination of *HindIII*-linearized pRS316 (*CEN URA3*) and a PCR-derived DNA fragment containing the *RAM1* gene

that was amplified from BY4741 genomic DNA. Second, the *XhoI-SacI* fragment from pWS1767 was subcloned into the same sites of pRS426 (2μ *URA3*).⁷⁹ Introduction of plasmids, plasmid digests, and PCR-derived DNA fragments into yeast strains was via a lithium acetate-based transformation procedure.⁸⁰

The synthetic oligonucleotides used for generating random Cxx sequences that underwent genetic screening were based on the CaaX encoding region of either *MFA1* or *YDJI* as encoded in pWS1024 and pWS1132, respectively. The forward PCR oligo encoded the Cxx sequence and was flanked by sequences on the 5' and 3' ends that were homologous to the target gene; the 5' sequence facilitates recombination and the 3' sequence facilitates PCR priming. All nucleotides were allowed at the x positions, allowing for the formation of all 400 Cxx permutations and two nonsense mutations (i.e. C-stop and Cx-stop). The reverse oligo matched a region in the polylinker sequence adjacent to the 3' UTR of each gene. The synthetic oligonucleotides used for generating specific Cxx sequences were as described above for random Cxx sequence but were individually designed to create the desired Cxx sequence. The synthetic oligonucleotides used to amplify the *RAM1* gene contained 5' sequences homologous to the recipient vector pRS316 to facilitate recombination and 3' sequences homologous to intergenic regions surrounding the *RAM1* gene to facilitate PCR priming such that 491 and 271 nucleotides of the 5' and 3' intergenic regions were amplified, respectively.

2.11.4 a-factor mating pheromone screen, halo assay, and mating test (These experiments were performed in the Schmidt laboratory, University of Georgia): *MATa* yeast lacking the *MFA1* and *MFA2* a-factor genes (SM2331) were co-transformed with digested pWS1024 (*MluI*, *SphI*) and a PCR product encoding randomized Cxx sequences. The transformation mix was

plated on synthetic complete agar plates lacking leucine (SC-leucine) and incubated at 30 °C for 72-96 hours to allow for colony formation. Colony counts were determined before replica plating the colonies onto an SC-leucine plate (replica plate) and a minimal media plate (diploid-selective) containing a thin lawn of IH1793 yeast. Plates were incubated at 30 °C for 72-96 hours, diploid colonies were identified, and the corresponding *MATa* parent colony recovered from the SC-leucine replicate plate. The *MATa* strains were individually cultured to saturation, spotted onto a lawn of *MAT α sst2-1* yeast (RC757), and strains visually scored for strength of halo production. Plasmids were isolated and sequenced from the strongest halo producing strains. For figure production, plasmid transformants of SM2331 were cultured to saturation in selective SC-leucine liquid media, cultures pinned onto SC-leucine plates, plates incubated for 24-36 hours at 30 °C, and the dense spots of growth were replica transferred onto a thin lawn RC757 yeast. Plates were scanned as described below after incubation at 30 °C for 16-20 hours.

Quantitative mating was performed as previously described.^{6, 18} *MATa* strains derived from SM2331 to express indicated **a**-factor Cxx mutants were cultured to saturation in selective liquid media, diluted to $A_{600} \sim 1.0$ using fresh culture media, then mixed with an excess of IH1793 *MAT α lys1* strain cultured and diluted in the same manner but with non-selective YPD. The number of colony forming units (CFUs) were determined on both SC-lysine and synthetic minimal media agar plates (SD) using empirically determined dilutions; SC-lysine selects for the total of *MATa* haploid and *MATa/ α* diploid cells, while SD selects for diploids only. Mating frequencies ($CFU_{diploid}/CFU_{total}$) were determined for each mutant and were reported as a percentage relative to a strain producing wild type **a**-factor.

2.11.5 Thermotolerance screen and assays (These experiments were performed in the

Schmidt laboratory, University of Georgia): The Ydj1p screen was performed essentially as previously described.⁶ In brief, yeast lacking the *YDJ1* gene (yWS304) were co-transformed with the PCR product encoding randomized Cxx sequences and digested pWS1132 (*NheI*). A portion of the transformation mix was plated on SC-uracil solid media and incubated at 25 °C for 96 hours to assess the total number of CFUs in the mix. The remaining transformation mix was plated on YPD solid media and incubated at 40 °C for 96 hours. Plasmids were recovered from thermotolerant colonies, sequenced, and re-introduced into yWS304 to confirm plasmid-linked thermotolerance prior to detailed thermotolerance analysis involving incubation at various temperatures (25 °C, 37 °C, or 40 °C). In brief, saturated cultures grown at room temperature in SC-uracil liquid media were serially diluted into YPD, dilutions pinned onto YPD solid media, and plates incubated for several days at desired temperature. Each experiment was performed at least twice on separate days, and each strain was evaluated in duplicate within each experiment.

2.11.6 Estimate of Cxx complexity in a-factor and thermotolerance screens (These

experiments were performed in the Schmidt laboratory, University of Georgia): The GLUE-IT algorithm was used to estimate coverage of the screen.⁸¹ The algorithm takes into account the CFUs evaluated for each screen and the number and redundancy of the codons used for amino acid randomization. The number of colonies associated with transformation of linearized plasmids or PCR products alone (i.e. false positives) were not counted toward the CFU total. The false positive rate was typically low (<2%) relative to co-transformed sample. In the case of the thermotolerance screen, the CFU value derived from growth observed on SC-uracil solid media at 25 °C (i.e. ~8,400) was adjusted to 14% of its value to account for the observation

that incubation at 40 °C reduces transformation efficiency.¹⁹

2.11.7 Immunoblot analysis for protein prenylation in yeast (These experiments were performed in the Schmidt laboratory, University of Georgia): Whole cell lysates of mid-log yeast were prepared as previously described, separated by SDS-PAGE (14%), transferred onto nitrocellulose, and blots incubated with rabbit anti-Ydj1p primary antibody (courtesy of Dr. Avrom Caplan) and HRP-conjugated goat anti-rabbit secondary antibody (Kindle Biosciences, Greenwich, CT).^{18, 82} Immune complexes were detected using a KwikQuant Imager at multiple exposure times after development of blots with the KwikQuant Western Blot Detection Kit (Kindle Biosciences).

2.11.8 Image analysis for yeast plates and immunoblot films (These experiments were performed in the Schmidt laboratory, University of Georgia): A flat-bed scanner was used to image plates at 300 dpi (grayscale). Plates were scanned face down without lids using a black background. Digitized TIFF images of plates and immunoblots were imported into Photoshop for minor adjustments (i.e. image rotation, contrast, cropping, etc.) then copied to PowerPoint for final figure assembly. Contrast settings within Photoshop were adjusted for all plate images to be identical and to maximize dynamic range of signal; settings for immunoblot images were unchanged.

2.11.9 Expression and purification of FTase and GGTase-I: Rat FTase and GGTase-I were expressed in BL21(DE3) *E. coli* and purified as previously described.^{6, 40}

2.11.10 RP-HPLC-based assay for screening the reactivity of dns-GCxx peptides and

assessing prenylation preference by FTase: Dns-peptides (3 μM) were diluted into 1x FTase reaction buffer (50 mM HEPPSO-NaOH, pH 7.8, 5 mM TCEP, 5 mM MgCl_2 ; 50 μL total) and incubated for 20 minutes in 0.65 mL low-adhesion microcentrifuge tubes. Prenylation reactions were initiated by adding an enzyme mix (200 nM rat FTase, 10 μM FPP or GGPP, in 1x FTase reaction buffer). Reactions were incubated at 33 $^\circ\text{C}$ for 16 hours and then quenched with an equal volume of 20% acetic acid in isopropanol. RP-HPLC analysis was performed at ambient temperature on an Agilent 1260 HPLC system with auto-sampler, UV-Vis, and fluorescence detection using a C18 reversed-phase analytical column (Zorbax XDB-C18) with a linear gradient from 30% acetonitrile in 25 mM ammonium acetate to 100% acetonitrile flowing at 1 mL/min over 30 minutes; peptides and products were detected by fluorescence (λ_{ex} 340 nm, λ_{em} 496 nm). Chromatogram analysis and peak integration was performed using Chemstation for LC (Agilent Technologies).

For prenyl donor preference assays, the reactivity of dns-GCxx peptides (CFT, CFV, CGF, CMF, and CVF) was evaluated as described above with varying concentration of FPP and GGPP (10 μM FPP only, 7.5 μM FPP + 2.5 μM GGPP, 5 μM FPP + 5 μM GGPP, 2.5 μM FPP + 7.5 μM GGPP, and 10 μM GGPP only).

2.11.11 Fluorescence-based assay for screening reactivity of dns-GCxx peptides,

determining prenyl donor saturating concentration, and determining steady-state kinetic

parameters: Steady-state kinetic parameters were determined for FTase from a time-dependent increase in fluorescence (λ_{ex} 340 nm, λ_{em} 520 nm) upon prenylation of the dansylated peptide,

with assays performed with 0.5–10 μM dansylated peptide, 100 nM purified rat FTase, and 10 μM FPP or GGPP in 1x FTase reaction buffer at 33 °C in a 96-well plate (Corning); reactivity screening was performed using 3 μM peptide. Peptides were incubated in reaction buffer for 20 minutes prior to reaction initiation by addition of FTase and prenyl donor. The fluorescence was monitored over a period of 7-8 hours at 33 °C in the BioTek H1 Synergy plate reader (λ_{ex} 340 nm, λ_{em} 520 nm) with fluorescence measured at intervals of 30-40 seconds. Initial velocity for prenylation of dns-GCxx peptides was determined from a time-dependent increase in fluorescence upon prenylation of the dansylated peptide. To confirm that 10 μM FPP and GGPP represented a saturating concentration of these cosubstrates (Figure 2.15), assays were performed as described above with 3 μM dns-GCFT peptide, 100 nM purified rat FTase, and 2–10 μM FPP or GGPP in 1x FTase reaction buffer at 33 °C in a 96-well plate (Corning). The initial velocities for dns-GCFT prenylation using both FPP and GGPP prenyl donors decrease less than 2-fold when the prenyl donor concentration is reduced from 10 μM to 2 μM , consistent with 10 μM representing saturating prenyl donor (Figure 2.15).

To obtain steady state ($k_{\text{cat}}/K_{\text{m}}$) parameters for peptide reactivity, the total fluorescence change observed upon reaction completion was divided by the initial concentration of the peptide substrate in a given reaction to yield a conversion factor from fluorescence units to product concentration (μM). These values were averaged over several peptide concentrations to give an amplitude conversion (AmpConv), whose units are fluorescence units per micromolar of product formed (FI/ μM). The linear initial rate, whose units are fluorescence intensity per second (FI/Sec), was converted to a velocity ($\mu\text{M}/\text{sec}$) using equation 1, where V is velocity ($\mu\text{M}/\text{s}$), R is the velocity (FI/s), and AmpConv is the ratio described above (FI/ μM).

$$V = R/\text{AmpConv} \text{ (equation 1)}$$

The reaction velocities (V) were divided by the enzyme concentration (μM) to get $V/[E]$ ratios having units of sec^{-1} . A steady-state kinetic parameter (k_{cat}/K_m) was determined from a fit of the Michaelis-Menten equation to the dependence of the initial velocity divided by the enzyme concentration ($V/[E]$) on the peptide concentration in presence of saturating prenyl donor ($10 \mu\text{M}$). Errors represent the standard deviation from three replicate measurements.

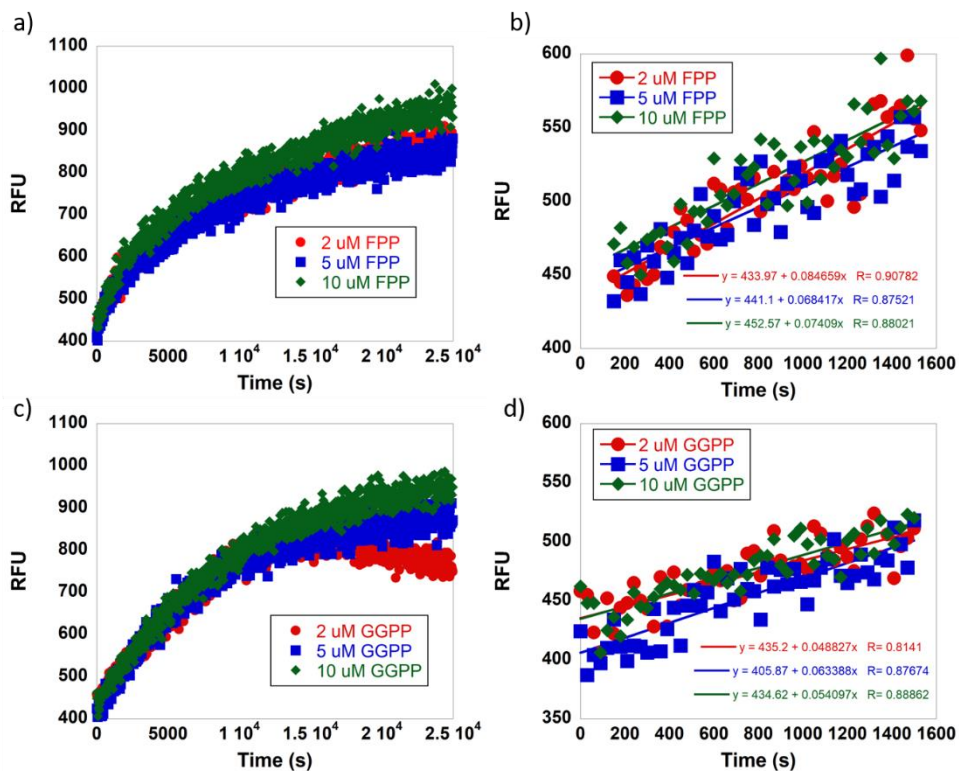


Figure 2.15. Determination of saturating FPP and GGPP concentrations for FTase-catalyzed prenylation of dns-GCFT. a) Time course for FTase-catalyzed farnesylation of dns-GCFT in the presence of various FPP concentrations (2 μM, red; 5 μM, blue; 10 μM, green); b) Determination of initial velocities for FTase-catalyzed farnesylation of dns-GCFT in the presence of various FPP concentrations (2 μM, red; 5 μM, blue; 10 μM, green). c) Time course for FTase-catalyzed geranylgeranylation of dns-GCFT in the presence of various GGPP concentrations (2 μM, red; 5 μM, blue; 10 μM, green); b) Determination of initial velocities for FTase-catalyzed geranylgeranylation of dns-GCFT in the presence of various GGPP concentrations (2 μM, red; 5 μM, blue; 10 μM, green). This figure has been reused with permission from reference 44 (Appendix II).

2.11.12 RP-HPLC-based and fluorescence-based assays for screening the reactivity of dns-GCxx peptides by GGTase-I: Dns-peptides (3 μ M) were diluted into 1x GGTase-I reaction buffer (50 mM HEPPSO-NaOH, pH 7.8, 5 mM TCEP; 50 μ L total) and incubated for 20 minutes in 0.65 mL low-adhesion microcentrifuge tubes. Prenylation reactions were initiated by adding an enzyme mix (200 nM rat GGTase-I, 10 μ M GGPP, in 1x reaction buffer). Reactions were incubated at 33 °C for 16 hours then quenched with an equal volume of 20% acetic acid in isopropanol. RP-HPLC analysis was performed similarly to reactions with FTase. The fluorescence-based assay was monitored over a period of 10 hours at 33 °C in the BioTek H1 Synergy plate reader (λ_{ex} 340 nm, λ_{em} 520 nm) with fluorescence measured at intervals of 37 seconds.

2.11.13 LC-MS analysis of dns-GCxx peptides modified by FTase (LC-MS experiments were performed in the Castaneda laboratory with assistance from Tongyin Zheng, Syracuse University): *In vitro* reactions with dns-GCxx peptides (3 μ M) were prepared in 1x FTase reaction buffer in the presence of rat FTase (200 nM) and prenyl donor (10 μ M) and incubated at 33 °C for 16 hours before isolation of the farnesylated or geranylgeranylated peptide by RP-HPLC. Reactions (2 mL) were purified via semipreparative RP-HPLC (Zorbax Eclipse XDB-C18 column 9 x 250 mM) using a linear gradient of 30:70 TFA in water (0.05%):acetonitrile (HPLC grade) with a flow rate of 3.2 mL/min over 42 min. The peak corresponding to the prenylated peptide was detected by UV absorbance at 360 nm, with this peak collected and dried under reduced pressure overnight before re-dissolving in 50% acetonitrile. Product peptide mass was determined by LC-MS (ESI) using a Shimadzu LCMS-8040 mass spectrometer with a mobile phase of 5% ACN, 95% water used at a flow rate of 0.2

mL/min using 5 μ L of purified prenylated peptide dissolved in 50% ACN and DI water; peak intensity was monitored from $m/z = +200$ to $+2000$.

2.11.14 Determination of tipifarnib inhibition of dns-GCxx peptide prenylation: Assays were performed as described in our plate-reader based activity screening, with varying concentrations of tipifarnib (0-500 nM) included in the reaction. Initial slopes (fluorescence change per second) were determined for each reaction and normalized to the reaction without tipifarnib. Normalized slope values were plotted against tipifarnib concentration and analyzed using the equation shown below to calculate IC₅₀ values.

$$\text{Normalized Slope} = 1 - [\text{tipifarnib}]/([\text{tipifarnib}] + \text{IC}_{50})$$

2.11.15 Construction of eGFP-KRas-CLL/-CWI/-CQL reporter protein plasmids: The vector plasmids encoding for eGFP-KRas-Cxx were prepared by PCR using the pEGFP-KRas vector obtained from the Casey Lab (Duke University) serving as a template and -CLL, -CWI, and -CQL C-terminal sequence and *KpnI* restriction site present in the 3' primers (Integrated DNA Technology, Coralville, IA):

eGFP-KRas-CLL:

5'-GAAAAGAAGTCAAAGACAAAGAGTACTGGATGTCTGCTGTAAGGTACCCTAAG-3'

eGFP-KRas-CWI:

5'-GAAAAGAAGTCAAAGACAAAGAGTACTGGATGTTGGATCTAAGGTACCCTAAG-3'

eGFP-KRas-CQL:

5'-GAAAAAGAAGTCAAAGACAAAGAGTACTGGATGTGAACTGTAAGGTACCCTAAG-3'

The PCR reaction (50 μ L) consisted of 1x Standard OneTaq buffer, 10 mM dNTPs, 125 ng reverse and forward primers each, 10 ng template plasmid, and OneTaq DNA polymerase (0.25 μ L, 5U/ μ L). The PCR reactions were performed in a BioRad Mycycler thermal cycler using the following program: Initial denaturation (94°C, 1 min); thirty cycles of denaturation (94°C, 30 sec), annealing (56°C, 1 min), and extension (68°C, 2 min); final extension (68°C, 5 min); and a final hold (10°C, ∞). PCR products were purified using BIO Basic Inc. EZ-10 Spin Column PCR purification Kit following the manufacturer's protocol. Following digestion by *NheI* and *KpnI*, the eGFP-KRas-Cxx insert was ligated into the pEGFP-KRas plasmid using the Quick Ligase kit (NEB), following the manufacturer's instructions. Insert ligation was verified by analytical restriction digest and gene sequencing (Genewiz).

2.11.16 Site-directed mutagenesis of eGFP-KRas-CLL reporter protein to generate 6

remaining -Cxx sequences: PCR mutagenesis primers were designed to obtain the desired Cxx sequence per manufacturer's protocols (Stratagene) and were synthesized by Integrated DNA Technologies. Primers were dissolved in ultra-pure water and concentrations were measured by UV absorbance at 260 nm (1 OD= 33 μ g/mL). Each PCR mutagenesis reaction (50 μ L) contained the following components: 10x Pfu reaction buffer (5 μ L), template plasmid (10 ng), forward primer (125 ng), reverse primer (125 ng), dNTP mixture (1 μ L of 10 mM). The reaction was gently mixed, centrifuged, and 1 μ L of Pfu Turbo DNA polymerase (Agilent) was added. PCR mutagenesis reactions were performed in a BioRad Mycycler thermal cycler using the following temperature program: Initial denaturation (95°C, 1 min); 18 cycles of denaturation

(95°C, 50 sec); annealing (60°C, 50 sec) and extension (68°C, 12 min) followed by final extension (68°C, 12 min). Following PCR, reactions were treated with DpnI (1 µL, 10 units/ µL) and incubated at 37°C for 1 hour. Z-competent DH5α E. coli cells (Zymo Research) were thawed on ice for 10 minutes and then transformed with 5 µL of the PCR reaction following which the cells were plated on pre-warmed LB-Amp plates and incubated overnight at 37°C. Two colonies were picked from each plate and inoculated into LB media (5 mL) containing 100 µg/ mL ampicillin and incubated with shaking (225 rpm) overnight at 37°C. Following overnight growth, a 10% glycerol stock was prepared stored at -80°C. Plasmid DNA was purified from the remaining saturated culture using EZ-10 spin column DNA purification kit (BioBasic) per the manufacturer's protocol. The mutations were confirmed by DNA sequencing (Genewiz).

2.11.17 Transfection and visualization of eGFP-KRas-Cxx fusion proteins in HEK293 cells:

HEK293 cells were maintained in 75 mL vented tissue culture flasks (Celltreat), and were split once reaching 80% confluency. Cells were grown in complete DMEM (DMEM supplemented with 10% fetal bovine serum (FBS) and 1 % (v/v) penicillin-streptomycin (MediaTech) in 5% CO₂ at 37°C. After allowing cells to adhere for 24 hours in complete DMEM media, a reaction mixture consisting of 1 µg DNA, 2 µL Turbofect reagent (Promega), and supplement free DMEM for a total volume of 500 µL was prepared and incubated at RT for 20 min. During this time, fresh complete DMEM was added to the HEK293 cells to a total volume of 1 mL per well. The reaction mixture was then added dropwise to 6x10⁴ HEK293 cells in a 24-well plate and incubated at 37°C, 5% CO₂ with humidity, for 24 hours. Following incubation, live cells were imaged using a Zeiss Axio Vert.A1 inverted fluorescence microscope with a 470/40 nm excitation filter, a 495 nm beam splitter and a 525/50 nm emission filter to verify successful

fluorescent protein expression and analyze fluorescence localization.

2.11.18 Site-directed mutagenesis of pJExpress414-eGFP-CVLL reporter protein to -

CVLS/-CLL/-CVL sequences: PCR mutagenesis primers were designed to obtain the desired C-terminal sequence per manufacturer's protocols (Stratagene) and were synthesized by Integrated DNA Technologies. Primers were dissolved in ultra-pure water and concentrations were measured by UV absorbance at 260 nm (1 OD= 33 µg/mL). Each PCR mutagenesis reaction (50 µL) contained the following components: 10x Pfu reaction buffer (5 µL), template plasmid (10 ng), forward primer (125 ng), reverse primer (125 ng), dNTP mixture (1 µL of 10 mM). The reaction was gently mixed, centrifuged, and 1 µL of Pfu Turbo DNA polymerase (Agilent) was added. PCR mutagenesis reactions were performed in a BioRad Mycycler thermal cycler using the following temperature program: Initial denaturation (95°C, 1 min); 18 cycles of denaturation (95°C, 50 sec); annealing (60°C, 50 sec) and extension (68°C, 12 min) followed by final extension (68°C, 12 min). Following PCR, reactions were treated with DpnI (1 µL, 10 units/ µL) and incubated at 37°C for 1 hour. Z-competent DH5α E. coli cells (Zymo Research) were thawed on ice for 10 minutes and then transformed with 5 µL of the PCR reaction following which the cells were plated on pre-warmed LB-Amp plates and incubated overnight at 37°C. Two colonies were picked from each plate and inoculated into LB media (5 mL) containing 100 µg/ mL ampicillin and incubated with shaking (225 rpm) overnight at 37°C. Following overnight growth, a 10% glycerol stock was prepared stored at -80°C. Plasmid DNA was purified from the remaining saturated culture using EZ-10 spin column DNA purification kit (BioBasic) per the manufacturer's protocol. The mutations were confirmed by DNA sequencing (Genewiz).

2.11.19 Expression and purification of pJExpress414-eGFP-CVLS/-CVL/-CLL: Chemically competent BL21 (DE3) E. coli were transformed with pJExpress414-eGFP-CVLS/-CVL/-CLL vectors. Following transformation and antibiotic selection, a colony from the transformation plate was inoculated into LB media (5 mL) containing 100 µg/mL ampicillin. Cultures were incubated and shaken at 225 rpm for 4 h at 37°C and then transferred to 0.5 liter of prewarmed auto-induction media (5 g tryptone, 2.5 g yeast extract, 10 mL 50X 5052 media [25% glycerol, 10% lactose, 2.5% glucose], 25 mM Na₂HPO₄, 25 mM KH₂PO₄, 50 mM NH₄Cl, 5 mM Na₂SO₄, 2 mM MgSO₄, 100 µL trace metals [50 µM FeCl₂, 20 µM CaCl₂, 10 µM MnCl₂, 10 µM ZnCl₂], 100 µg/mL ampicillin. Expression cultures were incubated for 19 h at 37°C with shaking. Cells were harvested by centrifugation and resuspended in 50 mL resuspension buffer (20 mM NaH₂PO₄, 300 mM NaCl, and 10 mM imidazole). Bacterial cell suspensions were lysed by sonication, clarified by centrifugation, and purified by affinity chromatography using a Ni-NTA HisTrap column (GE S4 Healthcare). Fractions containing the protein were combined and concentrated using a centrifugal concentrator. Concentrated samples were buffer exchanged to 50 mM Tris buffer (pH 7.8), divided into 20 µL aliquots, and stored at -20°C. Protein concentration was determined using the molar absorption of eGFP at 488 nm.

2.11.20 Farnesylation of purified His₆-eGFP-CVLS/-CVL/-CLL: 2 µM eGFP-CVLS/-CVL/-CLL were incubated with both 1X reaction buffer (50 mM HEPPSO-NaOH, pH7.8, 5 mM TCEP) and 5 mM MgCl₂ (0.5 mL total) for 20 minutes in 1.5 mL low-adhesion eppendorf tube. Farnesylation reactions were initiated by adding an enzyme mix (0.5 mL) containing 200 nM

FTase, 5 mM MgCl₂, 1X reaction buffer, and 10 μM FPP. Reactions were incubated at RT for 16 hours under foil before storage at -80°C. Negative controls were also set up without FPP.

2.11.21 Site-directed mutagenesis of pCAF1-eGFP-CVLS vector to obtain -CVL/-CLL/-

SVLS/-SVL/-SLL vectors: PCR mutagenesis primers were designed to obtain the desired C-terminus sequence per manufacturer's protocols (Stratagene) and were synthesized by Integrated DNA Technologies. Primers were dissolved in ultra-pure water and concentrations were measured by UV absorbance at 260 nm (1 OD= 33 μg/mL). Each PCR mutagenesis reaction (50 μL) contained the following components: 10x Pfu reaction buffer (5 μL), template plasmid (10 ng), forward primer (125 ng), reverse primer (125 ng), dNTP mixture (1 μL of 10 mM). The reaction was gently mixed, centrifuged, and 1 μL of Pfu Turbo DNA polymerase (Agilent) was added. PCR mutagenesis reactions were performed in a BioRad Mycycler thermal cycler using the following temperature program: Initial denaturation (95°C, 1 min); 18 cycles of denaturation (95°C, 50 sec); annealing (60°C, 50 sec) and extension (68°C, 12 min) followed by final extension (68°C, 12 min). Following PCR, reactions were treated with DpnI (1 μL, 10 units/ μL) and incubated at 37°C for 1 hour. Z-competent DH5α E. coli cells (Zymo Research) were thawed on ice for 10 minutes and then transformed with 5 μL of the PCR reaction following which the cells were plated on pre-warmed LB-Amp plates and incubated overnight at 37 °C. Two colonies were picked from each plate and inoculated into LB media (5 mL) containing 100 μg/mL ampicillin and incubated with shaking (225 rpm) overnight at 37 °C. Following overnight growth, a 10% glycerol stock was prepared stored at -80°C. Plasmid DNA was purified from the remaining saturated culture using EZ-10 spin column DNA purification kit (BioBasic) per the manufacturer's protocol. The mutations were confirmed by DNA sequencing (Genewiz).

2.11.22 Preparation of HEK293 cells expressing eGFP-CVLS/-CVL/-CLL/-SVLS/-SVL/-

SLL: The mammalian cell line HEK293 (ATCC) was maintained in 75 mL vented tissue culture flasks (Celltreat), and were split upon reaching 80% confluency. The cells were grown in complete DMEM (Dulbecco's Modified Eagle's Medium supplemented with 10% fetal bovine serum (FBS) and 1% (v/v) penicillin streptomycin (MediaTech)) in a humidified atmosphere with 5% CO₂ at 37 °C. For expression of the eGFP reporter proteins, 2 x 10⁵ cells were placed in 2 mL of complete DMEM per well of a tissue culture treated 6-well plate (Corning) (total of 5 wells). The cells were incubated 24-28 hours prior to transfection. The DNA-transfection reagent complex was prepared by incubating 4 µg of each reporter protein expression plasmid pCAF-eGFP-CVLS/-SVLS/-CVL/-SVL/-CLL/-SLL and 6 µL of the Turbofect transfection reagent (Thermo Scientific) in a total volume of 500 µL supplement free DMEM for 15 minutes at room temperature. The cells were then transfected with the prepared DNA-transfection reagent complex by drop wise addition into the wells of a 6-well tissue culture plate. Following transfection for 24 h, live cells were imaged using a Zeiss Axio Vert.A1 inverted fluorescence microscope with a 470/40 nm excitation filter, a 495 nm beam splitter and a 525/50 nm emission filter to verify fluorescent protein expression. The cells were then scraped and resuspended in PBS followed by centrifugation to harvest the cell pellet. The cell pellets were stored at -80 °C.

2.11.23 Preparation and analysis of proteins by PLQ (PLQ experiments were performed in

the Krylov laboratory, York University): Prior to the CE experiments, HEK293 cells were centrifuged for 2 min at ~13000 × g (Eppendorf 5417R centrifuge with F45-30-11 rotor (Fisher

scientific, PA, USA)) at 4 °C and the supernatant was collected. The obtained supernatant as well as purified proteins were diluted with the sample buffer consisting of 50 mM HEPES sodium salt (NaHEPPSO), 10 mM MgCl₂, 5 mM tris(2-carboxyethyl)- phosphine hydrochloride (TCEP), and 10 mg/mL bovine serum albumin (BSA) at pH 7.8. The BSA was added to reduce adsorption of the proteins onto capillary surface.

PLQ analysis was carried out with MDQ-PACE instrument (Sciex, formerly BeckmanCoulter, Caledon, ON, Canada) using laser-induced fluorescence (LIF) detection with excitation at 488 nm and emission at 520 nm for the detection of eGFP derivatives. Fused silica capillaries with total length of 50 cm were preconditioned by sequential washing with 100 mM HCl, 100 mM NaOH, Milli-Q water and running buffer (25 mM Borax, 20 mM SDS, pH 10.0) each for 2 min at 30 psi. The samples were injected into the capillary by 0.5 psi pressure pulse of 10 s. Electrophoretic separation was carried out with a positive electrode at the injection end of the capillary, with electric field strength of 15 kV at 25 °C.

References 2.12

1. Mann, M.; Jensen, O. N., Proteomic analysis of post-translational modifications. *Nature biotechnology* **2003**, *21* (3), 255-261.
2. Marshall, C. J., Protein prenylation: a mediator of protein-protein interactions. *Science* **1993**, *259* (5103), 1865-1866.
3. Casey, P. J.; Seabra, M. C., Protein prenyltransferases. *Journal of Biological Chemistry* **1996**, *271* (10), 5289-5292.
4. Zhang, F. L.; Casey, P. J., Protein prenylation: molecular mechanisms and functional consequences. *Annual review of biochemistry* **1996**, *65* (1), 241-269.
5. Benetka, W.; Koranda, M.; Eisenhaber, F., Protein prenylation: An (almost) comprehensive overview on discovery history, enzymology, and significance in physiology and disease. *Monatshefte für Chemie/Chemical Monthly* **2006**, *137* (10), 1241.
6. Blanden, M. J.; Suazo, K. F.; Hildebrandt, E. R.; Hardgrove, D. S.; Patel, M.; Saunders, W. P.; Distefano, M. D.; Schmidt, W. K.; Hougland, J. L., Efficient farnesylation of an extended C-terminal C (x) 3X sequence motif expands the scope of the prenylated proteome. *Journal of Biological Chemistry* **2018**, *293* (8), 2770-2785.
7. Lau, H. Y.; Tang, J.; Casey, P. J.; Wang, M., Isoprenylcysteine carboxylmethyltransferase is critical for malignant transformation and tumor maintenance by all RAS isoforms. *Oncogene* **2017**, *36* (27), 3934-3942.
8. Feig, L. A.; Buchsbaum, R. J., Cell signaling: life or death decisions of ras proteins. *Curr Biol* **2002**, *12* (7), R259-61.
9. Blanden, M. J.; Ashok, S.; Hougland, J. L., Mechanisms of CaaX Protein Processing: Protein Prenylation by FTase and GGTase-I. **2020**.

10. Wang, M.; Casey, P. J., Protein prenylation: unique fats make their mark on biology. *Nature reviews Molecular cell biology* **2016**, *17* (2), 110.
11. Bonni, A.; Brunet, A.; West, A. E.; Datta, S. R.; Takasu, M. A.; Greenberg, M. E., Cell survival promoted by the Ras-MAPK signaling pathway by transcription-dependent and-independent mechanisms. *Science (New York, N.Y.)* **1999**, *286* (5443), 1358-1362.
12. Casey, P. J., Protein lipidation in cell signaling. *Science (New York, N.Y.)* **1995**, *268* (5208), 221-5.
13. Leung, K. F.; Baron, R.; Ali, B. R.; Magee, A. I.; Seabra, M. C., Rab GTPases containing a CAAX motif are processed post-geranylgeranylation by proteolysis and methylation. *The Journal of biological chemistry* **2007**, *282* (2), 1487-97.
14. Winter-Vann, A. M.; Casey, P. J., Post-prenylation-processing enzymes as new targets in oncogenesis. *Nature reviews. Cancer* **2005**, *5* (5), 405-12.
15. Michaelson, D.; Ali, W.; Chiu, V. K.; Bergo, M.; Silletti, J.; Wright, L.; Young, S. G.; Philips, M., Postprenylation CAAX processing is required for proper localization of Ras but not Rho GTPases. *Mol Biol Cell* **2005**, *16* (4), 1606-16.
16. Solski, P. A.; Helms, W.; Keely, P. J.; Su, L.; Der, C. J., RhoA biological activity is dependent on prenylation but independent of specific isoprenoid modification. *Cell growth & differentiation: the molecular biology journal of the American Association for Cancer Research* **2002**, *13* (8), 363.
17. Roberts, P. J.; Mitin, N.; Keller, P. J.; Chenette, E. J.; Madigan, J. P.; Currin, R. O.; Cox, A. D.; Wilson, O.; Kirschmeier, P.; Der, C. J., Rho Family GTPase modification and dependence on CAAX motif-signaled posttranslational modification. *The Journal of biological chemistry* **2008**, *283* (37), 25150-63.

18. Hildebrandt, E. R.; Cheng, M.; Zhao, P.; Kim, J. H.; Wells, L.; Schmidt, W. K., A shunt pathway limits the CaaX processing of Hsp40 Ydj1p and regulates Ydj1p-dependent phenotypes. *Elife* **2016**, *5*, e15899.
19. Berger, B. M.; Kim, J. H.; Hildebrandt, E. R.; Davis, I. C.; Morgan, M. C.; Hougland, J. L.; Schmidt, W. K., Protein Isoprenylation in Yeast Targets COOH-Terminal Sequences Not Adhering to the CaaX Consensus. *Genetics* **2018**, *210* (4), 1301-1316.
20. Casey, P. J.; Thissen, J. A.; Moomaw, J. F., Enzymatic modification of proteins with a geranylgeranyl isoprenoid. *Proceedings of the National Academy of Sciences* **1991**, *88* (19), 8631-8635.
21. Caplin, B. E.; Ohya, Y.; Marshall, M. S., Amino acid residues that define both the isoprenoid and CAAX preferences of the *Saccharomyces cerevisiae* protein farnesyltransferase. Creating the perfect farnesyltransferase. *The Journal of biological chemistry* **1998**, *273* (16), 9472-9.
22. Omer, C. A.; Kral, A. M.; Diehl, R. E.; Prendergast, G. C.; Powers, S.; Allen, C. M.; Gibbs, J. B.; Kohl, N. E., Characterization of recombinant human farnesyl-protein transferase: cloning, expression, farnesyl diphosphate binding, and functional homology with yeast prenyl-protein transferases. *Biochemistry* **1993**, *32* (19), 5167-5176.
23. Reiss, Y.; Seabra, M. C.; Armstrong, S. A.; Slaughter, C. A.; Goldstein, J. L.; Brown, M. S., Nonidentical subunits of p21H-ras farnesyltransferase. Peptide binding and farnesyl pyrophosphate carrier functions. *The Journal of biological chemistry* **1991**, *266* (16), 10672-7.
24. Fu, H.-W.; Casey, P. J., Enzymology and biology of CaaX protein prenylation. *Recent progress in hormone research* **1999**, *54*, 315-42; discussion 342.

25. Reid, T. S.; Terry, K. L.; Casey, P. J.; Beese, L. S., Crystallographic analysis of CaaX prenyltransferases complexed with substrates defines rules of protein substrate selectivity. *Journal of molecular biology* **2004**, *343* (2), 417-433.
26. Lane, K. T.; Beese, L. S., Thematic review series: lipid posttranslational modifications. Structural biology of protein farnesyltransferase and geranylgeranyltransferase type I. *Journal of lipid research* **2006**, *47* (4), 681-699.
27. Maurer-Stroh, S.; Eisenhaber, F., Refinement and prediction of protein prenylation motifs. *Genome biology* **2005**, *6* (6), R55.
28. Maurer-Stroh, S.; Koranda, M.; Benetka, W.; Schneider, G.; Sirota, F. L.; Eisenhaber, F., Towards complete sets of farnesylated and geranylgeranylated proteins. *PLoS computational biology* **2007**, *3* (4).
29. Hougland, J. L.; Lamphear, C. L.; Scott, S. A.; Gibbs, R. A.; Fierke, C. A., Context-Dependent Substrate Recognition by Protein Farnesyltransferase. *Biochemistry* **2009**, *48* (8), 1691-1701.
30. London, N.; Lamphear, C. L.; Hougland, J. L.; Fierke, C. A.; Schueler-Furman, O., Identification of a novel class of farnesylation targets by structure-based modeling of binding specificity. *PLoS computational biology* **2011**, *7* (10).
31. Hartman, H. L.; Hicks, K. A.; Fierke, C. A., Peptide specificity of protein prenyltransferases is determined mainly by reactivity rather than binding affinity. *Biochemistry* **2005**, *44* (46), 15314-15324.
32. Moores, S. L.; Schaber, M. D.; Mosser, S. D.; Rands, E.; O'Hara, M. B.; Garsky, V. M.; Marshall, M. S.; Pompliano, D. L.; Gibbs, J., Sequence dependence of protein isoprenylation. *Journal of Biological Chemistry* **1991**, *266* (22), 14603-14610.

33. Schaber, M.; O'hara, M.; Garsky, V.; Mosser, S.; Bergstrom, J.; Moores, S.; Marshall, M.; Friedman, P.; Dixon, R.; Gibbs, J., Polyisoprenylation of Ras in vitro by a farnesyl-protein transferase. *Journal of Biological Chemistry* **1990**, *265* (25), 14701-14704.
34. Hancock, J.; Cadwallader, K.; Paterson, H.; Marshall, C., A CAAX or a CAAL motif and a second signal are sufficient for plasma membrane targeting of ras proteins. *The EMBO journal* **1991**, *10* (13), 4033-4039.
35. Gao, J.; Liao, J.; Yang, G.-Y., CAAX-box protein, prenylation process and carcinogenesis. *American journal of translational research* **2009**, *1* (3), 312.
36. Hougland, J. L.; Gangopadhyay, S. A.; Fierke, C. A., Expansion of Protein Farnesyltransferase Specificity Using “Tunable” Active Site Interactions: Development of bioengineered prenylation pathways. *Journal of Biological Chemistry* **2012**, *287* (45), 38090-38100.
37. Hougland, J. L.; Hicks, K. A.; Hartman, H. L.; Kelly, R. A.; Watt, T. J.; Fierke, C. A., Identification of novel peptide substrates for protein farnesyltransferase reveals two substrate classes with distinct sequence selectivities. *Journal of molecular biology* **2010**, *395* (1), 176-90.
38. Long, S. B.; Casey, P. J.; Beese, L. S., Cocystal structure of protein farnesyltransferase complexed with a farnesyl diphosphate substrate. *Biochemistry* **1998**, *37* (27), 9612-9618.
39. Taylor, J. S.; Reid, T. S.; Terry, K. L.; Casey, P. J.; Beese, L. S., Structure of mammalian protein geranylgeranyltransferase type-I. *The EMBO journal* **2003**, *22* (22), 5963-74.
40. Gangopadhyay, S. A.; Losito, E. L.; Hougland, J. L., Targeted reengineering of protein geranylgeranyltransferase type I selectivity functionally implicates active-site residues in protein-substrate recognition. *Biochemistry* **2014**, *53* (2), 434-446.

41. Terry, K. L.; Casey, P. J.; Beese, L. S., Conversion of protein farnesyltransferase to a geranylgeranyltransferase. *Biochemistry* **2006**, *45* (32), 9746-55.
42. Maurer-Stroh, S.; Eisenhaber, F., Refinement and prediction of protein prenylation motifs. *Genome biology* **2005**, *6* (6), R55.
43. Yokoyama, K.; Zimmerman, K.; Scholten, J.; Gelb, M. H., Differential prenyl pyrophosphate binding to mammalian protein geranylgeranyltransferase-I and protein farnesyltransferase and its consequence on the specificity of protein prenylation. *Journal of Biological Chemistry* **1997**, *272* (7), 3944-3952.
44. Ashok, S.; Hildebrandt, E. R.; Ruiz, C. S.; Hardgrove, D. S.; Coreno, D. W.; Schmidt, W. K.; Hougland, J. L., Protein farnesyltransferase catalyzes unanticipated farnesylation and geranylgeranylation of shortened target sequences. *Biochemistry* **2020**, *59* (11), 1149-1162.
45. Caplan, A. J.; Tsai, J.; Casey, P. J.; Douglas, M. G., Farnesylation of YDJ1p is required for function at elevated growth temperatures in *Saccharomyces cerevisiae*. *The Journal of biological chemistry* **1992**, *267* (26), 18890-5.
46. Trueblood, C. E.; Boyartchuk, V. L.; Picologlou, E. A.; Rozema, D.; Poulter, C. D.; Rine, J., The CaaX proteases, Afc1p and Rce1p, have overlapping but distinct substrate specificities. *Molecular and cellular biology* **2000**, *20* (12), 4381-92.
47. Wang, Y. C.; Dozier, J. K.; Beese, L. S.; Distefano, M. D., Rapid analysis of protein farnesyltransferase substrate specificity using peptide libraries and isoprenoid diphosphate analogues. *ACS chemical biology* **2014**, *9* (8), 1726-35.
48. Leung, K. F.; Baron, R.; Seabra, M. C., Thematic review series: lipid posttranslational modifications. geranylgeranylation of Rab GTPases. *Journal of lipid research* **2006**, *47* (3), 467-75.

49. Boys, B. L.; Kuprowski, M. C.; Noël, J. J.; Konermann, L., Protein oxidative modifications during electrospray ionization: solution phase electrochemistry or corona discharge-induced radical attack? *Analytical chemistry* **2009**, *81* (10), 4027-4034.
50. Reid, T. S.; Long, S. B.; Beese, L. S., Crystallographic analysis reveals that anticancer clinical candidate L-778,123 inhibits protein farnesyltransferase and geranylgeranyltransferase-I by different binding modes. *Biochemistry* **2004**, *43* (28), 9000-8.
51. Pompliano, D. L.; Gomez, R. P.; Anthony, N. J., Intramolecular fluorescence enhancement: a continuous assay of Ras farnesyl:protein transferase. *Journal of the American Chemical Society* **1992**, *114* (20), 7945-7946.
52. Cassidy, P. B.; Dolence, J. M.; Poulter, C. D., Continuous fluorescence assay for protein prenyltransferases. *Methods in enzymology* **1995**, *250*, 30-43.
53. Reigard, S. A.; Zahn, T. J.; Haworth, K. B.; Hicks, K. A.; Fierke, C. A.; Gibbs, R. A., Interplay of isoprenoid and peptide substrate specificity in protein farnesyltransferase. *Biochemistry* **2005**, *44* (33), 11214-11223.
54. Alsina, M.; Fonseca, R.; Wilson, E. F.; Belle, A. N.; Gerbino, E.; Price-Troska, T.; Overton, R. M.; Ahmann, G.; Bruzek, L. M.; Adjei, A. A.; Kaufmann, S. H.; Wright, J. J.; Sullivan, D.; Djulbegovic, B.; Cantor, A. B.; Greipp, P. R.; Dalton, W. S.; Sebti, S. M., Farnesyltransferase inhibitor tipifarnib is well tolerated, induces stabilization of disease, and inhibits farnesylation and oncogenic/tumor survival pathways in patients with advanced multiple myeloma. *Blood* **2004**, *103* (9), 3271-7.
55. Sebti, S. M.; Adjei, A. A. In *Farnesyltransferase inhibitors*, Seminars in oncology, Elsevier: 2004; pp 28-39.

56. Ho, A.; Chau, N.; Bauman, J.; Bible, K.; Chintakuntlawar, A.; Cabanillas, M.; Wong, D.; Braña Garcia, I.; Brose, M.; Boni, V., 10460 Preliminary results from a phase II trial of tipifarnib in squamous cell carcinomas (SCCs) with HRAS mutations. *Annals of Oncology* **2018**, *29* (suppl_8), mdy287. 002.
57. Flynn, S. C.; Lindgren, D. E.; Hougland, J. L., Quantitative determination of cellular farnesyltransferase activity: towards defining the minimum substrate reactivity for biologically relevant protein farnesylation. *Chembiochem : a European journal of chemical biology* **2014**, *15* (15), 2205-10.
58. Chen, Z.; Otto, J. C.; Bergo, M. O.; Young, S. G.; Casey, P. J., The C-terminal polylysine region and methylation of K-Ras are critical for the interaction between K-Ras and microtubules. *Journal of Biological Chemistry* **2000**, *275* (52), 41251-41257.
59. Hancu, G.; Simon, B.; Rusu, A.; Mircia, E.; Gyeresi, A., Principles of micellar electrokinetic capillary chromatography applied in pharmaceutical analysis. *Advanced pharmaceutical bulletin* **2013**, *3* (1), 1-8.
60. Gong, F.; Yang, H.; Sun, W.; Cao, J.; Liu, W., Development and validation of a micellar electrokinetic capillary chromatography method for the determination of goserelin and related substances. *Electrophoresis* **2016**, *37* (4), 623-629.
61. Shala-Lawrence, A.; Blanden, M. J.; Krylova, S. M.; Gangopadhyay, S. A.; Beloborodov, S. S.; Hougland, J. L.; Krylov, S. N., Simultaneous Analysis of a Non-Lipidated Protein and Its Lipidated Counterpart: Enabling Quantitative Investigation of Protein Lipidation's Impact on Cellular Regulation. *Analytical chemistry* **2017**, *89* (24), 13502-13507.

62. Jennings, B. C.; Danowitz, A. M.; Wang, Y. C.; Gibbs, R. A.; Distefano, M. D.; Fierke, C. A., Analogs of farnesyl diphosphate alter CaaX substrate specificity and reactions rates of protein farnesyltransferase. *Bioorg Med Chem Lett* **2016**, *26* (4), 1333-6.
63. Troutman, J. M.; Andres, D. A.; Spielmann, H. P., Protein farnesyl transferase target selectivity is dependent upon peptide stimulated product release. *Biochemistry* **2007**, *46* (40), 11299-309.
64. Subramanian, T.; Liu, S.; Troutman, J. M.; Andres, D. A.; Spielmann, H. P., Protein Farnesyltransferase-Catalyzed Isoprenoid Transfer to Peptide Depends on Lipid Size and Shape, not Hydrophobicity. *Chembiochem : a European journal of chemical biology* **2008**, *9* (17), 2872-2882.
65. Hightower, K. E.; Casey, P. J.; Fierke, C. A., Farnesylation of nonpeptidic thiol compounds by protein farnesyltransferase. *Biochemistry* **2001**, *40* (4), 1002-10.
66. Storck, E. M.; Morales-Sanfrutos, J.; Serwa, R. A.; Panyain, N.; Lanyon-Hogg, T.; Tolmachova, T.; Ventimiglia, L. N.; Martin-Serrano, J.; Seabra, M. C.; Wojciak-Stothard, B.; Tate, E. W., Dual chemical probes enable quantitative system-wide analysis of protein prenylation and prenylation dynamics. *Nature chemistry* **2019**, *11* (6), 552-561.
67. Suazo, K. F.; Schaber, C.; Palsuledesai, C. C.; John, A. R. O.; Distefano, M. D., Global proteomic analysis of prenylated proteins in *Plasmodium falciparum* using an alkyne-modified isoprenoid analogue. *Scientific reports* **2016**, *6*, 38615.
68. Wang, Y.-C.; Distefano, M. D., Synthetic isoprenoid analogues for the study of prenylated proteins: Fluorescent imaging and proteomic applications. *Bioorganic Chemistry* **2016**, *64*, 59-65.

69. Kho, Y.; Kim, S. C.; Jiang, C.; Barma, D.; Kwon, S. W.; Cheng, J.; Jaunbergs, J.; Weinbaum, C.; Tamanoi, F.; Falck, J.; Zhao, Y., A tagging-via-substrate technology for detection and proteomics of farnesylated proteins. *Proceedings of the National Academy of Sciences of the United States of America* **2004**, *101* (34), 12479-12484.
70. Stein, V.; Kubala, M. H.; Steen, J.; Grimmond, S. M.; Alexandrov, K., Towards the systematic mapping and engineering of the protein prenylation machinery in *Saccharomyces cerevisiae*. *PLoS One* **2015**, *10* (3), e0120716.
71. Nguyen, U. T.; Guo, Z.; Delon, C.; Wu, Y.; Deraeve, C.; Franzel, B.; Bon, R. S.; Blankenfeldt, W.; Goody, R. S.; Waldmann, H.; Wolters, D.; Alexandrov, K., Analysis of the eukaryotic prenylome by isoprenoid affinity tagging. *Nature chemical biology* **2009**, *5* (4), 227-35.
72. Rashidian, M.; Kumarapperuma, S. C.; Gabrielse, K.; Fegan, A.; Wagner, C. R.; Distefano, M. D., Simultaneous dual protein labeling using a triorthogonal reagent. *Journal of the American Chemical Society* **2013**, *135* (44), 16388-96.
73. Chan, R. K.; Otte, C. A., Isolation and genetic analysis of *Saccharomyces cerevisiae* mutants supersensitive to G1 arrest by a factor and alpha factor pheromones. *Molecular and cellular biology* **1982**, *2* (1), 11-20.
74. Michaelis, S.; Herskowitz, I., The a-factor pheromone of *Saccharomyces cerevisiae* is essential for mating. *Molecular and cellular biology* **1988**, *8* (3), 1309-18.
75. Chen, P.; Sapperstein, S. K.; Choi, J. D.; Michaelis, S., Biogenesis of the *Saccharomyces cerevisiae* mating pheromone a-factor. *The Journal of cell biology* **1997**, *136* (2), 251-269.

76. Shoemaker, D. D.; Lashkari, D. A.; Morris, D.; Mittmann, M.; Davis, R. W., Quantitative phenotypic analysis of yeast deletion mutants using a highly parallel molecular bar-coding strategy. *Nature genetics* **1996**, *14* (4), 450-456.
77. Kevin R, O.; Vo, K. T.; Michaelis, S.; Paddon, C., Recombination-mediated PCR-directed plasmid construction in vivo in yeast. *Nucleic acids research* **1997**, *25* (2), 451-452.
78. Schmidt, W. K.; Tam, A.; Fujimura-Kamada, K.; Michaelis, S., Endoplasmic reticulum membrane localization of Rce1p and Ste24p, yeast proteases involved in carboxyl-terminal CAAX protein processing and amino-terminal a-factor cleavage. *Proceedings of the National Academy of Sciences of the United States of America* **1998**, *95* (19), 11175-80.
79. Sikorski, R. S.; Hieter, P., A system of shuttle vectors and yeast host strains designed for efficient manipulation of DNA in *Saccharomyces cerevisiae*. *Genetics* **1989**, *122* (1), 19-27.
80. Elble, R., A simple and efficient procedure for transformation of yeasts. *BioTechniques* **1992**, *13*, 18-20.
81. Firth, A. E.; Patrick, W. M., GLUE-IT and PEDEL-AA: new programmes for analyzing protein diversity in randomized libraries. *Nucleic Acids Res* **2008**, *36* (Web Server issue), W281-5.
82. Kim, S.; Lapham, A.; Freedman, C.; Reed, T.; Schmidt, W., Yeast as a tractable genetic system for functional studies of the insulin-degrading enzyme. *J Biol Chem.* **2005**, *280* (30), 27481-27490.

Chapter 3: Investigating photo-switchable FPP analogs as donors

for FTase

The work presented herein is unpublished.

Syntheses and characterization of both azo-benzene FPP analogs were completed by our collaborator Johannes Morstein from the Trauner Group (Department of Chemistry, New York University).

3.1 Introduction

Given prenylation's impact on many signaling pathways, gaining a comprehensive understanding of its function in terms of time and space represents an intriguing challenge and is limited by the current utilization of genetic or pharmacological interventions. Spatiotemporal details of prenylated proteins are lost when studied under *in vitro* conditions with purified protein. Genetic approaches such as gene knockouts lack temporal precision as they eliminate the function of prenylated proteins at all times and positions. While small molecules offer better temporal control, they suffer from off-target issues.¹ And although several functionalized isoprenoid analogs have been developed (see Chapter 1), their utility is limited to identification of prenylated proteins and does not offer the dynamic control that may influence membrane localization in a reversible manner. An ideal approach for probing the role of a specific prenylated protein in its native environment is one that allows for spatial and temporal control on a time frame and spatial scale comparable to that which occurs naturally.²⁻⁵

Light is a promising external chemical and biological modulator of protein function because it exhibits a high level of spatiotemporal resolution, is generally non-invasive (for a range of wavelengths) and well-tolerated by most chemical and biochemical elements leading to minimal interference with living systems, and does not cause contamination. Moreover, its wavelength and intensity can be precisely controlled allowing for unparalleled manipulations of biological phenomena.^{1,5} Light can influence the biological activity of synthetic molecules that are modified with a light-sensitive group by changing their pharmacokinetic or pharmacodynamic properties. This approach is termed photopharmacology.¹

The most widely used method for rendering biomolecules light sensitive is the “caging” approach, in which, a key functional group is protected with a light-sensitive “caging” group.

This causes the biomolecule to be in its inactive form until the caging group is removed with light. There are several examples of light-sensitive protecting groups used in biological studies.⁶⁻
⁹ However, this approach is limited by the irreversible nature of this photochemistry because once “uncaged”, the bioactive molecule remains active until it is removed or degraded. In contrast, “photoswitches” represent a class of chemical compounds that may undergo a reversible change in their structure and properties multiple times. While several classes of such light-responsive compounds have been developed, azobenzene has received considerable attention in biological applications.^{1-4, 10} Azobenzene groups are relatively small, allowing them to be easily incorporated into a drug-like molecule of low molecular weight. Furthermore, they can be synthesized through a wide variety of methods, including classical azo-coupling to Mills reactions or the cross-couplings of hydrazine derivatives followed by oxidation.^{10, 11} The repertoire of azobenzene incorporated compounds has grown substantially recently.

Photoirradiation of azobenzene results in a *trans* to *cis* isomerization that is accompanied by a large change in geometry and a considerable change in polarity.¹² The *trans* conformation of azobenzene is 10-12 kcal mol⁻¹ more stable than the *cis* isomer, which means that *trans* is the dominant isomer (>99.99%) in the dark at equilibrium.^{2, 12, 13} The *trans* conformation is near planar and has a dipole moment near zero.^{14, 15} A substantial amount of the *cis* isomer can be induced by irradiation with 340 nm light, which causes azobenzene to adopt a bent confirmation with its phenyl rings twisted out of the plane from the azo group and has a dipole moment of ~3 Debye (Figure 3.1).¹⁴ Relaxation to the thermodynamically more stable *trans*-isomer can be achieved by either irradiation with ~450 nm light or may proceed spontaneously by thermal isomerization in the absence of light. The photoisomerization events occur with high quantum yields and minimal photo-bleaching.^{2, 14} Moreover, photo-induced isomerization of azobenzene

results in a substantial difference between the end-to-end distance of each isomer and isomerization occurs on a picosecond timescale, much faster than most biological events.^{14, 16, 17}

Photoswitchable lipids have emerged as tools useful in the control of cell signaling in a reversible manner.^{3, 10} They rely on the incorporation of an azobenzene photoswitch in the hydrophobic tail and mediate optical control of lipid function by reversible, light-induced isomerization between a *cis* and *trans* isomer, as described. In comparison to caged lipids, photoswitchable lipids require less intense radiation and do not lead to the formation of side products. To date, photoswitchable lipids have been applied in the optical modulation of ion channels,¹⁸⁻²⁰ the fatty acid receptor GPR40,²¹ lipid rafts,²² lipid vesicle budding and fission,²³ lipid-protein interactions in canonical lipid signaling and sphingolipid metabolism.^{24, 25}

Inspired by the success of recent studies on photoswitchable lipids in modulating cell signaling events in various contexts,³ we examined the reactivity of two FPP azobenzene-containing “azologs” (AzoFPP1 and AzoFPP2) developed by the Trauner Group (Department of Chemistry, New York University) (Figure 3.2) in reactions with mammalian prenyltransferases. As with other compounds incorporating azobenzene, azo-FPP analogs favor their thermally stable *trans* isoform but can be isomerized to their less stable *cis* isoform by irradiation at 365 nm. Moreover, both azologs thermally relax to the *trans* isomer with a half-life of ~24 hours or can be induced by irradiation with 460 nm light allowing reversible control (Figure 3.3). We tested these Azo-FPP analogs in a proof of principle *in vitro* assay to validate incorporation by protein prenyltransferase using peptide substrates. This work moves towards the goal of utilizing the photo-isomerization ability of these azologs in cells to modulate membrane localization behavior and thus potentially influence protein function and consequential downstream events in cells.

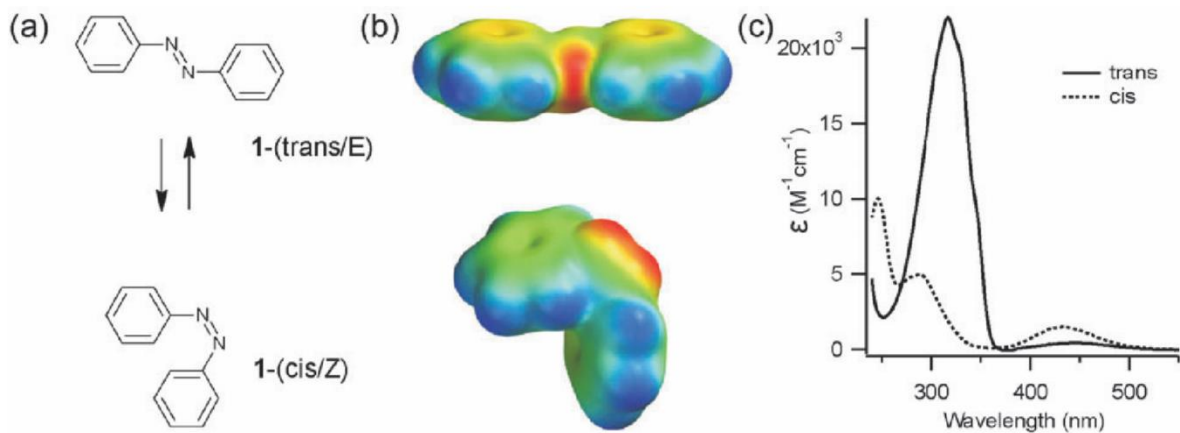


Figure 3.1. Structure and absorption spectra of *trans*- and *cis*-azobenzene: (a) Structures of *trans* and *cis* isomers of azobenzene. (b) Space-filling models colored by electrostatic potential (red—negative to blue—positive). (c) Electronic absorption spectra of the *trans* and *cis* isomers of azobenzene dissolved in ethanol. This figure has been reproduced from Reference 2 with permission from The Royal Society of Chemistry (Appendix III).

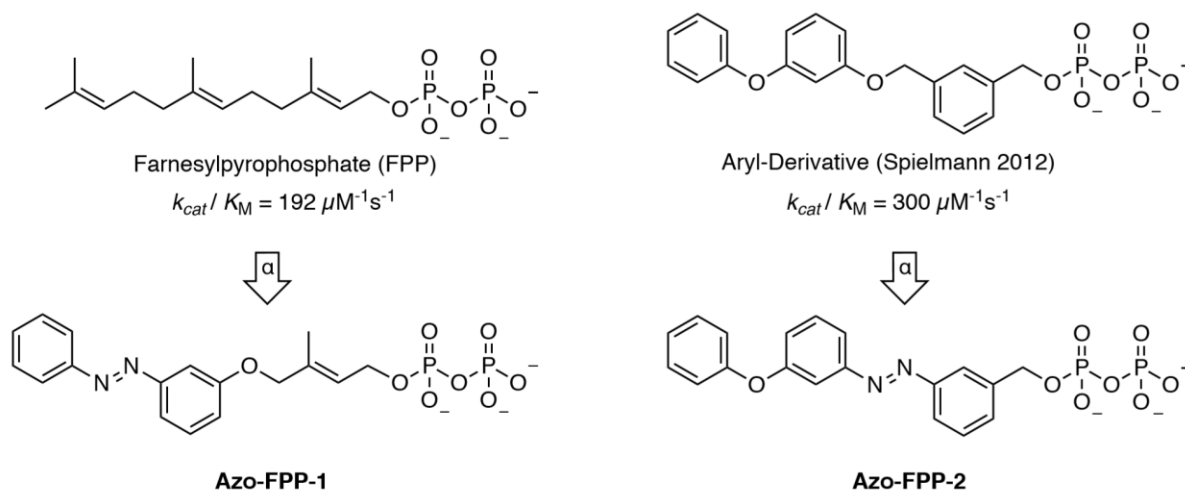


Figure 3.2. Structures of Azo-FPP1 and Azo-FPP2. Both azologs were inspired by farnesylpyrophosphate (FPP) and an aryl-derivative FPP analog²⁶, respectively.

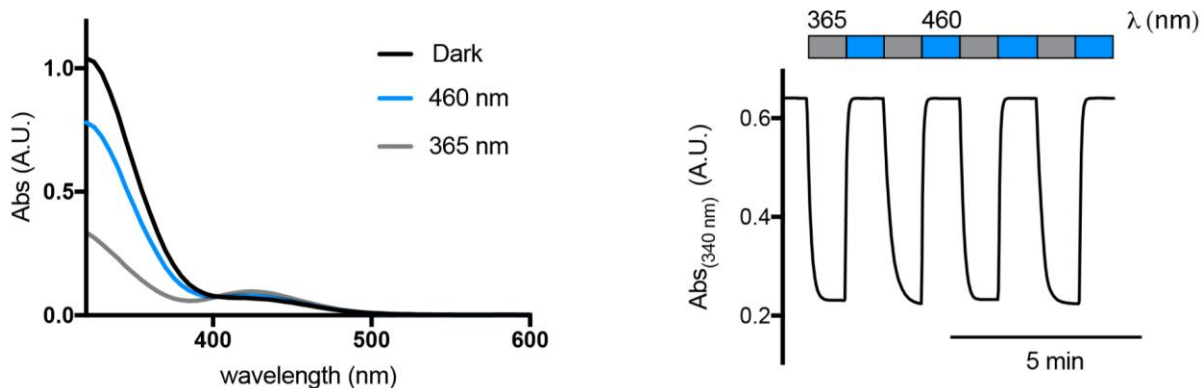


Figure 3.3. Photophysical properties of Azo-FPP1. Ultraviolet-visible spectra of Azo-FPP1 in the dark-adapted (black, *trans*), 365 nm-adapted (gray, *cis*) and 460 nm-adapted (blue, *trans*) photostationary states. Reversible cycling between photoisomers with alternating illumination at 365/460 nm. A.U., arbitrary units. Azo-FPP2 exhibited similar photophysical properties (data not shown). This data was collected and analyzed by our collaborator Johannes Morstein from the Trauner Group (Department of Chemistry, New York University).

3.2 WT FTase-catalyzed prenylation of dns-GCVLS peptide using Azo-FPP1

We performed an initial assay to validate incorporation of the two azologs without any irradiation by monitoring the reaction between the canonical FTase/GGTase-I peptide substrates dns-GCVLS and dns-GCVLL, respectively with Azo-FPP donors by reverse phase HPLC.²⁷⁻³⁰ HPLC analysis indicated that of the two Azo-FPP analogs, Azo-FPP1 was incorporated in a reaction with FTase and dns-GCVLS whereas Azo-FPP2 was unable to be utilized by FTase as a donor (Figure 3.4). In contrast, GGTase-I did not accept either of the two analogs as the prenyl donor in a reaction with dns-GCVLL (Figure 3.5).

Following confirmation that Azo-FPP1 could serve as a substrate for FTase, we probed the photo-isomerization of Azo-FPP1 and whether we could detect the two different isomers by monitoring reactions via HPLC. After incubating peptide reactions with FTase and Azo-FPP1 overnight in the dark, reactions were stopped by adding stop solution and irradiated for three minutes with either 365 nm light to induce the *cis*-isomer favoring photo-stationary state or with 460 nm light to enrich the *trans*-isomer favoring photo-stationary state prior to HPLC analysis of the modified peptides (see Materials and Methods). By this approach, we were able to unambiguously assign distinct peaks in the HPLC chromatogram to the peptide substrates appended with the two different photo-isomers of the Azo-FPP1 group (Figure 3.6). This study supported further testing of Azo-FPP1 to determine its steady-state reaction parameters with FTase and canonical FTase substrates.

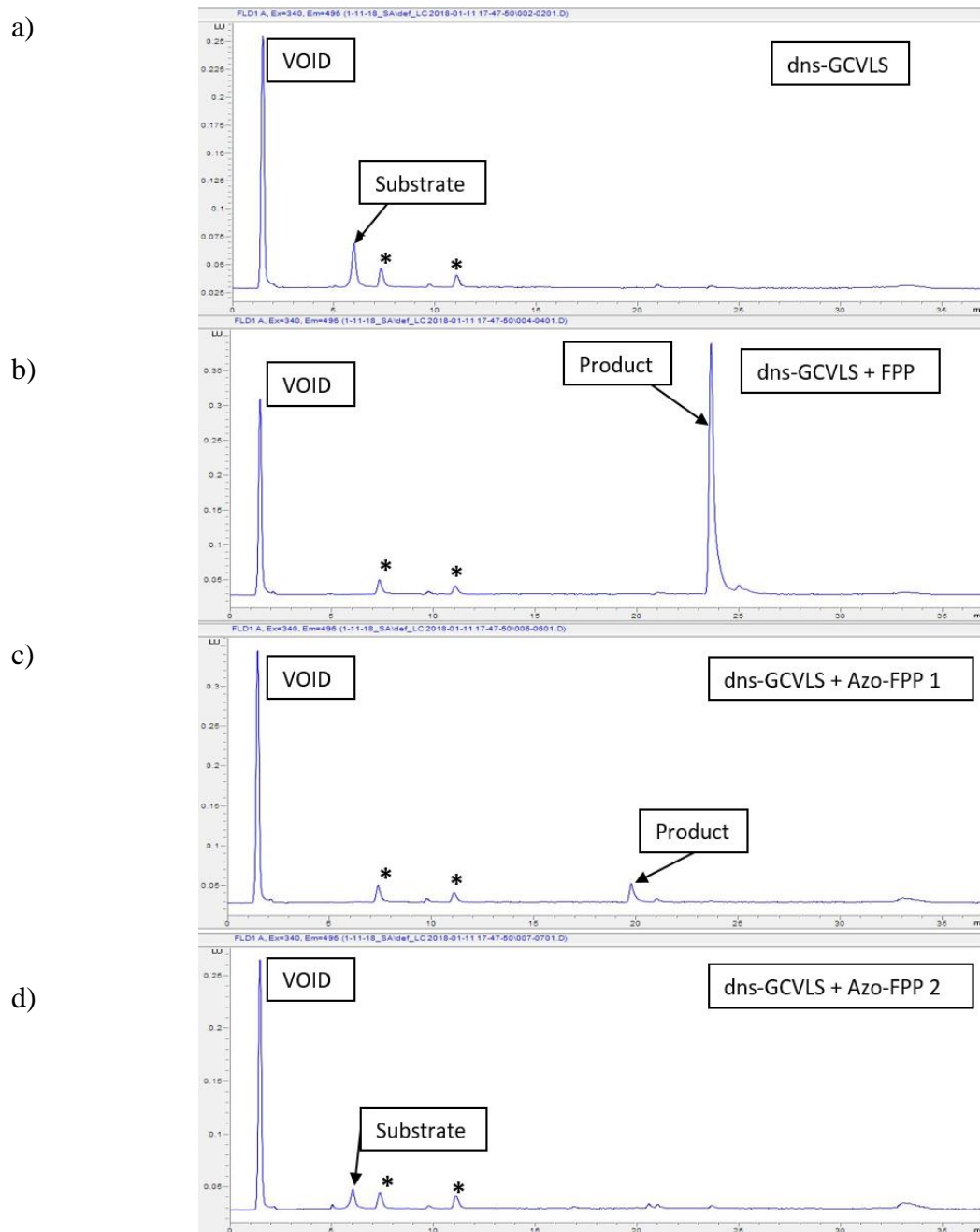


Figure 3.4. Modification of dns-GCVLS by FTase using Azo-FPP analogs as monitored by RP-HPLC. a) Negative control consisting of peptide and FTase only. b) Peptide reaction with FTase and FPP (positive control). c) Peptide reaction with FTase and Azo-FPP1. d) Peptide reaction with FTase and Azo-FPP2. Asterisks represent background peaks. Reactions and HPLC analysis carried out as described in Materials and Methods.

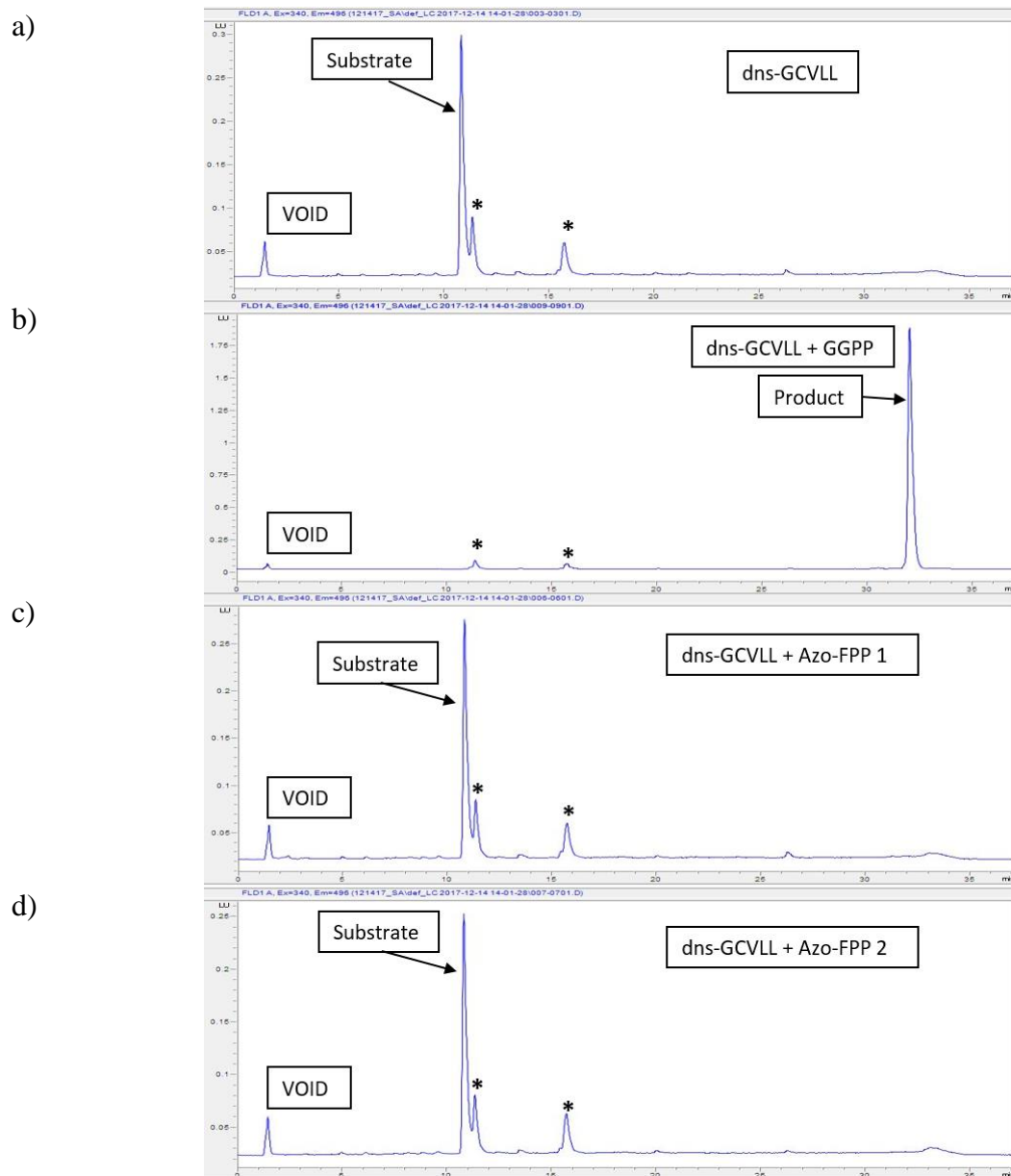


Figure 3.5. Modification of dns-GCVLL by GGTase-I using Azo-FPP analogs as monitored by RP-HPLC. a) Negative control consisting of peptide and GGTase-I only. b) Peptide reaction with GGTase-I and GGPP (positive control). c) Peptide reaction with GGTase-I and Azo-FPP1. d) Peptide reaction with GGTase-I and Azo-FPP2. Asterisks represent background peaks. Reactions and HPLC analysis carried out as described in Materials and Methods.

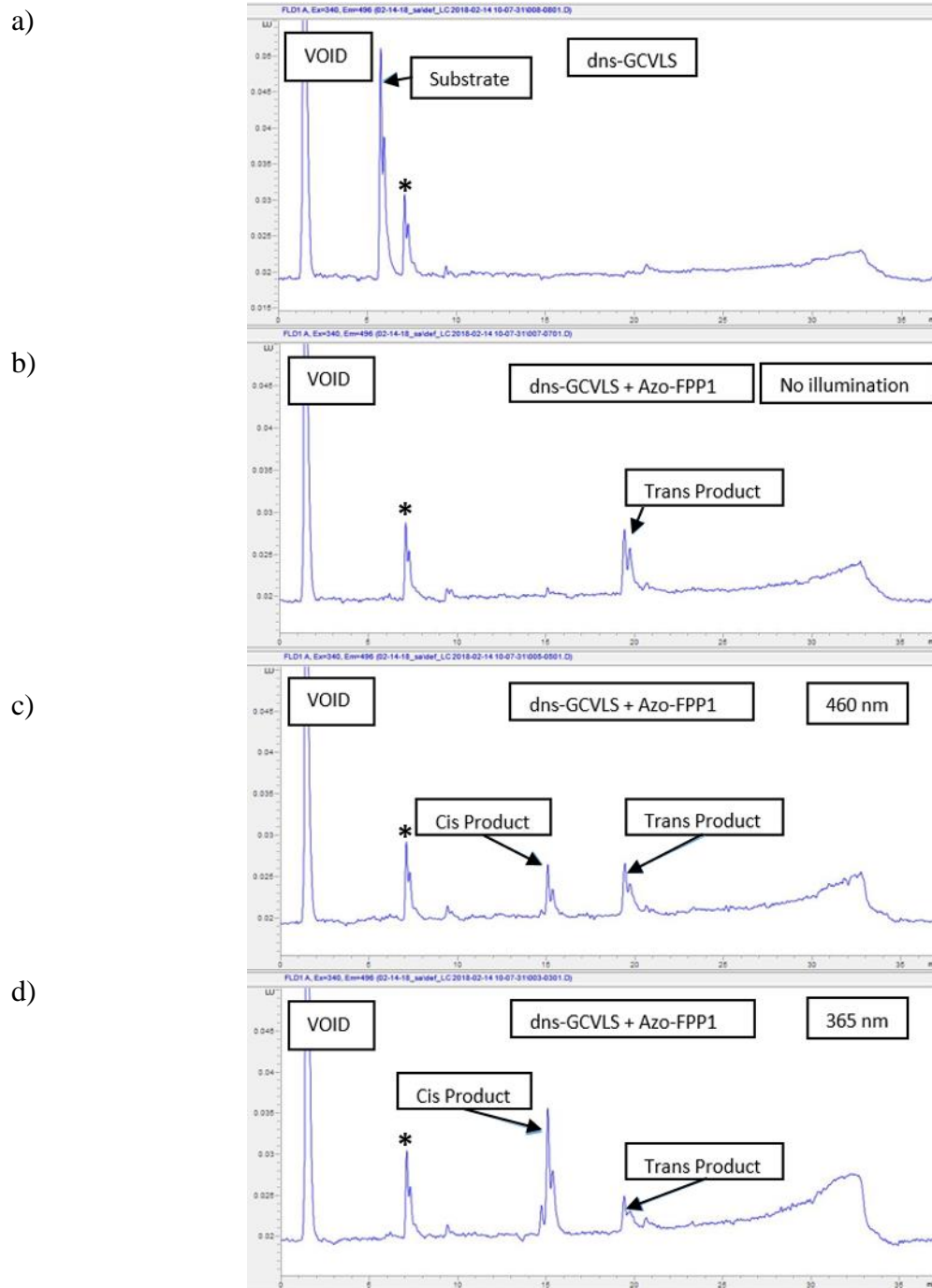


Figure 3.6. RP-HPLC detection of modified dns-GCVLS with photoisomers of Azo-FPP1 generated by post-enzymatic reaction illumination. A) Negative control consisting of peptide only. b) Peptide reaction with Azo-FPP1 (non-illuminated post-reaction). c) Peptide reaction with Azo-FPP1 (illuminated with 460 nm light post-reaction). d) Peptide reaction with Azo-FPP1 (illuminated with 365 nm light post-reaction). Asterisks represent background peaks. Reactions, illumination, and HPLC analysis were carried out as described in Materials and Methods.

3.3 Azo-FPP1 exhibits sufficient reactivity with FTase to be considered for cellular studies

To completely define the functional role of prenylated proteins in their native environment by use of azologs, it is imperative to establish if Azo-FPP1 can be utilized inside cells by endogenous FTase. Following confirmation of FTase's ability to incorporate Azo-FPP1 onto purified peptides, we determined steady-state parameters for Azo-FPP1 with FTase and canonical FTase substrates by carrying out a time course study. This allows us to gauge the reactivity of the azolog and compare its reactivity to known FPP analogs that have been successfully used in cell studies. To determine the time-course of FTase-catalyzed prenylation using Azo-FPP1, reactions with dns-GCVLS were stopped at various time points and product conversion was determined via RP-HPLC. In our initial studies, we assessed the time required to reach completion for both the *trans* and *cis* isomers (Figures 3.7 and 3.8). We determined the peptide prenylation reaction with *trans* Azo-FPP1 reached complete conversion to product more quickly than the *cis* Azo-FPP1 isomer reaction, suggesting that the *trans* isomer is a more reactive substrate for FTase under these conditions. More specifically, the time required to reach reaction completion was 120 minutes for *trans* Azo-FPP1 compared to 240 minutes required for the *cis* isomer for reaction completion (Figure 3.9).

We also tested parallel reactions with FTase and farnesyl pyrophosphate containing a terminal alkyne group (AlkC15OPP). This allowed us to compare the reactivity of *trans* Azo-FPP1 with another FPP analog prenyl donor which has been successfully used in cells to prenylate canonical and non-canonical substrates.³¹⁻³³ Since peptide modification with the AlkC15OPP probe results in a greater fluorescence enhancement than the AzoFPP1 analog, HPLC chromatograms were analyzed at by UV absorbance of 340 nm for the dansyl group to allow direct comparison between these two analogs. The extent of reaction progress at any one

point was calculated based on the integration of the UV absorbance peak, which was converted to concentration by normalization to the final peak integration with the assumption of 100% conversion to product. Through this analysis, we found the non-irradiated Azo-FPP1 donor showed comparable reactivity to AlkC15OPP with reactions involving both analogs going to completion in approximately 120 minutes (Figure 3.10). This supports that *trans* Azo-FPP1 is sufficiently reactive to support cell-based studies for protein modification with this light-switchable farnesyl group, provided that this analog can enter the cell.

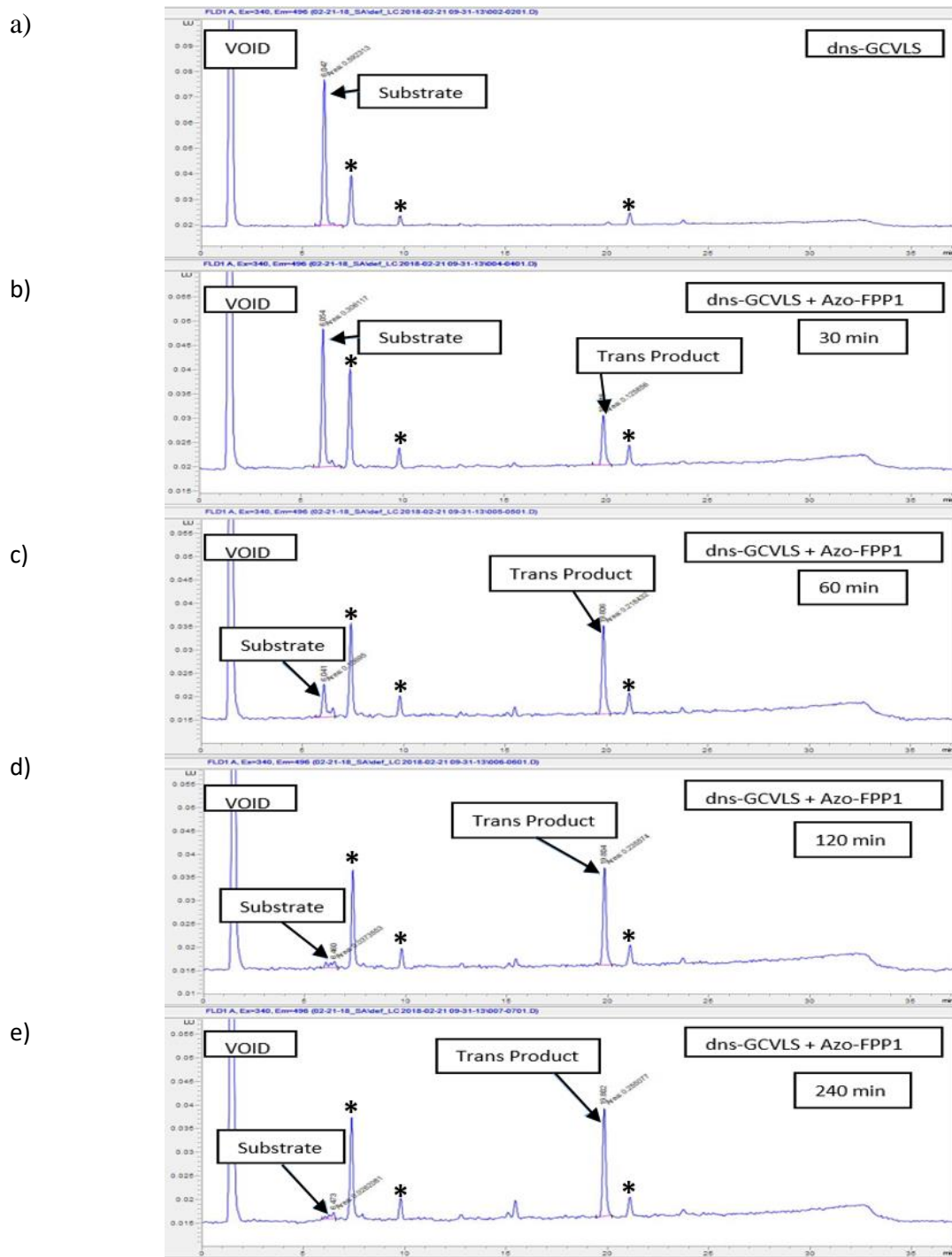


Figure 3.7. RP-HPLC detection of dns-GCVLS modified with *trans*-Azo-FPP1 at various time points under no illumination. a) Negative control consisting of peptide only. b) Peptide reaction with Azo-FPP1 at 30 mins. c) Peptide reaction with Azo-FPP1 at 60 mins. d) Peptide reaction with Azo-FPP1 at 120 mins. e) Peptide reaction with Azo-FPP1 at 240 mins. Asterisks represent background peaks. Reactions and HPLC analysis carried out as described in Materials and Methods.

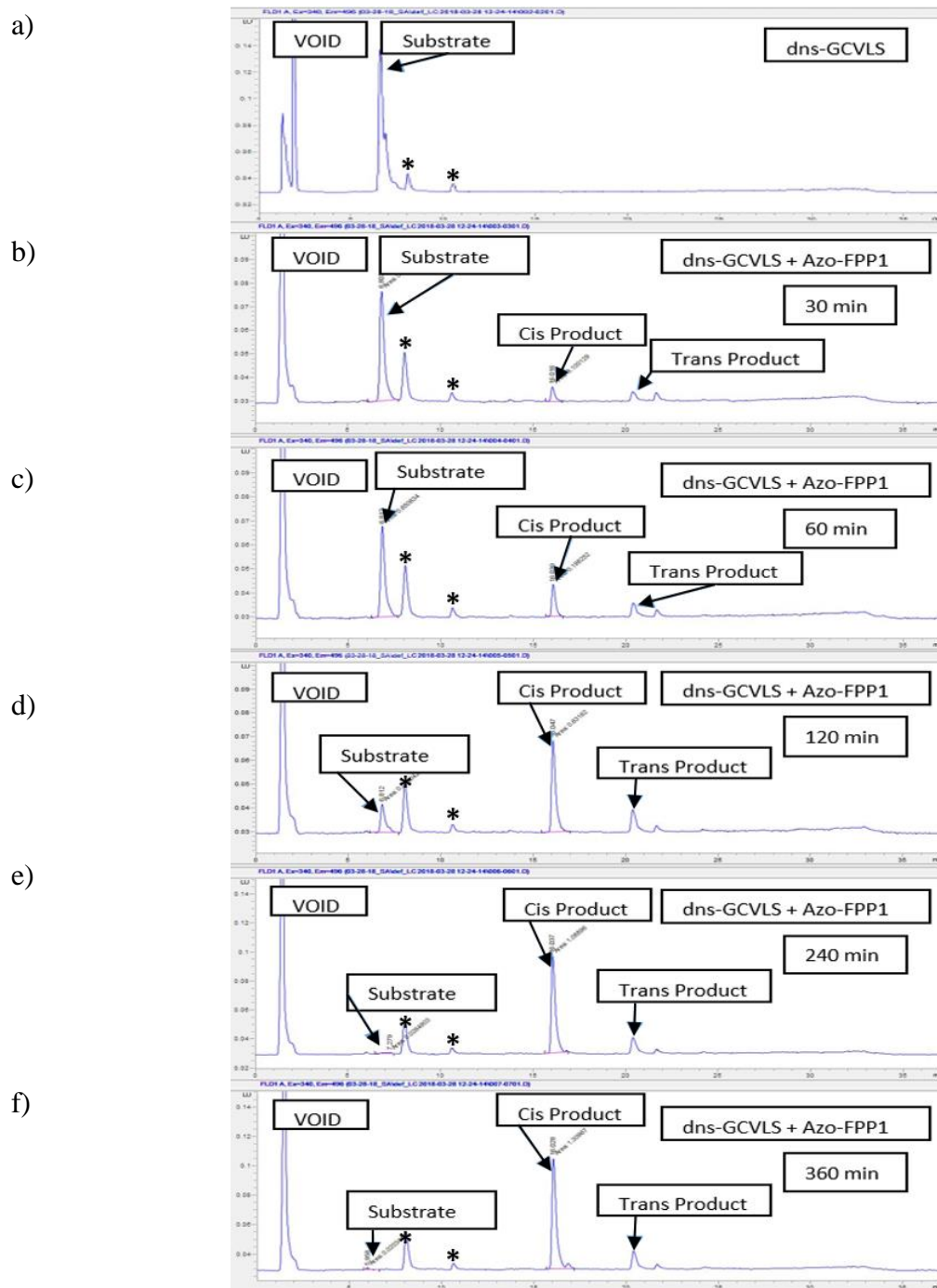


Figure 3.8. RP-HPLC detection of dns-GCVLS modified with *cis*-Azo-FPP 1 at various time points after illumination with 365 nm light. a) Negative control consisting of peptide only. b) Peptide reaction with Azo-FPP1 at 30 mins. c) Peptide reaction with Azo-FPP1 at 60 mins. d) Peptide reaction with Azo-FPP1 at 120 mins. e) Peptide reaction with Azo-FPP1 at 240 mins. f) Peptide reaction with Azo-FPP1 at 360 mins. Asterisks represent background peaks. Reactions, illumination, and HPLC analysis were carried out as described in Materials and Methods.

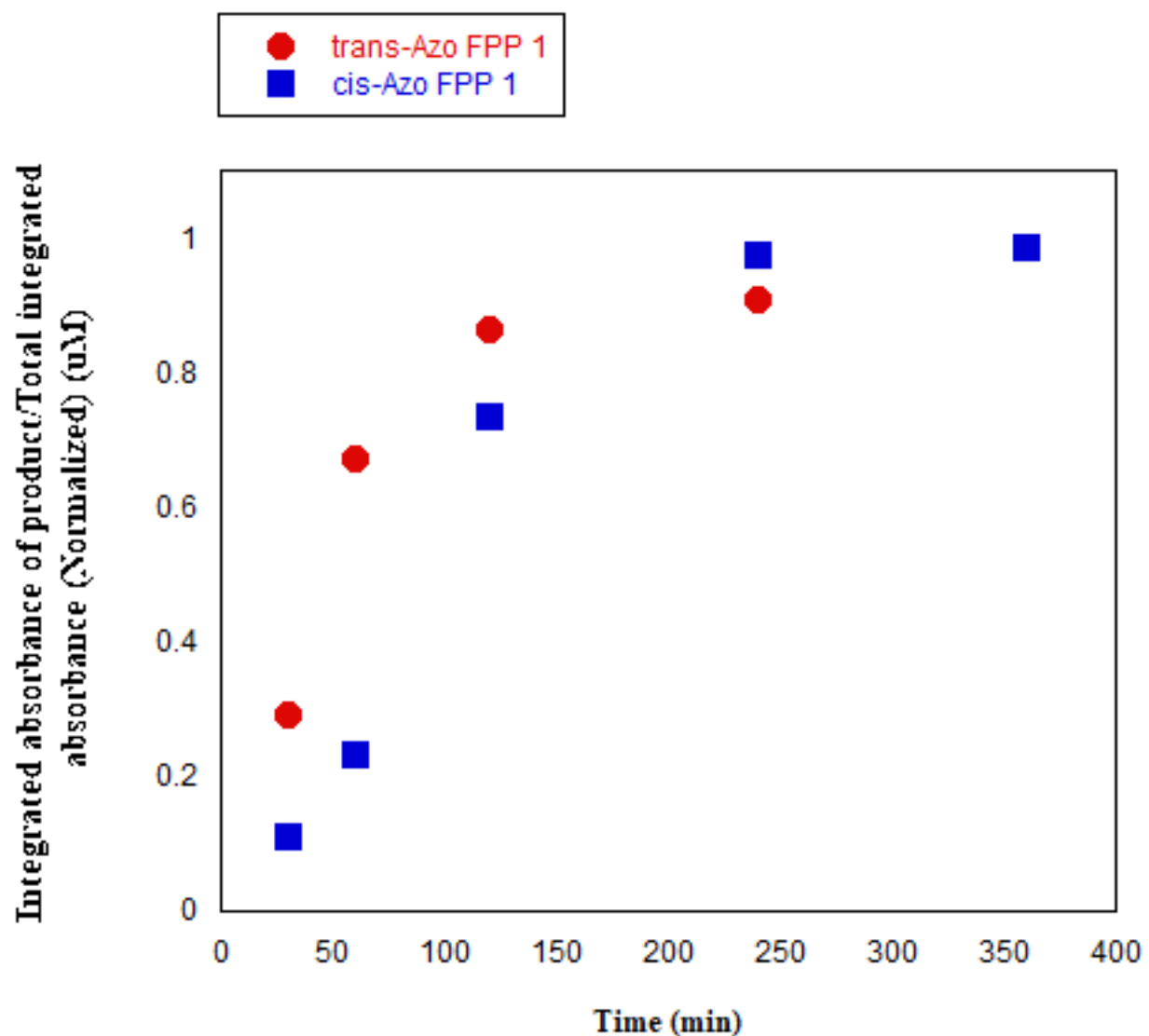


Figure 3.9. Time course for FTase-catalyzed modification of dns-GCVLS by both photoisomers of Azo-FPP1. Data reflect integration of substrate and product peaks shown in Figures 3.7 and 3.8, as described in the Materials and Methods. Reactions with the *trans*-isomer are represented in red, while the *cis*-isomer reactions are shown in blue.

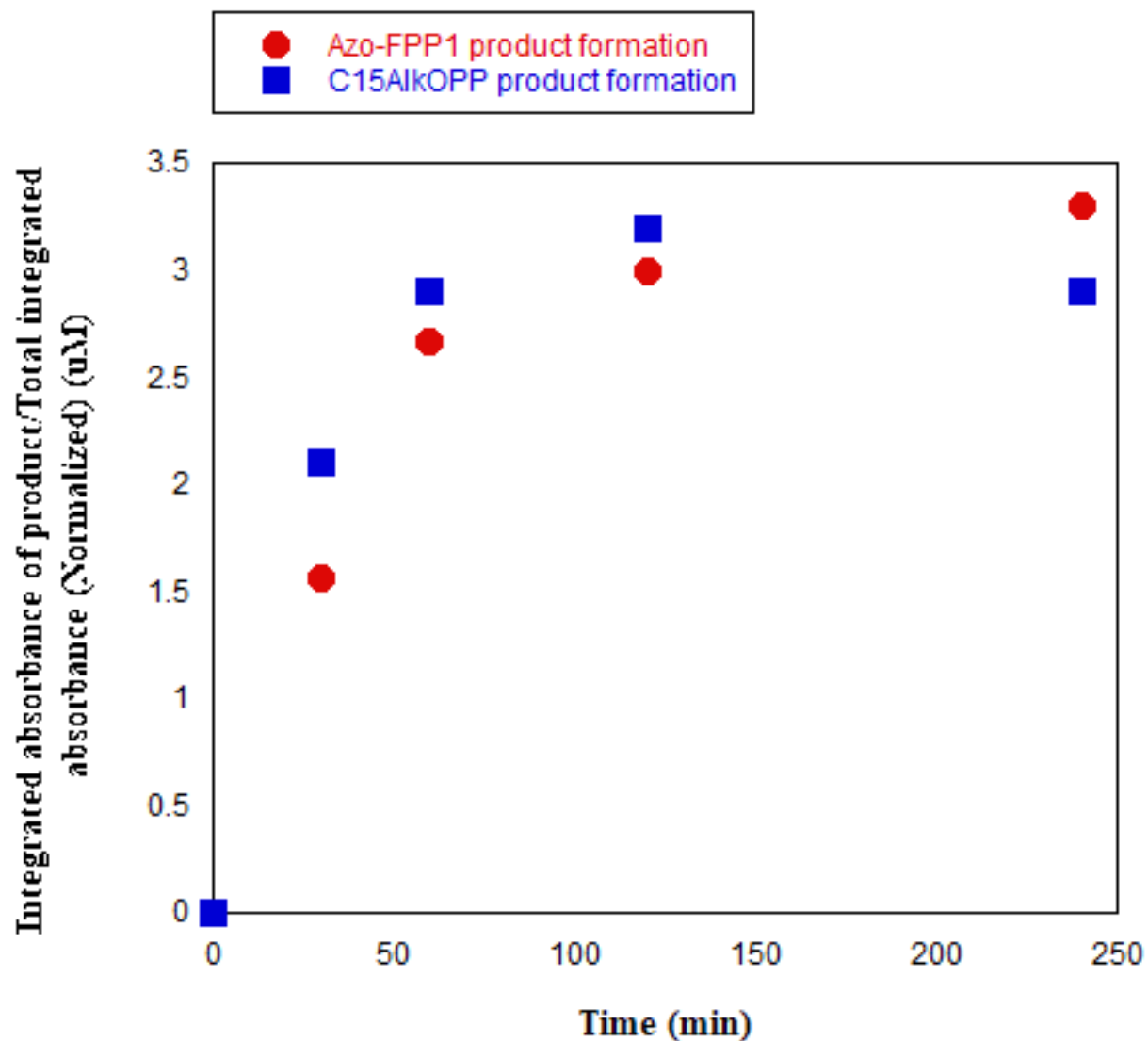


Figure 3.10. Time course for FTase-catalyzed modification of dns-GCVLS by both *trans* Azo-FPP1 and AlkC15OPP. Data reflect integration of substrate and product peaks, as described in the Materials and Methods. Reactions with the *trans*-Azo-FPP1 are represented in red, while the C15AlkOPP reactions are shown in blue.

3.4 Conclusions

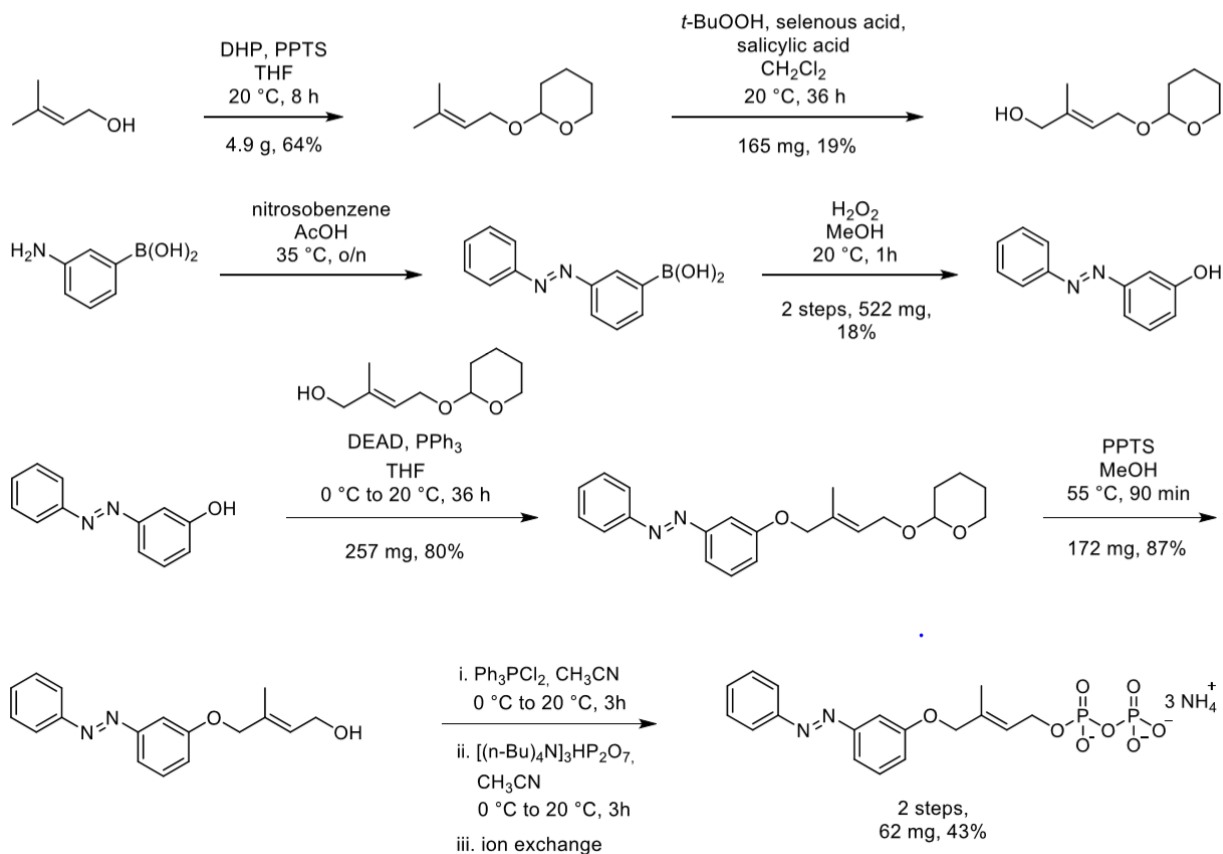
We employed an *in vitro* RP-HPLC based assay to determine whether FTase and/or GGTase-I can incorporate two different prenyl donor analogs with azobenzene in their hydrophobic chain to target peptide substrates. These azologs represent intriguing molecules as they are photo-sensitive, with dramatic structural changes controllable by light irradiation. This photoswitching ability could be harnessed to potentially mediate membrane localization behavior of prenylated proteins. Our initial analysis showed that FTase, but not GGTase-I, can utilize Azo-FPP1 as a viable donor to modify the canonical dns-GCVLS peptide substrate. This observation again speaks towards the flexibility exhibited by FTase in substrate selection in comparison to GGTase-I.^{33, 34} As for the preference of FTase for Azo-FPP1 over Azo-FPP2, we speculate that the aryl-ether moiety of Azo-FPP2 could be out of plane when bound to FTase and is not recognized by FTase. Alternatively, the location of the azobenzene in the middle of Azo-FPP2, rather than the distal end as in Azo-FPP1, is not as well accommodated by FTase. Moreover, Azo-FPP1 is more structurally similar to FPP than Azo-FPP2 is to FPP, which could also explain FTase selectivity of Azo-FPP1. These hypotheses require further investigation, perhaps through mutagenesis studies. In addition, we were able to observe the two different *trans* and *cis* photostationary states of Azo-FPP1 when bound to peptide substrate (dns-GCVLS) in our HPLC analysis, consistent with the distinct polarity / hydrophobicity predicted for these two isomers. These results suggest that due to the differing polarities observed, irradiation of Azo-FPP1 in cells could potentially modulate membrane localization behavior of proteins modified with Azo-FPP1.

In terms of reactivity, comparison with a known prenyl analog successfully used in cell studies provided useful insight that non-irradiated Azo-FPP1 exhibits sufficient reactivity to be

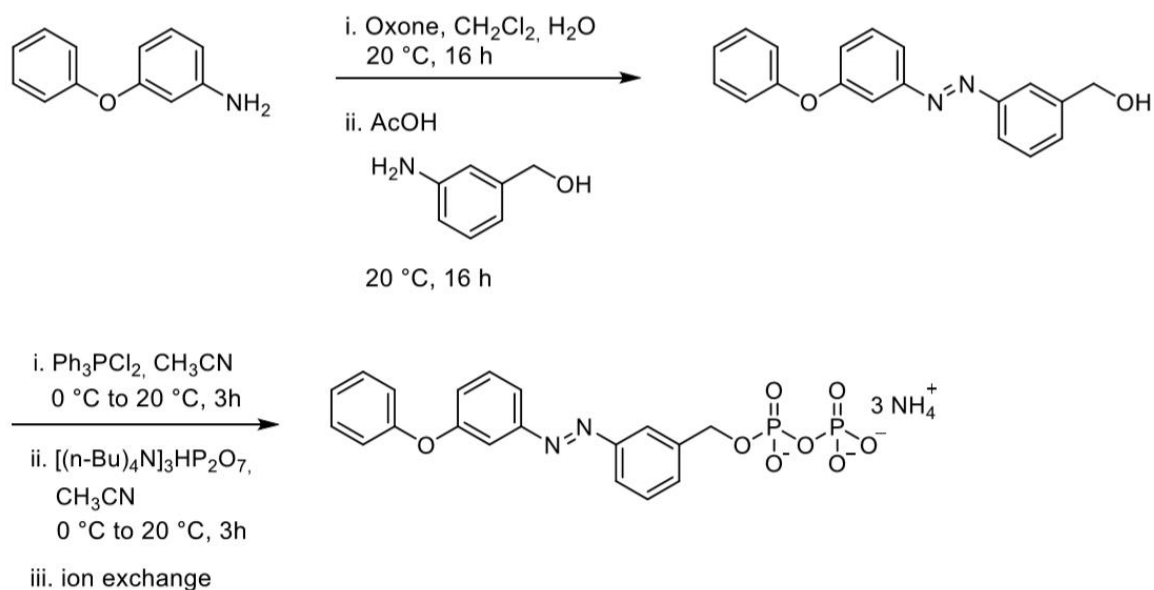
applied in cellular studies with endogenously expressed FTase.³³ As noted above, for these studies this azolog would need to cross the plasma membrane from the cell growth media in order to be utilized for protein modification within the cell. Current efforts by our collaborators are underway to test the utility of Azo-FPP1 in cell-based studies of protein modification, membrane localization, and biological function. Success in these studies will open interesting new options for modulating the behavior of lipidated proteins modified by Azo-FPP1, which could help further define the functional roles of prenylated proteins and investigate associated signaling pathways within biological systems.

3.5 Materials and Methods

3.5.1 Synthetic schemes of Azo-FPP analogs (Both synthetic procedures were completed by Johannes Morstein of the Trauner Group (Department of Chemistry, New York University):



Synthesis Scheme 3.1: Chemical synthesis of Azo-FPP1. This synthetic procedure was performed by our collaborator Johannes Morstein from the Trauner Group (Department of Chemistry, New York University).



Synthesis Scheme 3.2: Chemical synthesis of Azo-FPP2. This synthetic procedure was performed by our collaborator Johannes Morstein from the Trauner Group (Department of Chemistry, New York University).

3.5.2 Assessing activity of Azo-FPP analogs with FTase and dns-GCVLS via RP-HPLC:

dns-GCVLS (3 μM) were incubated with both 1x reaction buffer (50 mM HEPPSO-NaOH, pH 7.8, 5 mM TCEP) and 5 mM MgCl₂ (50 μL total) for 20 minutes in 0.65 mL low-adhesion eppendorf tubes. Peptide reactions were initiated by adding an enzyme mix (50 μL) containing 100 nM FTase, 5 mM MgCl₂, 1x reaction buffer, and 10 μM prenyl donor [FPP (positive control), Azo-FPP1 or Azo-FPP2]. Reactions were incubated at RT for 16 hours before adding an equal volume of 20% acetic acid in isopropanol to stop the reaction. HPLC analysis was performed at ambient temperature on an Agilent 1260 HPLC system with auto-sampler, UV-Vis, and fluorescence detection using a C18 reversed-phase analytical column (Zorbax XDB-C18) with a linear gradient from 30% acetonitrile in 25 mM ammonium acetate to 100% acetonitrile flowing at 1 mL/min over 30 minutes; peptides and products were detected by fluorescence (λ_{ex}

340 nm, λ_{em} 496 nm).

3.5.3 Assessing activity of Azo-FPP analogs with GGTase-I and dns-GCVLL via RP-

HPLC: dns-GCVLL (3 μ M) was incubated with both 1x reaction buffer (50 mM HEPPSO-NaOH, pH 7.8, 5 mM TCEP) (50 μ L total) for 20 minutes in 0.65 mL low-adhesion eppendorf tubes. Peptide reactions were initiated by adding an enzyme mix (50 μ L) containing 100 nM GGTase-I, 1x reaction buffer, and 10 μ M prenyl donor [FPP (positive control), Azo-FPP1 or Azo-FPP2]. Reactions were incubated at RT for 16 hours before adding an equal volume of 20% acetic acid in isopropanol to stop the reaction. HPLC analysis was performed at ambient temperature on an Agilent 1260 HPLC system with auto-sampler, UV-Vis, and fluorescence detection using a C18 reversed-phase analytical column (Zorbax XDB-C18) with a linear gradient from 30% acetonitrile in 25 mM ammonium acetate to 100% acetonitrile flowing at 1 mL/min over 30 minutes; peptides and products were detected by fluorescence (λ_{ex} 340 nm, λ_{em} 496 nm).

3.5.4 Detection of Azo-FPP1 photoisomers via RP-HPLC analysis: dns-GCVLS (3 μ M) was incubated with both 1x reaction buffer (50 mM HEPPSO-NaOH, pH 7.8, 5 mM TCEP) and 5 mM MgCl₂ (50 μ L total) for 20 minutes in 0.65 mL low-adhesion eppendorf tubes. Peptide reactions were initiated by adding an enzyme mix (50 μ L) containing 100 nM FTase, 5 mM MgCl₂, 1x reaction buffer, and 10 μ M Azo-FPP1. Reactions were incubated at RT for 16 hours before adding an equal volume of 20% acetic acid in isopropanol to stop the reaction. Following, the reaction mixtures were illuminated with either 365 nm or 460 nm LED lights for three

minutes before performing the HPLC analysis. HPLC analysis was performed at ambient temperature on an Agilent 1260 HPLC system with auto-sampler, UV-Vis, and fluorescence detection using a C18 reversed-phase analytical column (Zorbax XDB-C18) with a linear gradient from 30% acetonitrile in 25 mM ammonium acetate to 100% acetonitrile flowing at 1 mL/min over 30 minutes; peptides and products were detected by fluorescence (λ_{ex} 340 nm, λ_{em} 496 nm).

3.5.5 Time course study to determine reactivity of *trans*- and *cis*-Azo-FPP1: Peptide mix consisting of dns-GCVLS (3 μM) incubated with both 1x reaction buffer (50 mM HEPPSO-NaOH, pH 7.8, 5 mM TCEP) and 5 mM MgCl_2 (50 μL total) for 20 minutes in 0.65 mL low-adhesion eppendorf tubes. Before peptide reactions were initiated by adding an enzyme mix (50 μL) containing 100 nM FTase, 5 mM MgCl_2 , 1x reaction buffer, and 10 μM Azo-FPP1, the enzyme mix was either non-illuminated or illuminated with 365 nm LED light (*cis* isomer) for 3 minutes in dark. Reactions were incubated at RT for different time points; 30 minutes, 60 minutes, 120 minutes, 240 minutes, or 360 minutes. HPLC analysis was performed at ambient temperature on an Agilent 1260 HPLC system with auto-sampler, UV-Vis, and fluorescence detection using a C18 reversed-phase analytical column (Zorbax XDB-C18) with a linear gradient from 30% acetonitrile in 25 mM ammonium acetate to 100% acetonitrile flowing at 1 mL/min over 30 minutes; peptides and products were detected by fluorescence (λ_{ex} 340 nm, λ_{em} 496 nm). Reaction progress was calculated by % peptide conversion to prenylated product, with substrate and product peaks assigned per retention times:

$$\% \text{ conversion} = \text{Product Integration} / (\text{Product} + \text{Substrate Integration})$$

3.5.6 Time course study to gauge reactivity of non-illuminated Azo-FPP1 in comparison to

AlkC15OPP: To probe the reactivity of Azo-FPP1 and to determine if the reactivity of Azo-FPP1 is sufficient to potentially support cell-based metabolic labeling, this analogue was compared with C15AlkOPP (an isoprenoid alkyne analogue from DiStefano Lab, University of Minnesota) using a time course experiment with peptide substrate. A peptide mix consisting of dns-GCVLS (3 μ M) was incubated with both 1x reaction buffer (50 mM HEPPSO-NaOH, pH 7.8, 5 mM TCEP) and 5 mM MgCl₂ (50 μ L total) for 20 minutes in 0.65 mL low-adhesion eppendorf tubes. Peptide reactions were initiated by adding an enzyme mix (50 μ L) containing 100 nM FTase, 5 mM MgCl₂, 1x reaction buffer, and either 10 μ M Azo-FPP1 or C15AlkOPP. Following addition of equal volume of 20% acetic acid in isopropanol stop solution at different time intervals, 30 minutes, 60 minutes, 120 minutes, and 240 minutes; reaction mixtures were analyzed by reverse-phase HPLC to determine the extent of peptide prenylation by both donor substrates. Since the C15AlkOPP probe results in a greater fluorescence enhancement/detection on the HPLC, UV chromatograms were analyzed at absorbance of 340 nm for the dansyl group. Reaction progress was obtained by calculating the concentration of product formation (μ M) with normalization to the UV absorbance observed upon reaction completion. HPLC analysis was performed at ambient temperature on an Agilent 1260 HPLC system with auto-sampler, UV-Vis, and fluorescence detection using a C18 reversed-phase analytical column (Zorbax XDB-C18) with a linear gradient from 30% acetonitrile in 25 mM ammonium acetate to 100% acetonitrile flowing at 1 mL/min over 30 minutes; peptides and products were detected by fluorescence (λ_{ex} 340 nm, λ_{em} 496 nm).

3.6 References

1. Velema, W. A.; Szymanski, W.; Feringa, B. L., Photopharmacology: beyond proof of principle. *J Am Chem Soc* **2014**, *136* (6), 2178-91.
2. Beharry, A. A.; Woolley, G. A., Azobenzene photoswitches for biomolecules. *Chem Soc Rev* **2011**, *40* (8), 4422-37.
3. Hull, K.; Morstein, J.; Trauner, D., In Vivo Photopharmacology. *Chem Rev* **2018**, *118* (21), 10710-10747.
4. Szymanski, W.; Beierle, J. M.; Kistemaker, H. A.; Velema, W. A.; Feringa, B. L., Reversible photocontrol of biological systems by the incorporation of molecular photoswitches. *Chem Rev* **2013**, *113* (8), 6114-78.
5. Hoorens, M. W. H.; Szymanski, W., Reversible, Spatial and Temporal Control over Protein Activity Using Light. *Trends Biochem Sci* **2018**, *43* (8), 567-575.
6. Brieke, C.; Rohrbach, F.; Gottschalk, A.; Mayer, G.; Heckel, A., Light-controlled tools. *Angew Chem Int Ed Engl* **2012**, *51* (34), 8446-76.
7. Ellis-Davies, G. C., Caged compounds: photorelease technology for control of cellular chemistry and physiology. *Nat Methods* **2007**, *4* (8), 619-28.
8. Klan, P.; Solomek, T.; Bochet, C. G.; Blanc, A.; Givens, R.; Rubina, M.; Popik, V.; Kostikov, A.; Wirz, J., Photoremovable protecting groups in chemistry and biology: reaction mechanisms and efficacy. *Chem Rev* **2013**, *113* (1), 119-91.
9. Lee, H. M.; Larson, D. R.; Lawrence, D. S., Illuminating the chemistry of life: design, synthesis, and applications of "caged" and related photoresponsive compounds. *ACS Chem Biol* **2009**, *4* (6), 409-27.

10. Broichhagen, J.; Frank, J. A.; Trauner, D., A roadmap to success in photopharmacology. *Acc Chem Res* **2015**, *48* (7), 1947-60.
11. Merino, E., Synthesis of azobenzenes: the coloured pieces of molecular materials. *Chem Soc Rev* **2011**, *40* (7), 3835-53.
12. Rau, H., Spectroscopic Properties of Organic Azo Compounds. *Angewandte Chemie International Edition in English* **1973**, *12* (3), 224-235.
13. Bandara, H. M.; Burdette, S. C., Photoisomerization in different classes of azobenzene. *Chem Soc Rev* **2012**, *41* (5), 1809-25.
14. Fliegl, H.; Kohn, A.; Hattig, C.; Ahlrichs, R., Ab initio calculation of the vibrational and electronic spectra of trans- and cis-azobenzene. *J Am Chem Soc* **2003**, *125* (32), 9821-7.
15. Tsuji, T.; Takeuchi, H.; Egawa, T.; Konaka, S., Effects of molecular structure on the stability of a thermotropic liquid crystal. Gas electron diffraction study of the molecular structure of phenyl benzoate. *J Am Chem Soc* **2001**, *123* (26), 6381-7.
16. Sporlein, S.; Carstens, H.; Satzger, H.; Renner, C.; Behrendt, R.; Moroder, L.; Tavan, P.; Zinth, W.; Wachtveitl, J., Ultrafast spectroscopy reveals subnanosecond peptide conformational dynamics and validates molecular dynamics simulation. *Proc Natl Acad Sci U S A* **2002**, *99* (12), 7998-8002.
17. Ihalainen, J. A.; Bredenbeck, J.; Pfister, R.; Helbing, J.; Chi, L.; van Stokkum, I. H.; Woolley, G. A.; Hamm, P., Folding and unfolding of a photoswitchable peptide from picoseconds to microseconds. *Proc Natl Acad Sci U S A* **2007**, *104* (13), 5383-8.
18. Frank, J. A.; Moroni, M.; Moshourab, R.; Sumser, M.; Lewin, G. R.; Trauner, D., Photoswitchable fatty acids enable optical control of TRPV1. *Nat Commun* **2015**, *6*, 7118.

19. Leinders-Zufall, T.; Storch, U.; Bleyemehl, K.; Mederos, Y. S. M.; Frank, J. A.; Konrad, D. B.; Trauner, D.; Gudermann, T.; Zufall, F., PhoDAGs Enable Optical Control of Diacylglycerol-Sensitive Transient Receptor Potential Channels. *Cell Chem Biol* **2018**, *25* (2), 215-223 e3.
20. Lichtenegger, M.; Tiapko, O.; Svobodova, B.; Stockner, T.; Glasnov, T. N.; Schreibmayer, W.; Platzer, D.; de la Cruz, G. G.; Krenn, S.; Schober, R.; Shrestha, N.; Schindl, R.; Romanin, C.; Groschner, K., An optically controlled probe identifies lipid-gating fenestrations within the TRPC3 channel. *Nat Chem Biol* **2018**, *14* (4), 396-404.
21. Frank, J. A.; Yushchenko, D. A.; Fine, N. H. F.; Duca, M.; Citir, M.; Broichhagen, J.; Hodson, D. J.; Schultz, C.; Trauner, D., Optical control of GPR40 signalling in pancreatic beta-cells. *Chem Sci* **2017**, *8* (11), 7604-7610.
22. Frank, J. A.; Franquelim, H. G.; Schwille, P.; Trauner, D., Optical Control of Lipid Rafts with Photoswitchable Ceramides. *J Am Chem Soc* **2016**, *138* (39), 12981-12986.
23. Pernpeintner, C.; Frank, J. A.; Urban, P.; Roeske, C. R.; Pritzl, S. D.; Trauner, D.; Lohmuller, T., Light-Controlled Membrane Mechanics and Shape Transitions of Photoswitchable Lipid Vesicles. *Langmuir* **2017**, *33* (16), 4083-4089.
24. Frank, J. A.; Yushchenko, D. A.; Hodson, D. J.; Lipstein, N.; Nagpal, J.; Rutter, G. A.; Rhee, J. S.; Gottschalk, A.; Brose, N.; Schultz, C.; Trauner, D., Photoswitchable diacylglycerols enable optical control of protein kinase C. *Nat Chem Biol* **2016**, *12* (9), 755-62.
25. Morstein, J.; Hill, R. Z.; Novak, A. J. E.; Feng, S.; Norman, D. D.; Donthamsetti, P. C.; Frank, J. A.; Harayama, T.; Williams, B. M.; Parrill, A. L.; Tigyi, G. J.; Riezman, H.; Isacoff, E. Y.; Bautista, D. M.; Trauner, D., Optical control of sphingosine-1-phosphate formation and function. *Nat Chem Biol* **2019**, *15* (6), 623-631.

26. Subramanian, T.; Pais, J. E.; Liu, S.; Troutman, J. M.; Suzuki, Y.; Leela Subramanian, K.; Fierke, C. A.; Andres, D. A.; Spielmann, H. P., Farnesyl diphosphate analogues with aryl moieties are efficient alternate substrates for protein farnesyltransferase. *Biochemistry* **2012**, *51* (41), 8307-19.
27. Moores, S. L.; Schaber, M. D.; Mosser, S. D.; Rands, E.; O'Hara, M. B.; Garsky, V. M.; Marshall, M. S.; Pompliano, D. L.; Gibbs, J. B., Sequence dependence of protein isoprenylation. *J Biol Chem* **1991**, *266* (22), 14603-10.
28. Strickland, C. L.; Windsor, W. T.; Syto, R.; Wang, L.; Bond, R.; Wu, Z.; Schwartz, J.; Le, H. V.; Beese, L. S.; Weber, P. C., Crystal structure of farnesyl protein transferase complexed with a CaaX peptide and farnesyl diphosphate analogue. *Biochemistry* **1998**, *37* (47), 16601-11.
29. Boutin, J. A.; Marande, W.; Petit, L.; Loynel, A.; Desmet, C.; Canet, E.; Fauchere, J. L., Investigation of S-farnesyl transferase substrate specificity with combinatorial tetrapeptide libraries. *Cellular signalling* **1999**, *11* (1), 59-69.
30. Krzysiak, A. J.; Scott, S. A.; Hicks, K. A.; Fierke, C. A.; Gibbs, R. A., Evaluation of protein farnesyltransferase substrate specificity using synthetic peptide libraries. *Bioorg Med Chem Lett* **2007**, *17* (20), 5548-5551.
31. Rashidian, M.; Song, J. M.; Pricer, R. E.; Distefano, M. D., Chemoenzymatic reversible immobilization and labeling of proteins without prior purification. *Journal of the American Chemical Society* **2012**, *134* (20), 8455-67.
32. Palsuledesai, C. C.; Ochocki, J. D.; Kuhns, M. M.; Wang, Y. C.; Warmka, J. K.; Chernick, D. S.; Wattenberg, E. V.; Li, L.; Arriaga, E. A.; Distefano, M. D., Metabolic

Labeling with an Alkyne-modified Isoprenoid Analog Facilitates Imaging and Quantification of the Prenylome in Cells. *ACS chemical biology* **2016**, *11* (10), 2820-2828.

33. Blanden, M. J.; Suazo, K. F.; Hildebrandt, E. R.; Hardgrove, D. S.; Patel, M.; Saunders, W. P.; Distefano, M. D.; Schmidt, W. K.; Hougland, J. L., Efficient farnesylation of an extended C-terminal C (x) 3X sequence motif expands the scope of the prenylated proteome. *Journal of Biological Chemistry* **2018**, *293* (8), 2770-2785.

34. Ashok, S.; Hildebrandt, E. R.; Ruiz, C. S.; Hardgrove, D. S.; Coreno, D. W.; Schmidt, W. K.; Hougland, J. L., Protein farnesyltransferase catalyzes unanticipated farnesylation and geranylgeranylation of shortened target sequences. *Biochemistry* **2020**, *59* (11), 1149-1162.

Chapter 4: Development of a FRET assay to monitor protein prenylation within cells

The work presented herein is unpublished.

FLIM-FRET microscopy and analysis was performed by Peter Calvert (Center for Vision Research, Upstate Medical University). HEK293 cell maintenance and preparation for microscopy was assisted by Himanshu Malhotra from the Calvert Lab (Center for Vision Research, Upstate Medical University).

David W. Coreno (Syracuse University) assisted with expression and purification of His₆-PDE δ .

4.1 Introduction

As described in Chapter 2, membrane localization studies in mammalian cells using the modified eGFP-KRas fusion protein did not provide evidence for the prenylation of non-canonical Cxx sequences. This could be because Cxx sequences are not prenylated inside cells as *in vitro* steady-state analysis showed that the sequences tested are not as reactive as the most reactive CaaX sequences (see section 2.6).¹ Or these Cxx proteins are modified by FTase, but are shunted (i.e. not proteolysed and methylated following prenylation) as several of the sequences tested were recovered from a Ydj1p-based assay.^{2,3} Therefore, membrane localization studies would not help identify potential substrates in a mammalian context, as post-processing of prenylated proteins is often required for localization at the plasma membrane.

To expand our ability to monitor protein prenylation, we aimed to develop a FRET based assay that would allow us to detect prenylation of Cxx sequences in cells. Förster Resonance Energy Transfer (FRET) is a photo-physical process by which energy (non-radiative) is transferred from an excited state of one fluorophore (termed the donor (D^*)) to another fluorophore (the acceptor (A)) via a dipole-dipole interaction.⁴ For this energy transfer to occur, a number of criteria must be satisfied. First, the absorption spectra of the acceptor must have sufficient overlap with the emission spectra of the donor. Second, the transition dipole moments of the donor and acceptor must be favorably aligned. Finally, the donor and acceptor must be near each other for energy transfer to occur (generally within ~ 10 nm).⁵⁻⁷ The energy transfer rate from the donor to the acceptor decreases with the sixth power of the distance. Due to the dependence on the distance between the donating and the accepting fluorophores, FRET has become a valuable tool for studying biological phenomena.⁸⁻¹¹ By labeling different proteins

with the donor and the acceptor, FRET can be used to ascertain if proteins interact with each other.

One common approach for monitoring FRET utilizes the increase in acceptor fluorescence due to the energy transfer from the donor.¹² However, these measurements must account for the concentration dependence of the fluorescence intensities of the donor and the acceptor. In addition, there can be complications from ‘donor bleed through’ due to the overlap of the donor fluorescence into the acceptor emission band and non-FRET fluorescence from directly excited acceptor molecules. Therefore, such measurements require careful calibration of these factors using data of samples containing only the donor and only the acceptor.¹³⁻¹⁶

In addition to the fluorescence intensity, detecting changes in the fluorescence/excited state lifetime of a donor molecule provides another option for monitoring FRET. When a molecule absorbs a photon, it enters an electronically excited singlet state. From this excited state, the molecules can return to the ground state by emitting a photon, by internally converting the absorbed energy into heat, by passing the energy to its molecular environment, or by crossing into the triplet state and returning to the ground state by phosphorescence or internal conversion.¹⁷ For a homogenous population of molecules, the resulting fluorescence decay can be fit to a single exponential function. The time constant of this function, the fluorescence lifetime, is the reciprocal sum of the rate constants of all possible return paths. The fluorescence lifetime is dependent on the fluorescent molecule’s conformation and the way the molecule interacts with its environment.¹⁸ Of all fluorescence parameters, it is the fluorescence decay function that provides the most direct insight into the molecular interactions with its biological environment.¹⁸ For *in cellulo* studies, fluorescence lifetime imaging microscopy (FLIM) of the

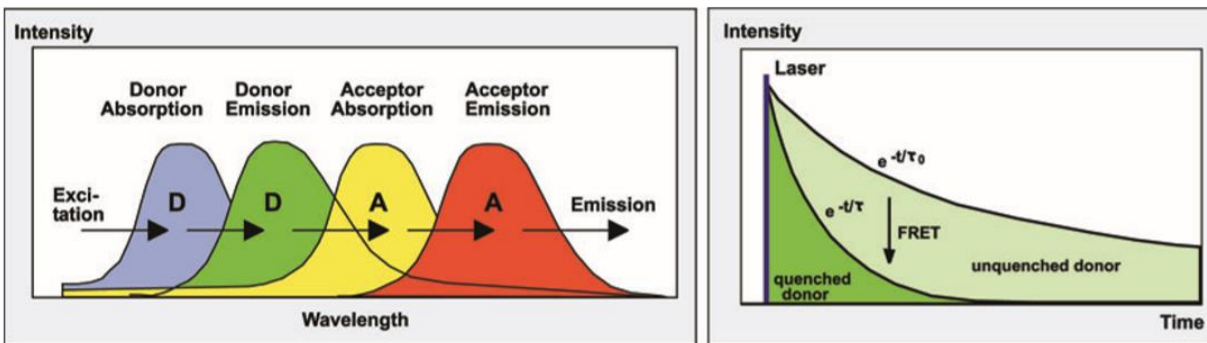
donor is the gold standard for FRET measurements as FRET results in a quenching of the donor fluorescence and thus, decreases the donor lifetime (Figure 4.1).^{6, 7, 18, 19}

To establish a FRET assay for assessing the prenylated state of non-canonical Cxx sequences in cells, a prenyl binding protein is required which will associate with the modified “Cxx” protein. This bimolecular association can be used to place donor and acceptor groups in proximity to allow FRET between them. The cytoplasmic prenyl binding factor PDE δ has been reported as a binding partner for various prenylated small G proteins including K/HRas and non-prenylated small G proteins such as Arl1 and Arl3.²⁰⁻²³ PDE δ has also been proposed to assist in H/N/KRas signaling in a similar way to Rho- and Rab-GDIs (Guanine-nucleotide Dissociation Inhibitors) that bind to prenylated GDP-bound small G-proteins and thus constitute a cytoplasmic pool of inactive G-proteins.²⁰ The Bastiaens group showed that PDE δ plays a role in modulating cell signaling through Ras family G proteins by sustaining their dynamic distribution in cellular membranes.²⁴ Moreover, they also showed that farnesylation of target proteins was necessary for the observed modulation by PDE δ . This work utilized FLIM-FRET to study the impact of PDE δ on the dynamic distribution of multiple prenylated Ras proteins and inspired the efforts reported in this chapter.²⁴

The work herein describes development of a FRET based assay which would allow for the detection of prenylated non-canonical Cxx motifs in a biological context. First, we attempted an *in vitro* characterization using purified His₆-mCherry-PDE δ fusion protein with purified eGFP protein appended with prenylation motifs to determine if PDE δ binds prenylated non-canonical Cxx sequences. Followed by studies that utilized purified His₆-PDE δ with purified prenylated dansyl peptides. We also report initial studies towards *in cellulo* characterization utilizing FLIM-

FRET to detect binding of non-canonical Cxx sequences in the context of two different fusion proteins.

Figure 4.1. Fluorescence resonance energy transfer. Left panel: FRET is an interaction of two fluorophore molecules with the emission band of one overlapping the absorption band of the other. Right panel: FRET results in a quenching of the donor fluorescence and consequently, decrease in the donor lifetime. This figure has been reused with permission from reference 18 (Appendix IV).



4.2 Establishing an *in vitro* FRET assay to assess binding of mCherry-PDE δ and prenylated eGFP-fusion peptide

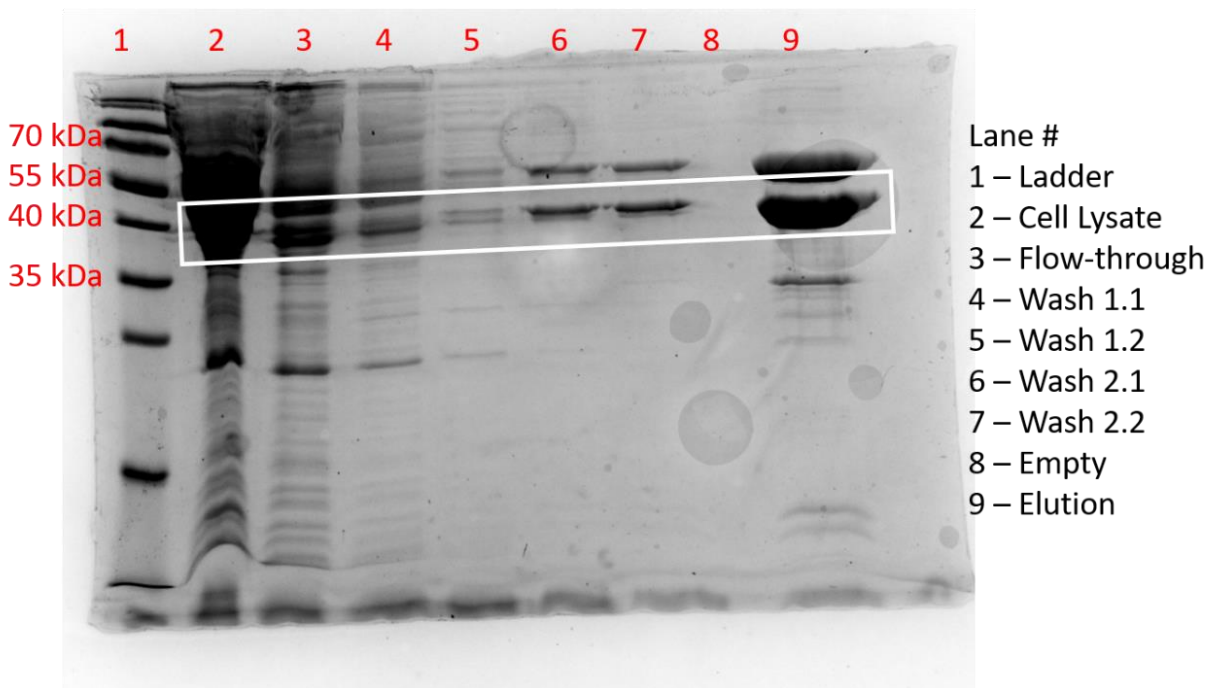
We aimed to design another system for detecting prenylation of non-canonical sequences inside a mammalian cell. This assay is based on a mCherry-PDE δ fusion protein, the mammalian plasmid for which was generously provided by the Bastiaens Group (Max Planck Institute of Molecular Physiology). Phosphodiesterase 6 (PDE6) delta subunit (PDE δ) is a cytoplasmic prenyl binding factor that has been proposed to assist in H/N/KRas intracellular trafficking by binding to the prenylated domain.^{21,22} In their study, Chandra et al. demonstrated the role of PDE δ in modulating signaling through Ras family G proteins by using a FRET system consisted of mCherry-PDE δ and various Ras proteins fused to the monomeric yellow fluorescent protein Citrine.²⁴ Interactions between the prenylated mCitrine-Ras proteins and mCherry-PDE δ produced a FRET signal allowing them to visualize the direct interaction of these two proteins. We aimed to develop a similar FRET signaling system to investigate prenylation of non-canonical Cxx sequences in cells.

Towards that goal, we first investigated whether this system would be viable for monitoring Cxx prenylation within an intact cell by establishing an *in vitro* model assay. After sequence confirmation of the mammalian mCherry-PDE δ vector, the mCherry-PDE δ insert was cloned into a pET-28a bacterial expression vector. The pET-28a vector inserts a His-tag at the N-terminus of the expressed protein to allow for affinity purification. Successful cloning was confirmed via sequencing. Expression of His₆-mCherry-PDE δ in a bacterial cell culture was visually detected by the bright pink color change in the bacterial culture and visualization of a pink band when analyzing the cell lysate on SDS-PAGE gel. While the predicted molecular weight for His₆-mCherry-PDE δ is 46.8 kDa, the pink band representing the fluorescent protein

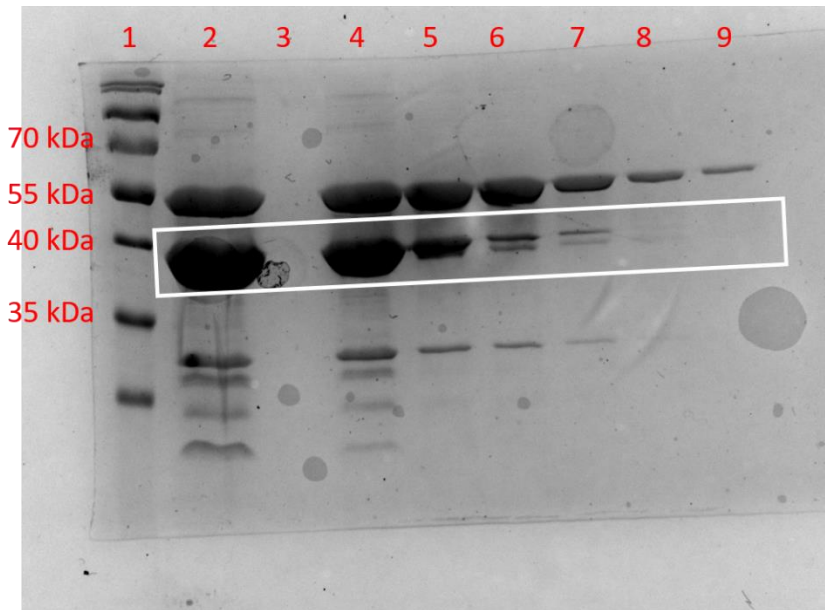
was observed to run aberrantly low closer to the 40 kDa ladder band suggesting incomplete denaturation of the expressed protein (Figure 4.2A). Following protein expression, the His₆-mCherry-PDE δ protein was purified using Nickel resin-based metal affinity chromatography (Figure 4.2B). Again, His₆-mCherry-PDE δ 's pink band was observed to run aberrantly low when analyzed via a denaturing SDS-PAGE. Of note, we also observed two bands for the purified protein when diluted. A non-denaturing SDS-PAGE analysis was carried out on purified His₆-mCherry-PDE δ where only a single band was observed running at ~40 kDa, consistent with the non-denatured protein exhibiting lower apparent molecular weight (Figure 4.2C).

Figure 4.2. Expression and purification of His₆-mCherry-PDE δ shown in white. A) Denaturing SDS-PAGE gel analysis of His₆-mCherry-PDE δ purification. B) Serial dilution of purified His₆-mCherry-PDE δ under denaturing conditions. C) Purified His₆-mCherry-PDE δ under non-denaturing conditions; the doublet in gel B) lane 2 collapses to the lower band in C). Bands on all three SDS-PAGE Gels were assigned for the expressed and purified protein based on the visualization of a clear pink band. His₆-mCherry-PDE δ was expressed and purified as described in Materials and Methods.

A)

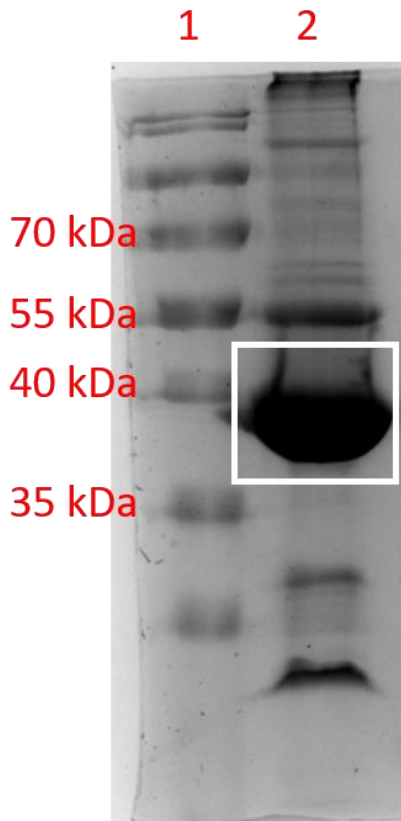


B)



Lane #
1 – Ladder
2 – 1:1 His₆-mCherry-PDE δ
3 – Empty
4 – 1:2 His₆-mCherry-PDE δ
5 – 1:5 His₆-mCherry-PDE δ
6 – 1:10 His₆-mCherry-PDE δ
7 – 1:20 His₆-mCherry-PDE δ
8 – 1:50 His₆-mCherry-PDE δ
9 – 1:100 His₆-mCherry-PDE δ

C)



Lane #
1 – Ladder
2 – 1:1 His₆-mCherry-PDE δ

Following expression and purification, His₆-mCherry-PDE δ was used in assays to measure FRET activity that would reflect binding to a prenylated eGFP fluorescent protein. A binding event is expected to produce a FRET signal, as the mCherry and eGFP fluorescent proteins are compatible with FRET given their overlapping emission (eGFP) and absorption (mCherry) spectra.²⁵ To ensure the two protein constructs were FRET compatible, emission spectral scans of both His₆-mCherry-PDE δ and eGFP-CVIA were performed. However, as shown in Figure 4.3A and 4.3B, we observed a strong emission from His₆-mCherry-PDE δ at the excitation wavelengths of 420 nm and 450 nm, where we expected to only observe emission from eGFP. Moreover, we found that both fluorescent fusion proteins emit at 510 nm during an excitation scan, where we again expected to only see eGFP emit (Figure 4.3C). These unexpected excitation and emission spectral results for His₆-mCherry-PDE δ suggest that it is not an ideal FRET pair for eGFP, at least for this *in vitro* analysis.

Despite these results, purified prenylated eGFP-CVIA and mCherry-PDE δ were incubated together under foil and analyzed on the plate reader at 15- and 60-minute increments by exciting eGFP at 488 nm and observing emission of mCherry at 610 nm. A negative control with purified non-prenylated eGFP-CVIA was also analyzed (Figure 4.4). No appreciable change in mCherry fluorescence was observed between the two tested conditions, suggesting that binding between the two proteins was not achieved.

Figure 4.3. Spectral characterization of His₆-mCherry-PDE δ and eGFP-CVIA. A) Emission spectral scan of His₆-mCherry-PDE δ and eGFP-CVIA obtained via plate-reader monitoring ($\lambda_{ex} = 420$ nm) B) Emission spectral scan of His₆-mCherry-PDE δ and eGFP-CVIA obtained via plate-reader monitoring ($\lambda_{ex} = 450$ nm) C) Excitation spectral scan of His₆-mCherry-PDE δ and eGFP-CVIA obtained via plate-reader monitoring ($\lambda_{em} = 510$ nm).

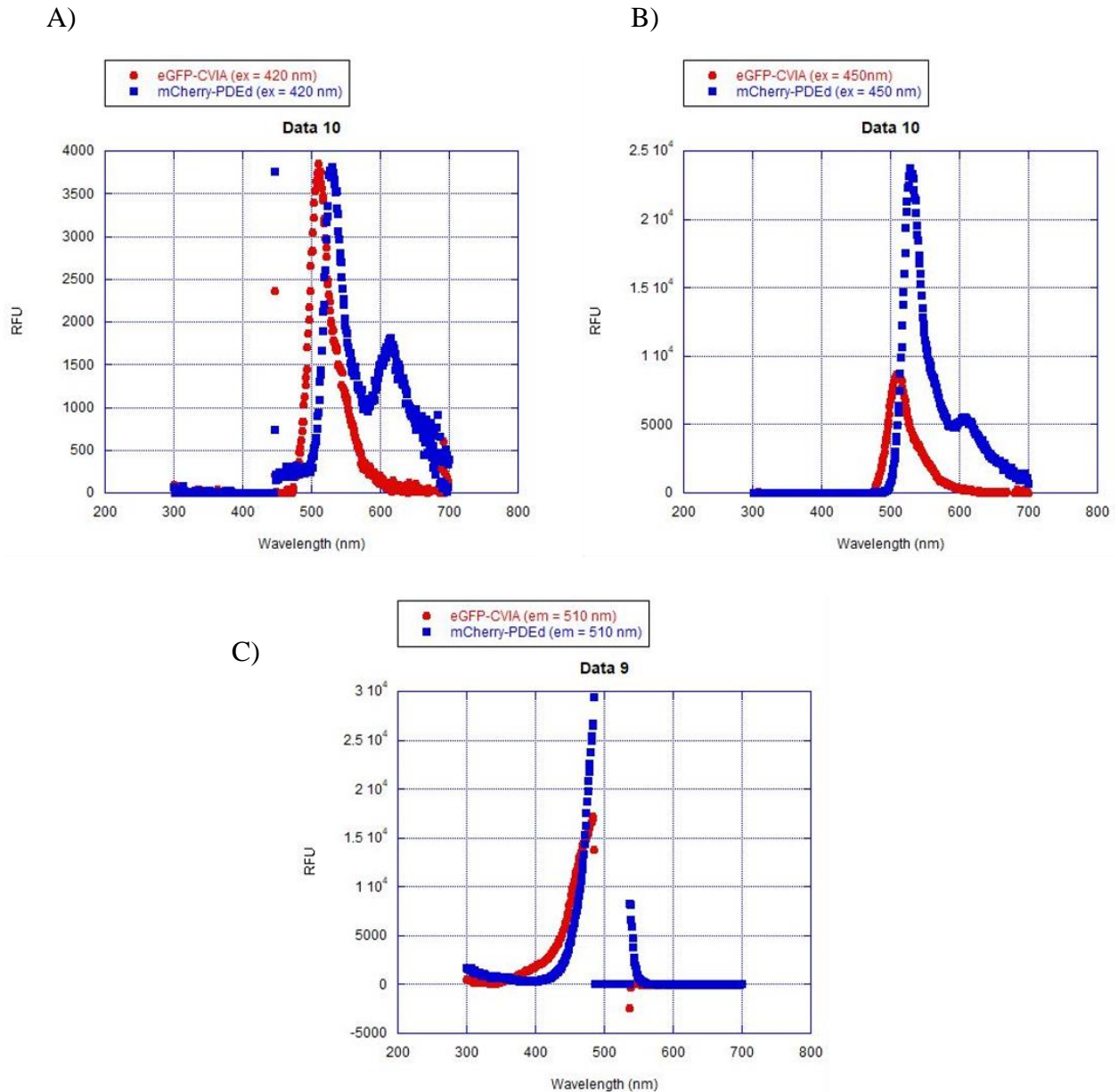
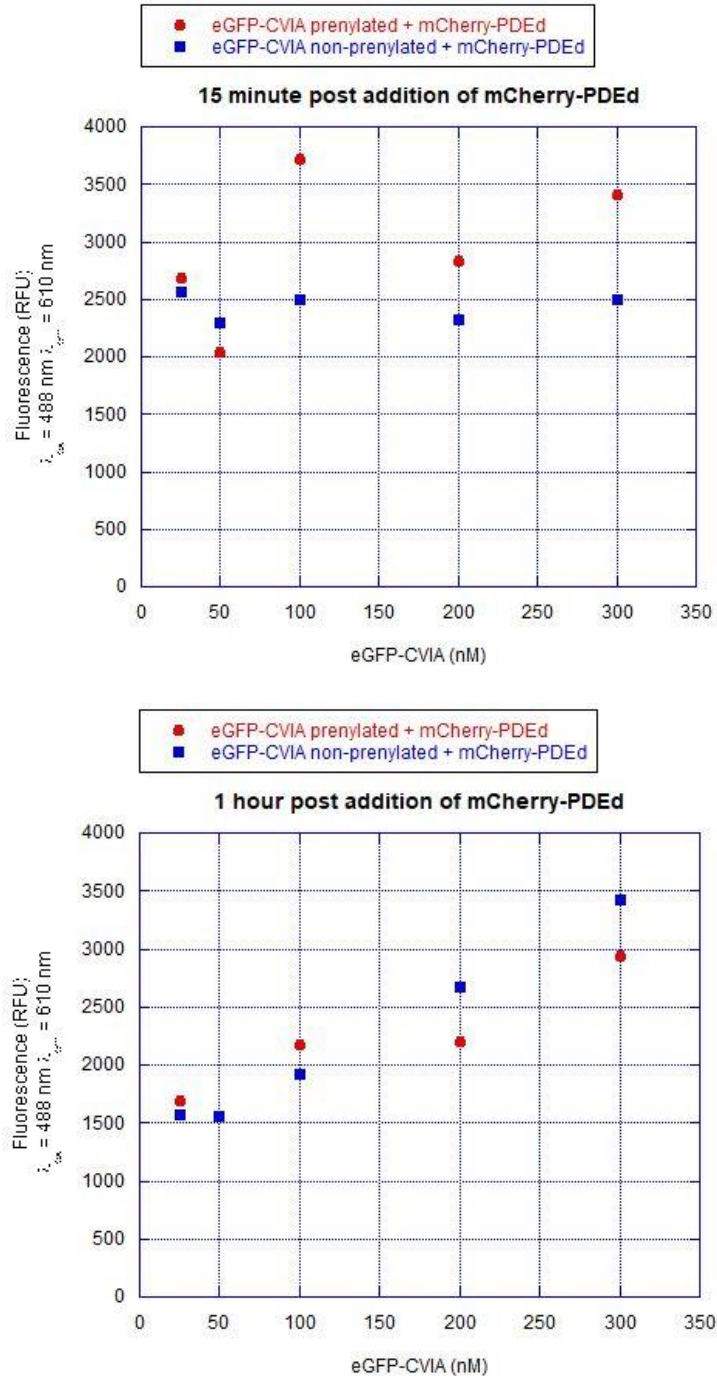


Figure 4.4. FRET analysis to assess binding interaction of His₆-mCherry-PDE δ with farnesylated and non-farnesylated eGFP-CVIA at 15- and 60-minutes post-incubation. Fluorescence measurements obtained via plate-reader monitoring of FRET-based emission from mCherry ($\lambda_{ex} = 488 \text{ nm}$, $\lambda_{em} = 610 \text{ nm}$), which do not provide evidence for FRET.



4.3 Expression and purification of PDE δ and development of FRET assay using PDE δ and a prenylated dansyl-peptide

With our initial efforts to measure FRET activity between His₆-mCherry-PDE δ and prenylated eGFP-CVIA unfruitful, we sub-cloned PDE δ into the pET-28a vector to directly examine binding of a prenylated dansyl-peptide and PDE δ based on previous work.²⁶ This system utilizes direct excitation of tryptophan residues in PDE δ and FRET-based emission from the dansyl fluorophore in the peptide. Successful sub-cloning was verified via Sanger sequencing. Expression of His₆-PDE δ was verified by the visualization of a prominent band on a non-denaturing SDS-PAGE gel at ~20 kDa corresponding to the His₆-PDE δ molecular weight (~17.4 kDa). The His₆-PDE δ protein was purified using Ni²⁺-affinity resin (Figure 4.5).

Following purification of His₆-PDE δ protein, assays were performed to determine the presence of FRET signal indicating binding of farnesylated dns-GCVLS to His₆-PDE δ . Spectral scans of His₆-PDE δ in presence of farnesylated dns-GCVLS were obtained by exciting the tryptophan residues in His₆-PDE δ at 282 nm and monitoring dansyl group emission at 515 nm. Negative controls consisted of His₆-PDE δ with non-farnesylated dns-GCVLS, His₆-PDE δ alone, and both prenylated and non-prenylated dns-GCVLS alone. Emission spectral scans were carried out following overnight incubation (see Materials and Methods). These scans did not provide a consistent increase in fluorescence signal from the dansyl group in the peptide- His₆-PDE δ sample compared to negative control of His₆-PDE δ only and/or His₆-PDE δ with non-prenylated dns-GCVLS peptide (Figure 4.6). Inconsistency in readings between wells makes interpreting results more difficult. We failed to observe any consistent increase in fluorescence of the dansyl group for the prenylated peptide in presence of His₆-PDE δ , suggesting that PDE δ does not bind the prenylated dns-GCVLS peptide under the conditions tested.

These results are not overly surprising as studies have shown that PDE δ prefers binding proteins that are processed post-prenylation, including a crystal structure of PDE δ bound to KRas protein.^{26, 27} Specifically, PDE δ exhibits a greater affinity for proteins that are carboxymethylated at their C-terminus following prenylation. In our assay, the dns-GCVLS peptide used still has the three amino acids following the prenylated cysteine. In comparison, the *in vitro* study performed by Zhang and co-workers utilized synthesized prenylated dansyl-cysteines with a carboxymethyl moiety following the prenyl cysteine. Based on the crystal structure and the Zhang study, we reasoned that the binding pocket of PDE δ may not be able to accommodate the extra amino acids present in our tested peptide.

Figure 4.5. Serial dilution of purified His₆-PDE δ analyzed by SDS-PAGE Gel under non-denaturing conditions, MW = 17.4 kDa, as shown in white. His₆-PDE δ was expressed and purified as described in Materials and Methods.

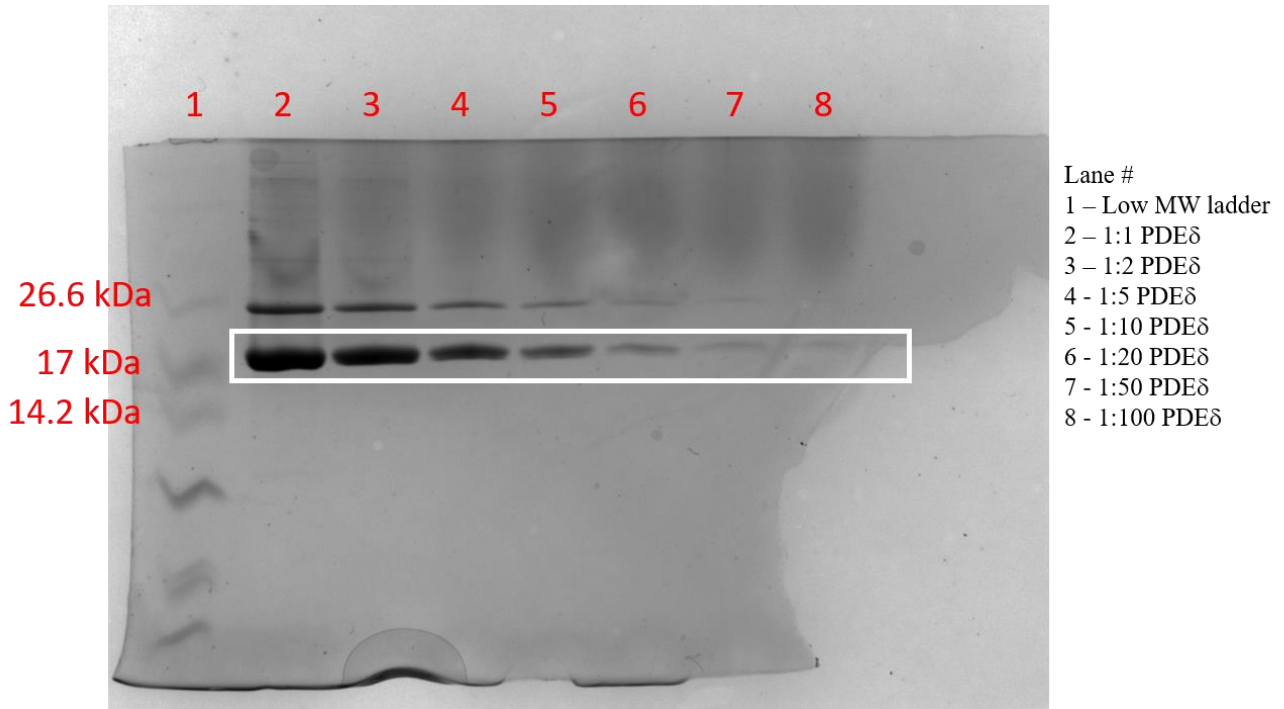
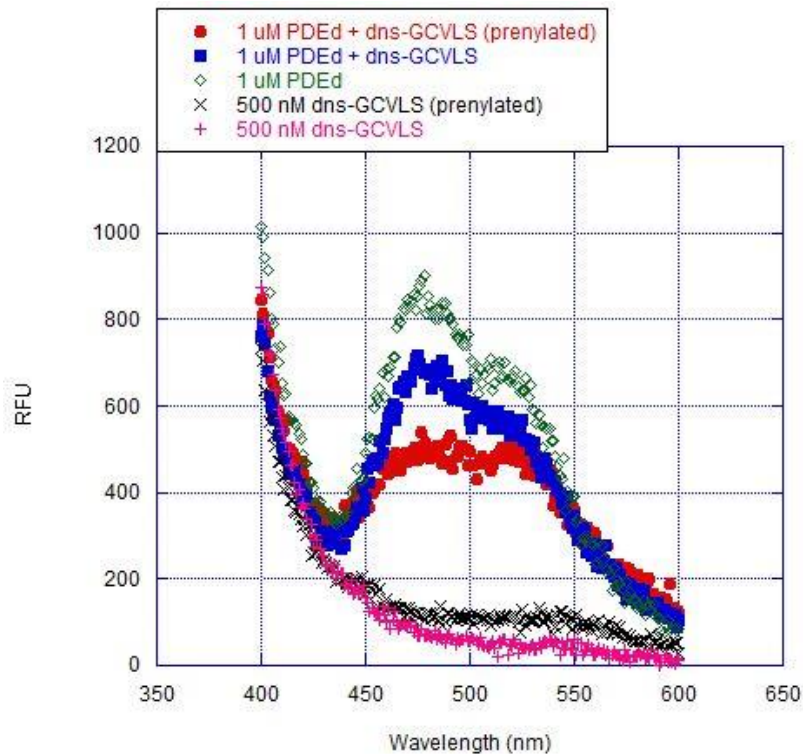
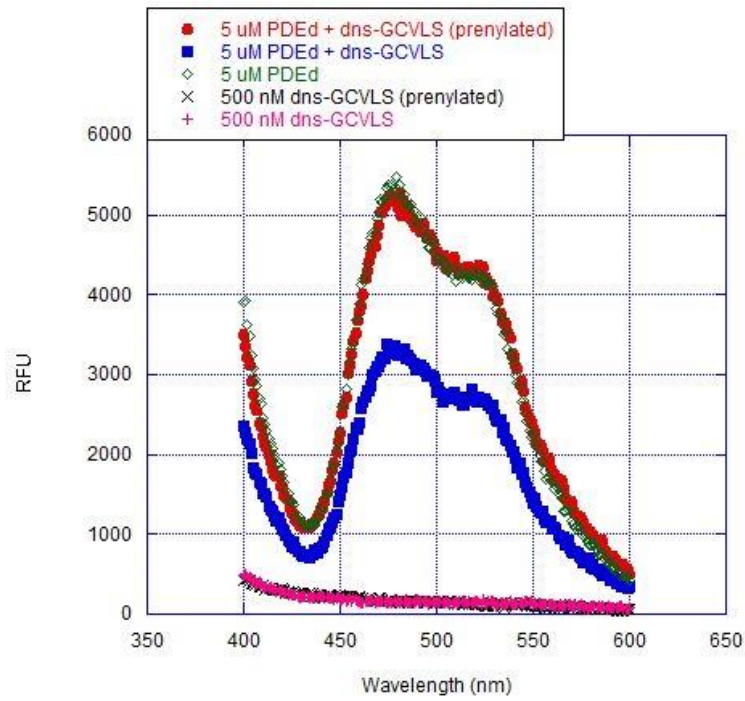
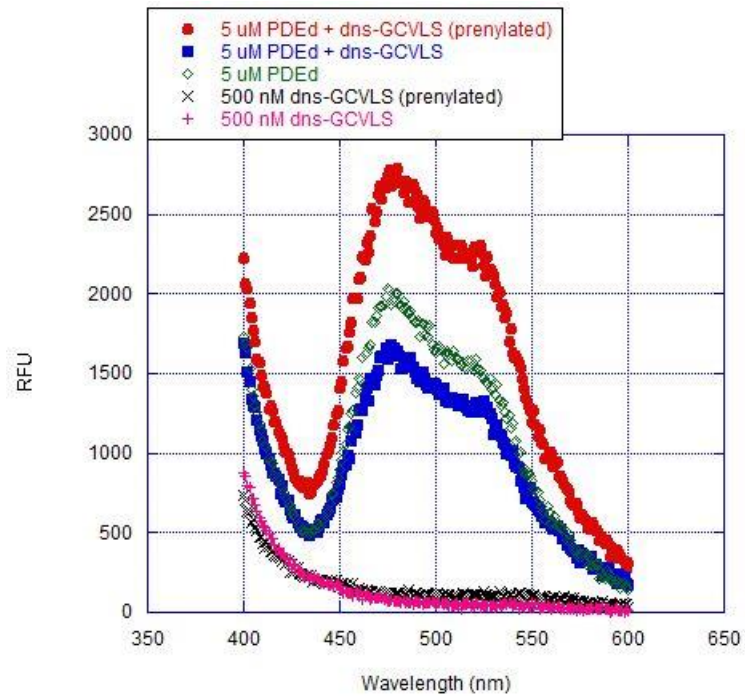


Figure 4.6. FRET measurements to determine binding interaction of PDE δ with farnesylated and non-farnesylated dns-GCVLS via plate-reader. A) 1 μ M PDE δ incubated with 500 nM prenylated or non-prenylated dns-GCVLS peptide overnight. B) 5 μ M PDE δ incubated with 500 nM prenylated or non-prenylated dns-GCVLS (two separate trials). Emission spectral scans were obtained ($\lambda_{\text{ex}} = 282$ nm, $\lambda_{\text{em}} = 400$ -600 nm) the following day as described in Materials and Methods.

A)



B)



4.4 Investigating prenylation of non-canonical Cxx sequences in HEK293 cells via FLIM-FRET using GRK1 protein construct

Note: FLIM-FRET microscopy and analysis was performed by Peter Calvert (Center for Vision Research, Upstate Medical University). Cell maintenance and preparation was assisted by Himanshu Malhotra from the Calvert Lab (Center for Vision Research, Upstate Medical University).

Despite unsuccessful efforts towards the development of an *in vitro* FRET assay based on mCherry-PDE δ or PDE δ binding prenylated eGFP or prenylated dansyl-peptides, respectively; we explored FLIM-FRET studies using live cells to gauge the prenylation status of non-canonical Cxx sequences in the context of two mammalian fluorescent fusion proteins, mCherry and eGFP. This work was based on an established study where the Bastaeins group used FLIM-FRET to delineate the spatial organization of Ras proteins conferred by PDE δ activity.²⁴

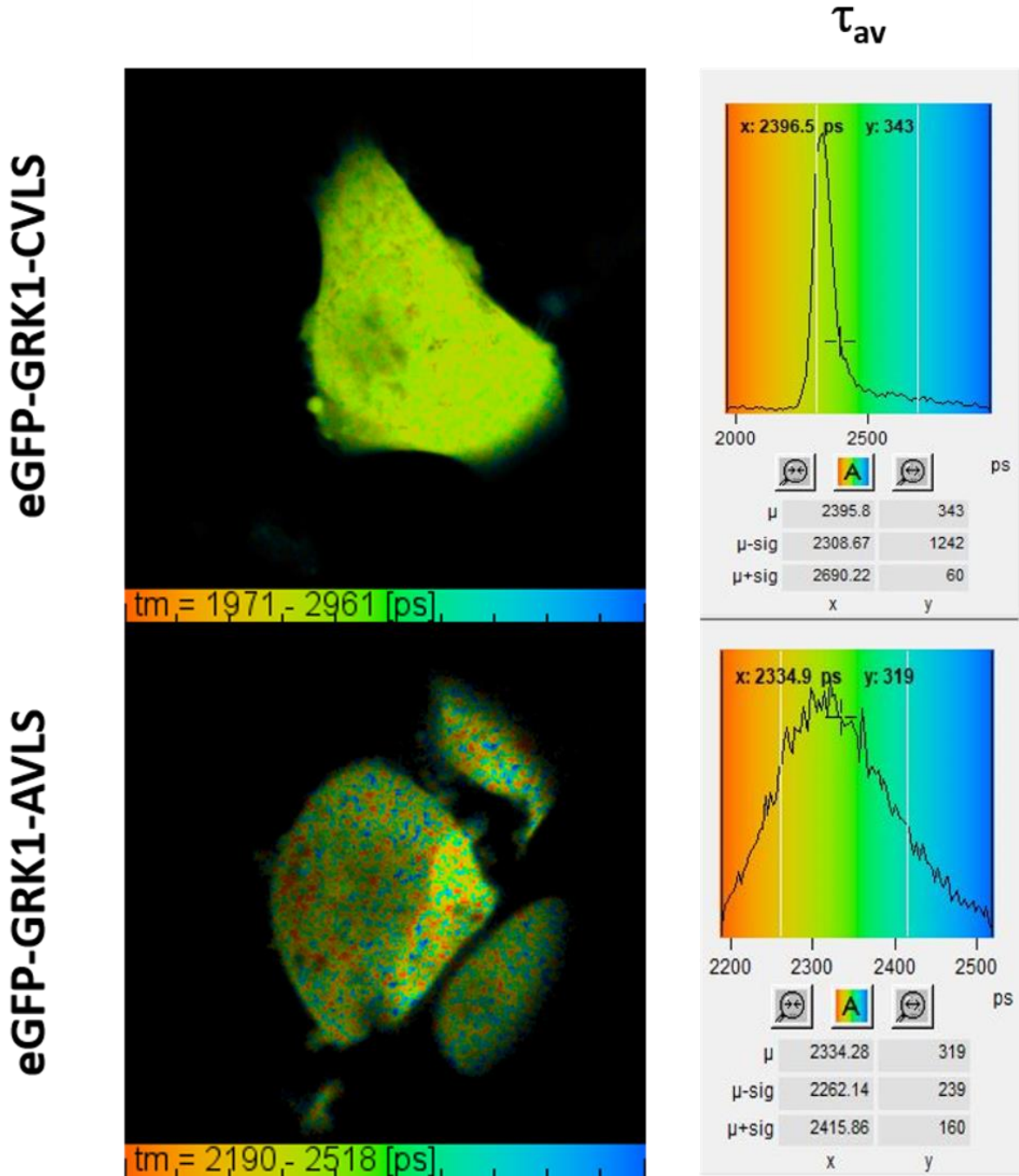
In collaboration with the Calvert Group (Upstate Medical University), we designed FLIM-FRET experiments utilizing mCherry-PDE δ and an eGFP-GRK1 construct that was modified at its C-terminus to contain prenylation motifs of interest. We chose the eGFP-GRK1 construct for this study for several reasons. First, numerous studies have reported that PDE δ serves as a binding partner for GRK1, a rhodopsin kinase, for the proper localization of GRK1.^{28,}²⁹ Second, as described in Chapter 1, prenylated protein usually require a secondary signal in order to membrane associate. That signal can be an additional lipid modification, such as palmitoylation, or it can be in the form of electrostatic interactions with the negatively charged plasma membrane inner leaflet. The GRK1 sequence used in this study lacks multiple positively charged residues that would aid its membrane localization and is not known to go under any

further modifications once prenylated and processed, which makes this prenylated construct more cytosolically available for binding interactions with PDE δ . It is also important to note, however, that the Maza study utilized endogenously expressed PDE δ in rods of *Xenopus laevis* in contrast to the human PDE δ sequence we utilized in this study,³³ and that study used the GRK1 sequence expressed in *Xenopus laevis*, which is also different from the human form.

For this study, the eGFP-GRK1 construct was modified to contain the following C-terminal sequences: -CVLS, -AVLS, and -CVL. These sequences were selected based on known steady-state kinetic parameters (see section 2.6), representing the most active CaaX and Cxx sequences tested.¹ The alanine mutant serves as the negative control as it is not expected to be prenylated or modified in any form, while -CVLS serves as the positive control as it is known to be prenylated, processed, and bind to PDE δ .²⁴

We initially expressed only the eGFP-GRK1-CVLS/-AVLS constructs in HEK293 cells to establish a baseline FLIM-FRET signal that may result from the normal lifetime for eGFP or homoFRET, i.e. eGFP to eGFP energy transfer. Robust expression of eGFP-GRK1 bearing -CVLS and -AVLS sequences at their C-terminus was confirmed via fluorescence microscopy and the resulting FLIM-FRET signals were analyzed to exhibit similar lifetimes for both eGFP donor (Figure 4.7). Both eGFP-GRK1-CVLS and eGFP-GRK1-AVLS expressed proteins showed lifetimes of approximately 2300-2400 ps. The fluorescence lifetimes observed are shorter than the reported lifetime of eGFP at 2800 ± 70 ps (Mamontova), suggesting that homoFRET might be playing a role in the values obtained (Figure 4.7). Moreover, eGFP-GRK1-CVLS expression was found to be diffuse throughout the cell, making it available to bind with mCherry-PDE δ .

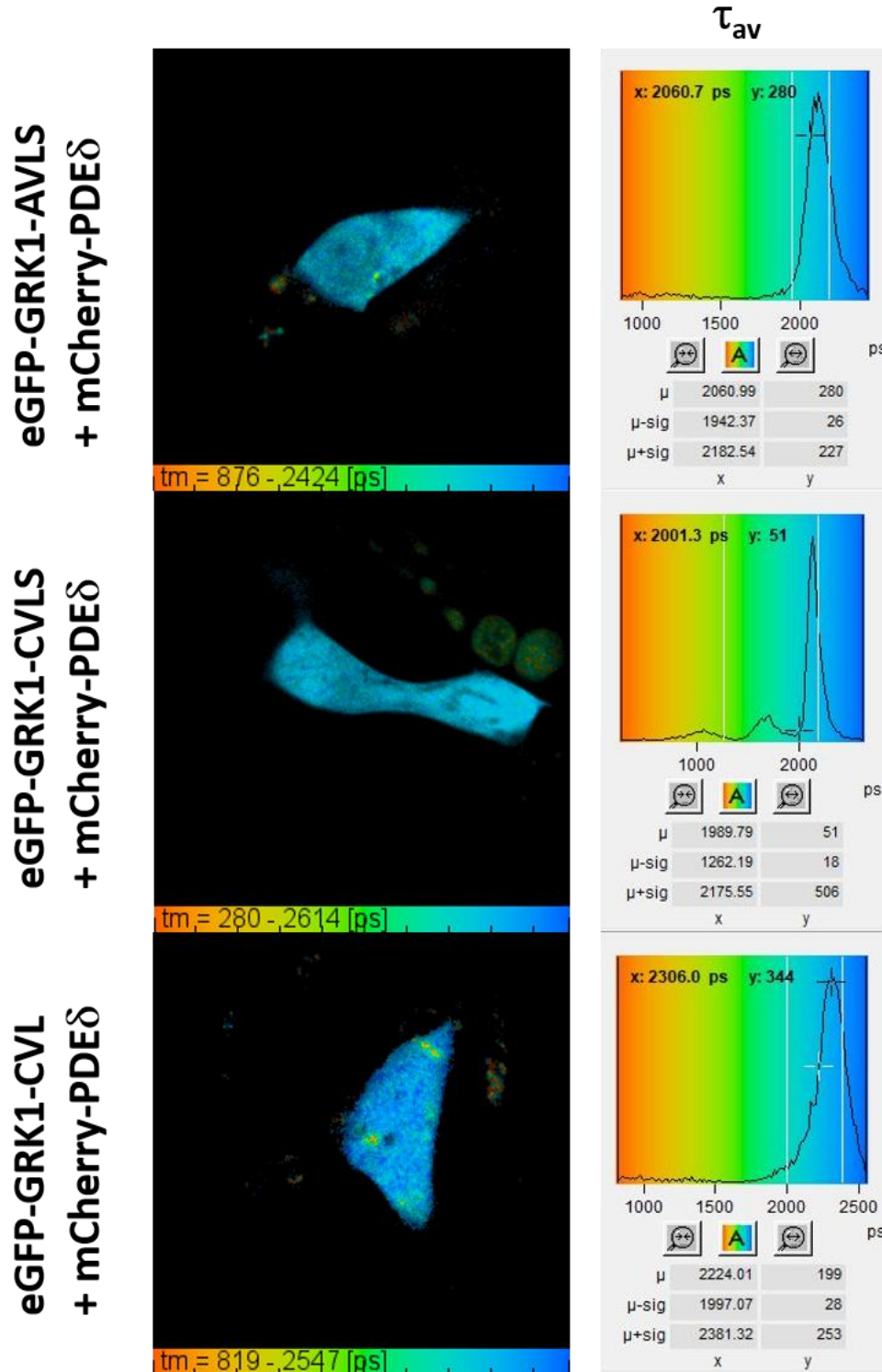
Figure 4.7. FLIM-FRET measurements in HEK293 cells expressing either eGFP-GRK1-CVLS or eGFP-GRK1-AVLS. Left panel: HEK293 cells transfected with eGFP-GRK1-CVLS or eGFP-GRK1-AVLS demonstrating diffuse fluorescence. Right panel: Mean fluorescence lifetime plots of each respective sample.



Following FLIM-FRET measurements of eGFP-GRK1 constructs alone, co-expression of mCherry-PDE δ and eGFP-GRK1 constructs was performed in HEK293 cell with protein expression verified by fluorescence microscopy. FLIM-FRET studies of co-transfected cells were then performed and analyzed. In these experiments, a successful binding interactions would be indicated by a larger reduction in the fluorescence lifetime of eGFP-GRK1-CVLS (presumed prenylated) with mCherry-PDE δ than any changes observed with eGFP-GRK1-AVLS which is expected to not be prenylated. In our experimental analysis, eGFP-GRK1-AVLS co-expressed with mCherry-PDE δ exhibited a lower lifetime compared to eGFP-GRK1-AVLS alone (Figure 4.8). The lifetime of eGFP-GRK1-CVLS in presence of mCherry-PDE δ was similarly lower in comparison to eGFP-GRK1-CVLS by itself. Moreover, we detected small peaks at a lower fluorescence lifetime in the FLIM plot which correspond to a small proportion of the expressed eGFP-GRK1-CVLS population in presence of mCherry-PDE δ (Figure 4.8), suggesting binding of fraction of eGFP-GRK1-CVLS by mCherry-PDE δ likely due to prenylation. However, the majority of the FLIM signal from eGFP-GRK1-CVLS in presence of mCherry-PDE δ was comparable with the signal generated by the co-expression of eGFP-GRK1-AVLS and mCherry-PDE δ . This highlights that these results should be interpreted carefully and require further control experimentation, such as the co-expression of the eGFP-GRK1 constructs with mCherry only to examine the possibility for non-prenylation dependent interactions with PDE δ . In the case of the eGFP-GRK1-CVL construct expressed with mCherry-PDE δ , the FLIM-FRET results were comparable to the negative control involving only eGFP-GRK1 constructs, suggesting that a significant binding event between eGFP-GRK1-CVL and mCherry-PDE δ did not occur (Figure 4.8). Again, a control experiment with the eGFP-GRK1 constructs and mCherry only will help

interpret these results and provide a comprehensive assessment about the viability of this assay for detection of prenylation on Cxx sequences.

Figure 4.8. FLIM-FRET measurements in HEK293 cells co-expressing eGFP-GRK1-CVLS or eGFP-GRK1-AVLS or eGFP-GRK1-CVL and mCherry-PDE δ . Left panel: HEK293 cells co-transfected with eGFP-GRK1-CVLS or eGFP-GRK1-AVLS or eGFP-GRK1-CVL and mCherry-PDE δ . Right panel: Mean fluorescence lifetime plots of each respective sample.



4.5 Investigating prenylation of non-canonical Cxx sequences in HEK293 cells via FLIM-FRET using modified eGFP-KRas protein constructs with mCherry-PDE δ

Note: FLIM-FRET microscopy and analysis was performed by Peter Calvert (Center for Vision Research, Upstate Medical University). Cell maintenance and preparation was assisted by Himanshu Malhotra from the Calvert Lab (Center for Vision Research, Upstate Medical University).

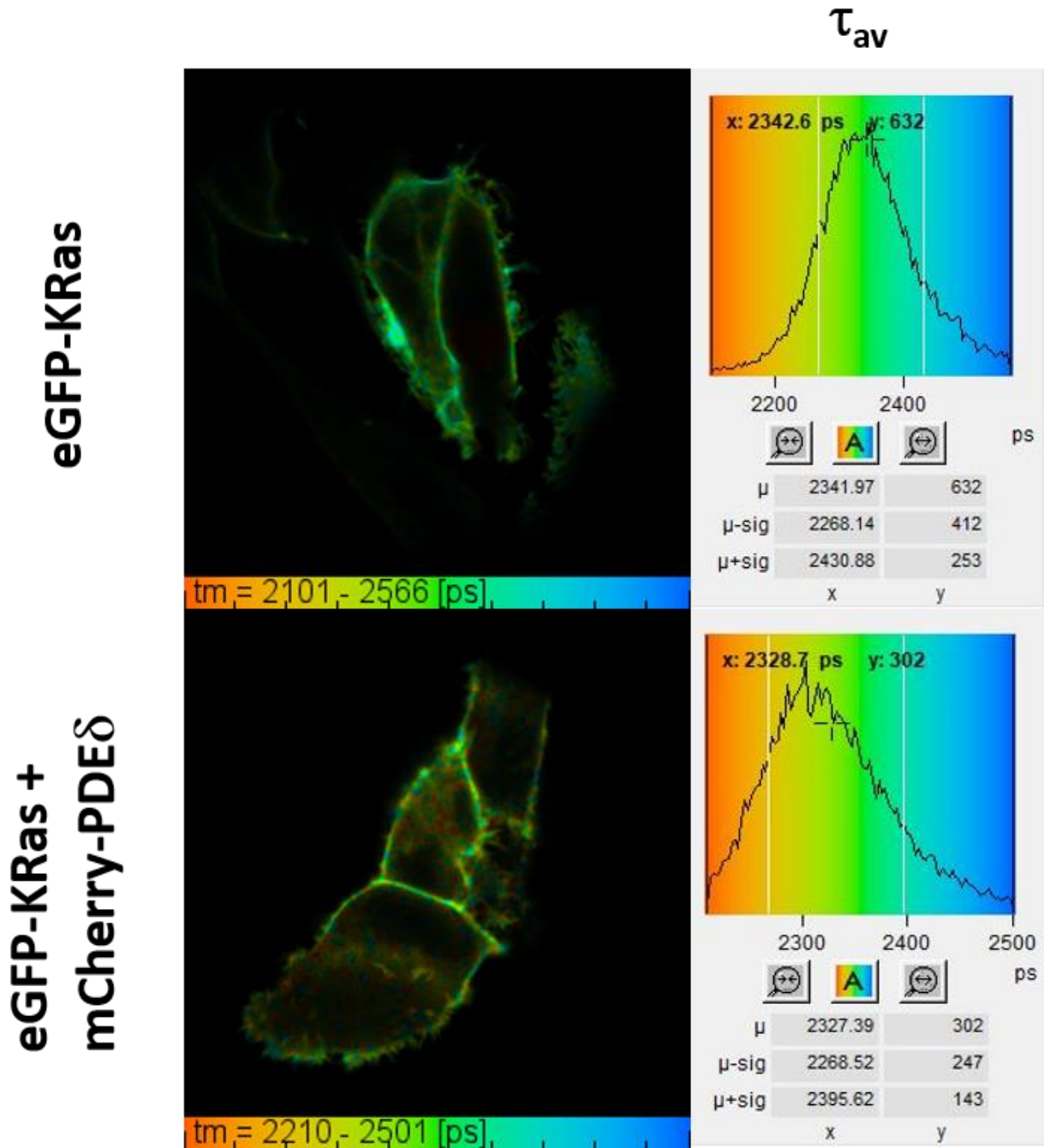
As described, the results from the FLIM-FRET analysis of live HEK293 cells co-expressing the modified eGFP-GRK1 constructs and mCherry-PDE δ did not provide a clear representation regarding PDE δ binding the GRK1 constructs that is dependent on prenylation. It is also important to note that the GRK1 construct utilized in that study was based on the *Xenopus Laevis* GRK1 protein's C-terminal amino acid sequence, which differ from the human version, while the PDE δ protein expressed in live cells is of human origin. Therefore, it is conceivable that these two proteins do not bind or bind as well as their respective human orthologs. To mitigate the possibility that the observed lack of significant difference in FLIM signal between the positive and negative controls is due to the utilization of cross-species proteins, we employed a known binding partner of human PDE δ , human KRas protein.^{24, 27, 30}

For this study, only an initial test with eGFP-KRas that has a canonical -CVIM motif was carried out in the presence and absence of mCherry-PDE δ . Using live cells, completely processed prenylated eGFP-KRas with its canonical C-terminus motif is expected to membrane localize and bind PDE δ .^{27, 31} PDE δ is proposed to play a role in continuously sequestering mislocalized KRas from endomembranes to ultimately restore KRas enrichment on the plasma membrane.³² Consequently, the cytosolic fraction of prenylated KRas available to bind with

mCherry-PDE δ is minimal compared to the GRK1 construct tested in section 4.4.²⁴ Therefore, it is not surprising that the FLIM-FRET results observed from the co-expression of eGFP-KRas and mCherry-PDE δ in live HEK293 cells do not provide evidence for any binding interactions. As shown in Figure 4.9, membrane localization of eGFP-KRas at the plasma membrane and the lifetime of eGFP-KRas in presence of mCherry-PDE δ was comparable to the lifetime of eGFP-KRas by itself. This result was expected and is in agreement with prior reports.²⁴

While the results from this experiment do not provide evidence for PDE δ binding due to the aforementioned reason, this system might still prove useful for detecting prenylation of non-canonical Cxx sequences. This is because KRas membrane localization is not only dependent on farnesylation, but the polybasic residues upstream of the prenylated cysteine that utilize electrostatic interactions to membrane associate with the negatively charged inner leaflet.³¹ Chandra and co-workers were able to increase the cytosolic fraction of KRas by mutating the polybasic lysine residues to negatively charged glutamate residues and demonstrated a lower lifetime for the mutated mCitrine-KRas construct in presence of mCherry-PDE δ , suggestive of binding interactions.²⁴ Therefore, future work should aim to utilize a KRas construct that is more available in the cytosol for assessing binding with PDE δ .

Figure 4.9. FLIM-FRET measurements in HEK293 cells co-expressing eGFP-KRas and mCherry-PDE δ . Left panel: HEK293 cells transfected with eGFP-KRas or co-transfected with eGFP-KRas and mCherry-PDE δ . Right panel: Mean fluorescence lifetime plots of each respective sample.



4.6 Conclusions

In this study, both *in vitro* and *in vivo* FRET-based techniques were explored to investigate prenylation of non-canonical Cxx sequences. *In vitro* FRET assays to evaluate binding of the prenylated protein/peptide to PDE δ using mCherry-PDE δ with prenylated eGFP-CVIA and PDE δ alone with prenylated dns-GCVLS did not yield consistent FRET behavior indicative of any binding events. We suggest that these negative results may arise from the presence of unprocessed prenylated protein/peptide. Specifically, PDE δ exhibits a higher affinity for prenylated substrates that have a carboxymethyl moiety following the prenylated cysteine compared to prenylated substrates that still have an intact CaaX motif.²⁶

In a more biologically relevant context, FLIM-FRET was utilized to assess binding of fluorescent protein constructs by mCherry-PDE δ that is dependent on prenylation of the fluorescent protein construct. FLIM-FRET provides a powerful avenue for quantifying binding interactions. Two different fluorescent constructs were used in this study including the C-terminal 18 amino acid sequence of rhodopsin kinase (GRK1) protein, and full-length KRas. It is important to note that the modified eGFP-GRK1C18 constructs were based on the GRK1 protein expressed in *Xenopus Laevis* and are expected to be cytosolic when prenylated, while the eGFP-KRas construct is based on human KRas protein and is expected to membrane associate following prenylation and processing. PDE δ has been reported to bind both prenylated proteins.²⁰⁻²⁴

For the eGFP-GRK1 constructs expressed with mCherry-PDE δ , the FLIM-FRET analysis provided some evidence for the binding of eGFP-GRK1-CVLS by mCherry-PDE δ through the presence of eGFP subpopulations with markedly reduced fluorescence lifetimes. However, the test construct of eGFP-GRK1-CVL with mCherry-PDE δ provided results similar to the negative

control. Overall, these initial results are not conclusive and do not completely rule out the utilization of this assay for detecting Cxx prenylation, but would be aided by the addition of a negative control in which the eGFP-GRK1 constructs are co-expressed with mCherry only to fully evaluate their lifetimes and binding potential. Further, utilization of the human GRK1 protein sequence is recommended to assuage any discriminatory behavior human PDE δ might exhibit towards the *Xenopus Laevis* GRK1.

Leveraging human KRas, a known binding partner for PDE δ , also proved unfruitful in this FLIM-FRET based study. The results indicated a clear membrane associative behavior for eGFP-KRas, demonstrating the lack of cytosolic KRas available to bind PDE δ and produce a FRET signal. Increasing the cytosolic fraction of prenylated KRas by mutating the lysine rich area of KRas to glutamate residues would provide a better system for evaluating the viability of this assay for detecting prenylation of non-canonical 3mer sequences.

Lastly, it is important to mention PDE δ 's binding preference again and how that may influence the utility of this proposed assay. As described in section 4.3, PDE δ exhibits a higher affinity for farnesylated proteins that are processed compared to their unprocessed counterparts.^{26, 27} Therefore, it is important to consider if PDE δ can serve as a potential binding partner for non-canonical sequences that are longer compared to processed farnesylated canonical sequences. Future work towards the development of this detection method should take this into account and aim to employ a mutagenesis strategy based on the proteins crystal structure that would facilitate binding of longer PDE δ substrates.

4.7 Materials and Methods

4.7.1 Construction of pET28a-mCherry-PDE δ bacterial vector: The mammalian vector for mCherry-PDE δ obtained from Bastiaens Group (Max Planck Institute of Molecular Physiology) was sequence verified to confirm the presence of both *EcoRI* and *NheI* restriction sites (Genewiz). Both the mammalian inserts and the pET28a vectors were double digested using *EcoRI* and *NheI*-HF restriction enzymes in a reaction containing 1 μ g DNA, 2 μ L 10x Buffer, 1 μ L of each restriction enzyme in 20 μ L total volume. The double digest reaction was incubated for 2 hours at RT and then ran on a 0.8 % agarose gel to confirm successful digestion. The digested products were purified from the gel using EZ-10 Spin Column DNA Gel Extraction kit (BioBasic) per the manufacturer's protocol. 1 μ g of the double digested pET28a vector was ligated with a 3-fold molar excess of the mCherry-PDE δ insert to get the pET28a-mCherry-PDE δ vector. The ligation reaction was carried out as follows: 50 ng double digested pET28a vector, 33.8 ng mCherry-PDE δ insert, 2X QuickLigase buffer (10 μ L), and 1 μ L of Quick ligase enzyme (NEB) were added in a total reaction volume of 20 μ L. A negative control reaction without the mCherry-PDE δ insert was also carried out. The reactions were incubated at RT for 5 min before chilling them on ice and adding 2 μ L of each the ligation reaction and the negative control into separate tubes with 100 μ L of DH5 α cells. After transformation, DH5 α cells were incubated for 30 min on ice. 250 μ L 1X LB Media was added to each transformed cell tube and shaken for 1 hour at 37°C before plating the cells on LB-Kan plates and incubating overnight at 37°C. Colonies from the ligation reaction plate were inoculated into 5 mL of LB containing 50 μ g/mL kanamycin and incubated overnight at 37°C with shaking at 225 rpm. The plasmids from the overnight cultures were purified using the EZ-10 spin column plasmid purification kit

(BioBasic) per manufacturer's protocol and sequenced (Genewiz) to confirm the presence of mCherry-PDE δ insert in the pET28a vector.

4.7.2 Expression and purification of pET28a-mCherry-PDE δ protein: Chemically competent BL21 (DE3) E. coli were transformed with pET28a-mCherry-PDE δ vector. Following transformation and antibiotic selection, a colony from the transformation plate was inoculated into LB media (5 mL) containing 50 μ g/mL kanamycin. Cultures were incubated and shaken at 225 rpm for 4 h at 37°C and then transferred to 0.5 liter of prewarmed auto-induction media (5 g tryptone, 2.5 g yeast extract, 10 mL 50X 5052 media [25% glycerol, 10% lactose, 2.5% glucose], 25 mM Na₂HPO₄, 25 mM KH₂PO₄, 50 mM NH₄Cl, 5 mM Na₂SO₄, 2 mM MgSO₄, 100 μ L trace metals [50 μ M FeCl₂, 20 μ M CaCl₂, 10 μ M MnCl₂, 10 μ M ZnCl₂], 50 μ g/mL kanamycin. Expression cultures were incubated for 19 h at 37°C with shaking. Cells were harvested by centrifugation and resuspended in 50 mL resuspension buffer (20 mM NaH₂PO₄, 300 mM NaCl, and 10 mM imidazole). Bacterial cell suspensions were lysed by sonication, clarified by centrifugation, and purified by affinity chromatography using a Ni-NTA HisTrap column (GE S4 Healthcare). Fractions containing the fluorescent protein were combined and concentrated using a centrifugal concentrator. Concentrated samples were buffer exchanged to 50 mM Tris buffer (pH 7.5), divided into 20 μ L aliquots, and flash frozen with liquid nitrogen for storage at -80°C. Protein concentration was determined using the molar absorption of mCherry at 587 nm.

4.7.3 Construction of pET28a-PDE δ bacterial vector: The vector plasmid encoding for PDE δ was prepared by PCR using the pET28a-mCherry-PDE δ vector with a 5' primer containing the

*Bam*HI restriction site and a 3' primer containing the *Hind*III restriction site (synthesized by IDT, Inc.). The PCR reaction (50 μ L) consisted of 1x Standard OneTaq buffer, 10 mM dNTPs, 125 ng reverse and forward primers each, 10 ng template plasmid, and OneTaq DNA polymerase (0.25 μ L, 5U/ μ L). The PCR reactions were performed in a BioRad Mycycler thermal cycler using the following program: Initial denaturation (94°C, 1 min); thirty cycles of denaturation (94°C, 30 sec), annealing (56°C, 1 min), and extension (68°C, 2 min); final extension (68°C, 5 min); and a final hold (10°C, ∞). PCR products were purified using BIO Basic Inc. EZ-10 Spin Column PCR purification Kit following the manufacturer's protocol. Following digestion by *Bam*HI and *Hind*III of the amplified product and pET28a, the PDE δ insert was ligated into the pET28a plasmid using the Quick Ligase kit (NEB), following the manufacturer's instructions. Insert ligation was verified by analytical restriction digest and gene sequencing (Genewiz).

4.7.4 Expression and purification of pET28a-PDE δ : Chemically competent BL21 (DE3) *E. coli* were transformed with pET28a-PDE δ vector. Following transformation and antibiotic selection, a colony from the transformation plate was inoculated into LB media (5 mL) containing 50 μ g/mL kanamycin. Cultures were incubated and shaken at 225 rpm for 4 h at 37°C and then transferred to 0.5 liter of prewarmed auto-induction media (5 g tryptone, 2.5 g yeast extract, 10 mL 50X 5052 media [25% glycerol, 10% lactose, 2.5% glucose], 25 mM Na₂HPO₄, 25 mM KH₂PO₄, 50 mM NH₄Cl, 5 mM Na₂SO₄, 2 mM MgSO₄, 100 μ L trace metals [50 μ M FeCl₂, 20 μ M CaCl₂, 10 μ M MnCl₂, 10 μ M ZnCl₂], 50 μ g/mL kanamycin. Expression cultures were incubated for 19 h at 37°C with shaking. Cells were harvested by centrifugation and resuspended in 50 mL resuspension buffer (20 mM NaH₂PO₄, 300 mM NaCl, and 10 mM imidazole). Bacterial cell suspensions were lysed by sonication, clarified by centrifugation, and

purified by affinity chromatography using a Ni-NTA HisTrap column (GE S4 Healthcare). Fractions containing the protein were combined and concentrated using a centrifugal concentrator. Concentrated samples were buffer exchanged to 50 mM Tris buffer (pH 7.8), divided into 20 μ L aliquots, and stored at -20°C . Protein concentration was determined using the molar absorption of PDE δ at 280 nm.

4.7.5 Farnesylation of purified eGFP-CVIA: Purified eGFP-CVIA was provided by Elizabeth Cleverdon, Hougland Laboratory. 5 μ M eGFP-CVIA was incubated with both 1X reaction buffer (50 mM HEPPSO-NaOH, pH7.8, 5 mM TCEP) and 5 mM MgCl_2 (.5 mL total) for 20 minutes in 1.5 mL low-adhesion eppendorf tube. Farnesylation reaction was initiated by adding an enzyme mix (.5 mL) containing 100 nM FTase, 5 mM MgCl_2 , 1X reaction buffer, and 10 μ M FPP. Reaction was incubated at RT for 16 hours under foil before removing excess FPP through use of a 0.5 mL illustra NAP-5 column (GE Healthcare). NAP-5 column was equilibrated with 50 mM Tris-HCl (10 mL, pH7.8) before application of the 1 mL reaction sample. Elution followed with 50 mM Trish-HCl (1.0 mL, pH 7.8) into a low-adhesion eppendorf tube. Concentration of the protein was calculated using UV-Vis absorbance of the eluent at 488 nm.

4.7.6 FRET assay to probe mCherry-PDE δ binding prenylated eGFP-CVIA: 300 nM mCherry-PDE δ was incubated in 50 mM Tris-HCl (pH 7.8) at RT for 20 mins under foil before adding prenylated eGFP-CVIA at various concentration, including, 25 nM, 50 nM, 100 nM, 200 nM, and 500 nM in a 96-well plate (Corning). Fluorescence measurements were obtained 15- and 60-mins post-incubation in the BioTek H1 Synergy plate reader (λ_{ex} 488 nm, λ_{em} 610 nm).

Relative fluorescence units were plotted against eGFP-CVIA concentrations. Controls consisted of a non-prenylated eGFP-CVIA negative control.

4.7.7 Farnesylation and purification of dns-GCVLS: 3 μ M dns-GCVLS was incubated with both 1X reaction buffer (50 mM HEPPSO-NaOH, pH7.8, 5 mM TCEP) and 5 mM $MgCl_2$ (.5 mL total) for 20 minutes in 1.5 mL low-adhesion eppendorf tube. Farnesylation reaction was initiated by adding an enzyme mix (.5 mL) containing 100 nM FTase, 5 mM $MgCl_2$, 1X reaction buffer, and 10 μ M FPP. Reaction was incubated at RT for 16 hours under foil. Following overnight incubation, the peptide reaction was purified by semi-preparative reverse phase HPLC (Zorbax Eclipse XDB column, 9.4 x 250 mm) using a gradient mobile phase of 30%-100% acetonitrile in aqueous 0.05 % trifluoroacetic acid (TFA) over 30.2 minutes, at a flow rate of 4.2 mL/min. Prenylated dansyl peptide elution was detected by fluorescence (λ_{ex} 340 nm, λ_{em} 496 nm), and fractions containing the prenylated peptide were collected and dried under vacuum at room temperature and resuspended in 1:1 H₂O: acetonitrile. Concentration of the protein was calculated using UV-Vis absorbance of the eluent at 340 nm.

4.7.8 FRET assay to probe PDE δ binding prenylated dns-GCVLS: 500 nM or 1 μ M prenylated or non-prenylated dns-GCVLS were incubated in 1X reaction buffer (50 mM HEPPSO-NaOH, pH7.8, 5 mM TCEP) at RT for 20 mins under foil before adding 3 or 5 μ M PDE δ in a 96-well plate (Corning). Spectral scans were obtained post-overnight incubation in the BioTek H1 Synergy plate reader (λ_{ex} 282 nm, λ_{em} 320-550 nm). Relative fluorescence units were plotted against emission wavelengths. Controls consisted of a non-prenylated dns-GCVLS and

PDEδ only negative controls.

4.7.9 Generation of pCDNA-eGFP-GRK1ct18 mammalian vectors: The vector plasmids encoding for eGFP-GRK1ct18-C/Axx(x) were prepared by PCR using the XOP-eGFP-GRK1ct18 vector obtained for the Calvert Lab, Upstate Medical University serving as a template. 5' primer containing the *BamHI* restriction site and 3' primers containing -CVLS, -AVLS, -CVL, and -AVL C-terminal sequences and *NotI* restriction site were designed (IDT, Inc.). The PCR reaction (50 μL) consisted of 1x Standard OneTaq buffer, 10 mM dNTPs, 125 ng reverse and forward primers each, 10 ng template plasmid, and OneTaq DNA polymerase (0.25 μL, 5U/μL). The PCR reactions were performed in a BioRad Mycycler thermal cycler using the following program: Initial denaturation (94°C, 1 min); thirty cycles of denaturation (94°C, 30 sec), annealing (56°C, 1 min), and extension (68°C, 2 min); final extension (68°C, 5 min); and a final hold (10°C, ∞). PCR products were purified using BIO Basic Inc. EZ-10 Spin Column PCR purification Kit following the manufacturer's protocol. Following digestion by *BamHI* and *NotI*, the eGFP-GRK1ct18-C/Axx(x) inserts were ligated into the pCDNA plasmid using the Quick Ligase kit (NEB), following the manufacturer's instructions. Insert ligation was verified by analytical restriction digest and gene sequencing (Genewiz).

4.7.10 Transfection and FLIM-FRET analysis of various eGFP-GRK1ct18 and eGFP-KRas fusion proteins in HEK293 cells: HEK293 cells were maintained in 75 mL vented tissue culture flasks (Celltreat) and were split once reaching 80% confluency. Cells were grown in complete DMEM (DMEM supplemented with 10% fetal bovine serum (FBS) and 1 % (v/v) penicillin-

streptomycin (MediaTech) in 5% CO₂ at 37°C. For co-expression of the eGFP-GRK1ct18 and eGFP-KRas constructs and mCherry-PDE δ , 2 x 10⁵ cells were placed in 2 mL of complete DMEM per well of a tissue culture treated 6-well plate (Corning), each containing a 25 mm glass coverslip #1.5 thickness (Celltreat). The cells were incubated 24-28 hours prior to transfection. The DNA-transfection reagent complex was prepared by incubating 4 μ g each of eGFP-GRK1ct18 and eGFP-KRas (provided by Casey Lab, Duke University) and mCherry-PDE δ and 6 μ L of the Turbofect transfection reagent (Thermo Scientific) in a total volume of 500 μ L supplement free DMEM for 20 minutes at room temperature. The cells were then transfected with the prepared DNA-transfection reagent complex by drop wise addition into the wells of a 6-well tissue culture plate. Following transfection for 24-28 h, glass coverslips were prepared for imaging by washing with 1X PBS and placing them in an imaging chamber. FLIM-FRET microscopy and analysis was performed by Peter Calvert (Center for Vision Research, Upstate Medical University).

4.8 References

1. Hougland, J. L.; Lamphear, C. L.; Scott, S. A.; Gibbs, R. A.; Fierke, C. A., Context-dependent substrate recognition by protein farnesyltransferase. *Biochemistry* **2009**, *48* (8), 1691-701.
2. Hildebrandt, E. R.; Cheng, M.; Zhao, P.; Kim, J. H.; Wells, L.; Schmidt, W. K., A shunt pathway limits the CaaX processing of Hsp40 Ydj1p and regulates Ydj1p-dependent phenotypes. *Elife* **2016**, *5*, e15899.
3. Blanden, M. J.; Suazo, K. F.; Hildebrandt, E. R.; Hardgrove, D. S.; Patel, M.; Saunders, W. P.; Distefano, M. D.; Schmidt, W. K.; Hougland, J. L., Efficient farnesylation of an extended C-terminal C(x)3X sequence motif expands the scope of the prenylated proteome. *J Biol Chem* **2018**, *293* (8), 2770-2785.
4. Förster, T., Zwischenmolekulare energiewanderung und fluoreszenz. *Annalen der physik* **1948**, *437* (1-2), 55-75.
5. Jares-Erijman, E. A.; Jovin, T. M., FRET imaging. *Nature biotechnology* **2003**, *21* (11), 1387-1395.
6. Piston, D. W.; Kremers, G.-J., Fluorescent protein FRET: the good, the bad and the ugly. *Trends in biochemical sciences* **2007**, *32* (9), 407-414.
7. Vogel, S. S.; Thaler, C.; Koushik, S. V., Fanciful fret. *Sci. STKE* **2006**, *2006* (331), re2-re2.
8. Patterson, G. H.; Piston, D. W.; Barisas, B. G., Förster distances between green fluorescent protein pairs. *Analytical biochemistry* **2000**, *284* (2), 438-440.
9. Periasamy, A.; Clegg, R. M., *FLIM microscopy in biology and medicine*. CRC Press: 2009.

10. Hink, M. A.; Visser, N. V.; Borst, J. W.; van Hoek, A.; Visser, A. J., Practical use of corrected fluorescence excitation and emission spectra of fluorescent proteins in Förster resonance energy transfer (FRET) studies. *Journal of Fluorescence* **2003**, *13* (2), 185-188.
11. Periasamy, A., *Methods in cellular imaging*. Springer: 2013.
12. Zeug, A.; Woehler, A.; Neher, E.; Ponimaskin, E. G., Quantitative intensity-based FRET approaches—a comparative snapshot. *Biophysical journal* **2012**, *103* (9), 1821-1827.
13. Gordon, G. W.; Berry, G.; Liang, X. H.; Levine, B.; Herman, B., Quantitative fluorescence resonance energy transfer measurements using fluorescence microscopy. *Biophysical journal* **1998**, *74* (5), 2702-2713.
14. Hoppe, A.; Christensen, K.; Swanson, J. A., Fluorescence resonance energy transfer-based stoichiometry in living cells. *Biophysical journal* **2002**, *83* (6), 3652-3664.
15. Zal, T.; Gascoigne, N. R., Photobleaching-corrected FRET efficiency imaging of live cells. *Biophysical journal* **2004**, *86* (6), 3923-3939.
16. Chen, H.; Puhl 3rd, H. L.; Koushik, S. V.; Vogel, S. S.; Ikeda, S. R., Measurement of FRET efficiency and ratio of donor to acceptor concentration in living cells. *Biophysical journal* **2006**, *91* (5), L39-L41.
17. Lakowicz, J. R., *Principles of fluorescence spectroscopy*. Springer Science & Business Media: 2013.
18. Becker, W., Fluorescence lifetime imaging—techniques and applications. *Journal of microscopy* **2012**, *247* (2), 119-136.
19. Sun, Y.; Hays, N. M.; Periasamy, A.; Davidson, M. W.; Day, R. N., Monitoring protein interactions in living cells with fluorescence lifetime imaging microscopy. In *Methods in enzymology*, Elsevier: 2012; Vol. 504, pp 371-391.

20. Hanzal-Bayer, M.; Renault, L.; Roversi, P.; Wittinghofer, A.; Hillig, R. C., The complex of Arl2-GTP and PDE δ : from structure to function. *The EMBO journal* **2002**, *21* (9), 2095-2106.
21. Nancy, V.; Callebaut, I.; El Marjou, A.; de Gunzburg, J., The δ subunit of retinal rod cGMP phosphodiesterase regulates the membrane association of Ras and Rap GTPases. *Journal of Biological Chemistry* **2002**, *277* (17), 15076-15084.
22. Bhagatji, P.; Leventis, R.; Rich, R.; Lin, C.-j.; Silvius, J. R., Multiple cellular proteins modulate the dynamics of K-ras association with the plasma membrane. *Biophysical journal* **2010**, *99* (10), 3327-3335.
23. Chen, Y. X.; Koch, S.; Uhlenbrock, K.; Weise, K.; Das, D.; Gremer, L.; Brunsveld, L.; Wittinghofer, A.; Winter, R.; Triola, G., Synthesis of the Rheb and K-Ras4B GTPases. *Angewandte Chemie International Edition* **2010**, *49* (35), 6090-6095.
24. Chandra, A.; Grecco, H. E.; Pisupati, V.; Perera, D.; Cassidy, L.; Skoulidis, F.; Ismail, S. A.; Hedberg, C.; Hanzal-Bayer, M.; Venkitaraman, A. R., The GDI-like solubilizing factor PDE δ sustains the spatial organization and signalling of Ras family proteins. *Nature cell biology* **2012**, *14* (2), 148-158.
25. Albertazzi, L.; Arosio, D.; Marchetti, L.; Ricci, F.; Beltram, F., Quantitative FRET Analysis With the E0GFP-mCherry Fluorescent Protein Pair. *Photochemistry and photobiology* **2009**, *85* (1), 287-297.
26. Zhang, H.; Liu, X.-h.; Zhang, K.; Chen, C.-K.; Frederick, J. M.; Prestwich, G. D.; Baehr, W., Photoreceptor cGMP phosphodiesterase δ subunit (PDE δ) functions as a prenyl-binding protein. *Journal of Biological Chemistry* **2004**, *279* (1), 407-413.

27. Dharmaiah, S.; Bindu, L.; Tran, T. H.; Gillette, W. K.; Frank, P. H.; Ghirlando, R.; Nissley, D. V.; Esposito, D.; McCormick, F.; Stephen, A. G., Structural basis of recognition of farnesylated and methylated KRAS4b by PDE δ . *Proceedings of the National Academy of Sciences* **2016**, *113* (44), E6766-E6775.
28. Zhang, H.; Li, S.; Doan, T.; Rieke, F.; Detwiler, P.; Frederick, J.; Baehr, W., Deletion of PrBP/ δ impedes transport of GRK1 and PDE6 catalytic subunits to photoreceptor outer segments. *Proceedings of the National Academy of Sciences* **2007**, *104* (21), 8857-8862.
29. Maza, N. A.; Schiesser, W. E.; Calvert, P. D., An intrinsic compartmentalization code for peripheral membrane proteins in photoreceptor neurons. *Journal of Cell Biology* **2019**, *218* (11), 3753-3772.
30. Zimmermann, G.; Papke, B.; Ismail, S.; Vartak, N.; Chandra, A.; Hoffmann, M.; Hahn, S. A.; Triola, G.; Wittinghofer, A.; Bastiaens, P. I., Small molecule inhibition of the KRAS–PDE δ interaction impairs oncogenic KRAS signalling. *Nature* **2013**, *497* (7451), 638-642.
31. Hancock, J. F.; Paterson, H.; Marshall, C. J., A polybasic domain or palmitoylation is required in addition to the CAAX motif to localize p21ras to the plasma membrane. *Cell* **1990**, *63* (1), 133-139.
32. Schmick, M.; Vartak, N.; Papke, B.; Kovacevic, M.; Truxius, D. C.; Rossmannek, L.; Bastiaens, P. I., KRas localizes to the plasma membrane by spatial cycles of solubilization, trapping and vesicular transport. *Cell* **2014**, *157* (2), 459-471.
33. Maza, N. A.; Schiesser, W. E.; Calvert, P. D., An intrinsic compartmentalization code for peripheral membrane proteins in photoreceptor neurons. *Journal of Cell Biology* **2019**, *218* (11), 3753-3772.

Chapter 5: Conclusions and Future Work

5.1 Summary

Prenylation is a form of post-translational lipidation that is involved in cell signaling and growth, influencing protein structure, localization, and function.¹⁻⁵ For the past 30 years, the four-amino-acid, C-terminal “CaaX” box motif has served as the defining paradigm for prenyltransferase substrate recognition, as first identified through study of yeast mating factors and lamins.^{1, 3-11} Consequently, studies of prenylation targets for FTase and GGTase-I have mainly focused on amino acid selectivity within the CaaX motif. Numerous biochemical, crystallographic, and computational works have led to the development of general rules for selectivity based on the four amino acids and have greatly enhanced our understanding of these prenyltransferase substrate targets.^{7, 12-26}

Recently, yeast genetic screening utilizing the Hsp40 co-chaperone Ydj1p revealed that yeast FTase could efficiently prenylate shorter Cxx sequences.²⁷ This finding motivated fluorescent-based biochemical and cell-based studies at both the short peptide and full-length protein level. These determined that mammalian FTase can recognize and prenylate a three amino acid recognition motif in an *in vitro* context, as described. In addition, the recent finding that FTase can target longer C(x)₃X sequences has expanded the potential substrate scope for this enzyme.²⁸ A search of the human genome (as of May 2020) using Prosite results in 1074 proteins ending in a Cxx sequence with the potential to undergo prenylation, expanding the number of proteins that can be explored not only in humans but other organisms such as yeast. With previous studies and current computational prediction models restricted to four amino acids,

innovative approaches to determining the role of this novel selectivity will need to be addressed for such a large scale of potential prenylated proteins.

This finding suggests a broader impact for prenylation in a biological context and raises many new questions regarding the role of these Cxx proteins. With FTase and GGTase-I showing a stark contrast in their acceptance of these shorter sequences, it is sensible to question why these “sister” enzymes exhibit such a discrepancy in their flexibility for substrates. It is also important to question how FTase recognizes these shorter sequences, and to determine the biological role of potential Cxx proteins with both FPP and GGPP prenyl donors. Lastly, the work herein failed to capture any membrane localization behavior of potentially prenylated Cxx sequences in cells. This result suggests the potential for a shunt pathway in mammals, as seen with yeast, which would define a new cytosolic role for prenylation in mammalian systems.²⁹

The FLIM-FRET based system discussed in this work may prove useful in studying lipidation for these new Cxx sequences in cells. The ability of FLIM-FRET to provide quantitative information concerning potentially prenylated Cxx sequences as binding partners for PDE δ gives an opportunity to identify endogenous Cxx substrates and explore the aforementioned potential cytosolic function for prenylated Cxx substrates. However, this system requires further refinement as our studies to date have not provided evidence for binding of unprocessed prenylated substrates.

5.2 Future directions

5.2.1 Investigation of FTase vs. GGTase-I in Cxx substrate selectivity

One of the most surprising findings, after determining the ability of FTase to prenylate Cxx sequences using either FPP or GGPP prenyl donors, is the inability of GGTase-I to accept any of the sequences tested.²⁷ These two enzymes recognize the same classic CaaX motif with variations in the amino acids they accept and the type of isoprenoid group they select to attach to their respective substrates.^{3, 30, 31} FTase and GGTase-I exhibit distinct amino acid preference in the “X” position of the CaaX prenylation motif with FTase accepting X = M, Q, S, T, and A and GGTase-I most efficiently prenylating sequences of X = I or L.¹ These closely related enzymes have the ability to cross-talk in cells, with one enzyme rescuing prenylation of certain sequences when the other is inhibited.³² For example, KRas has been shown to be geranylgeranylated in the presence of FTase inhibitors. Despite the overlapping substrate selectivity of these two enzymes, not a single Cxx sequence tested was found to be accepted by GGTase-I.

With the aim of understanding the difference between the enzymes, one of the next steps is to determine the crystal structures of FTase interacting with Cxx motifs using both prenyl donors. The ability to prenylate these short sequences with both prenyl donors suggests a flexibility within the FTase active site not currently predicted through computational studies, and also not present in GGTase-I. Understanding the contact points and spacing of amino acids within the FTase binding site will provide valuable insight into why GGTase-I is much stricter in its substrate selectivity and moreover, how FTase is able to incorporate both prenyl groups on Cxx substrate targets.

5.2.2 Utilizing metabolic labeling to investigate prenylation of Cxx sequences in cells

One approach not yet utilized in this work for investigating prenylation of Cxx sequences inside cells is metabolic labeling. To provide definitive evidence for the prenylation of shortened sequences within human cells, the protein can be enriched through metabolic labeling with an alkyne-modified FPP analogue allowing subsequent conjugation with an affinity handle.³³ This approach was successfully employed in confirming the prenylation of a reporter protein bearing a longer C(x)₃X sequence.²⁸

In this approach, following transfection with a reporter protein bearing the sequence of interest, cells are incubated with the alkyne-modified FPP analogue for alkyne functionalization of the expressed protein. Subsequent derivatization with TAMRA-N₃ followed by in-gel imaging of TAMRA fluorescence allows for the visualization of the potentially prenylated Cxx target.²⁸
³³ Such an approach could prove fruitful in providing evidence for prenylation of non-canonical Cxx sequences inside cells.

5.2.3 Identification of endogenous Cxx proteins and the potential of a human shunt pathway

In light of the results presented in this work, this newly discovered activity of non-canonical Cxx sequences nearly doubles the number of proteins that can be potentially prenylated, even after rejecting sequences containing other cysteines within the motif. Through a Prosite search it was found that 1074 human proteins (accessed May 2020) follow a C-terminal Cxx sequence, with 847 of those sequences containing no other cysteine other than that required for prenylation (see Table 2.1). This is comparable to the 1208 potential Cxxx proteins in the

human proteome. These numbers underscore the importance of exploring and characterizing more Cxx proteins, to determine their prenylation state within the cell.

The Cxx sequences identified for analysis in this work from yeast used a screening tool that discriminates for proteins that are prenylated but not proteolyzed. This raises the question as to whether all Cxx sequences that serve as prenyltransferase substrates are unable or resistant to undergoing subsequent processing. This possibility makes identifying prenylated Cxx sequences through fluorescence microscopy difficult, as membrane localization can no longer be used as a proxy for prenylation. Despite this challenge, implications of this newly discovered Cxx sequence reactivity call for reassessing the role prenyl groups play beyond serving as a membranous anchor, with the possible existence and role of a “shunt pathway” in mammalian cells.²⁹

An ultimate goal in examining human Cxx proteins is to identify one such protein that undergoes endogenous prenylation. Due to the high number of potential proteins to test, this objective presents a “needle in the haystack” obstacle. However, while there are 1074 human proteins with a C-terminal Cxx sequence, the number of proteins with a unique Cxx sequence is 400, 85 of which have been tested in this work. While screening peptides via HPLC analysis can be performed quickly, production of the peptides required to test all 315 remaining sequences may prove to be a costly and time-consuming endeavor. This is even more true in testing potential Cxx prenylation substrates in a biological context; steps of cloning, transfection, imaging, and metabolic labeling of the proteins whose sequences produce a product peak on HPLC is even more of a financial and time-insensitive effort than the initial screening.

One reasonable approach to tackle the number of potential sequences is to employ a tactic similar to that used in this work to select peptides for an initial screening (see section 2.3). The

requirements used to select potential substrates could be further refined to exclude proteins with a C-terminal Cxx motif that results upon gene splicing. Protein splice variants are produced during regulation of gene expression and allow for a single gene to produce several functional proteins. By excluding such proteins, the complexity of proteins being examined can be reduced.

Moving towards yeast (and eventually other species), its smaller proteome makes for an easier target to finding potentially prenylated Cxx proteins. Future work could also include pathogenic organisms that employ either endogenous or host-mediated farnesylation, such as *Plasmodium falciparum*, *Candida albicans*, and *Legionella pneumophila*, all of which have a significantly lower number of potential targets.^{20, 33-39}

Overall, this work lays the foundation to examine Cxx sequence prenylation by yeast and mammalian FTase in biological systems. Moreover, we provide the first reported example of wild type FTase catalyzing peptide geranylgeranylation with comparable efficiency to farnesylation of the same sequences. This work expands both the peptide and prenyl donor substrate pools for FTase, which further highlights the truly remarkable degree of substrate flexibility exhibited by this enzyme. It supports further investigation of proteins terminating in Cxx sequences in cellular systems to determine their prenylation status and impact of such modification on the biological activities of Cxx proteins.

5.3 References

1. Benetka, W.; Koranda, M.; Eisenhaber, F., Protein prenylation: An (almost) comprehensive overview on discovery history, enzymology, and significance in physiology and disease. *Monatshefte für Chemie/Chemical Monthly* **2006**, *137* (10), 1241.
2. Casey, P. J., Lipid modifications of G proteins. *Current opinion in cell biology* **1994**, *6* (2), 219-225.
3. Casey, P. J.; Seabra, M. C., Protein prenyltransferases. *Journal of Biological Chemistry* **1996**, *271* (10), 5289-5292.
4. Marshall, C. J., Protein prenylation: a mediator of protein-protein interactions. *Science* **1993**, *259* (5103), 1865-1866.
5. Zhang, F. L.; Casey, P. J., Protein prenylation: molecular mechanisms and functional consequences. *Annual review of biochemistry* **1996**, *65* (1), 241-269.
6. Farnsworth, C. C.; Wolda, S. L.; Gelb, M. H.; Glomset, J. A., Human lamin B contains a farnesylated cysteine residue. *Journal of Biological Chemistry* **1989**, *264* (34), 20422-20429.
7. Hancock, J. F.; Magee, A. I.; Childs, J. E.; Marshall, C. J., All ras proteins are polyisoprenylated but only some are palmitoylated. *Cell* **1989**, *57* (7), 1167-1177.
8. Kitten, G.; Nigg, E., The CaaX motif is required for isoprenylation, carboxyl methylation, and nuclear membrane association of lamin B2. *The Journal of cell biology* **1991**, *113* (1), 13-23.
9. Powers, S.; Michaelis, S.; Broek, D.; Santa, A.-A. S.; Field, J.; Herskowitz, I.; Wigler, M., RAM, a gene of yeast required for a functional modification of RAS proteins and for production of mating pheromone α -factor. *Cell* **1986**, *47* (3), 413-422.

10. Sefton, B. M.; Buss, J. E., The covalent modification of eukaryotic proteins with lipid. *The Journal of cell biology* **1987**, *104* (6), 1449-1453.
11. Vorburger, K.; Kitten, G.; Nigg, E., Modification of nuclear lamin proteins by a mevalonic acid derivative occurs in reticulocyte lysates and requires the cysteine residue of the C-terminal CXXM motif. *The EMBO journal* **1989**, *8* (13), 4007-4013.
12. Gao, J.; Liao, J.; Yang, G.-Y., CAAX-box protein, prenylation process and carcinogenesis. *American journal of translational research* **2009**, *1* (3), 312.
13. Gutierrez, L.; Magee, A.; Marshall, C.; Hancock, J., Post-translational processing of p21ras is two-step and involves carboxyl-methylation and carboxy-terminal proteolysis. *The EMBO journal* **1989**, *8* (4), 1093-1098.
14. Gangopadhyay, S. A.; Losito, E. L.; Hougland, J. L., Targeted reengineering of protein geranylgeranyltransferase type I selectivity functionally implicates active-site residues in protein-substrate recognition. *Biochemistry* **2014**, *53* (2), 434-446.
15. Hancock, J.; Cadwallader, K.; Paterson, H.; Marshall, C., A CAAX or a CAAL motif and a second signal are sufficient for plasma membrane targeting of ras proteins. *The EMBO journal* **1991**, *10* (13), 4033-4039.
16. Hougland, J. L.; Gangopadhyay, S. A.; Fierke, C. A., Expansion of Protein Farnesyltransferase Specificity Using “Tunable” Active Site Interactions: Development of bioengineered prenylation pathways. *Journal of Biological Chemistry* **2012**, *287* (45), 38090-38100.
17. Hougland, J. L.; Lamphear, C. L.; Scott, S. A.; Gibbs, R. A.; Fierke, C. A., Context-dependent substrate recognition by protein farnesyltransferase. *Biochemistry* **2009**, *48* (8), 1691-1701.

18. Moores, S. L.; Schaber, M. D.; Mosser, S. D.; Rands, E.; O'Hara, M. B.; Garsky, V. M.; Marshall, M. S.; Pompliano, D. L.; Gibbs, J., Sequence dependence of protein isoprenylation. *Journal of Biological Chemistry* **1991**, *266* (22), 14603-14610.
19. Ota, I. M.; Clarke, S., Enzymatic methylation of 23-29-kDa bovine retinal rod outer segment membrane proteins. Evidence for methyl ester formation at carboxyl-terminal cysteinyl residues. *Journal of Biological Chemistry* **1989**, *264* (22), 12879-12884.
20. Al-Quadani, T.; Price, C. T.; London, N.; Schueler-Furman, O.; AbuKwaik, Y., Anchoring of bacterial effectors to host membranes through host-mediated lipidation by prenylation: a common paradigm. *Trends in microbiology* **2011**, *19* (12), 573-579.
21. Cui, G.; Wang, B.; Merz, K. M., Computational studies of the farnesyltransferase ternary complex part I: substrate binding. *Biochemistry* **2005**, *44* (50), 16513-16523.
22. Maurer-Stroh, S.; Eisenhaber, F., Refinement and prediction of protein prenylation motifs. *Genome biology* **2005**, *6* (6), R55.
23. Maurer-Stroh, S.; Koranda, M.; Benetka, W.; Schneider, G.; Sirota, F. L.; Eisenhaber, F., Towards complete sets of farnesylated and geranylgeranylated proteins. *PLoS computational biology* **2007**, *3* (4).
24. Lane, K. T.; Beese, L. S., Thematic review series: lipid posttranslational modifications. Structural biology of protein farnesyltransferase and geranylgeranyltransferase type I. *Journal of lipid research* **2006**, *47* (4), 681-699.
25. London, N.; Lamphear, C. L.; Hougland, J. L.; Fierke, C. A.; Schueler-Furman, O., Identification of a novel class of farnesylation targets by structure-based modeling of binding specificity. *PLoS computational biology* **2011**, *7* (10).

26. Reid, T. S.; Terry, K. L.; Casey, P. J.; Beese, L. S., Crystallographic analysis of CaaX prenyltransferases complexed with substrates defines rules of protein substrate selectivity. *Journal of molecular biology* **2004**, *343* (2), 417-433.
27. Ashok, S.; Hildebrandt, E. R.; Ruiz, C. S.; Hardgrove, D. S.; Coreno, D. W.; Schmidt, W. K.; Hougland, J. L., Protein farnesyltransferase catalyzes unanticipated farnesylation and geranylgeranylation of shortened target sequences. *Biochemistry* **2020**, *59* (11), 1149-1162.
28. Blanden, M. J.; Suazo, K. F.; Hildebrandt, E. R.; Hardgrove, D. S.; Patel, M.; Saunders, W. P.; Distefano, M. D.; Schmidt, W. K.; Hougland, J. L., Efficient farnesylation of an extended C-terminal C (x) 3X sequence motif expands the scope of the prenylated proteome. *Journal of Biological Chemistry* **2018**, *293* (8), 2770-2785.
29. Hildebrandt, E. R.; Cheng, M.; Zhao, P.; Kim, J. H.; Wells, L.; Schmidt, W. K., A shunt pathway limits the CaaX processing of Hsp40 Ydj1p and regulates Ydj1p-dependent phenotypes. *Elife* **2016**, *5*, e15899.
30. Hartman, H. L.; Hicks, K. A.; Fierke, C. A., Peptide specificity of protein prenyltransferases is determined mainly by reactivity rather than binding affinity. *Biochemistry* **2005**, *44* (46), 15314-15324.
31. Yokoyama, K.; Goodwin, G. W.; Ghomashchi, F.; Glomset, J.; Gelb, M. H., Protein prenyltransferases. Portland Press Ltd.: 1992.
32. Whyte, D. B.; Kirschmeier, P.; Hockenberry, T. N.; Nunez-Oliva, I.; James, L.; Catino, J. J.; Bishop, W. R.; Pai, J.-K., K- and N-Ras are geranylgeranylated in cells treated with farnesyl protein transferase inhibitors. *Journal of Biological Chemistry* **1997**, *272* (22), 14459-14464.

33. Suazo, K. F.; Schaber, C.; Palsuledesai, C. C.; John, A. R. O.; Distefano, M. D., Global proteomic analysis of prenylated proteins in *Plasmodium falciparum* using an alkyne-modified isoprenoid analogue. *Scientific reports* **2016**, *6*, 38615.
34. Ivanov, S. S.; Charron, G.; Hang, H. C.; Roy, C. R., Lipidation by the host prenyltransferase machinery facilitates membrane localization of *Legionella pneumophila* effector proteins. *Journal of Biological Chemistry* **2010**, *285* (45), 34686-34698.
35. Hast, M. A.; Nichols, C. B.; Armstrong, S. M.; Kelly, S. M.; Hellinga, H. W.; Alspaugh, J. A.; Beese, L. S., Structures of *Cryptococcus neoformans* protein farnesyltransferase reveal strategies for developing inhibitors that target fungal pathogens. *Journal of Biological Chemistry* **2011**, *286* (40), 35149-35162.
36. Selvig, K.; Ballou, E. R.; Nichols, C. B.; Alspaugh, J. A., Restricted substrate specificity for the geranylgeranyltransferase-I enzyme in *Cryptococcus neoformans*: implications for virulence. *Eukaryotic cell* **2013**, *12* (11), 1462-1471.
37. Piispanen, A. E.; Bonnefoi, O.; Carden, S.; Deveau, A.; Bassilana, M.; Hogan, D. A., Roles of Ras1 membrane localization during *Candida albicans* hyphal growth and farnesol response. *Eukaryotic cell* **2011**, *10* (11), 1473-1484.
38. Zverina, E. A.; Lamphear, C. L.; Wright, E. N.; Fierke, C. A., Recent advances in protein prenyltransferases: substrate identification, regulation, and disease interventions. *Current opinion in chemical biology* **2012**, *16* (5-6), 544-552.
39. Blanden, M. J.; Ashok, S.; Houglund, J. L., Mechanisms of CaaX Protein Processing: Protein Prenylation by FTase and GGTase-I. **2020**.

Appendix I: Reprint permission for reference 104 (Chapter 1)

7/14/2020

RightsLink Printable License

ELSEVIER LICENSE TERMS AND CONDITIONS

Jul 14, 2020

This Agreement between Sudhat Ashok ("You") and Elsevier ("Elsevier") consists of your license details and the terms and conditions provided by Elsevier and Copyright Clearance Center.

License Number	4860361408786
License date	Jul 01, 2020
Licensed Content Publisher	Elsevier
Licensed Content Publication	Elsevier Books
Licensed Content Title	Reference Module in Chemistry, Molecular Sciences and Chemical Engineering
Licensed Content Author	Melanie J. Blanden, Sudhat Ashok, James L. Hougland
Licensed Content Date	Jan 1, 2020
Licensed Content Pages	1
Start Page	
End Page	
Type of Use	reuse in a thesis/dissertation
I am an academic or government institution with a full-text	No

subscription to this journal and the audience of the material
consists of students and/or employees of this institute?

Portion	full chapter
Circulation	1
Format	both print and electronic
Are you the author of this Elsevier chapter?	Yes
Will you be translating?	No
Title	Thesis
Institution name	Syracuse University
Expected presentation date	Jul 2020
Requestor Location	Sudhat Ashok 702 Lancaster Avenue Syracuse, NY 13210 United States Attn:
Publisher Tax ID	98-0397604
Billing Type	Invoice
Billing Address	Sudhat Ashok 702 Lancaster Avenue Syracuse, NY 13210 United States Attn: Sudhat Ashok
Total	0.00 USD

Terms and Conditions

INTRODUCTION

1. The publisher for this copyrighted material is Elsevier. By clicking "accept" in connection with completing this licensing transaction, you agree that the following terms and conditions apply to this transaction (along with the Billing and Payment terms and conditions established by Copyright Clearance Center, Inc. ("CCC"), at the time that you opened your Rightslink account and that are available at any time at <http://myaccount.copyright.com>).

GENERAL TERMS

2. Elsevier hereby grants you permission to reproduce the aforementioned material subject to the terms and conditions indicated.

3. Acknowledgement: If any part of the material to be used (for example, figures) has appeared in our publication with credit or acknowledgement to another source, permission must also be sought from that source. If such permission is not obtained then that material may not be included in your publication/copies. Suitable acknowledgement to the source must be made, either as a footnote or in a reference list at the end of your publication, as follows:

"Reprinted from Publication title, Vol /edition number, Author(s), Title of article / title of chapter, Pages No., Copyright (Year), with permission from Elsevier [OR APPLICABLE SOCIETY COPYRIGHT OWNER]." Also Lancet special credit - "Reprinted from The Lancet, Vol. number, Author(s), Title of article, Pages No., Copyright (Year), with permission from Elsevier."

4. Reproduction of this material is confined to the purpose and/or media for which permission is hereby given.

5. Altering/Modifying Material: Not Permitted. However figures and illustrations may be altered/adapted minimally to serve your work. Any other abbreviations, additions, deletions and/or any other alterations shall be made only with prior written authorization of Elsevier Ltd. (Please contact Elsevier at permissions@elsevier.com). No modifications can be made to any Lancet figures/tables and they must be reproduced in full.

6. If the permission fee for the requested use of our material is waived in this instance, please be advised that your future requests for Elsevier materials may attract a fee.

7. Reservation of Rights: Publisher reserves all rights not specifically granted in the combination of (i) the license details provided by you and accepted in the course of this licensing transaction, (ii) these terms and conditions and (iii) CCC's Billing and Payment terms and conditions.

8. License Contingent Upon Payment: While you may exercise the rights licensed immediately upon issuance of the license at the end of the licensing process for the transaction, provided that you have disclosed complete and accurate details of your proposed use, no license is finally effective unless and until full payment is received from you (either by publisher or by CCC) as provided in CCC's Billing and Payment terms and conditions. If full payment is not received on a timely basis, then any license preliminarily granted shall be deemed automatically revoked and shall be void as if never granted. Further, in the event that you breach any of these terms and conditions or any of CCC's Billing and Payment terms and conditions, the license is automatically revoked and shall be void as if never

granted. Use of materials as described in a revoked license, as well as any use of the materials beyond the scope of an unrevoked license, may constitute copyright infringement and publisher reserves the right to take any and all action to protect its copyright in the materials.

9. Warranties: Publisher makes no representations or warranties with respect to the licensed material.

10. Indemnity: You hereby indemnify and agree to hold harmless publisher and CCC, and their respective officers, directors, employees and agents, from and against any and all claims arising out of your use of the licensed material other than as specifically authorized pursuant to this license.

11. No Transfer of License: This license is personal to you and may not be sublicensed, assigned, or transferred by you to any other person without publisher's written permission.

12. No Amendment Except in Writing: This license may not be amended except in a writing signed by both parties (or, in the case of publisher, by CCC on publisher's behalf).

13. Objection to Contrary Terms: Publisher hereby objects to any terms contained in any purchase order, acknowledgment, check endorsement or other writing prepared by you, which terms are inconsistent with these terms and conditions or CCC's Billing and Payment terms and conditions. These terms and conditions, together with CCC's Billing and Payment terms and conditions (which are incorporated herein), comprise the entire agreement between you and publisher (and CCC) concerning this licensing transaction. In the event of any conflict between your obligations established by these terms and conditions and those established by CCC's Billing and Payment terms and conditions, these terms and conditions shall control.

14. Revocation: Elsevier or Copyright Clearance Center may deny the permissions described in this License at their sole discretion, for any reason or no reason, with a full refund payable to you. Notice of such denial will be made using the contact information provided by you. Failure to receive such notice will not alter or invalidate the denial. In no event will Elsevier or Copyright Clearance Center be responsible or liable for any costs, expenses or damage incurred by you as a result of a denial of your permission request, other than a refund of the amount(s) paid by you to Elsevier and/or Copyright Clearance Center for denied permissions.

LIMITED LICENSE

The following terms and conditions apply only to specific license types:

15. **Translation:** This permission is granted for non-exclusive world **English** rights only unless your license was granted for translation rights. If you licensed translation rights you may only translate this content into the languages you requested. A professional translator must perform all translations and reproduce the content word for word preserving the integrity of the article.

16. **Posting licensed content on any Website:** The following terms and conditions apply as follows: Licensing material from an Elsevier journal: All content posted to the web site must maintain the copyright information line on the bottom of each image; A hyper-text must be included to the Homepage of the journal from which you are licensing at <http://www.sciencedirect.com/science/journal/xxxxx> or the Elsevier homepage for books at <http://www.elsevier.com>; Central Storage: This license does not include permission for a

scanned version of the material to be stored in a central repository such as that provided by Heron/XanEdu.

Licensing material from an Elsevier book: A hyper-text link must be included to the Elsevier homepage at <http://www.elsevier.com>. All content posted to the web site must maintain the copyright information line on the bottom of each image.

Posting licensed content on Electronic reserve: In addition to the above the following clauses are applicable: The web site must be password-protected and made available only to bona fide students registered on a relevant course. This permission is granted for 1 year only. You may obtain a new license for future website posting.

17. **For journal authors:** the following clauses are applicable in addition to the above:

Preprints:

A preprint is an author's own write-up of research results and analysis, it has not been peer-reviewed, nor has it had any other value added to it by a publisher (such as formatting, copyright, technical enhancement etc.).

Authors can share their preprints anywhere at any time. Preprints should not be added to or enhanced in any way in order to appear more like, or to substitute for, the final versions of articles however authors can update their preprints on arXiv or RePEc with their Accepted Author Manuscript (see below).

If accepted for publication, we encourage authors to link from the preprint to their formal publication via its DOI. Millions of researchers have access to the formal publications on ScienceDirect, and so links will help users to find, access, cite and use the best available version. Please note that Cell Press, The Lancet and some society-owned have different preprint policies. Information on these policies is available on the journal homepage.

Accepted Author Manuscripts: An accepted author manuscript is the manuscript of an article that has been accepted for publication and which typically includes author-incorporated changes suggested during submission, peer review and editor-author communications.

Authors can share their accepted author manuscript:

- immediately
 - via their non-commercial person homepage or blog
 - by updating a preprint in arXiv or RePEc with the accepted manuscript
 - via their research institute or institutional repository for internal institutional uses or as part of an invitation-only research collaboration work-group
 - directly by providing copies to their students or to research collaborators for their personal use
 - for private scholarly sharing as part of an invitation-only work group on commercial sites with which Elsevier has an agreement
- After the embargo period
 - via non-commercial hosting platforms such as their institutional repository
 - via commercial sites with which Elsevier has an agreement

In all cases accepted manuscripts should:

- link to the formal publication via its DOI

- bear a CC-BY-NC-ND license - this is easy to do
- if aggregated with other manuscripts, for example in a repository or other site, be shared in alignment with our hosting policy not be added to or enhanced in any way to appear more like, or to substitute for, the published journal article.

Published journal article (JPA): A published journal article (PJA) is the definitive final record of published research that appears or will appear in the journal and embodies all value-adding publishing activities including peer review co-ordination, copy-editing, formatting, (if relevant) pagination and online enrichment.

Policies for sharing publishing journal articles differ for subscription and gold open access articles:

Subscription Articles: If you are an author, please share a link to your article rather than the full-text. Millions of researchers have access to the formal publications on ScienceDirect, and so links will help your users to find, access, cite, and use the best available version.

Theses and dissertations which contain embedded PJAs as part of the formal submission can be posted publicly by the awarding institution with DOI links back to the formal publications on ScienceDirect.

If you are affiliated with a library that subscribes to ScienceDirect you have additional private sharing rights for others' research accessed under that agreement. This includes use for classroom teaching and internal training at the institution (including use in course packs and courseware programs), and inclusion of the article for grant funding purposes.

Gold Open Access Articles: May be shared according to the author-selected end-user license and should contain a [CrossMark logo](#), the end user license, and a DOI link to the formal publication on ScienceDirect.

Please refer to Elsevier's [posting policy](#) for further information.

18. **For book authors** the following clauses are applicable in addition to the above: Authors are permitted to place a brief summary of their work online only. You are not allowed to download and post the published electronic version of your chapter, nor may you scan the printed edition to create an electronic version. **Posting to a repository:** Authors are permitted to post a summary of their chapter only in their institution's repository.

19. **Thesis/Dissertation:** If your license is for use in a thesis/dissertation your thesis may be submitted to your institution in either print or electronic form. Should your thesis be published commercially, please reapply for permission. These requirements include permission for the Library and Archives of Canada to supply single copies, on demand, of the complete thesis and include permission for Proquest/UMI to supply single copies, on demand, of the complete thesis. Should your thesis be published commercially, please reapply for permission. Theses and dissertations which contain embedded PJAs as part of the formal submission can be posted publicly by the awarding institution with DOI links back to the formal publications on ScienceDirect.

Elsevier Open Access Terms and Conditions

You can publish open access with Elsevier in hundreds of open access journals or in nearly 2000 established subscription journals that support open access publishing. Permitted third

party re-use of these open access articles is defined by the author's choice of Creative Commons user license. See our [open access license policy](#) for more information.

Terms & Conditions applicable to all Open Access articles published with Elsevier:

Any reuse of the article must not represent the author as endorsing the adaptation of the article nor should the article be modified in such a way as to damage the author's honour or reputation. If any changes have been made, such changes must be clearly indicated.

The author(s) must be appropriately credited and we ask that you include the end user license and a DOI link to the formal publication on ScienceDirect.

If any part of the material to be used (for example, figures) has appeared in our publication with credit or acknowledgement to another source it is the responsibility of the user to ensure their reuse complies with the terms and conditions determined by the rights holder.

Additional Terms & Conditions applicable to each Creative Commons user license:

CC BY: The CC-BY license allows users to copy, to create extracts, abstracts and new works from the Article, to alter and revise the Article and to make commercial use of the Article (including reuse and/or resale of the Article by commercial entities), provided the user gives appropriate credit (with a link to the formal publication through the relevant DOI), provides a link to the license, indicates if changes were made and the licensor is not represented as endorsing the use made of the work. The full details of the license are available at <http://creativecommons.org/licenses/by/4.0>.

CC BY NC SA: The CC BY-NC-SA license allows users to copy, to create extracts, abstracts and new works from the Article, to alter and revise the Article, provided this is not done for commercial purposes, and that the user gives appropriate credit (with a link to the formal publication through the relevant DOI), provides a link to the license, indicates if changes were made and the licensor is not represented as endorsing the use made of the work. Further, any new works must be made available on the same conditions. The full details of the license are available at <http://creativecommons.org/licenses/by-nc-sa/4.0>.

CC BY NC ND: The CC BY-NC-ND license allows users to copy and distribute the Article, provided this is not done for commercial purposes and further does not permit distribution of the Article if it is changed or edited in any way, and provided the user gives appropriate credit (with a link to the formal publication through the relevant DOI), provides a link to the license, and that the licensor is not represented as endorsing the use made of the work. The full details of the license are available at <http://creativecommons.org/licenses/by-nc-nd/4.0>. Any commercial reuse of Open Access articles published with a CC BY NC SA or CC BY NC ND license requires permission from Elsevier and will be subject to a fee.

Commercial reuse includes:

- Associating advertising with the full text of the Article
- Charging fees for document delivery or access
- Article aggregation
- Systematic distribution via e-mail lists or share buttons

Posting or linking by commercial companies for use by customers of those companies.

20. Other Conditions:

v1.9

Questions? customercare@copyright.com or +1-855-239-3415 (toll free in the US) or +1-978-646-2777.

Appendix II: Reprint permission for reference 44 (Chapter 2)

7/6/2020

Rightslink® by Copyright Clearance Center



RightsLink®



Home



Help



Email Support



Sudhat Ashok ▾

Protein Farnesyltransferase Catalyzes Unanticipated Farnesylation and Geranylgeranylation of Shortened Target Sequences



Author: Sudhat Ashok, Emily R. Hildebrandt, Colby S. Ruiz, et al

Publication: Biochemistry

Publisher: American Chemical Society

Date: Mar 1, 2020

Copyright © 2020, American Chemical Society

PERMISSION/LICENSE IS GRANTED FOR YOUR ORDER AT NO CHARGE

This type of permission/license, instead of the standard Terms & Conditions, is sent to you because no fee is being charged for your order. Please note the following:

- Permission is granted for your request in both print and electronic formats, and translations.
- If figures and/or tables were requested, they may be adapted or used in part.
- Please print this page for your records and send a copy of it to your publisher/graduate school.
- Appropriate credit for the requested material should be given as follows: "Reprinted (adapted) with permission from (COMPLETE REFERENCE CITATION). Copyright (YEAR) American Chemical Society." Insert appropriate information in place of the capitalized words.
- One-time permission is granted only for the use specified in your request. No additional uses are granted (such as derivative works or other editions). For any other uses, please submit a new request.

[BACK](#)

[CLOSE WINDOW](#)

© 2020 Copyright - All Rights Reserved | [Copyright Clearance Center, Inc.](#) | [Privacy statement](#) | [Terms and Conditions](#)
Comments? We would like to hear from you. E-mail us at customer@copyright.com

Appendix III: Reprint permission for reference 2 (Chapter 3)

7/8/2020

RightsLink Printable License

JOHN WILEY AND SONS LICENSE TERMS AND CONDITIONS

Jul 08, 2020

This Agreement between Sudhat Ashok ("You") and John Wiley and Sons ("John Wiley and Sons") consists of your license details and the terms and conditions provided by John Wiley and Sons and Copyright Clearance Center.

License Number	4818240666338
License date	Apr 29, 2020
Licensed Content Publisher	John Wiley and Sons
Licensed Content Publication	Journal of Microscopy
Licensed Content Title	Fluorescence lifetime imaging – techniques and applications
Licensed Content Author	W. BECKER
Licensed Content Date	May 24, 2012
Licensed Content Volume	247
Licensed Content Issue	2
Licensed Content Pages	18
Type of use	Dissertation/Thesis
Requestor type	University/Academic
Format	Print and electronic

Portion	Figure/table
Number of figures/tables	1
Will you be translating?	No
Title	Thesis
Institution name	Syracuse University
Expected presentation date	Jun 2020
Portions	Figure 8.
	Sudhat Ashok 702 Lancaster Avenue
Requestor Location	Syracuse, NY 13210 United States Attn:
Publisher Tax ID	EU826007151
Total	0.00 USD
Terms and Conditions	

TERMS AND CONDITIONS

This copyrighted material is owned by or exclusively licensed to John Wiley & Sons, Inc. or one of its group companies (each a "Wiley Company") or handled on behalf of a society with which a Wiley Company has exclusive publishing rights in relation to a particular work (collectively "WILEY"). By clicking "accept" in connection with completing this licensing transaction, you agree that the following terms and conditions apply to this transaction (along with the billing and payment terms and conditions established by the Copyright Clearance Center Inc., ("CCC's Billing and Payment terms and conditions"), at the time that you opened your RightsLink account (these are available at any time at <http://myaccount.copyright.com>).

Terms and Conditions

- The materials you have requested permission to reproduce or reuse (the "Wiley Materials") are protected by copyright.
- You are hereby granted a personal, non-exclusive, non-sub licensable (on a stand-alone basis), non-transferable, worldwide, limited license to reproduce the Wiley Materials for the purpose specified in the licensing process. This license, **and any CONTENT (PDF or image file) purchased as part of your order,** is for a one-time use only and limited to any maximum distribution number specified in the license. The first instance of republication or reuse granted by this license must be completed within two years of the date of the grant of this license (although copies prepared before the end date may be distributed thereafter). The Wiley Materials shall not be used in any other manner or for any other purpose, beyond what is granted in the license. Permission is granted subject to an appropriate acknowledgement given to the author, title of the material/book/journal and the publisher. You shall also duplicate the copyright notice that appears in the Wiley publication in your use of the Wiley Material. Permission is also granted on the understanding that nowhere in the text is a previously published source acknowledged for all or part of this Wiley Material. Any third party content is expressly excluded from this permission.
- With respect to the Wiley Materials, all rights are reserved. Except as expressly granted by the terms of the license, no part of the Wiley Materials may be copied, modified, adapted (except for minor reformatting required by the new Publication), translated, reproduced, transferred or distributed, in any form or by any means, and no derivative works may be made based on the Wiley Materials without the prior permission of the respective copyright owner. **For STM Signatory Publishers clearing permission under the terms of the [STM Permissions Guidelines](#) only, the terms of the license are extended to include subsequent editions and for editions in other languages, provided such editions are for the work as a whole in situ and does not involve the separate exploitation of the permitted figures or extracts,** You may not alter, remove or suppress in any manner any copyright, trademark or other notices displayed by the Wiley Materials. You may not license, rent, sell, loan, lease, pledge, offer as security, transfer or assign the Wiley Materials on a stand-alone basis, or any of the rights granted to you hereunder to any other person.
- The Wiley Materials and all of the intellectual property rights therein shall at all times remain the exclusive property of John Wiley & Sons Inc, the Wiley Companies, or their respective licensors, and your interest therein is only that of having possession of and the right to reproduce the Wiley Materials pursuant to Section 2 herein during the continuance of this Agreement. You agree that you own no right, title or interest in or to the Wiley Materials or any of the intellectual property rights therein. You shall have no rights hereunder other than the license as provided for above in Section 2. No right, license or interest to any trademark, trade name, service mark or other branding ("Marks") of WILEY or its licensors is granted hereunder, and you agree that you shall not assert any such right, license or interest with respect thereto
- NEITHER WILEY NOR ITS LICENSORS MAKES ANY WARRANTY OR REPRESENTATION OF ANY KIND TO YOU OR ANY THIRD PARTY, EXPRESS, IMPLIED OR STATUTORY, WITH RESPECT TO THE MATERIALS OR THE ACCURACY OF ANY INFORMATION CONTAINED IN THE MATERIALS, INCLUDING, WITHOUT LIMITATION, ANY IMPLIED WARRANTY OF MERCHANTABILITY, ACCURACY, SATISFACTORY QUALITY, FITNESS FOR A PARTICULAR PURPOSE, USABILITY, INTEGRATION OR NON-INFRINGEMENT AND ALL SUCH WARRANTIES ARE HEREBY EXCLUDED BY WILEY AND ITS LICENSORS AND WAIVED

BY YOU.

- WILEY shall have the right to terminate this Agreement immediately upon breach of this Agreement by you.
- You shall indemnify, defend and hold harmless WILEY, its Licensors and their respective directors, officers, agents and employees, from and against any actual or threatened claims, demands, causes of action or proceedings arising from any breach of this Agreement by you.
- IN NO EVENT SHALL WILEY OR ITS LICENSORS BE LIABLE TO YOU OR ANY OTHER PARTY OR ANY OTHER PERSON OR ENTITY FOR ANY SPECIAL, CONSEQUENTIAL, INCIDENTAL, INDIRECT, EXEMPLARY OR PUNITIVE DAMAGES, HOWEVER CAUSED, ARISING OUT OF OR IN CONNECTION WITH THE DOWNLOADING, PROVISIONING, VIEWING OR USE OF THE MATERIALS REGARDLESS OF THE FORM OF ACTION, WHETHER FOR BREACH OF CONTRACT, BREACH OF WARRANTY, TORT, NEGLIGENCE, INFRINGEMENT OR OTHERWISE (INCLUDING, WITHOUT LIMITATION, DAMAGES BASED ON LOSS OF PROFITS, DATA, FILES, USE, BUSINESS OPPORTUNITY OR CLAIMS OF THIRD PARTIES), AND WHETHER OR NOT THE PARTY HAS BEEN ADVISED OF THE POSSIBILITY OF SUCH DAMAGES. THIS LIMITATION SHALL APPLY NOTWITHSTANDING ANY FAILURE OF ESSENTIAL PURPOSE OF ANY LIMITED REMEDY PROVIDED HEREIN.
- Should any provision of this Agreement be held by a court of competent jurisdiction to be illegal, invalid, or unenforceable, that provision shall be deemed amended to achieve as nearly as possible the same economic effect as the original provision, and the legality, validity and enforceability of the remaining provisions of this Agreement shall not be affected or impaired thereby.
- The failure of either party to enforce any term or condition of this Agreement shall not constitute a waiver of either party's right to enforce each and every term and condition of this Agreement. No breach under this agreement shall be deemed waived or excused by either party unless such waiver or consent is in writing signed by the party granting such waiver or consent. The waiver by or consent of a party to a breach of any provision of this Agreement shall not operate or be construed as a waiver of or consent to any other or subsequent breach by such other party.
- This Agreement may not be assigned (including by operation of law or otherwise) by you without WILEY's prior written consent.
- Any fee required for this permission shall be non-refundable after thirty (30) days from receipt by the CCC.
- These terms and conditions together with CCC's Billing and Payment terms and conditions (which are incorporated herein) form the entire agreement between you and WILEY concerning this licensing transaction and (in the absence of fraud) supersedes all prior agreements and representations of the parties, oral or written. This Agreement may not be amended except in writing signed by both parties. This Agreement shall be binding upon and inure to the benefit of the parties' successors, legal representatives, and authorized assigns.

- In the event of any conflict between your obligations established by these terms and conditions and those established by CCC's Billing and Payment terms and conditions, these terms and conditions shall prevail.
- WILEY expressly reserves all rights not specifically granted in the combination of (i) the license details provided by you and accepted in the course of this licensing transaction, (ii) these terms and conditions and (iii) CCC's Billing and Payment terms and conditions.
- This Agreement will be void if the Type of Use, Format, Circulation, or Requestor Type was misrepresented during the licensing process.
- This Agreement shall be governed by and construed in accordance with the laws of the State of New York, USA, without regards to such state's conflict of law rules. Any legal action, suit or proceeding arising out of or relating to these Terms and Conditions or the breach thereof shall be instituted in a court of competent jurisdiction in New York County in the State of New York in the United States of America and each party hereby consents and submits to the personal jurisdiction of such court, waives any objection to venue in such court and consents to service of process by registered or certified mail, return receipt requested, at the last known address of such party.

WILEY OPEN ACCESS TERMS AND CONDITIONS

Wiley Publishes Open Access Articles in fully Open Access Journals and in Subscription journals offering Online Open. Although most of the fully Open Access journals publish open access articles under the terms of the Creative Commons Attribution (CC BY) License only, the subscription journals and a few of the Open Access Journals offer a choice of Creative Commons Licenses. The license type is clearly identified on the article.

The Creative Commons Attribution License

The [Creative Commons Attribution License \(CC-BY\)](#) allows users to copy, distribute and transmit an article, adapt the article and make commercial use of the article. The CC-BY license permits commercial and non-

Creative Commons Attribution Non-Commercial License

The [Creative Commons Attribution Non-Commercial \(CC-BY-NC\) License](#) permits use, distribution and reproduction in any medium, provided the original work is properly cited and is not used for commercial purposes.(see below)

Creative Commons Attribution-Non-Commercial-NoDerivs License

The [Creative Commons Attribution Non-Commercial-NoDerivs License \(CC-BY-NC-ND\)](#) permits use, distribution and reproduction in any medium, provided the original work is properly cited, is not used for commercial purposes and no modifications or adaptations are made. (see below)

Use by commercial "for-profit" organizations

Use of Wiley Open Access articles for commercial, promotional, or marketing purposes requires further explicit permission from Wiley and will be subject to a fee.

Further details can be found on Wiley Online Library
<http://olabout.wiley.com/WileyCDA/Section/id-410895.html>

Other Terms and Conditions:

v1.10 Last updated September 2015

Questions? customercare@copyright.com or +1-855-239-3415 (toll free in the US) or +1-978-646-2777.

Appendix IV: Reprint permission for reference 18 (Chapter 4)

7/9/2020

Manage Account



Marketplace™

Order Number: 1047115

Order Date: 08 Jul 2020

Payment Information

Sudhat Ashok
suashok@syr.edu

Payment method: Invoice

Billing Address:

Sudhat Ashok
702 Lancaster Avenue
Syracuse, NY 13210
United States

+1 (516) 974-6817

suashok@syr.edu

Customer Location:

Sudhat Ashok
702 Lancaster Avenue
Syracuse, NY 13210
United States

Order Details

1. Chemical Society reviews

Billing Status:

Open

Order license ID	1047115-1
Order detail status	Completed
ISSN	1460-4744
Type of use	Republish in a thesis/dissertation
Publisher	ROYAL SOCIETY OF CHEMISTRY
Portion	Chart/graph/table/figure

0.00 USD

Republication Permission

LICENSED CONTENT

Publication Title	Chemical Society reviews	Country	United Kingdom of Great Britain and Northern Ireland
Author/Editor	Royal Society of Chemistry (Great Britain)	Rightsholder	Royal Society of Chemistry
Date	01/01/1972	Publication Type	e-Journal
Language	English	URL	http://www.rsc.org/csr

REQUEST DETAILS

Portion Type	Chart/graph/table/figure	Distribution	Worldwide
Number of charts / graphs / tables / figures requested	1	Translation	Original language of publication
		Copies for the disabled?	No

Format (select all that apply)	Print,Electronic	Minor editing privileges?	No
Who will republish the content?	Academic institution	Incidental promotional use?	No
Duration of Use	Life of current edition	Currency	USD
Lifetime Unit Quantity	Up to 499		
Rights Requested	Main product		

NEW WORK DETAILS

Title	Investigating photo-switchable FPP analogs as donors for FTase	Institution name	Syracuse University
Instructor name	Sudhat Ashok	Expected presentation date	2020-07-28

ADDITIONAL DETAILS

The requesting person / organization to appear on the license	Sudhat Ashok
--	--------------

REUSE CONTENT DETAILS

Title, description or numeric reference of the portion(s)	Fig. 1	Title of the article/chapter the portion is from	Azobenzene photoswitches for biomolecules
Editor of portion(s)	N/A	Author of portion(s)	Andrew A. Beharry and G. Andrew Woolley
Volume of serial or monograph	N/A	Publication date of portion	2011-08-01
Page or page range of portion	4423		

Total Items: 1

Subtotal: 0.00 USD

Order Total: 0.00 USD

Appendix V: Curriculum Vitae

Sudhat Ashok

4060 Harlem Rd., Amherst, NY 14226

Phone: (516) 974-6817 – Email: sudhatashok@gmail.com

EDUCATION

2017 – Present

Doctor of Philosophy – Chemistry, *Syracuse University*, Syracuse, New York, USA.

2015 – 2017

Master of Philosophy – Chemistry, *Syracuse University*, Syracuse, New York, USA.

2009 – 2014

Bachelor of Arts – Psychology, Chemistry & Cognitive Science Minor, *State University of New York, College at Geneseo*, Geneseo, New York, USA.

RESEARCH EXPERIENCE

2015 – Present **Graduate Research Assistant**, *Syracuse University*, Syracuse, New York, USA.

Advisor: Dr. James L. Houglund

Expanding the potential prenylome through unanticipated prenylation of non-canonical C-terminal peptide sequences

Investigating the prenylation of non-canonical Cxx C-terminal sequences through HPLC analysis, mass spectrometry, in cell studies, and steady-state kinetics via fluorescence-based assays.

2013 – 2014 **Undergraduate Research Assistant**, *SUNY Geneseo*, Geneseo, New York, USA.

Advisor: Dr. Vincent Markowski

Investigated the behavioral and neurological effects of developmental exposure to neurotoxic flame retardant, Deca-BDE in animal models via tissue collection, chemical preparation, histological tissue staining, microscopic analysis of stained tissue, and statistical analysis.

TEACHING EXPERIENCE

- 2016 – 2019 **Teaching Assistant**, *Syracuse University*, Syracuse, NY
Classes – Organic Chemistry Lab I and Proteins & Nucleic Acids Laboratory
Responsibilities included preparation and ordering of materials, maintenance of equipment, testing the validity of experiments prior to class, assisting and guiding students during laboratory, office hours, holding lecture-style study sessions, and grading of lab reports, quizzes, and exams.
- 2018 – 2020 **Undergraduate Student Research Mentor**, *Syracuse University*, Syracuse, NY
Supervisor: Dr. James Houglan
Training and guidance of an undergraduate student in biochemistry lab techniques, experiments, and scientific writing/presentations. Techniques mentored include protein purification via FPLC, bacterial cloning, DNA and protein gel analysis, PCR, HPLC, fluorescence assays and basic lab maintenance and solution making.

PUBLICATIONS

- Ashok, S., Hildebrandt, E., Ruiz, C. S., Hardgrove, D. S., Coreno, D., Schmidt, W., & Houglan, J. L. (2020). Protein farnesyltransferase catalyzes unanticipated farnesylation and geranylgeranylation of shortened target sequences. *Biochemistry*.
<https://doi.org/10.1021/acs.biochem.0c00081>
- Blanden, M. J., Ashok, S., & Houglan, J. L., Mechanisms of CaaX Protein Processing: Protein Prenylation by FTase and GGTase-I. Elsevier Inc: 2020
<https://doi.org/10.1016/B978-0-12-409547-2.14837-1>

CLINICAL EXPERIENCE

- January 2014 Rotated with Dr. Thomas Martin, DO – Lourdes Family Practice, Binghamton NY (80 hours).
- Spring 2019 Rotated with both Dr. Julius Gene Latorre and Dr. Elena Schmidt in Neuro-ICU – SUNY Upstate University Hospital, Syracuse NY (200 hours).

SELECTED PRESENTATIONS

October 2019 **Neurocritical Care Society Meeting – Vancouver, CA**

Presented poster: Safety of Cangrelor in Emergency Endovascular Stroke Recanalization, A Single Center Experience.

March 2019 **Syracuse University Life Sciences Research Showcase – Syracuse, NY**

Presented poster: Expanding the potential prenylome through unanticipated prenylation of non-canonical C-terminal peptide sequences.

August 2018 **ACS National Meeting – Boston, MA**

Presented poster on expanding the potential prenylome through unanticipated prenylation of non-canonical C-terminal peptide sequences.

May 2018 **UB Graduate Student Symposium – Buffalo, NY**

Presented poster: Expanding the potential prenylome through unanticipated prenylation of non-canonical C-terminal peptide sequences.

May 2014 **GREAT Day Poster Presentation – Geneseo, NY**

Presented poster on the behavioral and neurological effects of developmental exposure to neurotoxic flame retardant, Deca-BDE in animal models.

SELECTED CONTRIBUTIONS TO ABSTRACTS AND GRANT APPLICATION

May 2019 **Abstract: Safety of Cangrelor in Emergency Endovascular Stroke Recanalization, A Single Center Experience**

- Assisted in literature search and abstract write-up.

AWARDS

August 2018 **ACS Division of Biological Chemistry Travel Award**

LEADERSHIP AND VOLUNTEER EXPERIENCE

2019-2020 **Refugee & Immigrant Self-Empowerment (RISE) – Syracuse, NY**

Serving as a volunteer in the following programs at RISE:

- **After School Programs** – Assist students from 1st grade to high schoolers with homework, help explore their creativity through engaging activities, and simply play and remain active with one another.
- **Saturday Academy** – Volunteer at the Destiny Christian Center every Saturday for two hours where the program serves as an education resource for those who need assisted homework help and Regents test prep. Also serves as a creative outlet through engaging activities and field trips.
- **Youth Professionalization Program** – This program seeks to provide refugees and immigrants between ages 14 – 25 the skills and confidence they need to excel in school, the workplace, and in life through interactive workshops, one-on-one advisement, homework help, and resume building.

2009-2014 **Special Olympics – York, NY**

- Assisted with setting up various Olympics style tournaments for kids to participate in. Also helped present awards and announced the respective winners.

2013-2014 **Second and Third Annual Ghana Gala – Geneseo, NY**

- Hosted and helped set up the annual fundraising project to aid Ghana.

2012-2013 **Trans-fat for Transplants fundraiser – Geneseo, NY**

- Initiated and helped carry out an annual fundraiser to raise money to aid kidney transplants. Donations were made to the National Kidney Foundation.

2012 **Pre-teen group Camp Counselor – Driftwood Day Camp, Melville NY**

- Served as a camp counselor for children aged 7-9.